INTERACTIONS BETWEEN MYOFIBROBLASTS AND COLORECTAL CANCER (CRC) EPITHELIAL CELL LINES

MARAHAINI MUSA

St Hilda's College

A thesis submitted to the Division of Medical Sciences, University of Oxford, in partial fulfilment of the requirements for the degree of
Doctor of Philosophy in Oncology

Trinity term, 2018

Weatherall Institute of Molecular Medicine
University of Oxford

I dedicate this thesis to my parents and my siblings.

Thank you for always being there for me.

ABSTRACT

Myofibroblasts are an important cellular component of the tumour microenvironment and play an essential role in facilitating carcinogenesis through bidirectional communications with epithelial cells. Accumulation of myofibroblasts is associated with poor prognosis in colorectal cancers. Myofibroblasts are distinguished from skin fibroblasts by positive expression of amine oxidase, copper containing 3 (*AOC3*) and *NKX2-3*. The current project aims to study the *in vitro* interactions between myofibroblasts and colorectal cancer (CRC) epithelial cell lines and their effects on gene expression in myofibroblasts, primarily *AOC3* and *NKX2-3*.

In vitro interactions between myofibroblasts and CRC cell lines were analysed using various assays. An increase in cancer cell growth, myofibroblast migration and formation of bigger lumens in CRC cell lines was found in co-culture as compared to monoculture (**Chapter 3**). The results show high expression of NKX2-3 in all myofibroblasts, while AOC3 expression was more heterogeneous. These data suggest NKX2-3 to be a key mediator for maintaining the myofibroblast phenotype, while AOC3 serves as a negative indicator for their activation state. Knockdown experiments indicated *NKX2-3* to be a regulator for *AOC3* and *ACTA2* expression in myofibroblasts. *AOC3* expression in myofibroblasts is downregulated by TGFβ1, EGF, PDGF-AA and CC. Our data indicate that PDGF-AA and CC are significant players for the interactions between myofibroblasts and CRC cell lines. The fibroblast activation protein (FAP) was shown to be an indicator of myofibroblast activation whose regulation

by PDGF-AA differed between normal and cancer-derived myofibroblasts (**Chapter 4**). Lastly, we established a serum free chemically defined (NEW) medium which supports the growth of myofibroblasts but not CRC cell lines (**Chapter 5).**

In conclusion, our results illustrate *in vitro* cross-communication between myofibroblasts and CRC epithelial cell lines with a significant role for the PDGF-A and C/PDGFRA signalling pathway in the interactions between those two cell types. (295 words)

ACKNOWLEDGEMENTS

I would like to express my gratitude to everyone who has helped me make this thesis possible. I am extremely thankful for my supervisor, Professor Sir Walter Bodmer, for his guidance and support throughout my DPhil journey. Furthermore, I would like to thank the members of the Cancer and Immunogenetics (CIL) Laboratory at University of Oxford, including Dr Djamila Ouaret, Laura Coling, Dr Jennifer Wilding, Tom Barnes, Peter Kalugin, Jeff Liu and Mustak Ibn Ayub for their constant support and advice. I would like to especially thank Djamila for her tremendous help in guiding me on daily basis from the first moment I joined the lab. Many thanks also to my funding body (Ministry of Education, Malaysia and Universiti Sains Malaysia) for providing the scholarship for my research.

Additionally, I am thankful for my own little Malaysian family in Oxford especially Adli, Hajar, Najiah, Ilham, Megat, Hakimi, Jaezah, Zarina, Quek and Aizuddin, who has been my source of comfort over the past 3 years. I am also grateful for the constant support from my friends who are living thousand miles away from me especially Nis and Fatihah.

Finally, I would like to express my utmost gratitude to my parents and siblings for their love, support and encouragement.

DECLARATION

I, Marahaini Musa, hereby declare that work on which this thesis is based on my original work and that neither the whole work nor any part of it has been, is being or will be submitted for another degree in this or any other university. The work is original expect where listed by reference in the text.

SIGNED: .DATE: 22/11/2018

TABLE OF CONTENTS

CHAPTER 1

GENERAL INTRODUCTION

CHAPTER 2

MATERIALS AND METHODS

CHAPTER 3

IN VITRO STUDIES OF THE INTERACTIONS BETWEEN MYOFIBROBLASTS AND COLORECTAL CANCER (CRC) CELL LINES

CHAPTER 4

INFLUENCE OF GROWTH FACTORS ON THE REGULATION OF *AOC3* AND *NKX2-3*, TWO DIFFERENTIALLY EXPRESSED GENES IN MYOFIBROBLASTS

CHAPTER 5

DEVELOPMENT OF SERUM FREE DEFINED MEDIUM FOR MYOFIBROBLASTS

CHAPTER 6

GENERAL DISCUSSION

LIST OF FIGURES

LIST OF TABLES

LIST OF ABREVIATIONS

AOC3	Amine oxidase, copper containing 3
αSMA	Alpha-smooth muscle actin
BSA	Bovine serum albumin
CAF	Cancer associated fibroblast
cDNA	Complementary DNA
CM	Conditioned medium
CRC	Colorectal cancer
DAPI	4',6-diamidino-2-phenylindole
DMEM	Dulbecco's Modified Eagle Medium
DMSO	Dimethyl sulfoxide
dNTP	Deoxyribonucleotide triphosphate
ECL	Enhanced chemiluminescence
ECM	Extracellular matrix
EDTA	Ethylenediaminetetraacetic acid
EGF	Epidermal growth factor
EMT	Epithelial to mesenchymal transition
FAP	Fibroblast activation protein
FBS	Fetal bovine serum
FGF	Fibroblast growth factor
Fs	Fibroblasts
h	Hour
HGF	Hepatocyte growth factor
IGF1	Insulin-like growth factor 1

kDa	Kilodalton
mAb	Monoclonal antibody
MET	Mesenchymal to epithelial transition
Min	Minute
mRNA	Messenger ribonucleic acid
µg	Microgram
µL	Microliter
µm	Micrometer
µM	Micromolar
mg	Miligram
mL	Milliliter
mM	Millimolar
MFs	Myofibroblasts
ng	Nanogram
nM	Nanomolar
PBS	Phosphate buffered saline
PDGF	Platelet-derived growth factor
PVDF	Polyvinylidene difluoride
qRT-PCR	Quantitative reverse-transcription polymerase chain reaction
RNAse	Ribonuclease
RT	Reverse transcription
SDS	Sodium dodecyl sulfate
SF	Serum free medium
Sec	Second

SEM	Standard error of the mean
siRNA	Small interfering ribonucleic acid
TBS	Tris-buffered saline
TBST	Tris-buffered saline plus Tween-20
TCGA	The Cancer Genome Atlas
TEMED	N,N,N,N-Tetramethylethylene-diamine
TGFβ	Transforming growth factor beta
TNF-α	Tumour necrosis factor
UTR	Untranslated Region
VEGF	Vascular endothelial growth factor
Vim	Vimentin

CHAPTER 1

GENERAL INTRODUCTION

CHAPTER 1: GENERAL INTRODUCTION

1.1 Colonic crypt structure

The mammalian intestinal epithelium turnover is a rapid process which occurs throughout the life of the organism (Stappenbeck et la., 1998). The stable state of cell growth of normal colonic epithelium is sustained by a dynamic balance between continuous cell renewal and shedding of cells at the top of the colonic crypts. Stem and progenitor cells which can be found at the base of the crypt drive this process and give rise to various differentiated cell types (van der Flier and Clevers, 2009). The development and turnover of these stem cells are controlled by several signalling pathways which involve Wnt, Hedgehog and Noggin (Lickert et al., 2000; Wang et al., 2002; Haramis et al., 2004).

Stem cell daughters divide and move toward the upper crypt regions before gradually losing the capacity to proliferate and become more differentiated cells and eventually die by apoptosis (Lipkin, 1983; Traber, 1994; Hall et al., 1994). Mesenchymal cells of the intestine found in lamina propria include myofibroblasts, bone marrow-derived stromal cells and smooth muscle (Powell et al., 2011; Hsia et al 2016). The crypt is surrounded by extracellular matrix (ECM) that helps to maintain the intestine's three-dimensional architecture. The colonic crypt organization is shown in **Figure 1.1**.

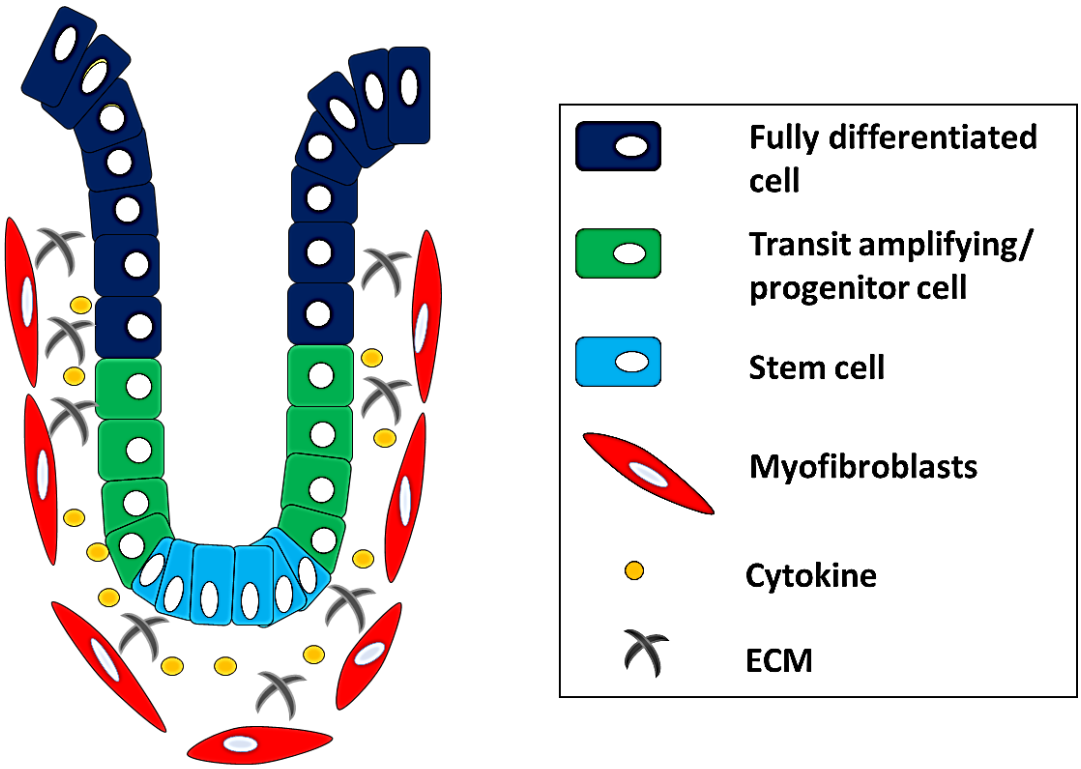

Figure 1.1

Illustration of the organization and different cell types in colonic crypt. Small numbers of stem cells are found at the bottom of the crypt. These cells differentiate into progenitor cells and subsequently into three types of fully differentiated cells: goblet cells, enterocytes and enteroendocrine cells. Myofibroblasts line the crypt of the colon and rectum and are separated from epithelial cells by ECM (extracellular matrix).

1.2 Microenvironment and its influence on colorectal cancer progression

The tumour microenvironment includes several components that play essential roles in determining the progress of malignancy in solid tumours. These can be divided into three major groups: cells of haematopoietic origin, cells of mesenchymal origin and non-cellular components. Depending on the origin of the tumour and stages of the cancer progression, these components may

present in different proportions. Major cell types of tumour microenvironment include myofibroblasts, macrophages, blood vessels and are associated with the ECM (Simon-Assmann et al., 1995; Pattabiraman and Weinberg, 2014). For the present study, we are going to focus more on the potential role of myofibroblasts, instead of other cell types, in promoting cancer progression.

Cross talk between tumour cells and adjacent stroma or microenvironment supports progression of many human solid tumours. Activated stroma makes up a significant proportion of various human solid tumours particularly non-small cell lung, pancreatic, breast and colorectal tumours (Yazhou et al., 2004). The presence of a high proportion of myofibroblast-rich stroma in individual tumours is normally associated with high-grade malignancy (Maeshima et al., 2002, Tsujino et al., 2007, Tothill et al., 2008, Farmer et al., 2009, Ootani et al., 2009). Investigation into the nature of the tumour-myofibroblasts interaction may therefore provide better insight on potential therapeutic avenues to eradicate the tumour (Eberlein et al., 2015). Contrary to this notion, Ozdemir et al. (2014) have reported that depletion of αSMA^{+} myofibroblasts leads to various adverse outcomes mainly by suppressing immune surveillance (increased CD4(+) Foxp3(+) the regulatory T cells – Tregs) which resulted in poor survival in a pancreatic ductal adenocarcinoma (PDAC) mouse model. These studies indicate that the complex role of myofibroblasts in cancer may variy depending on the type and progression of cancer. Bidirectional communication of tumour cells with activated stroma are mediated by secreted products such as cytokines, growth factors, chemokines, proteases and components of the ECM (Kaler et al., 2014; Brennen et al., 2004).

Colorectal cancer (CRC) is the third most commonly diagnosed malignancy worldwide and one of the leading causes of cancer death in both male and female (Torre et al., 2015). The approach of studying the treatment and related molecular characteristics of CRC has evolved over the past decades. Instead of focusing on the malignant cancer cells only, the scientific community started to explore the role of tumour microenvironment in driving the CRC progression. Accumulation of myofibroblasts around adenomatous colorectal polyps (Adegboyega et al., 2012) and primary tumour sites has been associated with poor prognosis and a higher rate of disease recurrence (Tsujino et al., 2007).

1.3 Stromal cell classification

Poor understanding of the stromal fibroblast has led to rather confusing and contradicting terminology on the different cell types found in the cancer microenvironment. Among many terms used to refer to stromal cells associated with colon cancer are cancer associated fibroblasts (CAFs), stromal fibroblasts, peritumoral fibroblasts, myofibroblasts or alpha-smooth muscle actin (αSMA)-positive myofibroblasts (Orimo and Weinberg, 2007, De Wever et al., 2008, Semba et al., 2009). αSMA defines the previously most commonly used phenotypic characteristic of myofibroblasts and is a main factor that contributes to the enhanced contractile force generation by these cells (Hinz et al., 2012). Myofibroblasts in the tumour context are generally referred to as tumour-associated fibroblasts or CAFs (Kalluri and Zeisberg, 2006) whose recruitment and activation are mainly influenced by the cytokines secreted by

cancer cells and infiltrated immune cells. This definition was derived from an early publication by Olumi et al. (1999) where he used a functionally based definition of CAFs to differentiate them from conventional fibroblasts. Based on their report and more recent study (Augsten, 2014), CAFs can be defined in simpler term as a form of activated myofibroblasts that possesses elevated expression of αSMA in comparison to fibroblasts in normal tissue. CAFs terminology is used in next sections in this thesis to refer to the population of activated myofibroblasts.

Single cell analysis provides more detailed information on the existence of different sub-populations of fibroblasts in the stroma. More recent study by Xie et al. (2018) has reported six mesenchymal cell types (myofibroblasts, *Col13a1* fibroblasts, *Col14a1* fibroblasts, lipofibroblasts, mesenchymal progenitors, mesothelial and endothelial cells) in normal lung and seven in fibrotic lung of mice (sub-population of cells mentioned before and addition of Pdgfrb high cells). A more thorough single cell transcriptomics of cellular stroma component of human colon has yet to be described in great details.

The association between various populations of stromal cells and prognosis of cancer has been explored by many researchers in the recent years. Costa et al. (2018) have reported on four CAF subsets in breast cancer characterized by specific phenotype and activation levels. In addition, Su et al. (2018) have described the presence of a subset of CAFs characterized by two cell-surface molecules ($CD10^+$ and $GPR77^+$) which correlate with poor response to chemotherapeutic agents in breast and lung cancer patients. Heterogeneity of

CAF populations also was described in pancreatic cancer whereby two spatially separated, reversible, and mutually exclusive subtypes of CAFs were found located either adjacent or distal from neoplastic cells (Öhlund et al., 2017). In the CRC context, poor prognosis of the cancer relates to the upregulation of mesenchymal genes expressed by tumour-associated stromal cells instead of epithelial tumour cells (Calon et al., 2015). In addition, pro-tumorigenic properties of CAFs in the colon were reported suggesting that CAFs increased the frequency of tumour-initiating cells which was greatly enhanced by transforming growth factor (TGF)-β signalling.

1.4 Myofibroblasts

Myofibroblasts can be found in normal tissues such as lymph nodes, blood vessels, uterine submucosa, intestinal villous core, lung septa and stroma of testis (Tomasek et al., 2002). These cells also were detected in reactive lesions, the locally aggressive fibromatoses, benign tumours and sarcomas (Fletcher, 1998). Pathologically, different tumours possess variability in the amount of myofibroblasts and heterogeneity of myofibroblasts in tumour stroma has been reported (Kojima and Ochiai, 2016). The origins of myofibroblasts are still a matter of debate among scientists and various research groups seem to be in agreement that sources of myofibroblast may differ between individuals, organs, animals, or particular injury models. Bochaton-Piallat et al. (2016) has described myofibroblasts as a phenotypic variant of many cell types which developed upon the appearance of appropriate stimuli.

A previous publication from our lab has defined pericryptal cells in the human colon as myofibroblasts, as originally identified by PR2D3 mAb staining (Richman et al., 1987), followed by the αSMA staining (Sappino et al., 1989) as well as supported by co-staining results with various markers to confirm these pericryptal cells are indeed $PR2D3^{+}$, αSMA^{+}, $Vimentin^{+}$ and $CD31^{-}$ (Hsia et al., 2016). **Table 1.1** shows markers that have been used to distinguish different cell types, namely myofibroblasts, fibroblasts, activated fibroblasts (TGFβ1-treated skin fibroblasts) and vascular smooth muscle cells (Hsia et al., 2016).

Cell type	AOC3	NKX2-3	SHOX2	αSMA	Desmin	Vimentin	Smoothelin	THY-1 CD90
Myofibroblasts	**+**	**+**	**-**	**+, ±**	**-**	**+**	**-**	**+**
Fibroblasts	**-**	**-**	**++**	**±**	**-**	**+**	**-**	**+**
Activated fibroblasts	**-**	**-**	**+**	**++**	**-**	**+**	**-**	**+**
Vascular smooth muscle cells	**+**	**+**	**-**	**+**	**+**	**-**	**+**	**-**

Table 1.1

Molecular markers for distinguishing among myofibroblasts, fibroblasts, activated fibroblasts and vascular smooth muscle cells.

Heterogeneous αSMA staining was found in myofibroblasts and skin fibroblasts (* +, ±: the majority of the myofibroblasts were stained by αSMA; ±: only a subset of fibroblasts was positive for αSMA). Table is taken from Hsia et al. (2016).

1.4.2 Markers for myofibroblasts

Microarray analysis between myofibroblasts and skin fibroblasts performed by our group suggested several differentially expressed genes (DEGs) as potential markers for myofibroblasts, namely *AOC3*, *NKX2-3* and *LRRC17* (Hsia et al., 2016). A specific gene for skin fibroblasts, *SHOX2*, also was identified. A volcano plot of the microarray data is summarized in **Figure 1.2**. In the next section, DEGs between myofibroblasts and fibroblasts (*AOC3*, *NKX2-3* and *LRRC17*) will be discussed.

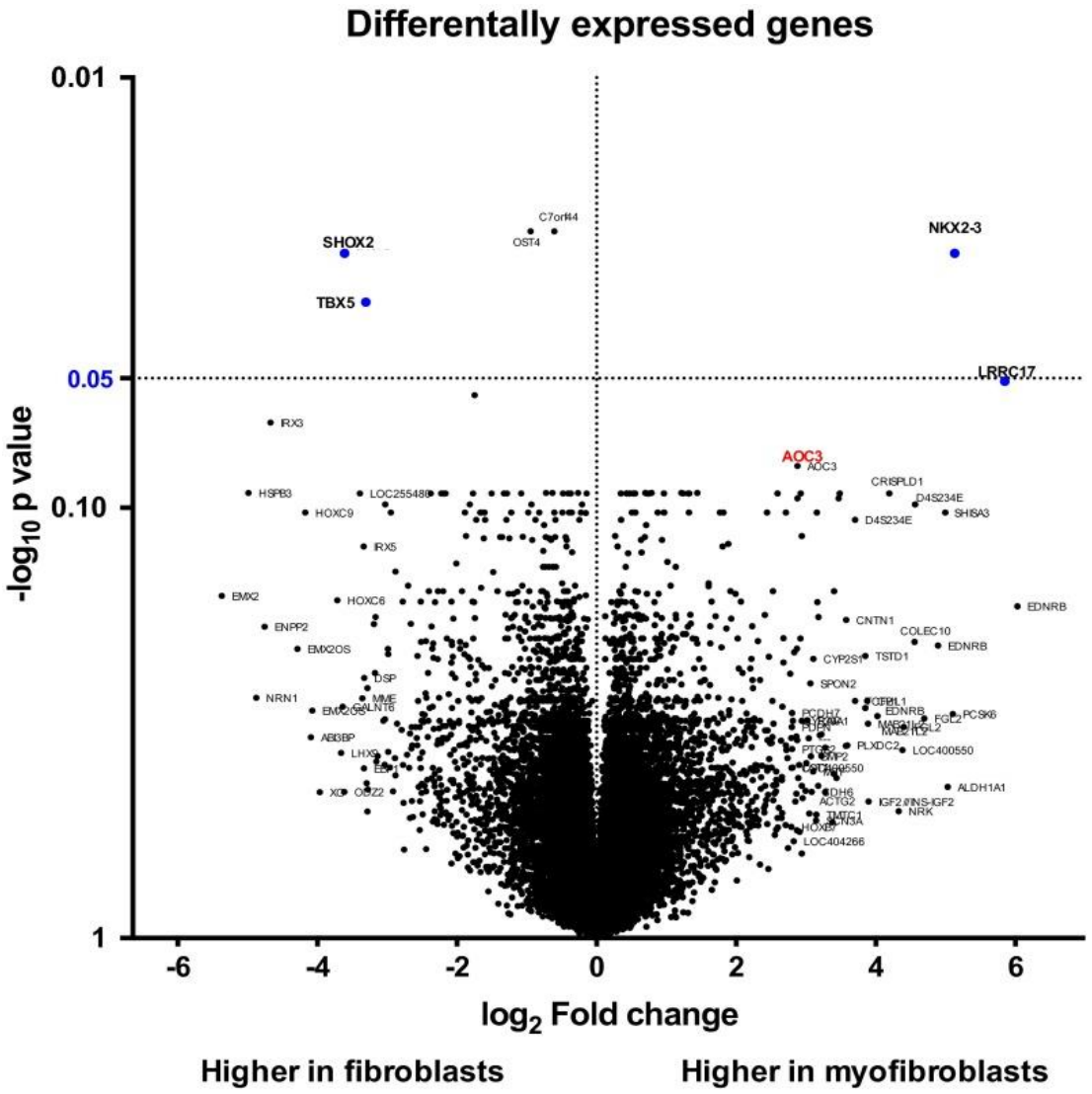

Figure 1.2

Volcano Plot representation of microarray data between myofibroblasts and fibroblasts

Microarray gene expression profiles of myofibroblast cultures group (positive foldchange) vs fibroblast cultures group (negative fold-change) were plotted according to the log2 fold change (X axis) and -log10 p-value (Y-axis). Significant changes in the gene expression were identified if the corrected p-value was less than 0.05 and fold change is greater than 2 (blue dots) (Image taken from Hsia et al., 2016).

1.5 Amine oxidase, copper containing 3 (AOC3)

1.5.1 The structure of AOC3 (VAP-1)

AOC3, (amine oxidase, copper containing 3) encodes vascular adhesion protein (VAP-1). AOC3 is one of the members of cell surface–expressed, semicarbazide-sensitive amine oxidases (SSAO; EC 1.4.3.6) family (Smith et al., 1998). This peripheral plasma membrane protein possesses 2 interrelated functions in the regulation of physiological trafficking and inflammation as both adhesive and an enzyme (Salmi and Jalkanen, 2001; 2005). AOC3 can serve as a traditional adhesion molecule on endothelial cells.

The human VAP-1 (hVAP-1) is a 180 kDa dimeric membrane glycoprotein consisting of a very short 4 amino acid N-terminal cytoplasmic tail, a single transmembrane segment and a sequence of large extracellular domains (Smith et al., 1998; Salmi and Jalkanen, 2001; 2005). The structure of a VAP-1 homodimer composed of chains A (A55–A761) and B (B57–B761). Each monomer (90 kDa glycoproteins) contains a copper atom, two calcium atoms and N-acetylglucosamine sugar units at two separate sites (Airenne et al., 2005). A soluble form of hVAP-1 has been found in humans which is presumably a product of the proteolytic cleavage of membrane bound hVAP-1 (Abella et al., 2004; Stolen et al., 2004). The molecular structure of hVAP-1 is the heart-shaped copper dependent amine oxidase (CAO) fold consisting of domains D2 (residues 55–169), D3 (residues 170–300), and D4 (residues 301–761) (Airenne et al., 2005). The structure of VAP-1 is illustrated in **Figure 1.3.**

1.5.2 Functional activity of AOC3 (VAP-1)

AOC3 oxidizes primary amines to the corresponding aldehyde, H_2O_2 and ammonium through enzymatic (deamination) reaction. At the first step of this two-step reaction involves the formation of a transient Schiff-base by the amine substrate with the enzyme. The enzyme is reduced, and the aldehyde is released. In the second part of the reaction, the enzyme is oxidized and returns to its original form which in a reaction, also leads to production of ammonium ions and hydrogen peroxide. A simplified enzymatic reaction of AOC3 is shown as below (reviewed by Jalkanen and Salmi, 2008):

$$R\text{-}CH_2\text{-}NH_2 + O_2 + H_2O \rightarrow R\text{-}CHO + NH_3 + H_2O_2$$

These products of VAP-1 enzymatic reaction, namely aldehyde, ammonium and hydrogen peroxide, activate NFκB-dependent chemokine secretion and adhesion molecule expression in liver endothelium (Lalor et al., 2007; Jalkanen et al., 2007) and may initiate oxidative stress due to formation hydroxyl free radicals from H_2O_2. VAP-1 is also detected in adipocytes and smooth muscle cells. *The in vitro* provision of SSAO substrates to these cells produced insulin-like effects on their metabolism, which is mediated via PI3-kinase activation by H_2O_2 (Marti et al., 1998; Enrique-Tarancó et al., 2000).

(A)

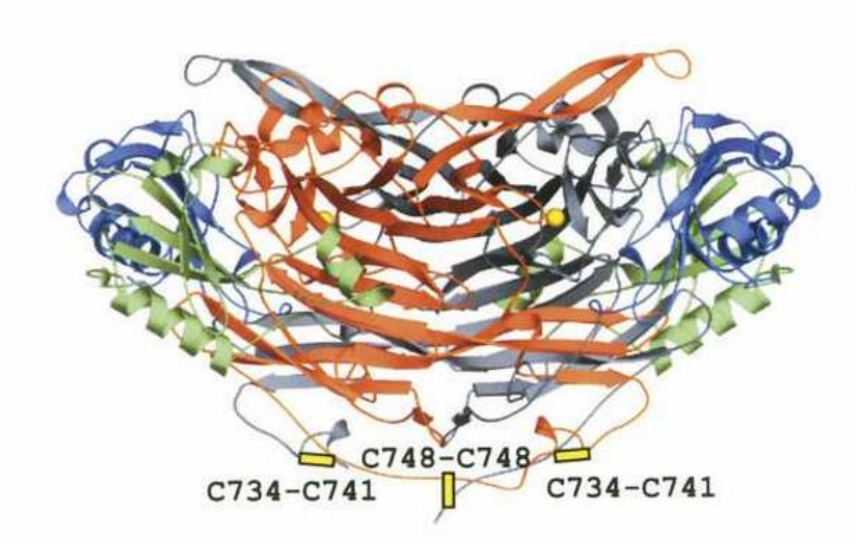

(B)

Figure 1.3

Structure of AOC3 (VAP-1).

The ribbons for hVAP-1are illustrated (A) where each domain is denoted with a different colour; D2, green; D3, blue; D4 of subunit A, orange; and D4 of subunit B, gray. The ECAO ribbon is shown in grey. The copper atom of the active site is indicated as a yellow sphere (Image taken from Airenne et al., 2005). (B) Molecular cloning of AOC3 indicated a type 2 glycoprotein with potential N-glycosylation sites and putative O-glycosylation sites (denoted by N or O and arrows). The transmembrane domain is between residues 5 and 27 (TMD: transmembrane domain) (Figure taken from Smith et al., 1998).

1.5.3 The role of AOC3/ VAP-1 in pathological condition

VAP-1 is found not only in endothelial cells but also in fibrotic septae where it co-localizes with αSMA^{+} myofibroblasts. Both *in vitro* hepatic stellate cells (HSC) and active myofibroblasts express VAP-1 and possess amine oxidase activity which is comparable to that of sinusoidal endothelial cells (SECs). Activated HSC induced *in vitro* migration of lymphocytes through amine oxidase enzymatic activity and this process was reduced either by H_2O_2 or GPCR signalling inhibition (Torok, 2015). Regulation of VAP-1 expression occurs in a tissue- and cell type-selective manner and upregulation of this gene required a correct micromilieu for it to happen (Arvilommi et al., 1997).

The expression of AOC3 is associated with the prognosis of various types of cancer (Toiyama et al., 2009; Yasuda et al., 2011; Kostoro et al., 2016). Higher mean levels of serum soluble VAP-1 (sVAP-1) level were detected in CRC patients than in controls, and it decreased with cancer progression. The sVAP also acts as an independent marker to predict lymph or hepatic metastasis. Levels of serum VAP-1 were found to be significantly higher in hepatocellular cancer patients when compared to controls (Kemik et al., 2010).

Others have reported conflicting findings on the association of levels of VAP expression and progression of cancer in various organs where strong expression of VAP-1 was found in some cancers including head and neck and liver cancers. Patients with lower sVAP-1 appear to have poor prognosis of CRC in comparison to those with higher sVAP-1 level (Toiyama et al., 2009). A similar

correlation with low sVAP-1 and poor prognosis in gastric cancer also was described (Yasuda et al., 2011). Wu et al. (2014) reported the association of monoamine oxidase A (MAO-1) expression with poor prognosis of cancer and it is correlated with the progression of prostate cancer and metastasis. It has been stated that serum sVAP-1 level is lower in CRC patients in comparison to controls (patients not having CRC). Western blot analysis also revealed lower VAP-1 protein level in CRC compared to its matched normal colon tissues (Ward et al., 2016).

It has been suggested that VAP-1 supports the lymphocyte recruitment where anti-VAP-1 mAbs blocks the natural killer (NK) adhesion and tumor infiltrating lymphocytes to VAP-1+ neovessels within the tumors (Irjala et al., 2001). VAP-1 knock-out mice of a melanoma mouse model has been shown to have impaired ability to form new tumour vessels. VAP-1 inhibition reduced tumour infiltration by CD8+ T cells and myeloid-derived suppressor cells (MDSCs) thus suggesting that VAP-1 supports tumorigenesis through the recruitment of immunosuppressive cells (Marttila-Ichihara et al., 2010).

1.6 NKX2-3

1.6.1 NKX2-3 expression and domain structure

NKX2-3 is another candidate marker for myofibroblasts. NKX2-3 (NK2 homeobox 3) located on chromosome 10q24, belongs to a family of genes that encode transcription factors which contain homeodomains and its function is

implicated in basic developmental processes. The NKX family in general is involved in the regulation of various fundamental cellular processes, including head patterning, cardiac and lung development, and neural cell specification (McGinnis and Krumlauf, 1992; Biben et al., 2002; Garcia-Fernàndez, 2005). Expression of Nkx2-3 is found in gut mesenchyme and spleen of embryonic and adult mice. This gene has a vital role in normal development and in the functions of the small intestine and spleen. Inactivation of the Nkx2-3 gene leads to a major defect in both organs and early postnatal death in most of the homozygous mutants (Pabst et al., 1999). **Figure 1.4** shows the domain architecture of human NKX2-3.

(A)

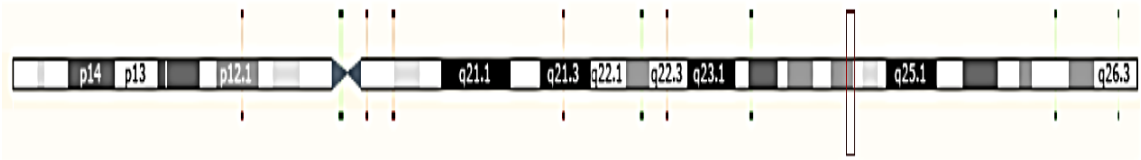

(B)

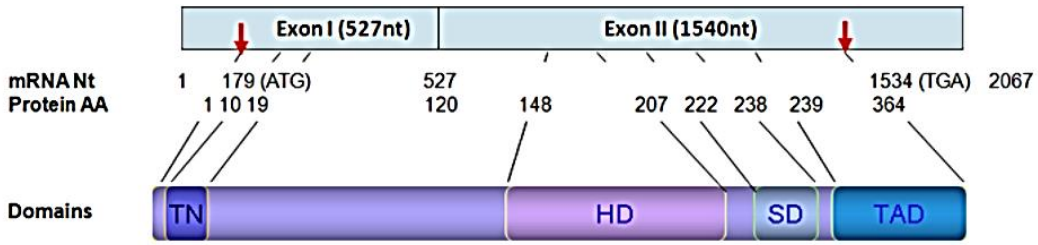

Figure 1.4

Human NKX2.3 mRNA and protein domains.

(A) NKX2-3 position on q arm of chromosome 10 is denoted by the box. (B) NKX2-3 gene is comprised of two exons of 527 and 1540 bp, respectively and

one intron of 1496 bp. The NKX2.3 protein is made up of 364 amino acids which includes a TN (tinman domain), HD (homeodomain), SD (NK2 specific domain) and TAD (transcriptional activation domain). Figure and data from ENSEMBL transcript (http://www.ensembl.org/index.html).

1.6.2 NKX2-3 and pathogenesis

Several NKX2 members have been identified as oncogenic drivers in solid tumours. NKX2-2 is associated as a vital transcription factor that contributes to the oncogenic transformation in Ewing's sarcoma (Smith et al., 2006). Weir et al. (2007) have identified NKX2-1 as a novel candidate proto-oncogene involved in a significant fraction of lung adenocarcinomas. Another member of the NKX2 family, NKX2-8 has been reported to act as a tumor suppressor in esophageal squamous cell carcinoma (ESCCs) where its downregulation leads to activation of NF-κB and ESCC angiogenesis (Lin et al., 2013). Studies also have demonstrated that NKX2-1, NKX2-2 and NKX2-5 frequently exhibit genomic rearrangements which result in dysregulation of expression in T-cell acute lymphoblastic leukaemia (Nagel et al., 2007; Homminga et al., 2011; Yamaguchi et al., 2013).

NKX2-3 polymorphism was associated with the susceptibility to inflammatory bowel disease (IBD) in Caucasian patients (The Wellcome Trust Case Control Consortium, 2007). CRC is one of the most serious complications of IBD, notably in ulcerative colitis (UC) where increased risk of developing CRC is found among these patients (Ekbom et al., 1990). Several studies have validated the association of single nucleotide polymorphisms (SNPs)

(rs10883365andrs1190140) in the NKX2-3 gene with Crohn's disease (CD) (Parkes et al., 2007; Meggyesi et al., 2010) and UC in Caucasian and Asian populations. A meta-analysis using 35358 subjects has established the association of NKX2-3 polymorphisms to IBD where a significantly greater CD or UC risk was detected in persons carrying a G allele at rs10883365 polymorphism (A/G) in comparison with those with a A allele (Odds ratio - OR = 1.226, 95% Confidence interval - CI: 1.177–1.277 and OR = 1.274, 95% CI: 1.175–1.382 respectively) (Lu et al., 2014). These findings corroborate with other studies where they reported that sequence variants in NKX2-3 gene predispose to development of CD and UC. The upregulation of NKX2-3 expression was detected in tissue samples from these patients (Fisher et al., 2008; Arai et al., 2011).

The functional roles of NKX2-3 are poorly understood and there is limited information on this gene's contribution to cancer development (Homminga et al., 2011). A more recent study has implied NKX2-3 in lymphomagenesis. NKX2-3 induces B-cell receptor signalling by phosphorylation of Lyn/Syk kinases. This in turn leads to activation of multiple integrins (LFA-1, VLA-4), adhesion molecules (ICAM-1, MadCAM-1) and the chemokine receptor type 4 (CXCR4). These molecules promote B cell migration, polarization and homing to splenic and extranodal tissues which results in malignant transformation via NF-kB and PI3K-AKT pathways (Robles et al., 2016). As for solid tumour, downregulation of NKX2-3 has been reported in colorectal cancer (Wang et al., 2008).

1.7 LRRC17

LRRC17, also known as P37NB, belongs to a member of the Leucine Rich Repeat (LRRC) superfamily. LRRs are 20–29-residue sequence motifs which can be found in various proteins with diverse functions and in many organisms such as viruses, bacteria, archae, and eukaryotes. Most of these proteins may play a part in protein-ligand and in protein–protein interactions; which includes innate immune response in mammals (Kobe and Deisenhofer, 1994; Kobe and Kajava, 2001; Matsushima et al., 2005a; Matsushima et al., 2005b).

The domain structure of LRRC17 is illustrated in **Figure 1.5**. Human LRRC17 contains ten leucine rich repeats (LRRs). The island region (IR) located at the centre of LRR region is 64–72 residues long. This IR comprises of a cluster of six Cys residues (Bella et al., 2008). LRRNT and LRRCT are Cys clusters including two or four Cys residues; the Cys clusters on the N- and C-terminal sides of the LRR arcs, respectively. The N-terminal part of the IR is suggested to act as a cap structure of the first block and its C-terminal part as a cap structure of the second block. The centre region of the IR with 22–30 residues is rich in Pro and hydrophilic residues (Matsushima et al., 2009).

Figure 1.5

Domain architecture of human LRRC17.

The blue circle indicates signal peptide and yellow box corresponds to LRR unit. Both LRRNT and LRRCT are shown in green. IR is denoted in dark green (Image taken from Matsushima et al., 2009).

LRRC17 has been implicated in osteoblast differentiation and proliferation (Kim et al., 2009). The expression of LRRC17 also has been associated with smooth muscle cells (Yu et al., 2005; Markowska et al., 2014). In the context of solid tumours, this gene has been identified as a triple negative breast cancer (TNBC) specific gene (Zaka et al., 2014). In contrast, microarray data analysis of primary breast tumours has shown estrogen induced the expression of LRRC17/ P37NB and its expression is correlated with estrogen receptor-positive (ER+) status (Chanrion et al., 2008). Due to the discrepancy between these reports, the correlation between LRRC17 expression and different cancer classifications still have yet to be determined. The differentially methylated region (DMR) of *LRRC17* is associated with survival, where better survival goes with higher methylation (Mathe et al., 2016). *LRRC17* also was expressed in neuroblastoma and influences the cell migration and invasion process (Lasorsa et al., 2016). Little is known of the functional activity of LRRC17 in a CRC context.

1.8 Fibroblast activation protein (FAP)

One of the most prominent genes to identify activated stromal fibroblast like cells or myofibroblasts is fibroblast activation protein alpha (*FAP*).

1.8.1 FAP expression in normal and cancer

FAP is a cell surface glycoprotein that shows a strong expression in stromal fibroblasts in over 90% of epithelial carcinomas, including CRC (Garin-Chesa et al., 1990; Rettig et al., 1993; 1994). The development of the FAP-specific monoclonal antibody F19 has shown a reaction with stromal myofibroblasts of cancer, also known as CAFs. No expression of FAP was found in the stroma of benign epithelial tumours, epithelial cells (normal and malignant), malignant hematopoietic cells and normal stromal fibroblasts of fetal colon, lung, cartilage, kidney and skeletal muscle.

1.8.2 Structure of FAP

FAP is a type II cell-surface-bound transmembrane glycoprotein (protease) comprised of 170 kDa homodimer that contains two N-glycosylated 97 kDa subunits (Aertgeerts et al., 2005). Its monomer structure is comprised of a large C-terminal extracellular domain and a short, single membrane-spanning domain that includes 760 amino acids, where most of this part consists of a hydrolytic area exposed laterally of the plasmalemma. Approximately 20 amino acids are

in the plasma membrane and 6 amino acids are located in the cytoplasmic region (Kelly, 2005).

The ectodomain crystal structure of FAP is shown in **Figure 1.6** where each subunit contains the β-propeller (residues 54-492) and the α/β hydrolase domain (residues 27-53 and 493-760). The FAP catalytic triad which is composed of residues Ser624, Asp702 and His734 is located between the interfaces of the β-propeller and the α/β-hydrolase domain (Aertgeerts et al., 2005). Dimerization of FAP is necessary for its catalytic (enzymatic) function (Park et al., 1999). FAP also can be found as a truncated, soluble form in human plasma, lacking the transmembrane domain (Lee et al., 2004; 2011).

(A)

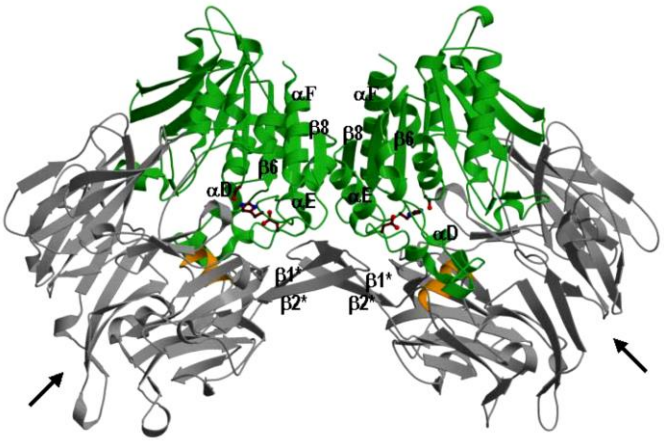

(B)

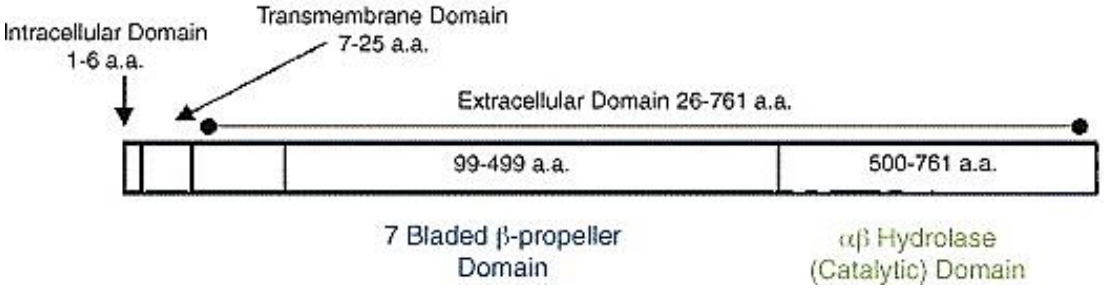

Figure 1.6

The structure of FAP.

FAP dimer represented in ribbon diagram (A). The β-propeller domain and α/β hydrolase domain are denoted in grey and green, respectively. Active-site residues Ser 624, Asp 702 and His 734 are shown in ball-and-stick symbols. The α-helix which contain the Glu-motif is indicated in yellow and Arrows show the direction of the central pore (Image taken from Aertgeerts et al., 2005). (B) The position and amino acid composition of FAP domains (Image taken from Cheng et al., 2005).

1.8.3 Functional activity of FAP

FAP possess dual-enzyme function as described below (Yu et al., 2010):

a) Dipeptidyl peptidase activity - This involve the cleavage of two amino acids off the N-terminus by FAP which occurs after a proline (Pro) residue
b) Endopeptidase activity – Enables FAP to cleave at a site of more than two amino acids from N-terminus of a protein. It is limited to the post-Pro bond after glycine-Pro (Gly-Pro)

FAP harbours a lot of interest among researchers as a potential therapeutic target for cancer. FAP has been speculated to promote tumour cell invasion. Gao et al., (2010) has reported that co-culture of human breast tumour stromal cells expressing FAP with breast cancer cells leads to faster migration of cancer cell and induction of EMT than did cancer cells co-incubated with FAP negative fibroblasts derived from the same tumour. It was shown that FAP expression is associated with metastatic burden in human colon cancer patients (Iwasa et al., 2005). Besides a huge interest in FAP as marker for tumour stroma, it is also being studied to dissect its role as a protease in other pathological conditions, including atherosclerosis (Brokopp et al., 2011; Keane et al., 2012). CAFs which express FAP have been reported to reduce the efficacy of treatment for pancreatic cancer. Elimination of these FAP+ stromal cells permitted immune control of tumour growth and revealed the efficacy of ‘check point’ immunotherapeutic antibodies, namely anti-cytotoxic T-lymphocyte-associated protein 4 (α-CTLA-4) and α-programmed cell death 1 ligand 1 (α-PD-L1) (Feig et al., 2013).

1.8.4 Substrates for FAP

The mechanism of the multiple functions of FAP, which involve a variety of different downstream pathways remains elusive despite many studies. Two physiological endopeptidase substrates for FAP were discovered, namely; denatured type I collagen (CN-I) (Park et al., 1999; Levy et al., 1999) and α2-antiplasmin (α2-AP) (Lee et al., 2004; 2011). Collagen fibres which constitute the largest components of ECM provide structural support for cells and tissues. The ECM regulates and affects essential biochemical and biomechanical processes as it binds certain growth factors and bioactive peptides (Frantz et al., 2010). Although FAP in its native form is unable to cleave the collagen fibres, partial digestion of collagen fibres by matrix metalloproteinase (MMP) 1 resulted in the unwinding of collagen fibres which enabled FAP to cleave these fibres as they are rich in Gly-Pro residues (Park et al., 1999; Christiansen et al., 2007). ECM remodelling is a common process that occurs in tumorigenesis and fibrosis. Soluble FAP (sFAP) cleaves α2-Antiplasmin (α2-AP), which is an inhibitor of plasmin and this leads to reduction in the rate of lysis of fibrin clots as plasmin dissolves fibrin clots during fibrinolysis. Thus, this FAP activity affects fibrinolysis and promotes scar tissue formation (Lee at al., 2006).

1.9 Cross talk between stromal cells and cancer cells

As mentioned earlier in this chapter, the bidirectional communication between the microenvironment (eg. cellular component such as myofibroblasts) and cancer cells may contribute to the tumorigenesis process. A wide variety of

cytokines such as interleukin-1, interleukin-6, tumour necrosis factor-α and growth factors (e.g. transforming growth factor (TGF)β1, epidermal growth factor (EGF), platelet-derived growth factor - PDGF) are secreted by both tumour and stromal cells through autocrine and/or paracrine mechanisms which can induce neovascularization and tumour growth as well as migration and invasion of cancer cells (Liotta and Kohn, 2001; Witsch et al., 2010; Erdogan and Webb, 2017). In cancer studies, associations between CAFs and tumour progression have been referred to in many publications. CAFs release various inflammatory mediators which include MMPs that can influence ECM modification and support the invasion and metastasis process (Lochter et al., 1998; Sternlicht et al., 1999; Kalluri and Zeisberg, 2006). CAFs also secrete other components and growth factors such as stromal derived factor-1 (SDF-1), VEGF, hepatocyte growth factor (HGF), insulin-like growth factor (IGF), nerve growth factor, WNT1, EGF and fibroblast growth factor 2 (FGF2), which can facilitate the growth of adjacent epithelial cells and formation of new blood vessel within the stroma (Kalluri and Zeisberg, 2006).

There is much yet to be discovered regarding the activation of myofibroblasts. Yeung et al. (2013) has reported substantial activation of myofibroblasts, stained with αSMA and anti-AOC3 in Hsia et al., (2016) in lymph nodes containing metastatic colorectal adenocarcinoma. Greater myofibroblast activation was observed in larger metastatic deposits. This finding suggests strong dependency of metastatic cancer cells on their microenvironment.

1.10 Culture medium to study myofibroblasts-CRC cells interactions

Some of the growth factors and cytokines mentioned above are detected, at various concentrations in the fetal bovine serum (FBS) that is used widely as a supplement to culture cells *in vitro* (Zheng et al., 2006). These components (eg. PDGF and TGFβ1) also can be found in human serum (Josh et al., 2013). Cocktails of different growth factors and components in serum are therefore used to provide essential supplements for cell grown in the absence of FBS.

An appropriate culture medium is the most important factor in cell culture technology. It supports cell survival and proliferation, as well as cellular functions, that directly determine the research outcome (Yao and Asayam, 2017). It is essential to select an appropriate medium with defined components that is suitable to culture myofibroblasts as the presence of numerous unidentified growth factors in FBS may influence the properties of myofibroblasts. The invention of serum free, defined medium with addition of specific, known components (which includes growth factors like PDGF, EGF, TGF) has enabled the study of cells in culture under more controlled conditions (Gstraunthaler, 2003). Different formulations of serum free media have been suggested to culture various types of cells (Chase et al., 2009; Chieregato et la., 2011; Martin et al., 2015).

1.11 Aims of this thesis

As discussed, a growing body of evidence has suggested bidirectional communication between myofibroblasts and cancer cells. The main goal of this thesis is to study *in vitro* the interactions between myofibroblasts and colorectal cancer (CRC) epithelial cell lines and its effects on differentially expressed genes in myofibroblasts. The thesis also will discuss the design of a serum free medium, which can potentially be used for myofibroblasts and CRC co-culture *in vitro*.

.

In summary, the primary aims of this thesis are as follows:

1. Design *in vitro* assays to evaluate the interactions between myofibroblasts and CRC cell lines (proliferation, differentiation, cell migration and invasion)
2. Characterize the expression of AOC3 and NKX2-3 in primary myofibroblasts derived from normal and cancerous colon tissues
3. Identify candidate growth factors that influence the expression of AOC3 and NKX2-3 in myofibroblasts
4. Evaluate the effects of growth factor treatments on other selected genes/ proteins in myofibroblasts such as FAP, αSMA and LRRC17
5. Study the effect of AOC3 and NKX2-3 knockdown in myofibroblasts in co-culture conditions with CRC cell line
6. Formulation of a serum free defined medium for myofibroblasts for prospective application in cell culture

CHAPTER 2

MATERIALS AND METHODS

CHAPTER 2: MATERIALS AND METHODS

2.1 Reagents and suppliers

Reagents and chemicals were acquired from Sigma-Aldrich (UK) unless stated otherwise. Cell culture flasks and plates were purchased from Corning (USA). All the cell lines were maintained in Gibco® cell culture media by Life Technologies.

2.2 Cell culture methods

2.2.1 Cell lines

All colorectal cancer (CRC) epithelial cell lines, myofibroblasts and fibroblasts used in this thesis were obtained from cryogenic storage of the Cancer and Immunogenetics laboratory (CIL) at the Weatherall Institute of Molecular Medicine (WIMM), Oxford, UK. Several of the CRC cell lines were selected to be included in the study, namely RKO, HT29, LS180, SW480, SW620, VACO400, OXCO1, NCIH716, HCT116, CC20, Lovo, SW1222, SKCO1, HDC9 and Colo320DM. The properties and details of the cell lines are summarized in **Table 2.1**. SW480 and SW620 have been isolated from the same patient. SW480 was established from a Dukes' stage B colon carcinoma of a 50-year-old male patient whereas SW620 is derived from a lymph node metastasis of the same patient (Leibovitz et al., 1976).

CRC cell lines	Catalogue number, Source	Differentiation state in Matrigel
RKO	ATCC® CRL-2577™	Non-lumen forming
HT29	ATCC® HTB-38™	Intermediate (poorly differentiated)
LS180	Kind gift from B.H.Tom, NW Uni Med Centre, Chicago	Lumen forming
SW480	ATCC® CCL-228™	Non-lumen forming
SW620	ATCC® CCL-227™	Non-lumen forming
VACO400	Dr Elizabeth Zborowska (obtained under an MTA, Case Western Reserve University, Cleveland, Ohio)	Non-lumen forming
OXCO1	Cerundolo, WIMM, Oxford	Non-lumen forming
NCIH716	ATCC® CCL-251™	Intermediate
HCT116	ATCC® CRL-247™	Non-lumen forming
CC20	A.R. Kinsella	Non-lumen forming
Lovo	ATCC® CRL-229™	Intermediate
SW1222	M. Herlyn, Wistar Institute	Lumen forming
SKCO1	ATCC® HTB-39™	Intermediate
HDC9	M. Schwab, DKFZ, Germany	Intermediate
Colo320DM	ATCC® CCL-220™	Non-lumen forming

Table 2.1

List of CRC epithelial cell lines used in this study.

Human foreskin fibroblasts and normal skin fibroblasts were also included in the research to enable the comparison between myofibroblasts and normal fibroblasts. CCD-18Co, a myofibroblast line from neonatal colonic mucosa, was acquired from American Type Culture Collection (ATCC, no. CRL1459). CCD-18Co was used as a main model for myofibroblasts based on previous work performed in our laboratory. CCD-18Co for up to passage 21 was used for subsequent experiments. Foreskin fibroblasts were purchased from ATCC and skin fibroblasts were derived from a healthy donor. The isolation of these skin fibroblasts was conducted in the Bodmer laboratory using the conventional enzymatic method.

2.2.2 Establishment of primary myofibroblasts

Primary myofibroblasts were derived from surgical samples. Colon tissue from patients, who underwent surgery for colorectal tumours (Oxford University Hospital, UK) were collected with informed consent (ethically approved under the OCHRe Biobank approval no. 09/H0606/5+5). The study using primary tissues was approved by the local research ethics committee. Isolation of myofibroblasts from normal and cancerous colonic regions was performed based on the examination by the pathologist.

In the current study, the primary cultures of myofibroblasts were isolated using collagenase enzymatic treatment. The acquired colon tissue was washed thoroughly with sterile phosphate buffered saline (PBS) and any fat or debris were removed using a scalpel. The specimen was dissected into smaller sections and transferred into a solution of collagenase IV (1 mg/mL; Worthington, Biochemical Corporation) prepared in Dulbecco's Modified Eagle's Medium (DMEM) (Invitrogen, CA). The tissue was minced into tiny pieces before being transferred into a Bijou tube. Then, the mixture was put under agitation for 3 h using a magnetic stirrer at 37˚C in a humidified incubator. Next, the tissue suspension was passed through a 100 µM nylon mesh (Pierce Biotechnology Inc, Rockford, IL, USA) to remove tissue clumps. The cells were collected after centrifugation at 250 x g for 5 min and transferred in a 24-well plate allowing cell attachment and growth. To minimise the risks of contamination, myofibroblasts were cultured in DMEM medium supplemented with 10% fetal bovine serum (FBS), 100 U/mL penicillin and 100 µg/mL streptomycin, 2 mM L-glutamine,

1:100 of 250 µg/mL of amphotericin and 1:100 of 10 mg/mL of neomycin. The cells were split and transferred to a 6-well plate once they had reached confluency. Cryovial stocks of these cultures was produced at the earliest possible passage (passage 2). The established primary myofibroblasts from this study are Myo 7395, Myo 8835C, Myo 8836, Myo 8849, Myo 8852C, Myo 8853, Myo 8872C, Myo 8873, Myo 0164C and Myo 0165. Primary myofibroblasts (Myo 6526, Myo 6550 and Myo 6551C) previously established from our lab were also included in the study. The details of the primary myofibroblast cultures (eg. localization site of the tissue) are summarized in **Table 2.2**. Primary cultures, which have a limited lifespan of maximum passage number of 10, were used for the experiments. Throughout this thesis, the term 'primary myofibroblasts' refers to myofibroblasts established from surgical samples, although technically after the first passage, myofibroblasts maintained in culture could be considered as already myofibroblast line. This is based on the traditional definition whereby the first harvesting and subculture of the cell population isolated from a tissue results in the formation of a cell line (Freshney, R.I., 1987).

Myofibroblasts	Location	Type of tissue
Myo 6526	Sigmoid colon	Normal
Myo 6550[1]	Sigmoid colon	Normal
Myo 6551C[1]	Sigmoid colon	Cancer
Myo 7395	Sigmoid colon	Normal
Myo 8835[2]	Sigmoid colon	Normal
Myo 8836C[2]	Sigmoid colon	Cancer
Myo 8849	Ascending colon	Normal
Myo 8852C[3]	Rectum	Cancer
Myo 8853[3]	Sigmoid colon	Normal
Myo 8872C[4]	Ascending colon	Cancer
Myo 8873[4]	Ascending colon	Normal
Myo 0164C[5]	Caecum	Cancer
Myo 0165[5]	Ascending colon	Normal

Table 2.2

The primary myofibroblasts isolated from surgical samples.

Myofibroblasts from the same patient are given identical numbers following the cell line name.

2.2.3 Cell culture conditions

All CRC cells, myofibroblasts and fibroblasts were grown, unless otherwise indicated, in complete medium consisting of DMEM supplemented with 10% FBS, 100 U/mL penicillin and 100 µg/mL streptomycin antibiotic solution and 2 mM L-glutamine in either 25cm^2 or 75cm^2 tissue culture flasks. The cells were maintained in a humidified incubator (37˚C, 10% CO_2) and culture medium was replaced every 2 or 3 days.

2.2.4 Cell culture maintenance

Cells were maintained in flasks with complete DMEM and passaged when they reached 70-80% confluence. Cells were split into new flasks by discarding the old medium and washed with sterile PBS before detached by adding 2 mL of trypsin/EDTA solution (Lonza, USA) and incubating for 5 min at 37˚C. Then, 10 mL of complete medium were added to neutralize the trypsin. The cell suspension was mixed gently to break the cell clumps. Subsequently, the cells were spun at 250 x g for 5 min and the cell pellet was resuspended with complete medium. Depending on the cell line growth characteristics, the cell suspension was split at 1:5 to 1:20 dilution for CRC cell lines and at 1:3 dilution for myofibroblasts and skin fibroblasts.

2.2.5 Cell counting

Automated counting of the cells was performed using Cellometer Auto T4 (Nexcelom Biosciences, USA). To count the cells, 20 µL of the cell suspension was loaded into the cell counting chamber and inserted into the Cellometer. The software allows the cell count from eight different areas of the cell counting chamber and gives directly the cell concentration per millilitres.

2.2.6 Cryopreservation and retrieval of cells

For cell storage, CRC cells, myofibroblasts and fibroblasts which reached 80% confluence were washed with PBS and detached with trypsin/EDTA solution before being centrifuged at 250 x g for 5 min. Cell pellets were then re-suspended with freezing medium which consists of a solution of FBS containing 10% dimethyl sulfoxide (DMSO). The cell suspension was then transferred to a sterile cryovial (Corning, USA). The vial was placed in Mr Frosty freezing container (Thermo Fisher). The collected vials from the container then were transferred to a -80˚C freezer overnight and subsequently into a liquid nitrogen tank at -196˚C for long term storage.

To retrieve the cells, the frozen cryovial was thawed in a 37˚C water bath for 1 min. The cell suspension then was mixed with 10 mL of medium and centrifuged at 250 x g for 5 min. The cell pellets then were re-suspended with 10 mL of medium and transferred into a 25 cm^2 or 75cm^2 cell culture flask.

2.5 Cell proliferation and viability assays - (Calcein AM) staining

Staining using calcein-acetoxymethyl ester (Calcein AM) was performed to analyse the viability of the cells. Calcein-AM (BioLegend, USA), a non-fluorescent lipophilic ester, is able to penetrate cellular membranes where the diacetate groups are rapidly cleaved by nonspecific cytosolic esterases. This will produce calcein (a fluorochromic alcohol), among other products, that chelates labile iron under quenching of the green fluorescence (Tenopoulou et al., 2007). For microscope viability assays, cultures were incubated for 30 min at 37˚C with serum free medium containing calcein AM (stock concentration of 1 mM) at 1:1000 dilution. Cells were then observed using a fluorescence microscope (Axio Observer.Z1, Zeiss) and representative pictures were taken.

2.4 Cell proliferation assay

To study the influence of myofibroblasts on the proliferation of the CRC cells using co-culture conditions, 8 x 10^4 CRC cells was seeded on top of a confluent layer of 4 x 10^4 CCD-18Co seeded on Matrigel® Growth Factor Reduced (GFR) Basement Membrane Matrix, Phenol Red-Free (BD Biosciences, USA). A total of 100 µL Matrigel layer were diluted with an equal volume of serum free culture medium (DMEM) and added to a 24-well plate. Control groups of CRC cells or myofibroblasts alone on Matrigel layer were included. The CRC cells and myofibroblasts were respectively pre-labelled with cell linker; PKH67 (red) and PKH26 (green) (Sigma-Aldrich, UK). After one week of co-culture, the morphology and the growth of the CRC cells was observed using a fluorescence

microscope. Parallel experiments without Matrigel were also conducted to assess its efficiency and influence as a substrate.

2.5 Differentiation assays

Two *in vitro* assays were designed to study the CRC cells differentiation under co-culture conditions with myofibroblasts. The first assay involves combination of both CRC cells (LS180) and myofibroblasts (CCD-18Co) in Matrigel solution to be co-cultured in a plate. Cells were counted after trypsinization and filtered through 20 µm filters (Celltrics, Partec GmbH) to acquire a single-cell suspension. A total of 1 x 10^3 LS180 cells and 1 x 10^4 of CCD-18Co were mixed in 40 µL of an ice-cold 1:1 mixture of Matrigel and DMEM. The resulting cell suspension was seeded in a 96-well plate. The Matrigel was left to harden at 37°C for 30 min, and serum free culture medium was then added to the wells. The cells were cultured for 14 days, with medium changes every 3 days.

The second assay was performed by seeding CRC cells in a Matrigel suspension on a myofibroblast lawn. The CRC cell (1 x 10^3 LS180) suspension was mixed with 40 µl Matrigel diluted with serum free DMEM (1:1) and cultured on top of a CCD-18Co lawn. The myofibroblast lawn consists of 2 x 10^4 CCD-18Co seeded in a 96-well plate 48 h prior to adding the CRC and Matrigel layer. The plate was incubated at 37˚C, 10% CO_2 for 14 days before staining with 10 µg/mL 4′6-diamidino-2-phenylindole (DAPI) (Sigma) and F-actin. The differentiation of LS180 was observed using a fluorescence microscope.

Quantification of the lumen size and number was performed using ImageJ software.

2.5.1 F-actin staining

Prior to the staining, the old medium was discarded, and the cells were washed with PBS (2 x 5 min). A total of 100 µL of 4% (v/v) paraformaldehyde (PFA) (VWR Chemicals, France) in PBS was added to the plate for 20 minutes. Then, PFA was discarded and the plate was washed with PBS (3 x 5 min) before 100 µL of 0.2% Triton-X in PBS was added for 10 minutes. The fluid was removed, and the wells were washed with 50 mmol/L glycine in PBS for 4 times. Next, 100 µL TRITC-phalloidin (stock concentration of 200 U/mL) in PBS (1:1000) was added and the plate was incubated at 4°C overnight. The plate was then washed 3 times with PBS. Then, 100 µL of DAPI in PBS was added to each well. The formation of lumen which is indicated by the F-actin staining was analyzed using a fluorescence microscope.

2.6 Treatment with conditioned medium (CM)

2.6.1 Preparation of conditioned medium (CM) from CRC cells

CRC cells (RKO, HT29, SW480, SW620 and OXCO1) were cultured in complete DMEM at 37˚C, 10% CO_2 until reaching 60% confluence. Cells were washed twice with PBS and incubated with serum free DMEM for 48 h, after what the CM was collected. The CM was filtered to remove any cell debris and

use immediately for experiments or stored in aliquots at -20˚C for no longer than 2 weeks until use.

2.6.2 Treatment with CM from CRC cells

To study the effect of CM from epithelial cells on the expression of selected genes in myofibroblasts, CCD-18Co cells were seeded and incubated with CM from RKO, HT29, SW480, SW620 and OXCO1 cells or with serum free DMEM as the control. After 72 h of treatment, a cell pellet from each group was collected and washed with PBS. Total RNA was extracted, and quantification of gene expression was performed using qRT-PCR.

2.7 Migration assay – Transwell assay

To analyse the role of CRC cells as chemoattractant, 2 x 10^4 epithelial cells (RKO, HT29, and LS180) were seeded in a 24-well plate. After 48 h, the medium was discarded and replaced with 800 µL of DMEM + 0.5% FBS. A total of 1 x 10^4 CCD-18Co cells were added in a Transwell insert with 8.0 µm pores (Greiner Bio-One, Germany). The insert was then transferred to the wells containing epithelial cells or to a well containing only DMEM + 0.5% FBS as a control.

After 48 h of co-culture, the insert was removed and non-migrated myofibroblasts on the inside of the insert were scraped off gently using a cotton swab. The insert was then stained with Kwik-Diff kit (Thermo Fisher Scientific,

UK). The cells were fixed for 5 sec (5 x 1 sec in fixative solution) followed by staining with eosin for 30 sec and methylene blue for 10 sec (5 x 2 sec). Then, the insert was rinsed with distilled water to remove excess staining solution and air-dried overnight. Migrated cells were examined using the EVOS® XL core microscope (Life Technologies, USA). A total of 5 fields were chosen randomly from an insert and the total of migrated cells was quantified using ImageJ software. Experiments were conducted in triplicate. The same methodology was used to study the migration of epithelial cells in co-culture conditions with myofibroblasts. In this experiment, myofibroblasts were cultured in the bottom chamber and epithelial cells were seeded in the upper chamber (Transwell insert).

2.8 Invasion assay

A total of 1 x 10^4 epithelial cells and 5 x 10^3 myofibroblasts or fibroblasts were separately mixed with a cold 1:1 mixture of Matrigel and DMEM serum free medium. Then, 3 µL of the Matrigel: cells solution was added to a single 48-well plate, forming a blob of cells, where for co-culture experiments, two individual blobs of epithelial cells and either myofibroblasts or fibroblasts are seeded apart from each other in the same well. For controls (monoculture), empty Matrigel blobs (50% Matrigel and serum free DMEM blob without any cells) were included in the same well with either epithelial cell, myofibroblast or fibroblast blobs. The plate was placed at 37˚C, 10% CO_2 until the gel hardened. Next, pure Matrigel was added to the well, to cover the area surrounding the blobs followed by an additional step of solidification of the Matrigel layer. Then, 300 µL

of serum free DMEM were added to the well and the plate was incubated in a humidified incubator. After 5 days of co-culture, cells were stained with 100 µL of Calcein AM labelling (1 µM) and 100 µL of DAPI (10 ng/mL). The cells were visualized using a fluorescence microscope. The assessment of lumen formation in LS180 was conducted at Day 7 using F-actin staining. The distance covered by invaded myofibroblasts and fibroblasts from triplicate experiments was measured using ImageJ software and compared to the control. The experimental layout of this assay is shown in **Figure 2.1**.

(A)

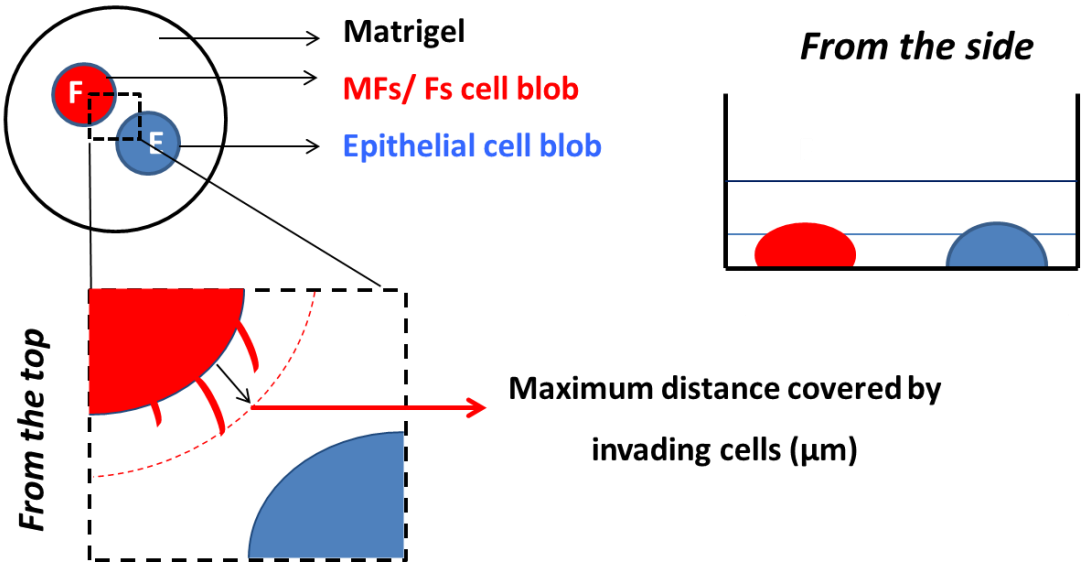

(B)

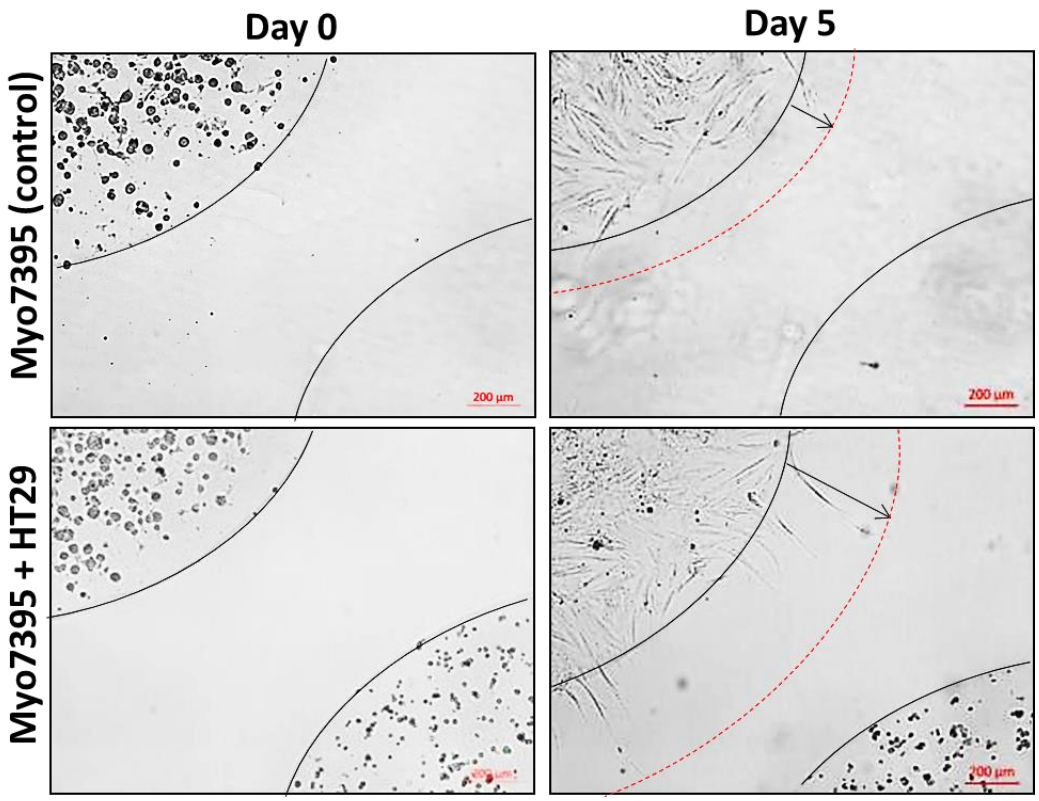

Figure 2.1

The Matrigel based blob invasion assay.

The experimental layout is illustrated in (A). An example of the quantification for the invasion assay is shown in (B). The boundary of each blob (either an empty blob or blob containing cells) is indicated by the black curved line. On day 0, the cells in the blob appear rounder and no invasion of cells out of the blob was found. After 5 days of experiment, myofibroblasts invaded the Matrigel layer which surrounds the Matrigel blobs. The red dotted line indicates the maximum distance of myofibroblast invasion (µm) from the edge of the Matrigel blob containing cells at the end of the experiment (Magnification: 5x) (MFs: myofibroblasts; Fs: fibroblasts).

2.9 Growth factor treatment

To study the influence of growth factors on differentially expressed genes in myofibroblasts, a screen using eight candidate growth factors was performed. The selected growth factors were transforming growth factor beta 1 (TGFβ1), epidermal growth factor (EGF), tumour necrosis factor-alpha (TNFα), basic fibroblast growth factor (FGF-β), hepatocyte growth factor (HGF), vascular endothelial growth factor (VEGF), platelet derived growth factor-AA (PDGF-AA), platelet derived growth factor-CC (PDGF-CC) and insulin-like growth factor 1 (IGF1). All the growth factor solutions were prepared using serum free culture medium (DMEM). **Table 2.3** shows the information for each growth factor used in the screening.

Growth factor	Working concentration	Source
TGFβ1	10 ng/mL	PeproTech
EGF	3 ng/mL	PeproTech
TNFα	20 ng/mL	Bio-Vision
FGF-β	1 ng/mL	Lonza
HGF	50 ng/mL	PeproTech
VEGF	20 ng/mL	Invitrogen
PDGF-AA	100 ng/mL	PeproTech
PDGF-CC	50 ng/mL	PeproTech
IGF1	40 ng/mL	Invitrogen

Table 2.3

Respective working concentrations and suppliers for the selected growth factors used in screening.

2.9.1 Blocking of EGFR

The specificity of EGF effects on the regulation of AOC3 in myofibroblasts was tested using an anti-EGF-receptor (EGFR) recombinant monoclonal antibody (cetuximab, clone C225, Merck). Selective binding of cetuximab to EGFR lead to competitive inhibition of endogenous ligand binding resulting in the inhibition of the associated downstream signalling (Mendelsohn and Baselga, 2003).

In this experiment, CCD-18Co was seeded in a 6-well plate and left to attach overnight in DMEM + 10% FBS. The cells then were incubated for 24 h in serum free medium. Next, the cells were pre-treated with cetuximab at 10 µg/mL for either 1 or 3 h before incubation with EGF for 72 h in serum free DMEM. Controls of cetuximab or EGF alone, diluted in serum free medium were included in the test. The experiment was repeated with a primary myofibroblast line – Myo 7395. Similar experimental setups using two monoclonal blocking antibodies to HER2 (a family of EGFR family), namely Trastuzumab and Pertuzumab (Roche, UK) (both at 20 µg/mL) also were performed. Cells were harvested for RNA extraction and subsequently analysed for AOC3 expression using qRT-PCR and western blots.

2.10 RNA methods

2.10.1 RNA extraction

Total RNA was extracted from cells using the RNeasy (Qiagen, USA) kit following the manufacturer's instructions. Prior to the RNA extraction, cells were washed with PBS and then 350 µl lysis buffer RLT was added. The cell lysates were left for 1 min to homogenize and diluted with 350 µL of 70% ethanol. Diluted samples were transferred into a RNeasy Mini spin column and centrifuged for 15 sec. The column was then washed with 700 µl RW1 buffer. The column was spun for 15 sec before 500 µL of wash buffer RPE was added twice to it. Total RNA was eluted with 40 µL of nuclease-free water. The quantification of the extracted RNA was done using Nano-Drop spectrophotometry. The RNA was stored at -20˚C until use.

2.10.2 Reverse transcription

Synthesis of the complementary DNA (cDNA) from RNA was performed using High Capacity cDNA Reverse Transcription kits (Applied Biosystems Inc., CA) according the manufacturer's instructions. Briefly, 10 ng/µL of diluted RNA was mixed with 10X RT buffer, 25X dNTP mix, 10X RT random primers, multiscribe transcriptase and RNAse free water. Reverse transcription was performed by using the thermal cycler and the optimized protocol; 25˚C for 10 min, 37˚C for 120 min and 85˚C for 5 min.

2.10.3 Gene expression analysis – Quantitative real-time PCR (qRT-PCR)

TaqMan® Gene Expression Assay, 20X FAM dye-labeled kit was used for the quantification of mRNA where pre-designed, manufacturer-validated primers and probes of genes of interests were added to the cDNA. The details of the TaqMan probes used in this study are shown in **Table 2.4**.

Target	Reference	Source
AOC3	Hs02560271_s1	Applied Biosystems
NKX2-3	Hs00414553_g1	Applied Biosystems
ACTA2	Hs00426835_g1	Applied Biosystems
FAP	Hs00990791_m1	Applied Biosystems
LRRC17	Hs00957873_m1	Applied Biosystems
SHOX2	Hs00243203_m1	Applied Biosystems
UBC	Hs00824723_m1	Applied Biosystems

Table 2.4
Summary of 20X TaqMan Gene Expression Assays details used in this thesis.

Briefly, cDNA was mixed with 20X TaqMan® Gene Expression Assay, 2X TaqMan® Universal PCR Master mix and nuclease-free water to make up the final volume of 20 µL/ reaction in MicroAmp Fast Optical 96-well Reaction plates (Life Technologies, USA) sealed with MicroAmp optical adhesive film (Life Technologies, USA). The samples then were run for qRT-PCR using a 7500 Fast Real Time PCR Systems machine (Applied Biosystems). Experiments were conducted in triplicate. The Ct values of the mRNA were normalized to a selected housekeeping gene – *ubiquitin C* (*UBC*) by using the comparative Ct method. The converted ∆Ct mean values of treatment groups were compared to the control. The calculation involved as follow:

Cycle threshold: Ct

$\Delta Ct = Ct_{Target} - Ct_{reference}$

The mean ΔCt was calculated from three independent experiments

Converted ΔCt mean value = $2^{(n - Mean\ \Delta Ct)}$

Where n = Arbitrary value greater than the highest ΔCt mean value

Rather than using the standard ΔΔCt method, which involves comparison to an arbitrarily identified reference sample, the actual ΔCt mean linear value was used. Since ΔCt is inversely proportional to the initial amounts of mRNAs, the ΔCt values were converted by deducting them from the highest (arbitrary) ΔCt value represented from the same experiment and converting these resulting values to a linear scale from a logarithmic value.

2.11 Protein Methods

2.11.1 Protein lysate preparation

Cells were cultured in 75 cm^2 cell culture flask until 70-80% confluence. Next, the cells were washed with ice cold PBS, then the cell were lysed with 100-500 µL radioimmunoprecipitation assay (RIPA) or lysis buffer (1% Nonidet P-40, 0.5% nordeoxycholate, 150 mM sodium chloride, 50 mM Tris base, pH 8.3) with protease inhibitor cocktail (Complete Protease Inhibitor Cocktail tablets, Roche,

Switzerland). The cells were kept on ice for 30 min with regular vortexing every 5-10 min followed by centrifugation at maximum speed 20000 x g (12000 rpm) for 20 min at 4˚C. Total cell lysate (supernatant) was collected and transferred into a new microfuge tube and stored at -20˚C until use. The pellet which consists of the cell debris was discarded.

2.11.2 BCA assay

The bicinchoninic acid colorimetric assay (BCA™ Protein Assay) (Pierce Chemical Company, USA) was used to determine the total concentration of protein in the protein lysate. The principle for this assay depends on the conversion of Cu^{2+} to Cu^{+} in an alkaline solution whereby the Cu^{+} will be detected by the BCA. This reaction results in the formation of purple colour. The protein concentration was measured spectrophotometrically by comparison with known standards. Protein standards at different working concentrations (0-2000 µg/mL) were prepared by diluting a vial of Albumin Standard (2 mg/mL, Pierce Chemical Company, USA) in lysis buffer. The BCA working reagent was prepared combining BCA solution A and B (50:1). A total of 200 µL of the working solution then was mixed with 25 µL of protein standards or the protein lysate of the sample in a 96-well plate. The microplate was incubated at 37˚C for 30 min and followed by absorbance reading at 562 nm using a plate reader (µQuant, Bio-Tek Instrument, USA). The absorbance value of the sample was extrapolated from the generated standard curve to derive the protein concentration.

2.12 Western blot

2.12.1 SDS poly-acrylamide gel electrophoresis

Electrophoresis of the protein samples was performed using a Mini-PROTEAN® vertical electrophoresis unit (Bio-Rad, USA). A total of 30 µg of protein was mixed with 5X sample buffer (16% (v/v) of 2 mM Tris HCl (pH 6.8), 50% (v/v) glycerol, bromophenol blue without 2-mercaptoethanol) before being spun for a few sec. The sample mixture then was loaded into each lane of the gel. The percentage of the gel to be run was determined by the size of the target protein (eg. AOC3 which is approximately 150 kDa and NKX2-3 at 39 kDa require a 10% and 12% gel respectively). A pre-stained rainbow molecular weight marker was included during the electrophoresis. The samples were stacked in a 4% upper gel and then resolved in a 10 or 12% separating gel at 90 V for approximately 2.5 h in 1X SDS running buffer (25 mM Tris base, 19.2 mM glycine and 0.1% SDS). The SDS gel was removed from the glass plate after the completion of the electrophoresis and submerged in semi-dry transfer buffer for a few min before immunoblotting.

2.12.2 Immunoblotting

For the transfer of the protein, polyvinylidene difluoride (PVDF) membrane (Amersham Biosciences, USA) was used. The membrane was activated by soaking in 100% methanol solution for 1 min and rinsed once in transfer buffer. Semi dry electrophoresis transfer method was applied whereby the proteins

were transferred to the PVDF membrane in semi dry transfer buffer (20% (v/v) methanol, 7.2 g glycine and 25% (v/v) ml Tris, pH: 7.5) at 12 V for 2 h. After the transfer, the membrane was stained with Ponceau S (0.1% (w/v) Ponceau S in 5% (v/v) acetic acid) to visualize the protein. The membrane then was washed 3x in distilled water for 5 min. Next, the membrane was submerged in blocking solution of 1% w/v bovine serum albumin (BSA in PBS for 40 min at room temperature on a rocking platform. The membrane was then incubated with primary antibody in blocking solution overnight at 4˚C before being washed for 15 min, 3 times with 1x TBS-T (Tris buffered saline, 0.1% Tween 20). Then, the membrane was incubated with secondary antibody for 2 h at room temperature before washing again (3 times for 15 min washing) with TBS-T solution. To detect the bands, the membrane was incubated with ECL Prime Western Blotting Detection System solution (GE Healthcare, UK) for 5 min and the blot was exposed to a film (Fujifilm Corporation, Japan). The film was developed in a dark room using a film processor.

2.13 Nuclear and cytoplasmic fraction preparation

Localization of AOC3 and NKX2-3 in the myofibroblasts was determined through the preparation of cytoplasmic and nuclear extracts from CCD-18Co using the Thermo Scientific™ NE-PER™ Nuclear and Cytoplasmic Extraction Reagents (Pierce Biotechnology, USA). Sub-confluence CCD-18Co cells were washed with PBS after harvesting and then spun at 500 x g for 3 min. Supernatant was removed and 100 µL of ice-cold CER I solution was mixed with the cell pellet. Then, the cell suspension was vortexed for 15 seconds followed by incubation

on ice for 10 min. Next, 5.5 µL of ice-cold CER II was added and the tube was vortexed for 5 sec and incubate on ice for 1 min. The tube was vortexed again for 5 sec and centrifuged for 5 min at 16000 x g. The supernatant (cytoplasmic extract) was transferred to a pre-chilled centrifuge tube and kept on ice. A total of 100 µL of NER was added to suspend the pellet, which contained nuclei. After vortex for 15 sec every 10 min for 40 min and centrifuged at 16000 x g, the supernatant (nuclear extract) was transferred to a pre-chilled tube. Both cytoplasmic and nuclear extracts were kept at -80˚C till use.

2.14 Immunofluorescence (IF) staining

For immunofluorescence staining, a total of 1 x 10^3 of myofibroblasts or 2 x 10^3 of CRC cells were seeded in 96-well plate. The cells were incubated in complete DMEM for 2 days before the staining. Prior to the staining, the cells were washed twice with PBS. For fixed staining, the cells were fixed either with 4% (v/v) PFA for 10 min at room temperature (RT) or with ice-cold methanol for 10 min at 4˚C. Live staining for AOC3 did not involve any fixation or permeabilization step. The fixed cells were permeabilized with 0.2% Triton in PBS solution for 10 min at RT before incubated with blocking solution (PBS + 2% FBS) for 30 min. The primary antibody containing solution diluted with washing buffer (PBS + 2% FBS) was added to the wells and the cells were kept at 4˚C for overnight. Next, the cells were washed with PBS (3 x 10 min) followed by incubation with secondary antibody for 1 h at RT. After washing with PBS, the cells were stained with DAPI (1: 10000) for 5 min. The staining was examined with fluorescence microscope

2.15 Flow cytometry

CCD-18Co cells were cultured to confluence then washed with PBS. Non-enzymatic Cell Dissociation Solution 1x (C5914, Sigma) was added to detach the cells and the cell suspension was centrifuged. The cell pellet was suspended in an adequate volume of wash buffer (PBS + 2% FBS) in a pre-labelled tube. The primary antibody (EGFR conjugated with Phycoerythrin) (Abcam, UK) or the isotype control was added to the cell suspension and the tube was incubated on ice for 45 min before washing buffer was added and the tube centrifuged at 250 x g for 5 min at 4˚C. Supernatant was discarded and the tube was tapped slightly to homogenize the cell pellet. Cells were re-suspended in wash buffer with DAPI (1:10000) for 10 min before being analysed using the Dako Cytomation CyAn ADP Flow Cytometer (Dako).

2.16 Immunohistochemistry (IHC) staining on (formalin-fixed paraffin-embedded) FFPE sections

For IHC staining, FFPE slides of the parental tumour were acquired from the BioBank, Oxford University Hospital. The correspond slides used for the staining were pairs of normal and tumour colon tissue, listed in **Table 2.5**. The slides were deparaffinized with Histo-Clear solution (National Diagnostics, UK) for 5 min (twice) and the slides were submerged in 100% ethanol solution for 5 min. Next, the slides were re-hydrated with 100% IMS (industrialized methylated spirit) solution (5 min) followed by 90% IMS (5 min), 70% IMS (2 min) and 70% IMS (2 min). Then, the slides were rinsed with PBS. Next, an antigen retrieval

step was performed by heating the slides at 100˚C for 20 min in a solution of EDTA (1mM, pH 8) and then cooled for 1 h at room temperature. The slides were washed with PBST (2 x 5 min) followed by blocking for 30 min with PBS + 2% FBS. Primary antibody diluted in PBS + 2% FBS was added to the slides and incubated overnight at 4˚C. The slides were washed with PBS (2 x 5 min) then stained with secondary antibody (dilution of 1: 150) for 1 h at room temperature. After washing with PBS, the slides were stained with DAPI (1: 10000, 10 min at RT). Vectashield solution was added and a coverslip was mounted on each slide. The staining was observed using a fluorescence microscope.

Myofibroblasts	Type of tissue
Myo 8835	Normal
Myo 8836C	Cancer
Myo 8852C	Cancer
Myo 8853	Normal
Myo 8872C	Cancer
Myo 8873	Normal

Table 2.5

The formalin-fixed paraffin embedded (FFPE) slides of parental tumour for IHC staining.

2.17 Antibodies

The details of antibodies used for western blot, immunofluorescence and immunohistochemistry are summarized in **Table 2.6**. Secondary antibodies were purchased from Life Technologies (USA) or DAKO (USA).

(A)

Antibody	Species	Supplier	Catalog number	Dilution/ Concentration
VAP-1 (TK8-14)	Mouse monoclonal IgG_{2a}	Santa Cruz	Sc-33670	WB 1:500 IF 1: 100 IHC 1: 50
NKX2-3	Rabbit polyclonal IgG	LSBio	LS-C30713	WB 1:1000 IF 1:100 IHC 1: 250
Fibroblast activation protein (FAP) (F19)	Mouse monoclonal	Olivia Newton-John Cancer Research Institute	-	WB: 5 µg/mL
Alpha smooth muscle actin (αSMA) (1A4)	Mouse monoclonal IgG_{2a}	Sigma	A 2547	WB 1:500 IF: 1:400 IHC: 1: 800
EpCAM (AUA1)	Mouse monoclonal	In house	-	IF: 1:100
Lamin A/C (4C11)	Mouse monoclonal IgG_{2a}	Cell Signaling	4777S	WB 1: 2000
Myosin heavy chain 11 (MYH11) (ID8)	Mouse monoclonal IgG_1	Santa Cruz	sc-65733	IF 1:250
β-tubulin (TUB 2.1)	Mouse monoclonal IgG_1	Sigma	T5201	WB 1: 5000
β-actin (AC-15)	Mouse monoclonal IgG1	Sigma	A5441	WB 1: 5000
α-tubulin (DM1A)	Mouse monoclonal IgG1	Abcam	ab7291	WB: 1: 5000

(B)

Method	Secondary antibody	Dilution	Supplier
Western blot	Goat anti-mouse (GAM)	1: 10000	Dako
	Swine anti-rabbit (SAR)	1: 10000	
	Rabbit anti-mouse (RAM)	1: 20000	
Immunofluorescence and immunohistochemistry staining	Alexa Fluor goat anti-mouse (GAM)-488	1: 200	Life Technologies
	Alexa Fluor donkey anti-rabbit (DAR)-555	1: 150	

Table 2.6

Antibody dilutions used in this study.

(A) The dilutions of primary antibodies used in this study. The list of secondary antibodies is shown in (B).

2.18 Transient siRNA transfection

Direct transfection was performed using Oligofectamine transfection reagent (Life Technologies, USA) to deliver short interfering RNAs (siRNAs) into myofibroblasts. Pre-designed siRNAs were purchased from GE Healthcare Dharmacon (USA). The target sequence of each siRNA is shown in **Table 2.7**.

siRNA	Catalog number	Concentration	Target Sequence
siGENOME SMARTpool siRNA Human AOC3	D-010143-01	5 nmol	CCACCUUGCUCAACUAUGA
siGENOME SMARTpool siRNA Human NKX2-3	D-016090-01	5 nmol	GGACAAGUCUCUGGAGCUU

Table 2.7

Details of the siRNAs used in the thesis.

Cells were seeded in 24-well or 6-well plates one day before the transfection in DMEM + 10% FBS without antibiotics. For the transfection in a 24-well plate format, 2.5 µL of 20 µM of the siRNA stock is diluted with 40 µL of serum free Opti-MEM® (Life Technologies, USA). This mixture then was added to the solution consisting of 2 µL Oligofectamine and 7.5 µL of serum free Opti-MEM followed by 20 min incubation at room temperature. As for the 6-well plate format, the siRNA complex comprised of 10 µL of 20 µM of siRNA stock solution in 40 µL of DMEM which is added to 4 µL Oligofectamine in 15 µL of DMEM. This siRNA complex was added to the cells and incubated at 37˚C for 4 h before DMEM containing 3X of the normal serum concentration was added. The transfection efficiency was evaluated after 24, 48 and 72 h post-transfection. Control groups of cells treated with scrambled RNA and untreated cells were included.

2.19 Senescence-associated beta-galactosidase staining

The senescence beta-galactosidase staining kit from Cell Signaling Technology (USA) was used to assess cell senescence. A total of 5 x 10^3 of myofibroblasts were seeded in a 24-well plate for 2 days until 50% confluence in complete medium Cells were then rinsed once with 1 mL of PBS and fixed for 15 min with a fixative (1X) solution provided in the kit. Next, the plate was rinsed twice with PBS before 1 mL of pH 6 beta-galactosidase staining solution (combination of 1X staining solution, 1X solution A, 1X solution B and 1 mg/mL X-gal stock solution) was added to the cells. The plate was sealed with parafilm to avoid evaporation. Next, the plate was incubated in a dry incubator without CO_2 for at least 18 h. The presence of CO_2 might alter the pH of the solution thus affecting the staining results. CCD-18CO at a very late passage (passage 21) were used as a positive control. Staining of the senescent cells is characterised by a dark blue green colour and was examined with light microscopy.

2.20 Serum free chemically-defined culture medium

To study the specific growth factors supporting the growth and attachment of myofibroblasts, a serum free chemically-defined medium was designed based on the medium formulation of PPRF-msc6 medium (Jung et al., 2010) (**Table 2.8**).

Component	Concentration
DMEM/Ham's F12 with glutamine	1X
Chemically defined lipid concentrate	0.1% v/v
Sodium bicarbonate	20.5 mM
HEPES	4.9 mM
Bovine insulin	4.01 µM
Human transferrin	0.318 mM
Putrescine dihydrochloride	55.9 µM
Sodium selenite	27 nM
Progesterone	0.018 µM
Heparin	0.7 U/mL
FGFβ	2 ng/mL
TGFβ1	1 ng/mL
Ascorbic acid	50 µg/mL
Fetuin	1 g/L
Hydrocorstisone	100 nM

Table 2.8

Components of the PPRF-msc6 medium.

Several components from the PPRF-msc6 medium formulation were selected to make a modified version of the original medium which was called modified PPRF medium (**Table 2.9**). This medium was then further optimized to make the final formulation of a serum free chemically defined medium which was then renamed as NEW medium.

Components	Concentrations	Company
DMEM F12 with GluTAMAX	1X	Life Technologies
FGFβ	2 ng/mL	Cell Guidance System
L-ascorbic acid-2-phosphate magnesium salt	50 µg/mL	Santa Cruz Biotech
Hydrocortisone	100 nM	Sigma
Fetuin	1.0 g/L	MP Biomedicals
Chemically defined lipid concentrates	0.1 % (v/v)	Life Technologies
TGFβ1	1 ng/mL	Peprotech

Table 2.9

Individual components of modified PPRF medium.

In the initial stage of medium development, the influence of modified PPRF medium on the growth of myofibroblasts was tested. A total of 5 x 10^2 CCD-18Co were seeded in complete DMEM (DMEM + 10% FBS) in a 24-well plate and left in the humidified incubator for overnight to allow cell attachment. The medium was then discarded and replaced with either modified PPRF medium, complete medium with addition of serum or basal medium alone (control group). CRC cells (HT29) and skin fibroblasts were also included in the comparisons to analyse the effect of the modified PPRF medium on cancer cells and normal fibroblasts' growth respectively (see Chapter 5).

The second stage of the experiment involved testing collagen type I as a substrate for direct seeding and culture of myofibroblasts using modified PPRF medium. The effect of collagen coating was studied by using collagen type I from rat tail (stock concentration: 3.6 mg/mL). The collagen was diluted using 17.5 mM acetic acid according to calculated concentrations:

$$C_{collagen}\ [\mu g/mL] = (A_{coating}\ [cm^2] \times 5\ \mu g/\ cm^2)/\ V\ [mL]$$

A 24-well plate was pre-coated with 1 mL of 20 µg/mL of collagen type I and incubated at 37˚C for 1 h. The plate was rinsed once with PBS and air-dried in the culture hood. CCD-18Co was then seeded in the pre-coated well with o8modified PPRF medium.

Modified PPRF medium was further optimized by omitting TGFβ1 from its formulation as previous data had shown its effect on the expression of AOC3 in myofibroblasts. The final formulation of this medium was then renamed as NEW medium. Each component of the NEW medium and their sources are listed in **Table 2.10.**

Components	Concentrations	Company
DMEM F12 with GluTAMAX	1X	Life Technologies
FGFβ	2 ng/mL	Cell Guidance System
L-ascorbic acid-2-phosphate magnesium salt	50 µg/mL	Santa Cruz Biotech
Hydrocortisone	100 nM	Sigma
Fetuin	1.0 g/L	MP Biomedicals
Chemically defined lipid concentrates	0.1 % (v/v)	Life Technologies

Table 2.10

Concentrations of the individual components in the NEW medium.

The influence of NEW medium on myofibroblasts (CCD-18Co, Myo 8873, Myo 0164C and Myo 0165) and a panel of CRC cell lines was evaluated where these cells were seeded on collagen type I coated plates and maintained in NEW

medium for 6 days. Calcein AM staining was performed to assess viability of the tested cell lines at the end of the experiment.

The NEW medium also was tested for the co-culture maintenance of myofibroblasts and CRC cell lines. In this experiment, CCD-18Co and CRC cell lines (HT29 or LS180) were mixed together in NEW medium and seeded on top of collagen coated plates. Cells were maintained for 6 days before stained for AUA1 and vimentin. Controls of monoculture (either myofibroblasts or CRC cell lines only) were included in the experiment.

2.22 Statistical methods

2.22.1 General data analysis

The data in this thesis were represented by the mean values ± standard error mean (SEM), assuming a normal distribution for the data. The p-values were calculated using an independent t-test, using the biological replicates (Microsoft Excel, Microsoft Corporation, USA). For statistical comparisons, p-value of less than 0.05 ($p<0.05$) was denoted by *, and $p<0.001$ was by **.

2.22.2 Microarray data analyses

Microarray data of the CRC cell line panel as well as from myofibroblasts and fibroblasts were obtained in Walter Bodmer's laboratory by sending RNA samples to the Paterson Institute for Cancer Research in Manchester for gene

expression analysis. The Human Genome Affymetrix GeneChip U133 plus 2.0 array was used to determine expression levels of 54,675 probe sets (covering 20,741 unique genes). The expression profiles between myofibroblasts and fibroblasts were compared using the Partek genomic suite (Partek, St Louis, Missouri, USA). Step-up correction for multiple testing was used (with a Benjamini and Hochberg step-up false discovery rate-corrected *p* value cut-off of 0.05) for genes with significant differential expression. The data on differentially expressed genes between normal skin fibroblasts and myofibroblasts described in this thesis are based on a previous article by Hsia et al. (2016) and have been deposited in the Gene Expression Omnibus (GEO) database, www.ncbi.nlm.nih.gov/geo (accession no. GSE77474).

CHAPTER 3

IN VITRO STUDIES OF THE INTERACTIONS BETWEEN MYOFIBROBLASTS AND COLORECTAL CANCER (CRC) CELL LINES

CHAPTER 3: *IN VITRO* STUDIES OF THE INTERACTIONS BETWEEN MYOFIBROBLASTS AND COLORECTAL CANCER (CRC) CELL LINES

3.1 Introduction

Bidirectional communications between CRC cells and myofibroblasts can be evaluated through *in vitro* co-culture conditions. The interactions between these two cell types may affect cell proliferation, migration, invasion and differentiation. Robust and valid *in vitro* assays need to be designed to determine the nature of these interactions. In this chapter, the influence of co-culture of myofibroblasts and CRC cells is discussed using various *in vitro* tests such as direct co-culture, Transwell assay and Matrigel-based experiments. Epithelial cells from several different cell lines and different lines of myofibroblasts were selected to assess the variations between different types of cells.

To address the influence of co-incubation on cell proliferation, we have chosen to use a direct co-culture method. The epithelial cells' differentiation also was assessed under co-incubation with CCD-18Co. Migration activity of myofibroblasts and CRC cells was studied using a Transwell assay, also known as the modified Boyden chamber. Subsequently, a Matrigel based invasion assay was designed to evaluate the invasion of myofibroblasts in the presence of epithelial cells. Matrigel was used in this assay to mimic the ECM in *in vivo* conditions. Several myofibroblasts and normal skin fibroblasts were included to compare the invasiveness of these cells under similar experimental conditions.

3.2 Results

3.2.1 Direct co-culture

The effect of the co-culture of CRC cells and myofibroblasts grown on either a Matrigel layer or normal culture plates without any Matrigel coating was analysed. **Figure 3.1** shows representative images of HT29 maintained in the presence of CCD-18Co under serum free conditions. PKH26-labelled HT29 (green) shows greater proliferation in co-culture with myofibroblasts (CCD-18Co labelled with PKH67, red) where bigger colonies were formed when compared to HT29 alone. This effect was more striking when both cells were grown on 1:1 Matrigel and DMEM (serum free) substrate (50% Matrigel) than on uncoated plates, where significantly smaller colonies of HT29 were observed. Similar observations were made with CCD-18Co where the myofibroblasts were growing at an optimum rate on a Matrigel layer in comparison to an uncoated surface (plastic). This finding proves that Matrigel acts as an efficient scaffold for cells to grow on. Quantification of the HT29 colony size, represented by total surface area covered by HT29, in monoculture and co-culture condition, either seeded on top of 50% Matrigel or plastic alone, performed using ImageJ software is shown in **Figure 3.1**.

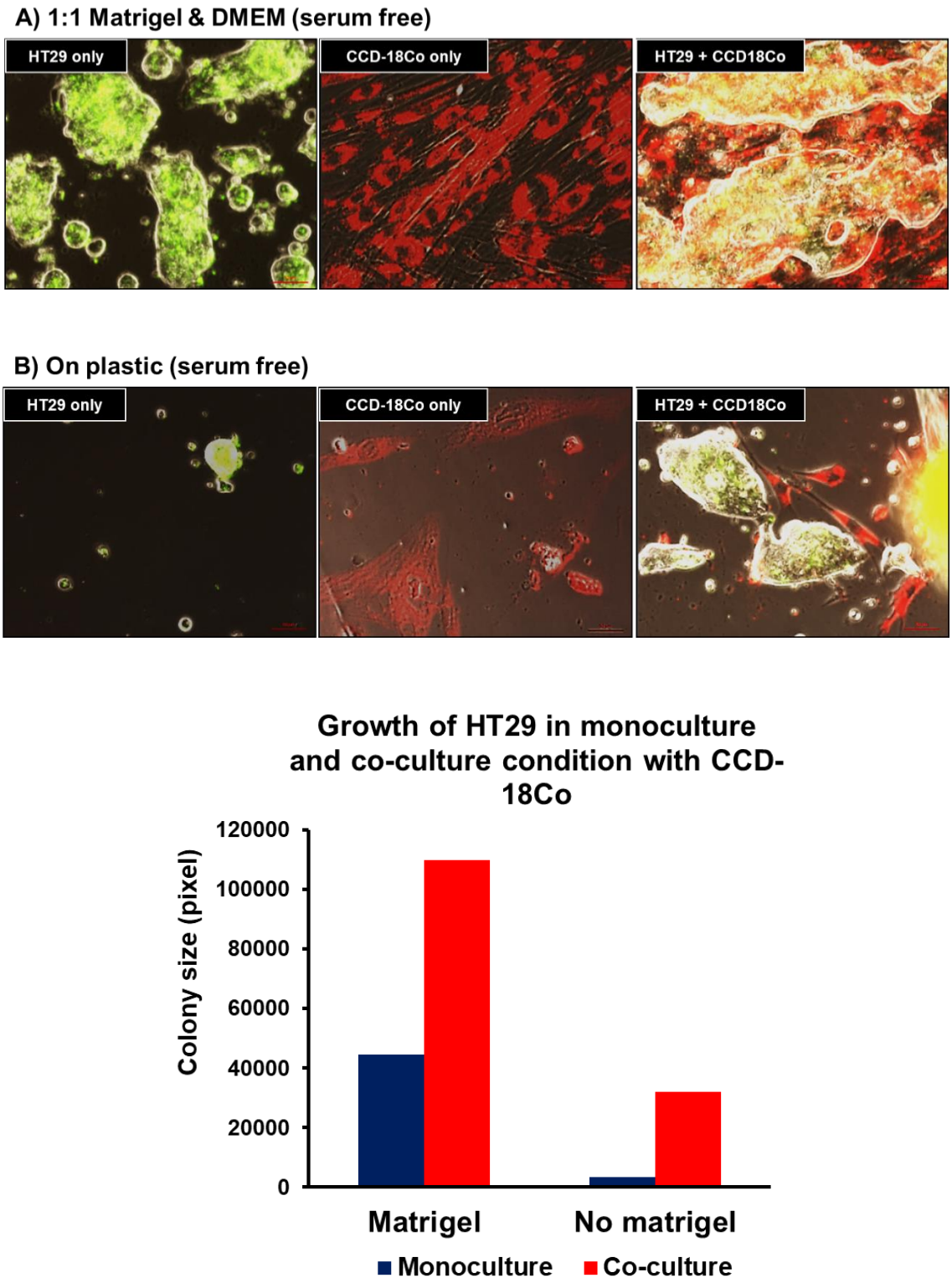

Figure 3.1

Co-culture of CCD-18Co with HT29 on (A) 1:1 Matrigel and DMEM (serum free) substrate and (B) uncoated surface (plastic).

Co-culture with CCD-18Co (PKH67 – Red) supports the growth of HT29 (PKH26 – Green). (A) Matrigel acts as a substrate and facilitates the proliferation of the HT29 cells. (B) The cells grew poorly after 8 days without serum, as seen for HT29 seeded on plastic alone. This is in agreement with Huschtscha et al., (1991) where it is stated that HT29 requires a coating (FBS coated) as one of the requirements to grow (Magnification: 20x) (Scale bar: 20 μm). Higher value of the total area covered by cells in a field, quantified using ImageJ software from a single experiment corresponds to greater colony size.

Similar co-culture experiments using a 50% Matrigel substrate were repeated with LS180 and RKO. As shown in **Figure 3.2**, there was an increase in the proliferation of LS180 in co-culture with CCD-18Co when compared to LS180 alone. This was illustrated by the bigger colonies and lumen size formed by LS180 grown in the presence of CCD-18Co. The LS180 colonies also appeared to be more flattened when compared to monoculture. RKO also grew better in the presence of CCD-18Co when compared with RKO alone. Quantitative analysis for this experiment is not performed as the it was difficult to define a surface area that is covered by CCD-18Co, both in monoculture and co-culture.

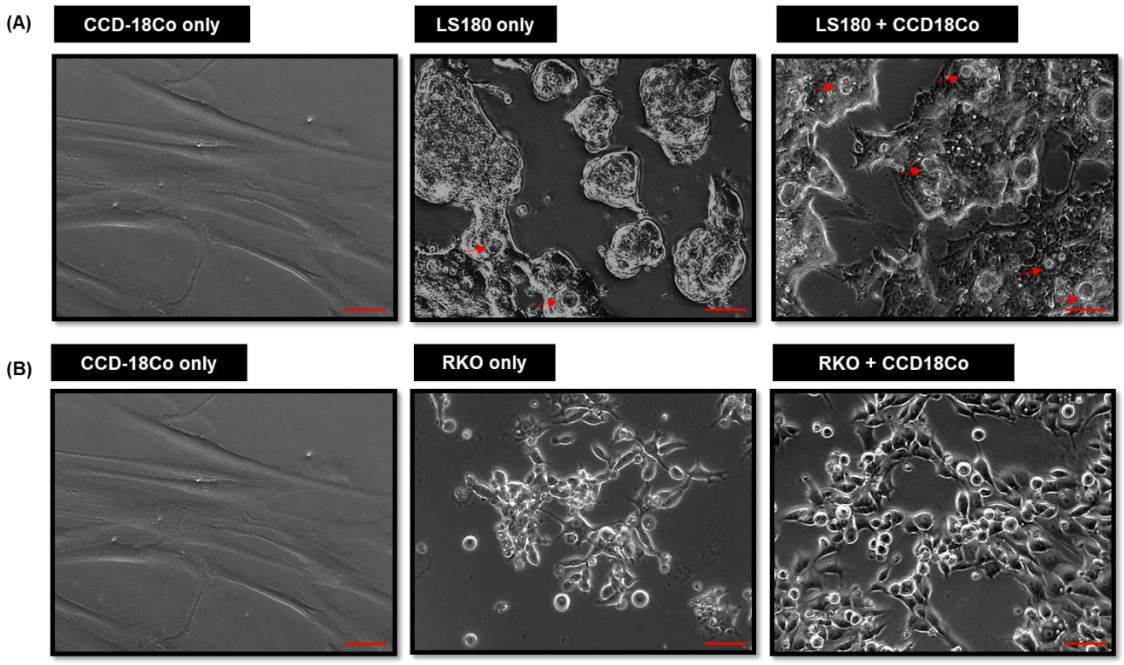

Figure 3.2

Co-culture of CCD-18Co with CRC cell lines (RKO and LS180) on 1:1 Matrigel and DMEM (serum free) substrate.

The growth of CRC cell line was significantly increased in co-culture with CCD-18Co after 8 days of incubation with serum free medium. Significant lumen formation was observed in co-culture of LS180 + CCD-18Co (shown by arrows) as compared to monoculture (LS180 alone) (Magnification: 20x) (Scale bar: 20 μm).

The effect of full Matrigel as a substrate for cells also was tested. For this experiment, either LS180 and RKO was co-cultured with CCD-18Co on a 100% Matrigel layer. **Figure 3.3** shows that a pure Matrigel layer was inefficient for the cell growth as compared to 50% Matrigel. This is indicated by the lack of cell proliferation, both for CCD-18Co and CRC cells, where the cells clumped together instead of spreading and attaching to the surface. A positive effect of the co-culture on the growth of RKO was observed where bigger 'islands' of cells were formed in RKO + CCD-18Co when compared to monoculture (RKO alone). The total area covered by cells was quantified using ImageJ software.

As seen in all direct co-culture of CRC cells and myofibroblasts, the effect on the growth of myofibroblasts after culturing together with CRC cells was inconclusive. This is mainly due to the morphology of myofibroblasts which was not as clearly defined as for CRC cells. A more accurate way to quantify both cells is to label each cell type (eg. PKH67 in Figure 3.1), and this would enable us to differentiate directly myofibroblasts and CRC cell lines in a mixed culture.

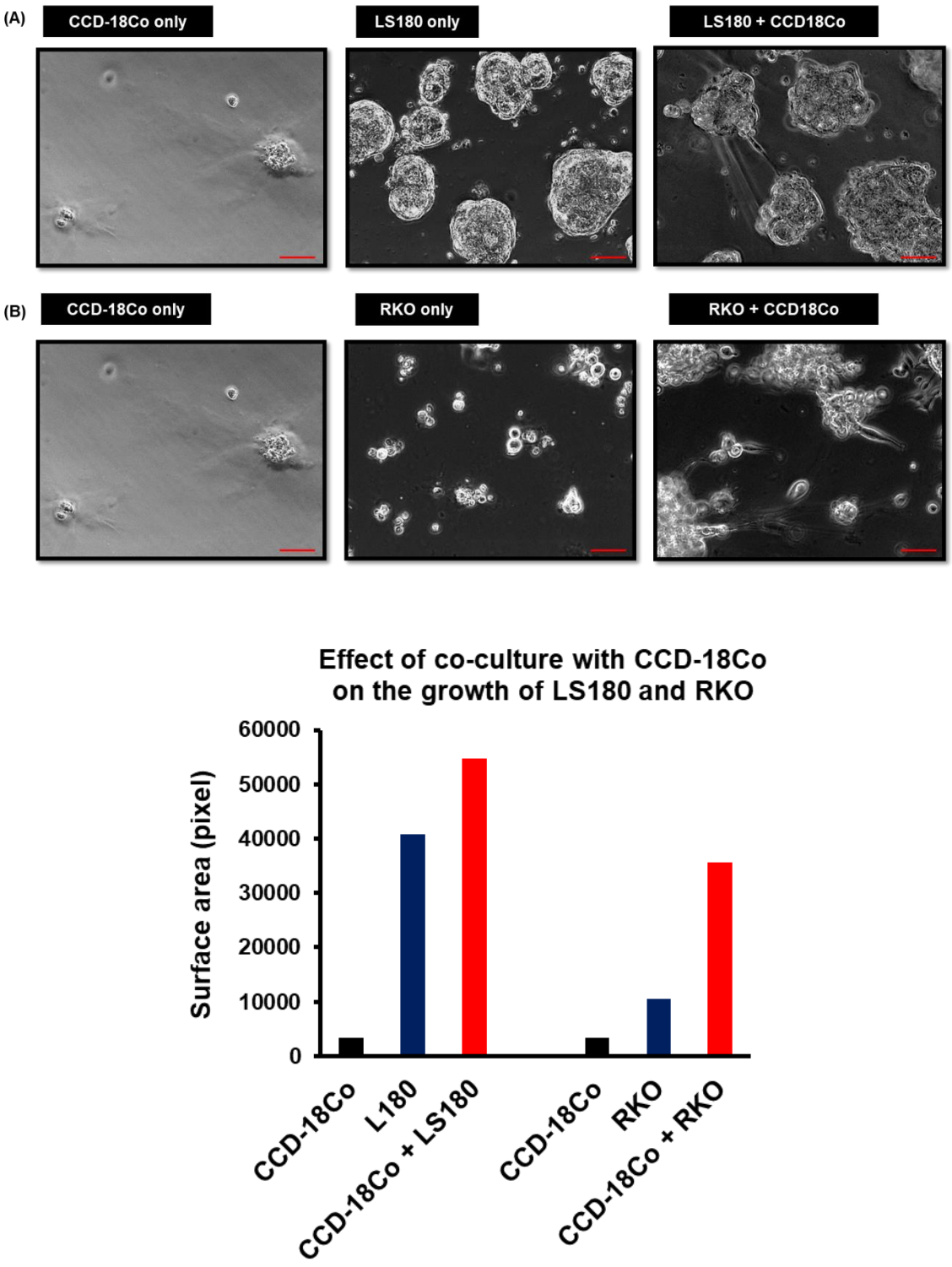

Figure 3.3

Co-culture of CCD-18Co with CRC cell lines (RKO and LS180) on full Matrigel substrate.

CRC cells and CCD-18Co clumped together forming clusters of cells on the Matrigel. Significant increase in cell numbers of both CCD-18Co and CRC cells

was seen in co-culture (more prominently in CCD-18Co + RKO) as compared to monoculture (Magnification: 20x) (Scale bar: 20 μm). Higher value of the total area covered by cells in a field, quantified using ImageJ software from a single experiment corresponds to greater cell growth.

3.2.2 Effect of co-culture on CRC cell differentiation

Our laboratory has shown that a subset of CRC cell lines when grown in Matrigel is able to form either large crypt like structures comprised of polarised cells surrounding a cell-free lumen that can be identified using F-actin staining, or instead form small non-lumen colonies. The three types of differentiated colorectal epithelial cells can be found in these lumen colonies (Ashley et al., 2013). Hence, lumen formation has been considered as an indication for the differentiation of CRC cell lines. In order to study the influence of co-culture with myofibroblasts on CRC cell differentiation we have performed two different types of Matrigel-based experiments. As illustrated by **Figure 3.4A**, the first assay consisted of layering a suspension of LS180 and Matrigel: DMEM (1:1) in the presence or absence of a myofibroblast lawn. There was a striking difference in the colony morphology and growth of LS180 after being co-cultured with CCD-18Co for 10 days, in comparison to monoculture (LS180 alone) (**Fig 3.4B**). A greater number of LS180 cells was found on co-culture, which suggests the positive influence of myofibroblasts on CRC cell proliferation. Moreover, LS180 colonies also appear to be more elongated and in close contact with the myofibroblasts. This contrasts with LS180 in monoculture where LS180 cells formed rounder and more uniform colonies. Notably, LS180 cells in co-culture gave rise to significantly larger lumens than LS180 alone.

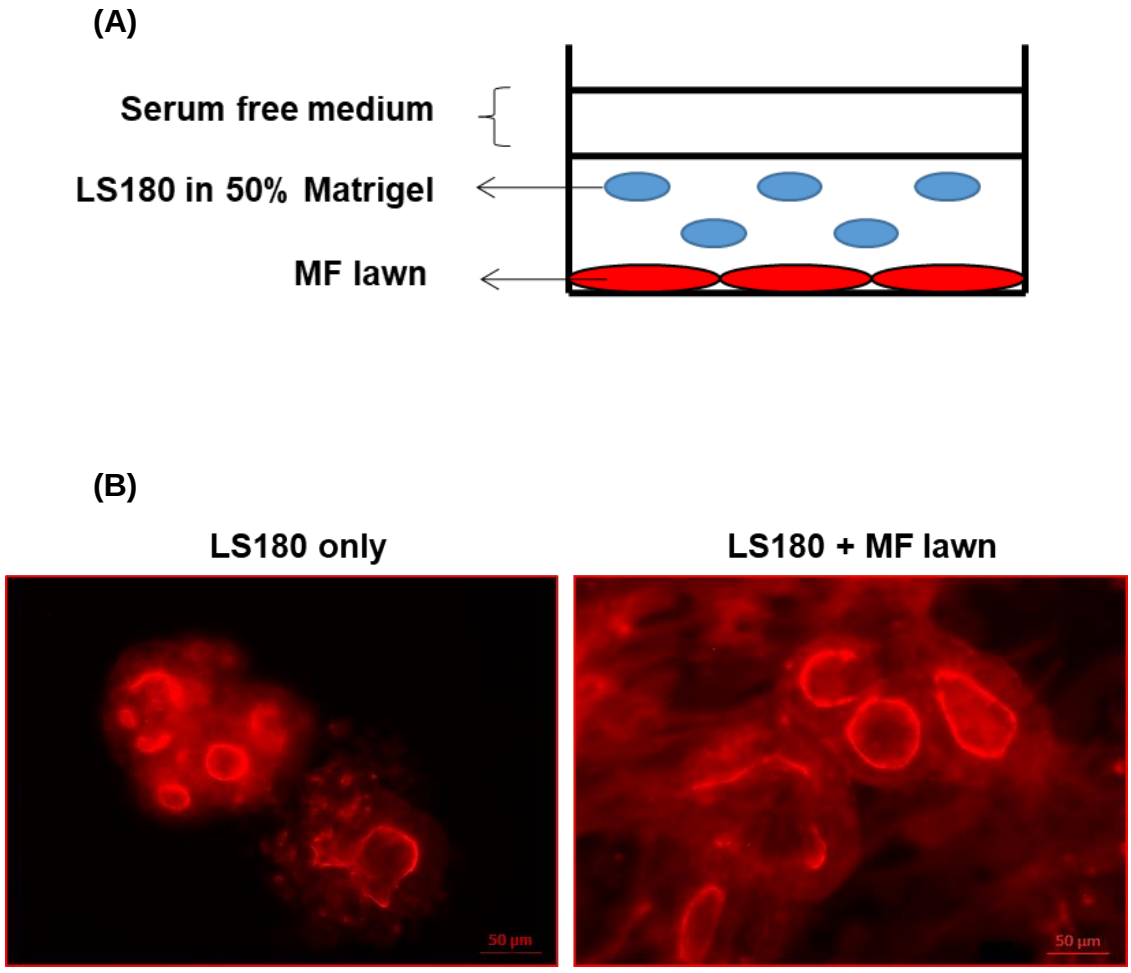

Figure 3.4

CCD-18Co supports the growth and lumen formation of LS180.

The experimental layout of the Matrigel-based differentiation assay is shown in (A). (B) Cells were incubated with serum free (DMEM alone) medium for 14 days. The lumens formed in LS180 co-culture group appeared to be more elongated and larger as compared to the control (LS180 alone). It is worth noting that LS180 is able to grow at an optimal rate in co-culture condition with myofibroblasts without the addition of serum, where both cell lines were maintained in serum free DMEM (DMEM alone). Hence, the presence of myofibroblasts may promote the growth of LS180 (MF: Myofibroblast) (Magnification: 20x).

The second assay was performed to confirm the effect of co-culture on CRC cell differentiation and is illustrated in **Figure 3.5A.** Here CCD-18Co and LS180 cells were directly mixed in 50% Matrigel solution. In comparison to LS180 alone, the sizes of LS180 lumens in the co-culture setting were significantly larger compared to the monoculture group as measured using ImageJ (**Fig 3.5B**). No significant difference was observed in the number of colonies between the two conditions.

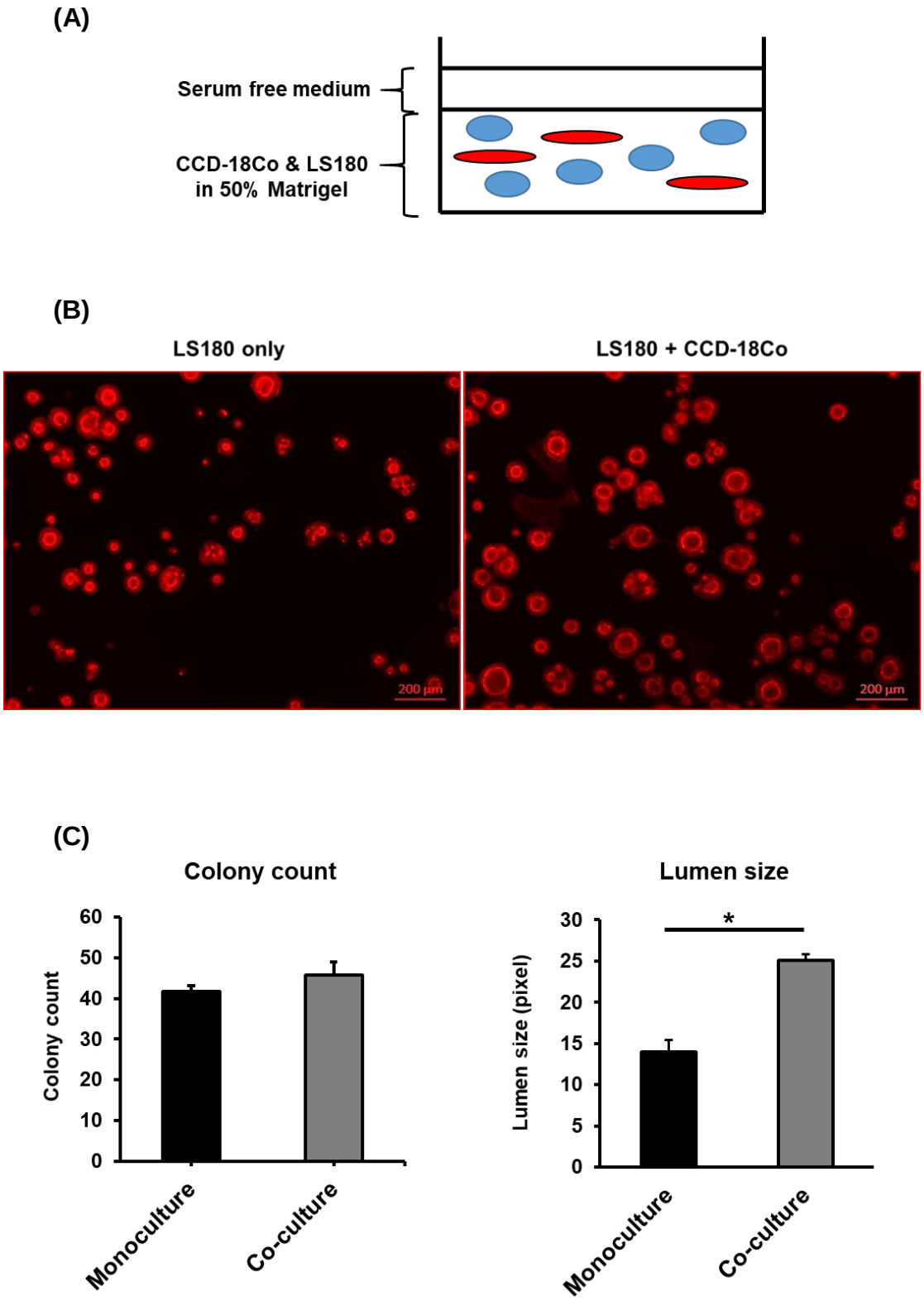

Figure 3.5

Co-culture with CCD-18Co supports the cell proliferation of LS180.

The experimental setup of the Matrigel-based differentiation assay is shown in (A). No significant difference in colony count between monoculture and co-

culture groups was found. Significantly larger size lumens (measured in length) were observed in LS180 + CCD-18Co after 14 days of culture as compared to LS180 alone, shown by F-actin staining (B). (Magnification: 5x) (*$p<0.05$ significant different when compared to monoculture from three biological replicates. The diameter of the lumens (length) from 45-50 cells in each field (3 fields for each group – monoculture and co-culture groups) was quantitated using ImageJ software. Average values of lumen size of both respective groups were recorded in **Figure 3.5C**.

3.2.3 Migration assay

A Transwell assay using a modified Boyden chamber was used to study the migration of CCD-18Co (**Fig 3.6A**) where CRC cells are seeded at the bottom of the well and CCD18CO are seeded in the Transwell insert. There was significant migration of CCD-18Co through the Transwell pores when compared to the control (without CRC cells) after 48 h of co-culture with CRC cells such as RKO, HT29 and LS180 under minimal serum conditions (0.5% FBS) (**Fig 3.6B**). The highest number of migrated CCD-18Co was found in the co-culture group with RKO, followed by HT29 and LS180.

(A)

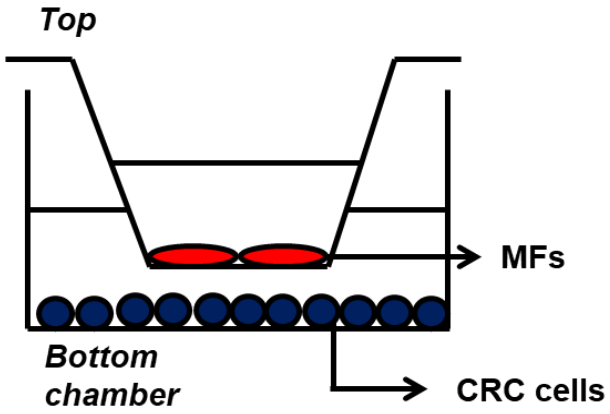

(B)

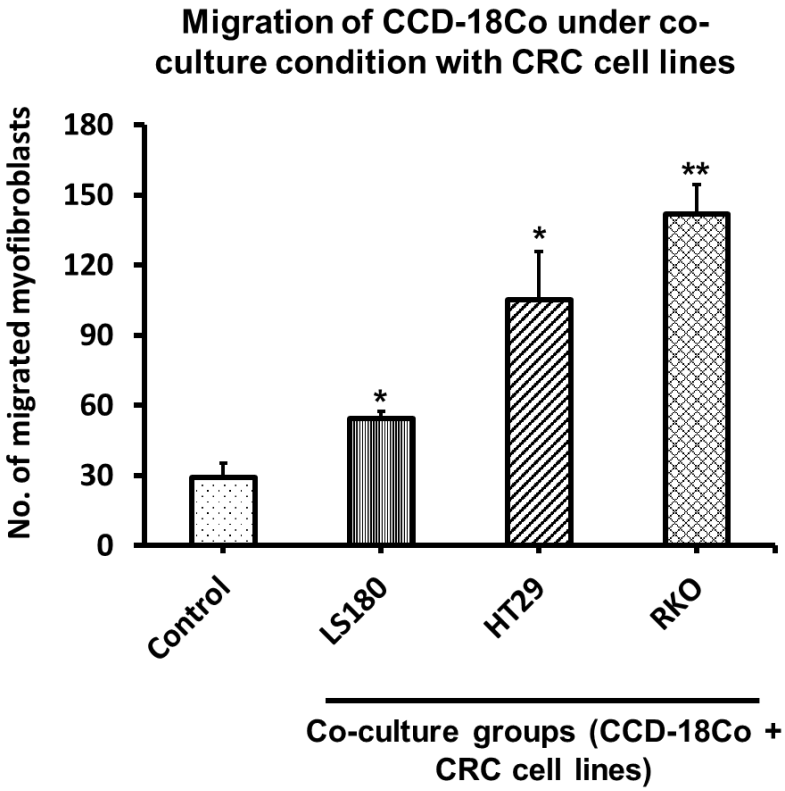

Figure 3.6

Epithelial cells support the migration of myofibroblasts.

The experimental layout of the migration assay is shown in (A). (B) Significant migration of CCD-18Co when co-cultured with CRC cells in comparison to control (Only DMEM + 0.5% medium, no CRC cell lines at the bottom) after 48 h of co-incubation (**p<0.001, *p<0.05 from three biological replicates) (MFs: Myofibroblasts).

The chemoattractant ability of CCD-18Co to induce the migration of CRC cells also was studied using another similar approach, namely reversing the positions of the CRC and MF cells (**Fig 3.7A**). **Figure 3.7B** shows the number of migrated CRC cells after 48 h of co-incubation with CCD-18Co. Both RKO and HT29 migrated significantly through the Transwell pores in comparison to the control (CRC cells only, absence of CCD-18Co). The results demonstrated that RKO cells were found to have significantly higher capacity of migration when compared to HT29, whereas LS180 did not show any migration. The highest number of migrated RKO cells was found in RKO + CCD-18Co co-culture, followed by co-culture of HT29. No significant migration of LS180 was found. Representative images of migrated and stained CRC cells with and without the presence of CCD-18Co are shown in **Figure 3.7B**.

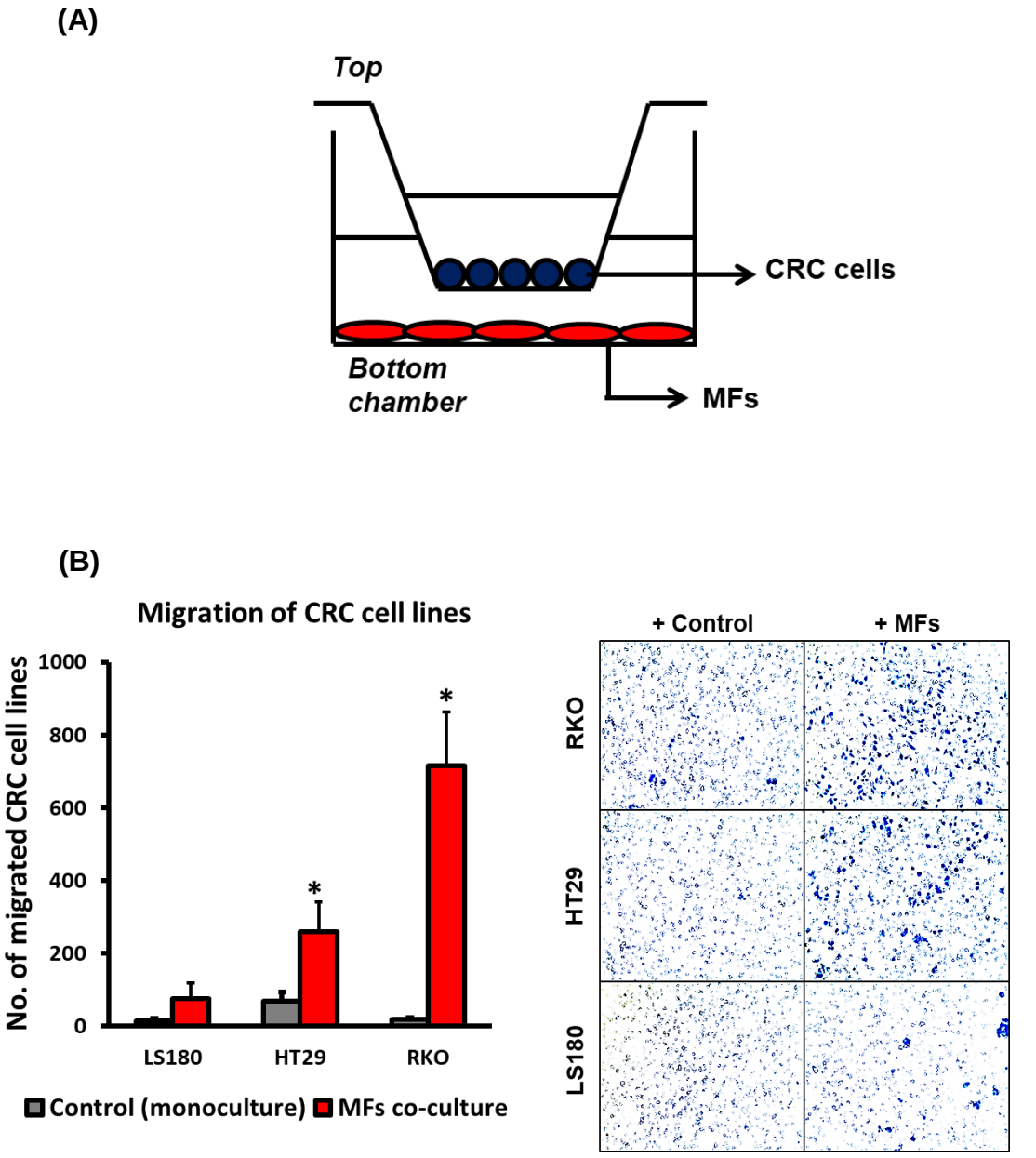

Figure 3.7

The presence of CCD-18Co influences the migration of CRC cells.

Figure 3.7A illustrates the experimental setup of the Transwell assay. Different CRC cells exhibit different abilities to migrate when co-incubated with CCD-18Co (MFs) (**Fig 3.7B**). Significant migration of CRC cells was observed in co-culture for RKO & HT29 (*$p<0.05$ from three biological replicates). Representative images from the assay show significantly higher numbers of migrated RKO compared to HT29 and LS180 in the presence of CCD-18Co (Migrated CRC cells stained in blue) (Magnification: 20x) (MFs: Myofibroblasts).

3.2.4 Invasion assay

The invasive property of myofibroblasts was analysed using a Matrigel-based "blob" assay. The different myofibroblast lines tested in our study showed different abilities to invade Matrigel under co-culture with CRC cells. The selection of CRC cells was based on their differentiation status in Matrigel (**Table 2.1**). After 6 days of co-culture, significant invasion of CCD-18Co was observed with all the selected CRC cells (RKO, HT29, LS180, SW480 and SW620) (**Fig 3.8B**) when compared to monoculture (myofibroblasts alone). SW620 induced the strongest effect on CCD-18Co invasion among other epithelial cells. Similar experiments were performed using two primary myofibroblasts (Myo 6526 and Myo 7395) from normal colon tissues as well as a pair of myofibroblasts from normal and cancerous colon tissues isolated from the same patient (Myo 6550 and Myo 6551C respectively). As illustrated in **Figure 3.8B and C**, apart from RKO, all CRC cell lines are inducing invasion of both Myo 6526 and Myo 7395. For the tumour/normal pair, the same pattern was found with the normal line Myo 6550 whereas the cancer derived Myo 6551C demonstrated some invasive properties only with the SW480 and SW620 cell lines (**Fig 3.8D and E**). Altogether, our data strengthen the evidence for invasive properties of myofibroblasts.

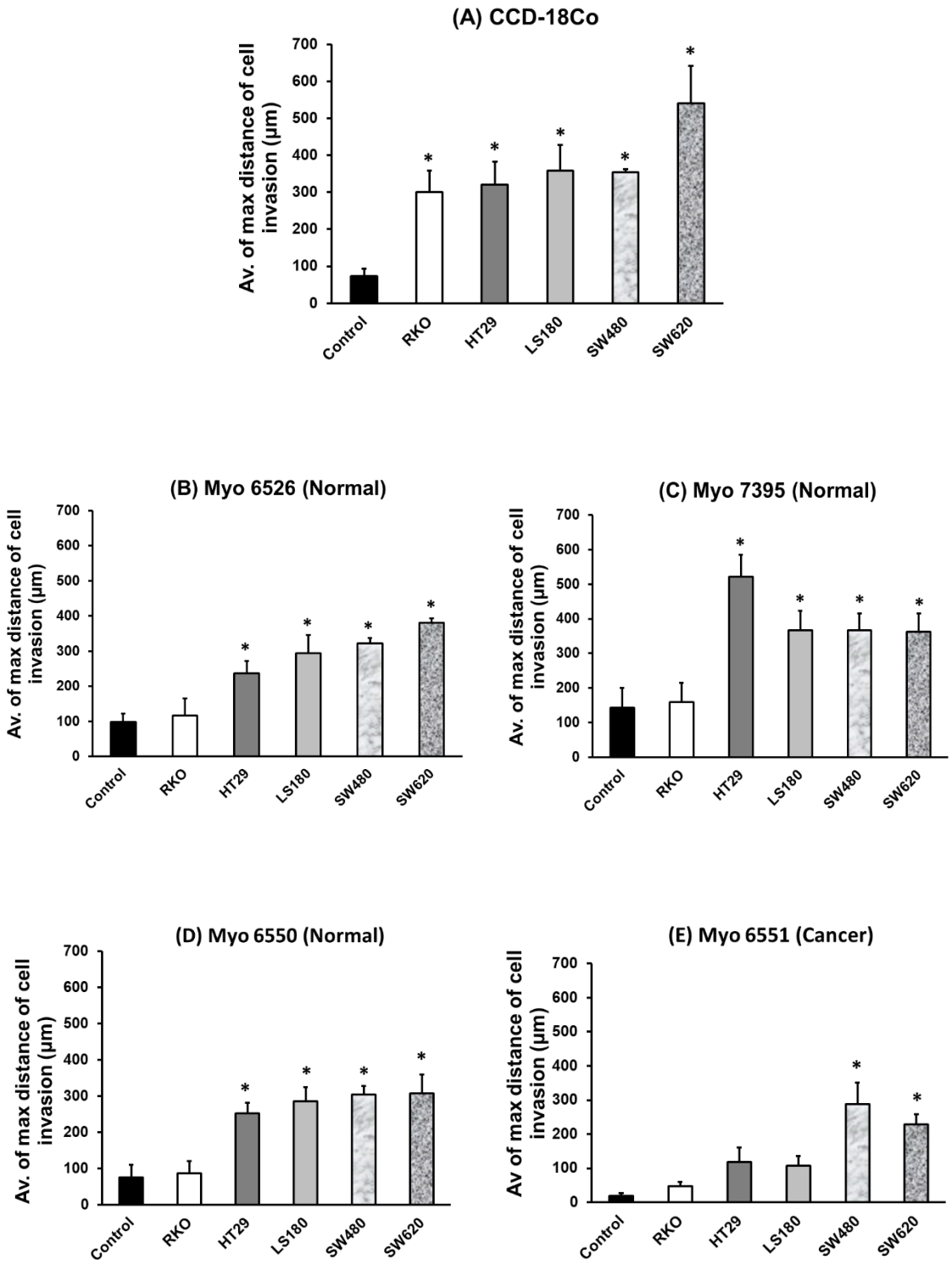

Figure 3.8

Invasion assay of (A) CCD-18Co; normal primary myofibroblasts: (B) Myo 6526 and (C) Myo 7395 and a pair of matched myofibroblasts from (D) normal (Myo 6550) and (E) cancerous tissue (Myo 6551C).

To study the invasion of myofibroblasts, a Matrigel-based invasion assay was conducted where either myofibroblasts or CRC cell lines were seeded in a Matrigel blob separated from each other by Matrigel layer. Both of the cell-containing blobs (myofibroblasts and CRC cell lines) were included in a same well for co-culture groups whereby monoculture involves only a blob of either myofibroblasts or CRC cells, seeded together with an empty Matrigel blob (control). In this assay, the average (Av) of maximum distance of myofibroblasts invasion from Matrigel blob when co-cultured either with CRC cells or empty blob (control) was measured after 6 days of incubation. Selected CRC cells from different cell lines possess different capacities to induce invasion of various myofibroblasts under co-culture condition (*$p<0.05$ from three biological replicates, significant different from control).

This Matrigel-based blob assay also was repeated to study the invasion of normal skin fibroblasts when co-cultured with CRC cells (**Fig 3.9**). No significant invasion of foreskin fibroblasts was found in the presence of selected epithelial cells. This differs from adult skin fibroblasts (skin fibro 3) where significant invasion was observed under co-culture with SW480 and SW620. Different expression profile between these two fibroblasts may contributed to this observation. For example, skin fibroblasts expressed high level of *PDGF-C* while low expression of this gene was found in foreskin fibroblasts (**Fig 4.21**).

Interestingly, our analysis revealed the different basal levels of invasion (monoculture, without presence of CRC cell lines) in both myofibroblasts and skin fibroblasts. The cancerous Myo 6551C has noticeably the lowest basal level of cell invasion when compared to the 4 normal myofibroblasts (CCD18Co, Myo 6526, 7395, and 6550) (**Fig 3.10**). Higher basal levels of invasion in skin fibroblasts were observed in the monoculture group in comparison to myofibroblasts.

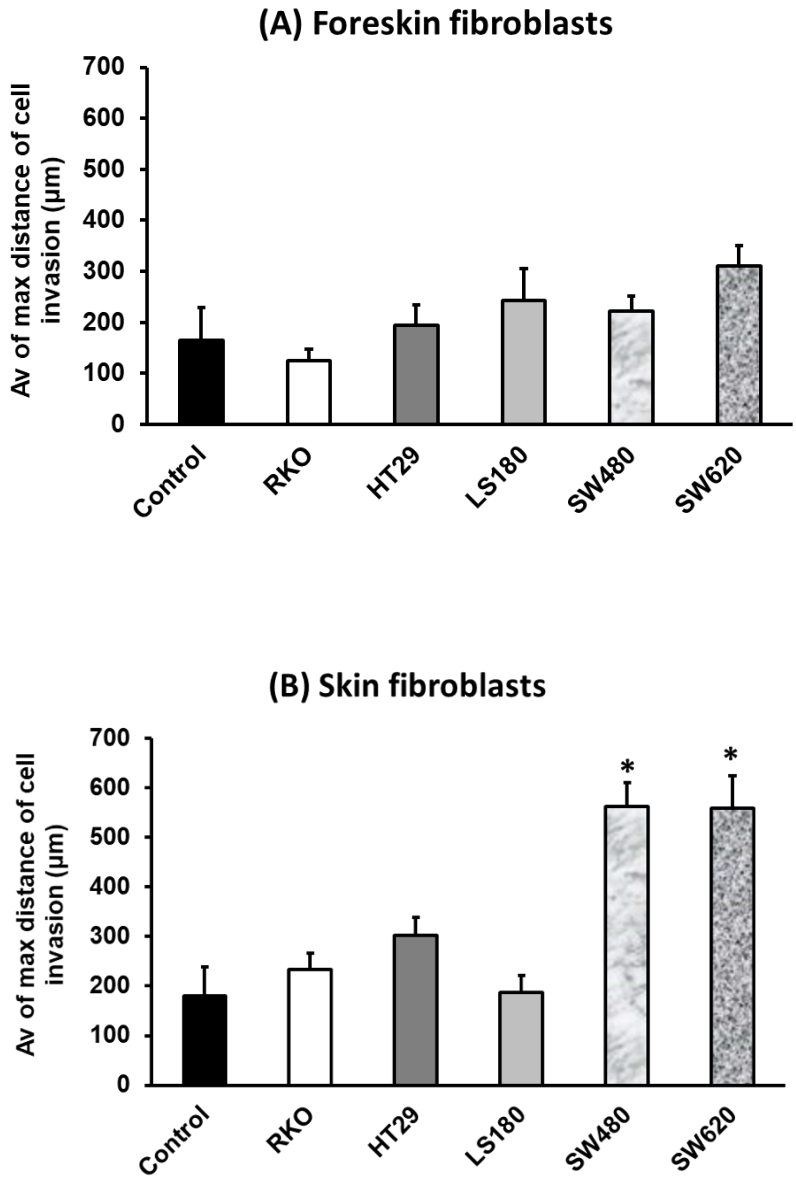

Figure 3.9

Invasion assay of (A) foreskin fibroblasts and (B) skin fibroblasts.

In this assay, the average (Av) of maximum distance covered by invaded skin fibroblasts from Matrigel blob when co-cultured either with CRC cells or empty blob (control) was measured after 6 days of incubation. Unlike with the observation with myofibroblasts, no CRC cell lines induced invasion of foreskin fibroblasts and only a subset of CRC cell lines could induce significant migration of skin fibroblasts (* $p<0.05$ from three biological replicates, compared to control).

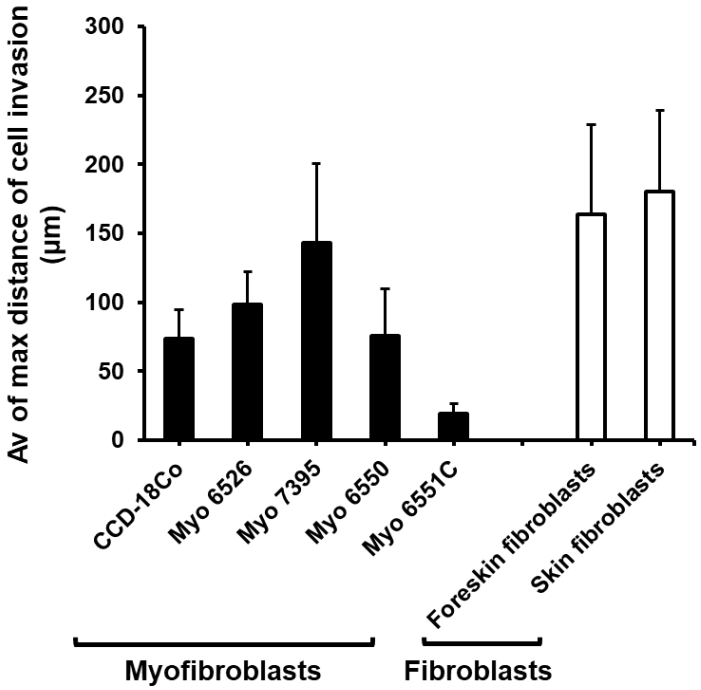

Figure 3.10

Basal level (monoculture) of myofibroblasts and skin fibroblasts invasion in monoculture conditions.

Foreskin and skin fibroblasts possess higher basal level (monoculture) of invasion in comparison to myofibroblasts. Myo 6551C has the lower basal invasive property when compared to its normal counterpart – Myo 6550 and other selected myofibroblast lines. As shown earlier in **Figure 3.8** and **3.9**, the basal level of cell invasion is lower in comparison to co-culture with CRC cell lines.

The viability of CRC cells under this experimental setup was verified using Calcein AM staining. **Figure 3.11** shows representative images of epithelial cells under monoculture and co-culture in the presence of CCD-18Co. No significant difference was observed in the morphology and growth of CRC cells in the Matrigel blob between the control and co-culture groups except in LS180 + CCD-18Co where more lumen formation can be seen when compared to LS180 alone. This corroborates the data shown previously in **Figure 3.4B** and **3.5B**.

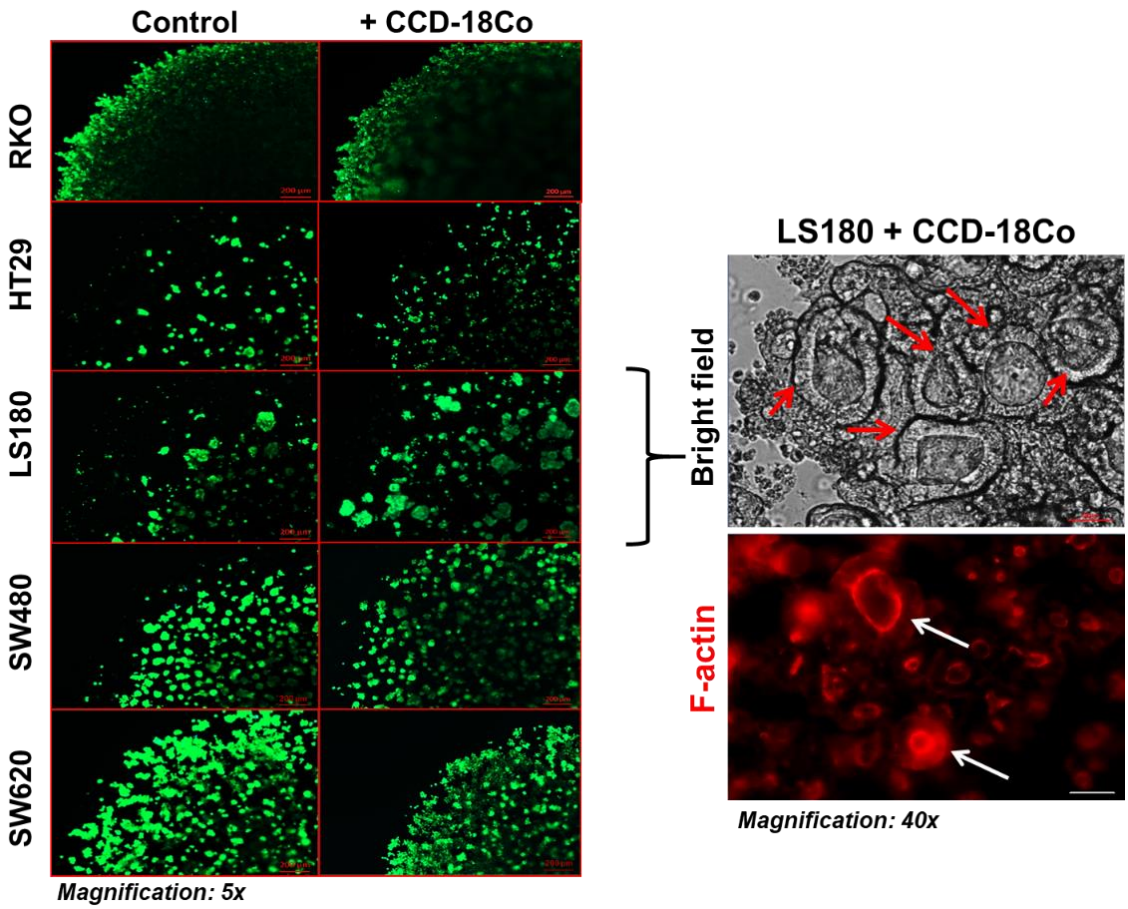

Figure 3.11

Viability and differentiation of CRC cells in Matrigel-based assay.

Calcein AM shows the viability of CRC cells cultured in Matrigel blob. Minimal DAPI staining was detected in tested CRC cells. No significant changes in the morphology of the epithelial cells from the CRC cell lines was observed except for LS180 co-culture where more prominent lumen formation was observed.

3.3 Discussion

This chapter discusses different *in vitro* assays that can be used to study various properties of myofibroblasts and CRC cells and their interactions, including cell proliferation, migration, invasion and differentiation under co-culture condition. All the assays were conducted under serum free (DMEM alone) or minimal serum (DMEM + 0.5% FBS) conditions to minimise the effect of serum on our observations and make it more specific to the co-culture conditions. This exclusion of serum was essential as serum has been found to improve cell proliferation and attachment as it is rich in essential components (eg. various growth factors).

We found that the CRC cell proliferation was poor in the absence of serum but greatly improved in co-culture with myofibroblasts. That observation was consistent across three different CRC cell lines regardless of their differentiated state (RKO, undifferentiated; HT29, poorly differentiated and LS180, well-differentiated).

Matrigel has components of the ECM such as laminin, collagens and fibronectin as well as growth factors and cytokines such as TGFβ1 that enhance the growth and adhesion of CRC cells and myofibroblasts. The concentration of Matrigel used was an important factor that can affect the results as both myofibroblasts and CRC cells did not grow well on full Matrigel. A more diluted Matrigel at 50% concentration proves to be optimal to culture both types of cells. The physical properties of Matrigel may contributed to these observations. It stems from

earlier studies which report on the influence of stiffness or compliance of ECM on cell signalling, that in tum affects the cell morphology, cell-cycle progression and differentiation. It is most likely that 100% Matrigel is not suitable to support CRC cells and myofibroblasts in *in vitro* conditions, when compared to more diluted Matrigel mixture. Thus, it is essential to modify the concentration of Matrigel used in the experiment to ensure an optimal growth and attachment of cells (Fischer et al., 2012).

A Matrigel based differentiation assay was conducted to study the differentiation of LS180 in the presence of myofibroblasts. Our lab has shown the ability of differentiated CRC cells to form lumen structures when grown in Matrigel. LS180 was selected for this assay due its well-established ability to form lumens. The result from the first assay shows more flattened colonies of LS180 that proliferate alongside the CCD-18Co as compared to the control, which were rounder in shape (**Fig 3.4**). The size of these lumens in the co-culture groups was significantly larger than in monoculture. This finding was supported by the second differentiation assay where larger lumens were observed when LS180 was co-cultured with CCD-18Co (**Fig 3.5**). The variation in the LS180 morphology observed through Matrigel based differentiation assays is probably due to different experimental layouts of the tests. LS180 either was seeded in Matrigel on top of myofibroblasts lawn or mixed with myofibroblasts in Matrigel solution before being added to a well. The presence of the myofibroblast layer attracts LS180 and migrated cancer cells grown very closely to the CCD-18Co cells, as shown in the first assay. In the second assay, as both LS180 and CCD-18Co were suspended in Matrigel, both cells proliferate separately, or formed

colonies of cells. This enables us to observe more clearly the individual cells of LS180 as there was no overlap of them and CCD-18Co as in first Matrigel assay. Both differentiation assays demonstrated the formation of bigger LS180 lumens when co-cultured with CCD-18Co. As shown in **Figure 3.5C**, in monoculture, the average lumen size of LS180 was approximately half of those in co-culture condition. Bigger lumens formed in LS180 co-cultured with CCD-18Co may illustrate the positive influence of myofibroblasts on the CRC cells differentiation and to some extent, on cell proliferation.

Greicius (2018) has reported that secreted R-spondins from pericryptal myofibroblasts, particularly R-spondin3 (RSPO3) increased the formation of epithelial cell organoids. Moreover, they also showed that RSPO3 supresses the expression of MUC2, which marks the differentiation of goblet cells. This study suggests the positive influence of myofibroblasts in promoting the proliferation and support of the stemness of epithelial cells through stimulation of WnT/ β-catenin signalling. Interestingly, our microarray data revealed low *RSPO3* expression in all primary myofibroblasts with exception of Myo 1998, which is derived from normal colon. The basis of differential RSPO expression between samples is remains unexplained. It seems likely that RSPO3 expression varies between different sources of myofibroblasts and this difference presumably would affect the growth and differentiation of epithelial cells in *in vivo*.

The Transwell assay was chosen to assess the migration properties of both myofibroblasts and epithelial CRC cells under co-culture. Very minimal numbers of migrated CCD-18Co cells were observed in the absence of CRC cells in the

bottom chamber. It is apparent from this assay that CRC cells secreted components that support the migration of myofibroblasts. Transwell assays of myofibroblasts also showed that the extent of migratory activity of CCD-18Co was dependant on the epithelial cell line used in the co-culture. The maximum number of migrated CCD-18Co cells were observed in the presence of RKO, when compared to HT29 and LS180. This suggests that RKO cells may secrete more growth factors or/and cytokines that promote the migration of CCD-18Co than do HT29 or LS180. For example, our microarray data shows higher mRNA level of *TGFβ1* in RKO in comparison to HT29 and LS180. A difference in the pro-migration activity of CCD-18Co on different CRC cells also was also observed. Thus, RKO and HT29 migrated significantly more in the presence of the myofibroblasts, than did LS180. The lack of specific secreted factors from CCD-18Co or the absence or low expression of receptors on LS180 could be an explanation of this result.

The invasion of myofibroblasts was also studied using a Matrigel based blob assay. Strong pro-invasive effects of CRC cell lines (RKO, HT29, LS180, SW480 and SW620) on CCD-18Co were observed. Similar results were obtained with other primary myofibroblasts from normal colon tissues except for co-culture with RKO. As described by the ATCC, although it is not an immortalized cell line, CCD-18Co may possess certain characteristics, including its gene expression profile, that vary from myofibroblasts that were established from patient's samples. One of the properties that differentiates these myofibroblasts from CCD-18Co is the population doubling rate (PDR), which refers to the total number of times the cells in the population have doubled since

their primary isolation in vitro. The PDR of CCD-18Co is significantly higher than other primary myofibroblasts used in this thesis. Primary myofibroblasts isolated from the surgical samples can be maintained in culture up to a maximum passage number of 10 unlike CCD-18Co that can be cultured till passage 20 before the cells start to senesce. In comparison to other primary myofibroblasts which derived from cancer and older patients, CCD-18Co was isolated from the colon of a much younger individual (2.5 months of age) (ATCC) which may explain the difference in the PDR between those myofibroblast lines.

As for the comparison between myofibroblasts from normal colon and tumour, the results from my experiments show that both cells have different basal levels of invasion in monoculture. Myo 6551C from cancerous tissues has a weak ability to invade the Matrigel layer even in the presence of CRC cells, unlike its normal counterpart – Myo 6550. This poor invasive ability of Myo 6551C may be due to its slow growth rate, which is typically seen with other primary myofibroblasts from tumour samples. These myofibroblasts may need different components or growth factors in the medium to support their proliferation *in vitro*.

No invasion of CRC cells into the Matrigel layer was seen although the cells were clearly viable from the Calcein AM staining. No significant changes were noticed in the morphology of the CRC cells under the same experimental conditions although the formation of larger lumens in the LS180 co-cultures was observed as in other assays described earlier. Even though the invasion Matrigel blob assay provides crucial information on the invasive properties of

different myofibroblasts, the fact that it presents little information of the effect of co-culture on CRC growth and morphology, shows the lack of versatility of this assay to portray the bidirectional communication between myofibroblasts and CRC cells.

Although these assays give insights on the bidirectional communications between myofibroblasts and CRC cell lines, there are still limitations that need to be addressed. As is true for many *in vitro* assays, there is a lack of specific and versatile experimental tests to evaluate the physiological process that occurs *in vivo*. For example, even though the Transwell assay has been considered as a mainstream experiment to study the migration of cells, it poses the question of the effect of increased proliferation in a co-culture setting which may influence the endpoint measurement of migrated cells. Ki-67, which is a cellular marker for proliferative cells may be included to assess the growth of cells (monoculture vs co-culture). This would verify that indeed increased numbers of stained cells in the insert of the Transwell assay are contributed by the pro-migration effect of the chemoattractant (cells at the bottom chamber) instead of greater growth of cells. Furthermore, the inability of these tests to reproduce the 3-dimensional architecture of tumour and its microenvironment at many levels in the colon also limits the information that can be acquired to further explain the relationships between myofibroblasts and epithelial cells. Considering the pros and cons of each test, the Matrigel based assay shown in **Figure 3.4** is more likely to mimic the *in vivo* physiological interaction between myofibroblasts and epithelial cells. Additional screening with other CRC cells using this assay will help to elucidate the nature of myofibroblasts/cancer cells bidirectional communications.

CHAPTER 4

INFLUENCE OF GROWTH FACTORS ON THE REGULATION OF *AOC3* AND *NKX2-3*, TWO DIFFERENTIALLY EXPRESSED GENES IN MYOFIBROBLASTS

CHAPTER 4: INFLUENCE OF GROWTH FACTORS ON THE REGULATION OF *AOC3* AND *NKX2-3*, TWO DIFFERENTIALLY EXPRESSED GENES IN MYOFIBROBLASTS

4.1 Introduction

Many publications have suggested the contribution of the reciprocal relationship between myofibroblasts and cancer cells in the progression of colon cancer. The communications between these two types of cells involve the secretion of growth factors, cytokines and chemokines from CRC cells that affect the properties of both of myofibroblasts and *vice versa*. These growth factors may lead to activation of the myofibroblasts in which these cells become more contractile and able to migrate and promote the invasion of cancer cells which eventually resulted in metastasis from primary site to the other organ(s).

This chapter discusses the influence of selected growth factors on the expression of *AOC3* and *NKX2-3*, which are two of the differentially expressed genes in myofibroblasts, in comparison to skin fibroblasts. Other associated genes expressed in myofibroblasts, specifically *ACTA2* (protein: alpha smooth muscle actin, αSMA) and *FAP* (fibroblasts activation protein, alpha) were also studied to elucidate the *in vitro* effects of these growth factors on their expression. Initial screening of AOC3 and NKX2-3 expression in different cell types (myofibroblasts, fibroblasts and CRC cells) was performed to prove the elevated relative expression of these genes in myofibroblasts. The *in vivo* expression of AOC3 was verified using immunohistochemistry staining of

patient’s colon samples (normal and cancer). The expression of AOC3 and NKX2-3 also was analysed in various primary myofibroblasts derived from different colon tissues. The expression level of AOC3 also was studied across different cell passages of myofibroblasts to find out if there was any correlation between AOC3 expression and cell senescence.

4.2 Results

4.2.1 Expression of AOC3 and NKX2-3 in different cell types

From microarray data, several differentially expressed genes between myofibroblasts and normal skin fibroblasts have been identified. As described by Hsia et al. (2016), *AOC3* and *NKX2.3* are two of the most highly differentially expressed genes in myofibroblasts. **Figure 4.1** shows the mRNA level of those genes in 8 different cell lines (4 myofibroblasts and 4 normal skin fibroblasts). The myofibroblasts which were included in the microarray analysis included CCD-18Co, a myofibroblasts purchased from ATCC, and three different primary myofibroblasts grown from patients' samples (Myo 1998, Myo 2020 and Myo 6024). The four normal skin fibroblasts include foreskin (F) fibroblasts and three other skin fibroblasts from three healthy adults (skin fibro_1, skin fibro_2 and skin fibro_3). None of the skin fibroblasts express *AOC3* at an apprecable level, while it is expressed at high levels in a subset of the myofibroblasts such as CCD-18Co, Myo 1998 and 2020. The transcription factor *NKX2-3* is, however, expressed at a significantly high level in all myofibroblasts, whereas all the skin fibroblasts only express this gene at a very low level (**Fig 4.1**).

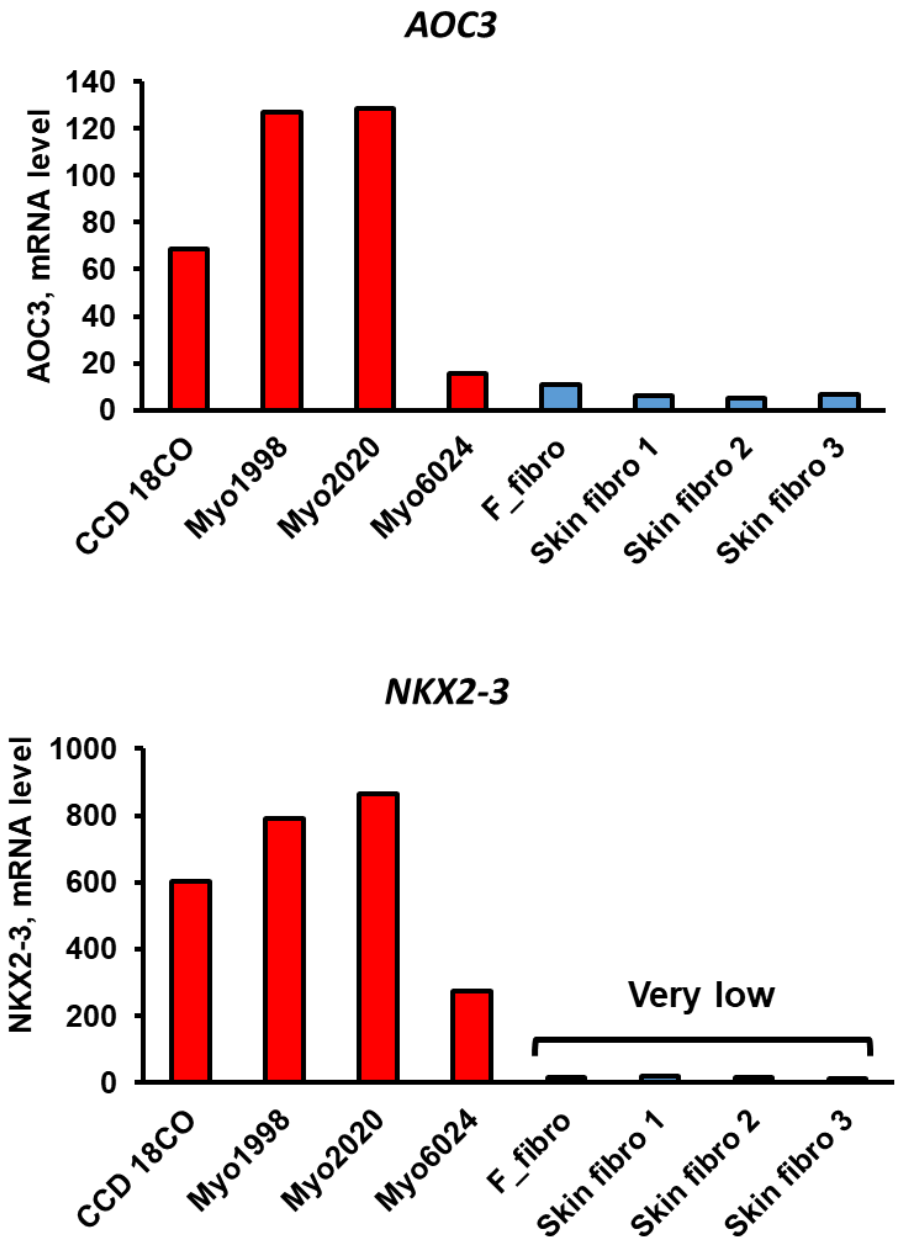

Figure 4.1

Expression of *AOC3* and *NKX2-3* in myofibroblasts and skin fibroblasts.

Microarray data shows high *AOC3* expression in all but one of the myofibroblasts (Myo 6024) as compared to various skin fibroblasts. *NKX2-3* is expressed at a high level in myofibroblasts whereas very low expression of this gene is detected in skin Fs in comparison to skin fibroblasts (Hsia et la., 2016) (F_fibro: foreskin fibroblasts).

The mRNA expression of *AOC3* and *NKX2-3* in the Bodmer CRC panel was extracted from the microarray data and the results are summarized in **Figure 4.2**. Only a small number of CRC cell lines shows detectable levels of *AOC3* and *NKX2-3*. It is worth noting that these mRNA values of *AOC3* and *NKX2-3* in CRC cell lines are relatively quite low (less than 200 for almost all the cell lines).

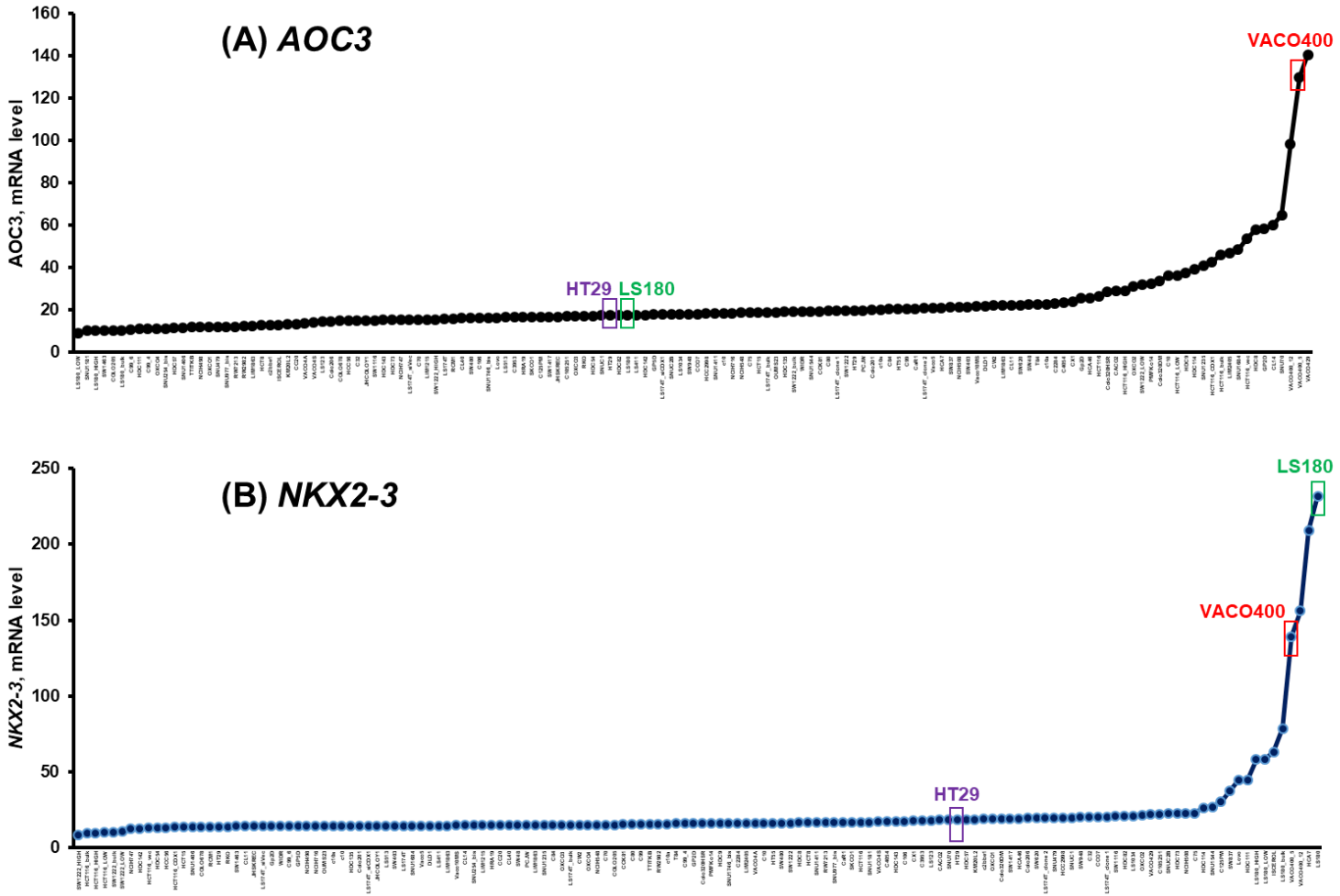

Figure 4.2

The mRNA levels of (A) *AOC3* and (B) *NKX2-3* in CRC cell lines.

x-axis: CRC cell lines, y-axis: mRNA level.

Screening of *AOC3* and *NKX2-3* expression in the three CRC lines that express it at different levels in the microarray data (High mRNA levels of *AOC3* and *NKX2-3* in VACO400, high expression of *NKX2-3* but low *AOC3* expression in LS180 and low mRNA levels of both *AOC3* and *NKX2-3* in HT29) and in CCD-18Co using qRT-PCR confirms the high expression of both genes in myofibroblasts in comparison to CRC cell lines (**Fig 4.3**). This result is verified at a protein level using western blots (**Fig 4.4A**) where a strong band for AOC3 was found in CCD-18Co whereas no band was detected for the CRC cell lines. As previously shown in our laboratory, the absence of serum increases the expression of AOC3. We therefore also compared the AOC3 expression under serum starvation and found that AOC3 is upregulated in CCD18Co which is in agreement with our previous finding (Hsia et al., 2016) but not in CRC cell lines as illustrated by the absence of band in the western blots.

The NKX2-3 protein expression in myofibroblast was compared to skin fibroblasts and CRC cells. **Figure 4.4B** shows the high expression of NKX2-3 in myofibroblasts (CCD-18Co, Myo 7395 and Myo 8853), while only quite faint bands were observed for skin fibroblasts and foreskin fibroblasts and finally no NKX2-3 expression was detectable in CRC cells (LS180, VACO400 and RW7213) including even LS180 which showed the highest relative expression of *NKX2-3* mRNA in the CRC cell line panel (**Figure 4.2)**.

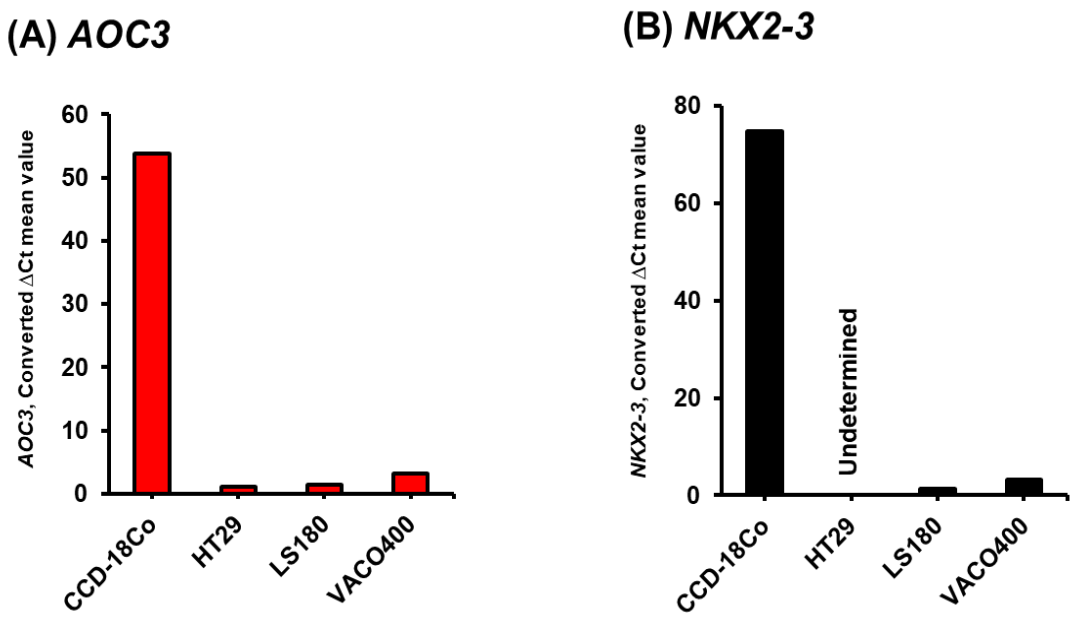

Figure 4.3

The expression of (A) *AOC3* and (B) *NKX2-3* in CCD-18Co and selected CRC cell lines (HT29, LS180 and VACO400), analysed by qRT-PCR.

Both *AOC3* and *NKX2-3* are expressed at very much higher levels in CCD-18Co than in the CRC lines, substantiating their use as markers for myofibroblasts.

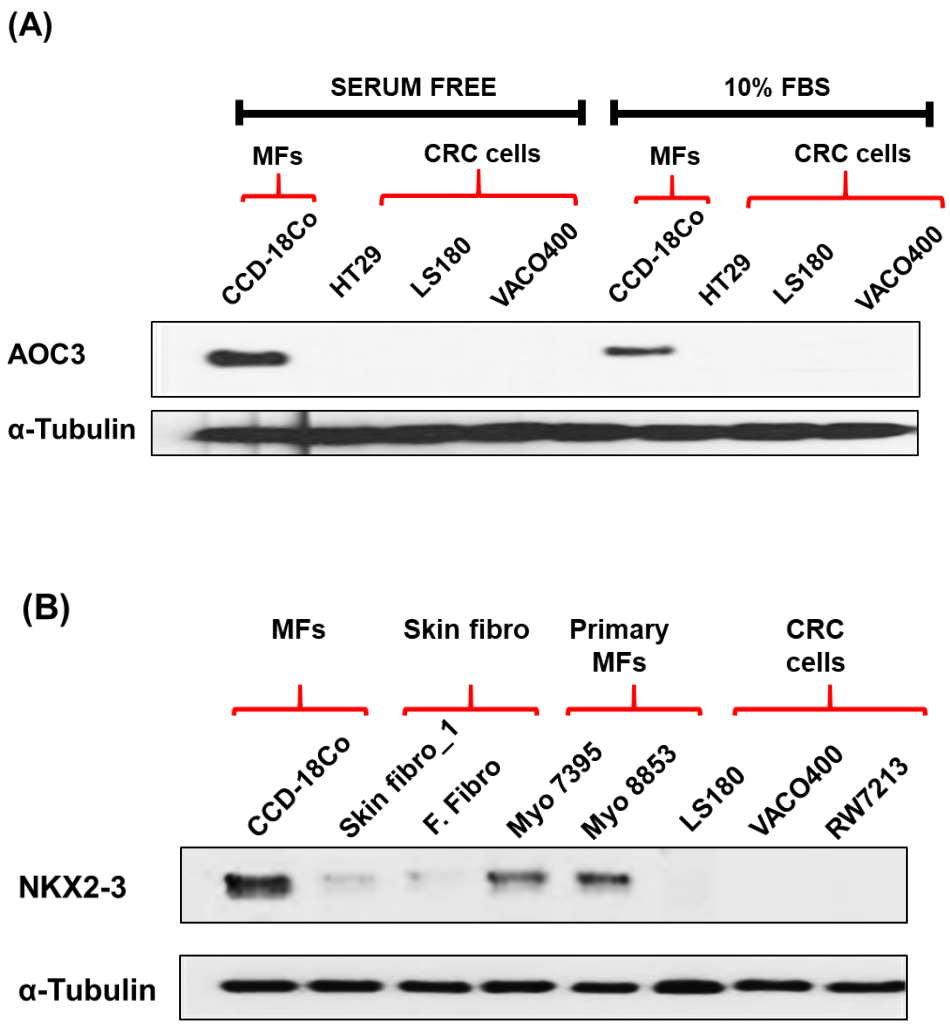

Figure 4.4

Protein expression of (A) AOC3 in serum free and full serum (10% FBS) and (B) NKX2-3 in different cell types.

AOC3 expression was upregulated in CCD-18Co under serum free condition. No detectable expression was observed for AOC3 in the selected CRC cell lines, regardless of treatment condition (presence or absence of serum). Strong NKX2-3 expression in MFs was detected. A very faint band was observed in skin Fs and no detectable band was found in CRC cell lines (MFs: myofibroblasts; F. fibro: foreskin fibroblasts; skin fibro_1: skin fibroblasts).

4.2.2 Localization of AOC3 and NKX2-3 in myofibroblasts

As shown in **Figure 4.5A**, AOC3 staining on live cells produced staining in the cytoplasmic region of CCD-18Co. The negative control for the AOC3 namely RKO shows no detectable AOC3 staining (**Fig 4.5B**).

Immunofluorescence staining also was conducted for NKX2-3 and we found that NKX2-3 staining pattern differs according to fixative solution that been used (**Fig 4.6A**). By using ice cold methanol as fixative solution, the staining of NKX2-3 in CCD-18Co was detected predominantly in the nucleus although faint staining was observed in cytoplasmic region of the myofibroblasts, which is in agreement with the localization of this protein according to GeneCards website (https://www.genecards.org/cgi-bin/carddisp.pl?gene=NKX2-3). The staining NKX2-3 in cold-methanol fixed CCD-18Co differs from those of PFA and glutaraldehyde-fixed cells. Cytoplasmic NKX2-3 staining in PFA and glutaraldehyde fixed-CCD-18Co is not in agreement with predicted localization of NKX2-3. Hence, NKX2-3 staining using the best available NKX2-3 antibody (LSBio) used in the present study, performed on cells fixed only in cold methanol is to be considered reliable for analysis. (**Fig 4.6A**).

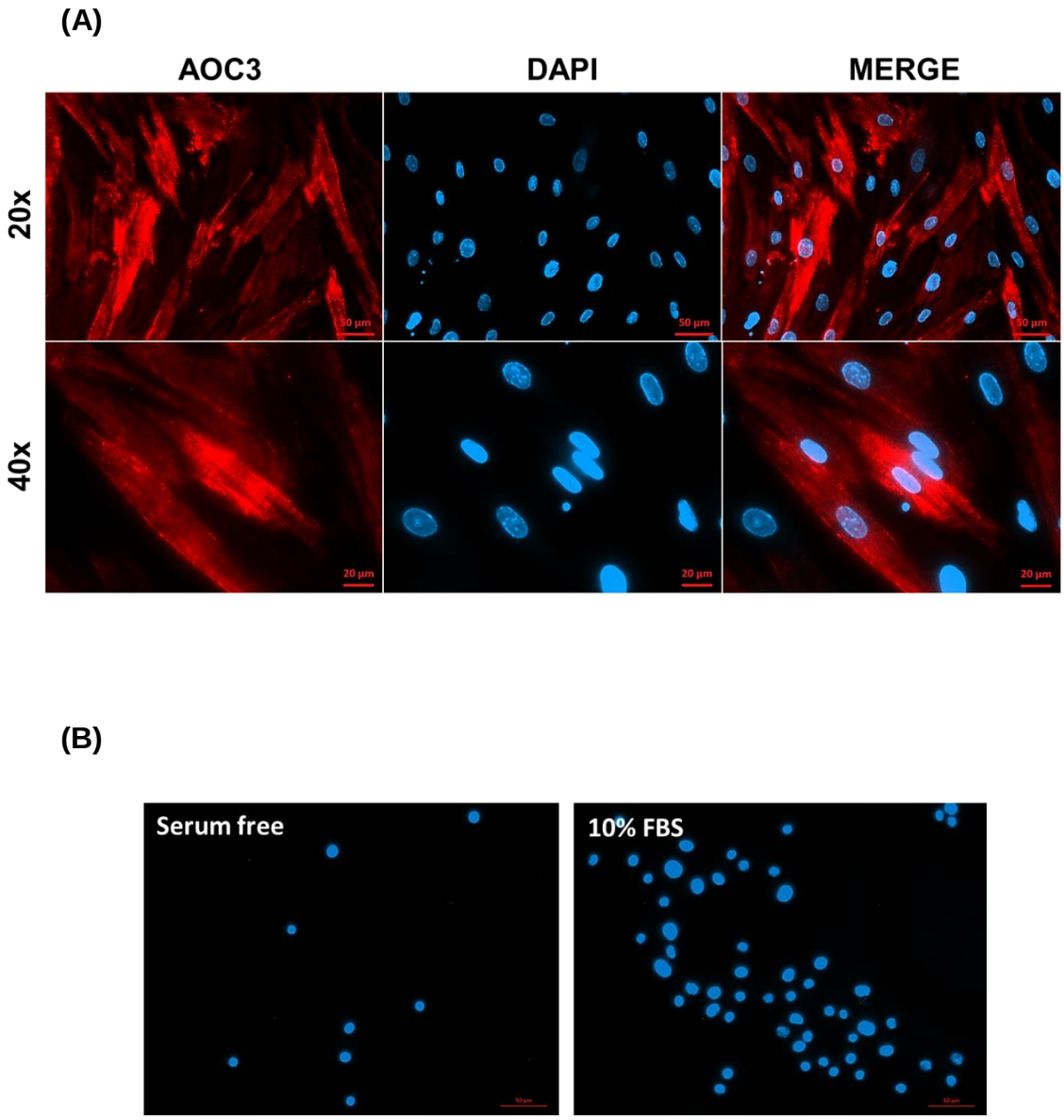

Figure 4.5

Positive immunofluorescence staining of AOC3 in myofibroblasts (CCD-18Co) and lack of AOC3 staining in CRC cell line (RKO).

Representative images of live staining of AOC3 (TK8-14, Santa Cruz) in CCD-18Co visualized at 20x and 40x magnification are shown in (A). (B) RKO was included in the IF staining (either been treated with serum free medium or 10% serum) as negative control for AOC3, shows no visible staining (Magnification: 20x). AOC3 (red), DAPI (blue).

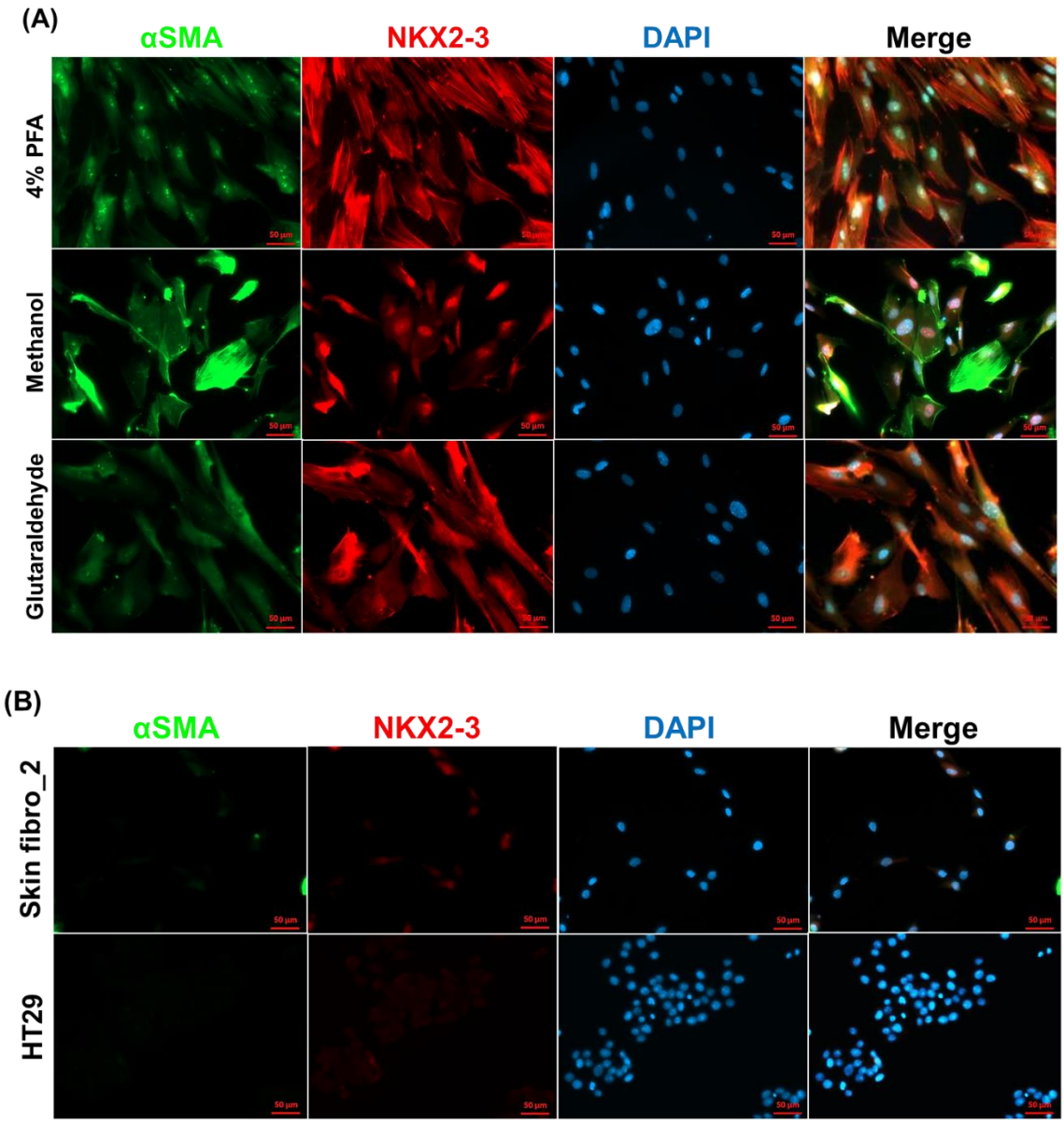

Figure 4.6

Localization and expression of NKX2-3 in different cell types

Variability in the NKX2-3 staining patterns in CCD-18Co, fixed with various fixative solution (4% PFA (paraformaldehyde), ice cold methanol or 0.02% glutaraldehyde) using the best commercially available antibody (LSBio) are shown in (A). Methanol fixation produced most accurate and reliable result of NKX2-3 staining indicated by strong NKX2-3 nuclear staining and much lower staining intensity in the cytoplasm. αSMA staining in CCD-18Co is included as positive control for myofibroblasts. (B) No visible staining of NKX2-3 and αSMA was observed in methanol fixed-skin fibroblasts and CRC cell line (HT29). NKX2-3 (red), αSMA (green), DAPI (blue) (Magnification: 20x).

To confirm the localization of both AOC3 and NKX2-3 in myofibroblasts shown by the IF staining, the expression of these proteins was verified in cytoplasmic and nuclear fractions of CCD-18Co (**Fig 4.7**). Notably, AOC3 is found to be expressed exclusively in the cytoplasm of CCD-18Co whereas NKX2-3 is expressed in both cytoplasm and nucleus. The appropriate loading controls were included: beta-tubulin and full length lamin A/C for respectively the cytoplasmic and nuclear compartments. In contrast to other publications where β-actin was found mainly in the cytoplasm fraction in comparison to nuclear extract (Sun et al., 2016), our data shows the detection of β-actin protein in both extracts of cytoplasm and nucleus. This is may be due to the poor quality of the antibody which contribute to its lack of specificity in assessing the localization of β-actin in cellular component extracts.

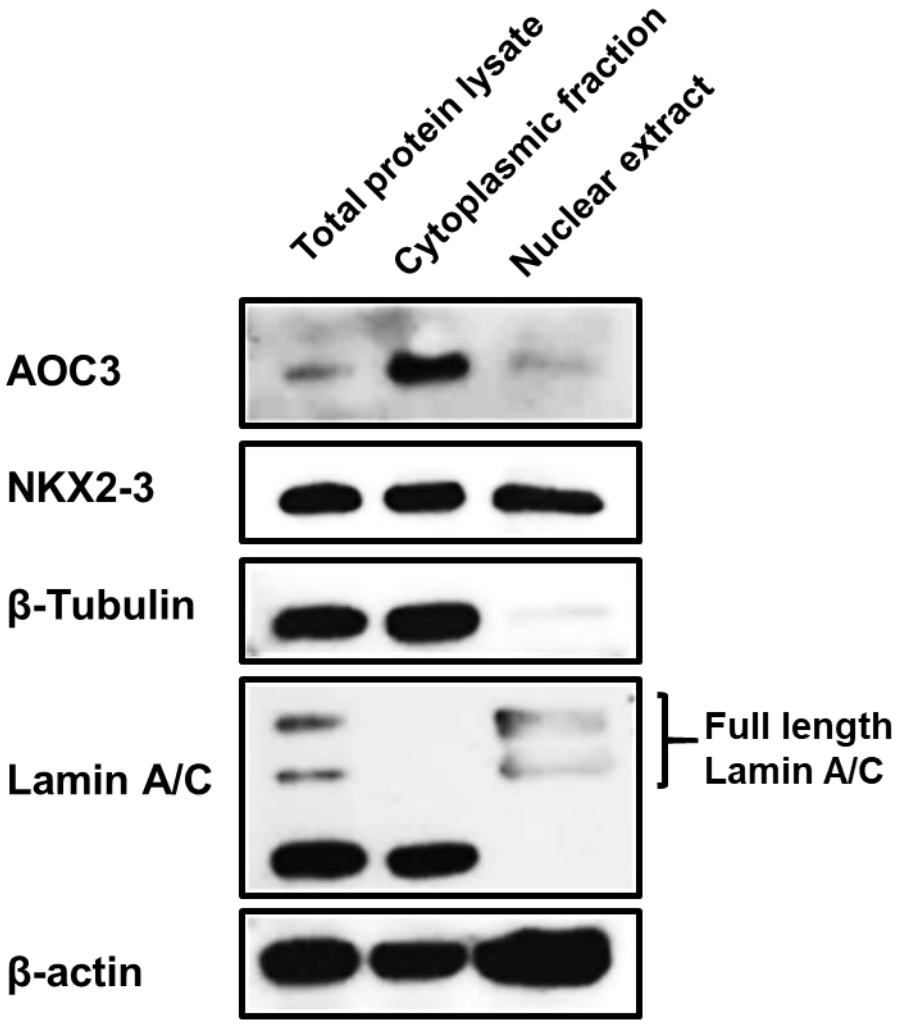

Figure 4.7

Localization of AOC3 & NKX2-3 in CCD-18Co.

AOC3 is predominantly being expressed in the cytoplasmic fraction whereas NKX2-3 can be found in both cytoplasmic and nuclear extract of CCD-18Co (Controls for; Cytoplasm: β-Tubulin, Nucleus - Lamin A/C).

4.2.3 Regulation of AOC3 and NKX2-3 expression in myofibroblasts

A more thorough screening was performed to compare the protein expression of both AOC3 and NKX2-3 in a panel of primary myofibroblasts. Western blot results (**Fig 4.8**) show that NKX2-3 is highly expressed across all primary MFs whereas AOC3 expression is more heterogeneous with the highest expression for Myo 7395 and Myo 8873 (both myofibroblasts derived from normal colon). Most of the selected myofibroblasts had no or low expression of AOC3 in the presence of 10% FBS. Skin fibroblasts were used as negative controls for NKX2-3 expression. Gene expression analysis of *AOC3* and *NKX2-3* in primary myofibroblasts cultured in normal culture medium (10% FBS) clearly validates high mRNA level of these two genes in myofibroblasts when compared to foreskin fibroblasts (**Fig 4.9**).

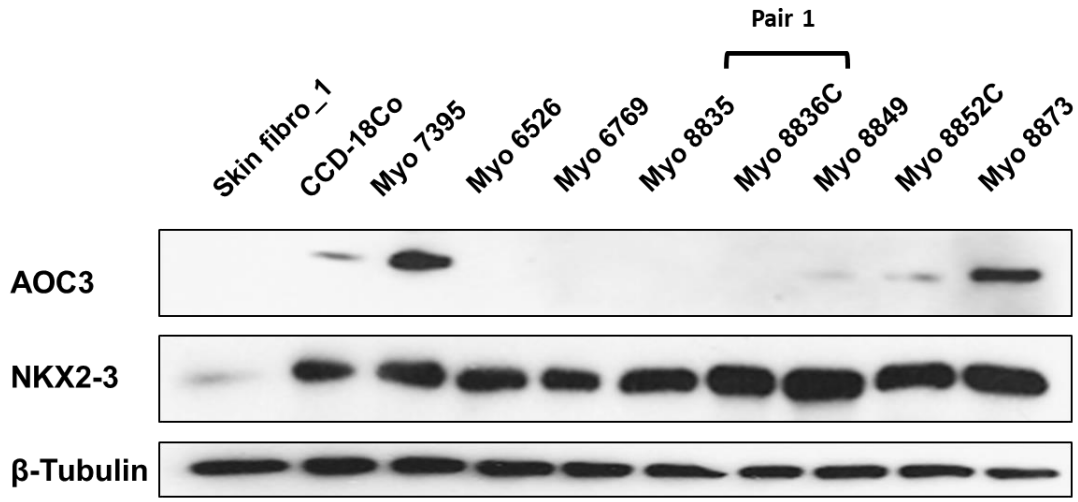

Figure 4.8

Screening of AOC3 and NKX2-3 protein expression across primary myofibroblasts after 3 days incubation in full medium (DMEM + 10% FBS).

NKX2-3 is highly expressed uniformly in all myofibroblasts while heterogenous expression of AOC3 was found across the myofibroblasts samples. Skin fibroblasts act as negative controls for the screening.

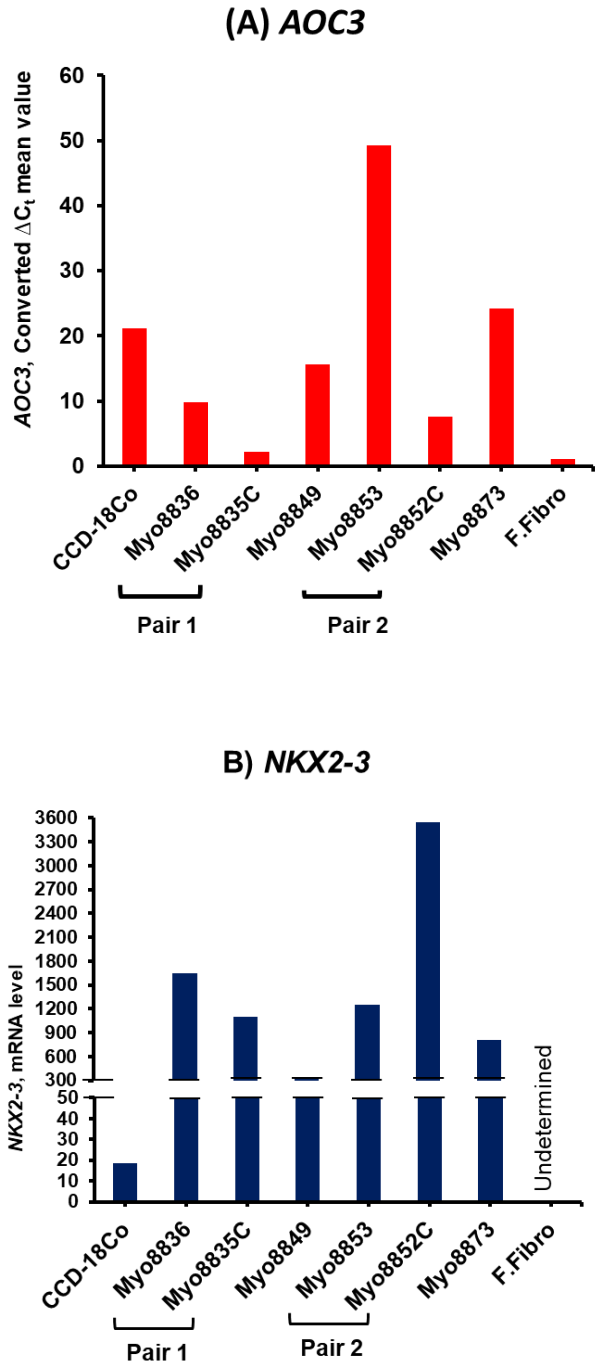

Figure 4.9

Screening of (A) *AOC3* and (B) *NKX2-3* gene expression in primary myofibroblasts maintained in full serum (10% FBS) using qRT-PCR.

Comparatively, *NKX2-3* is expressed at a much higher level compared to *AOC3* in myofibroblasts. CCD-18Co has lower expression of *NKX2-3* in comparison to other myofibroblasts. No detectable levels of *AOC3* and *NKX2-3* was found in F. fibro (F. fibro: foreskin fibroblasts).

To validate the expression level of and the influence of serum in AOC3 and NKX2-3, a screening using several of the established myofibroblasts was performed (**Fig 4.10**). Similar cell passage number for the three pairs of myofibroblasts (from cancerous and adjacent normal tissues) was used. The AOC3 expression is clearly upregulated in serum free condition in all myofibroblasts except for Myo8872C, which supports the previous finding. NKX2-3 expression seems to be higher under normal culture condition (presence of 10% serum) in comparison to treatment with serum free medium. Minor changes were observed in αSMA expression in different myofibroblasts between serum free condition and 10% FBS. It is worth noting that this result (**Fig 4.10**) represents two different western blot films. Inclusion of a control (cells with known positive/negative expression of screened protein) in every blot would provide a normalization for the reading of protein expression in tested cells.

The initial findings on the influence of serum on NKX2-3 expression was supported by the kinetics study of NKX2-3 expression in CCD-18Co under serum free and full serum condition. A clear upregulation of NKX2-3 seen in myofibroblasts maintained in full (10%) serum over time (**Fig 4.11A**). Immunofluorescence staining further validates this result where stronger NKX2-3 staining was detected in CCD-18Co cultured in the medium with 10% serum, in comparison to serum free condition (**Fig 4.11B**). A positive control for the myofibroblasts, αSMA was included in the experiment. Heterogeneous cytoplasmic αSMA staining was observed in CCD-18Co under both experimental conditions although stronger intensity of the staining can be detected in 10% FBS treated CCD-18Co.

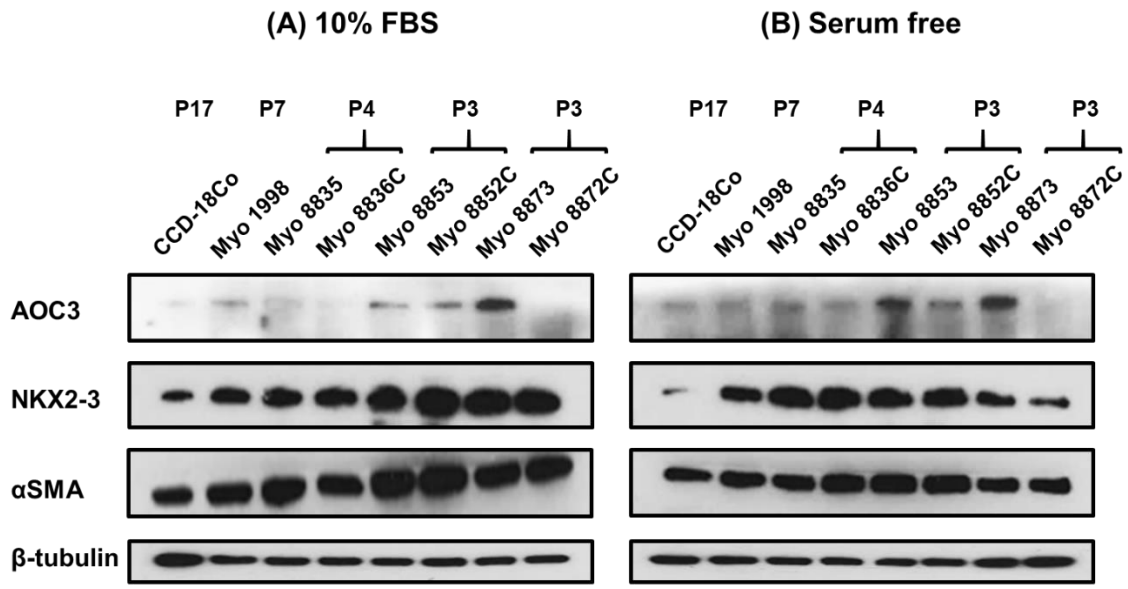

Figure 4.10

Expression of AOC3, NKX2-3 and αSMA across primary myofibroblasts after 72 h of incubation (A) full serum (DMEM + 10% FBS) and (B) serum free medium.

AOC3 expression in myofibroblasts was, as had been shown before, upregulated when treated with serum free medium when compared to 10% serum (FBS). Lower expression of AOC3 was found in myofibroblasts derived from cancerous tissues in comparison to their matched normal pair (Myo 8853 vs 8852C and Myo 8873 vs 8872C). Upregulation in the expression of NKX2-3 was observed in the presence of 10% FBS, most notably in CCD-18Co and Myo 8872C. Very little difference was seen in αSMA expression between serum free condition and 10% serum. Similar passage numbers for three myofibroblasts pairs were included in the experiment (P = cell passage number).

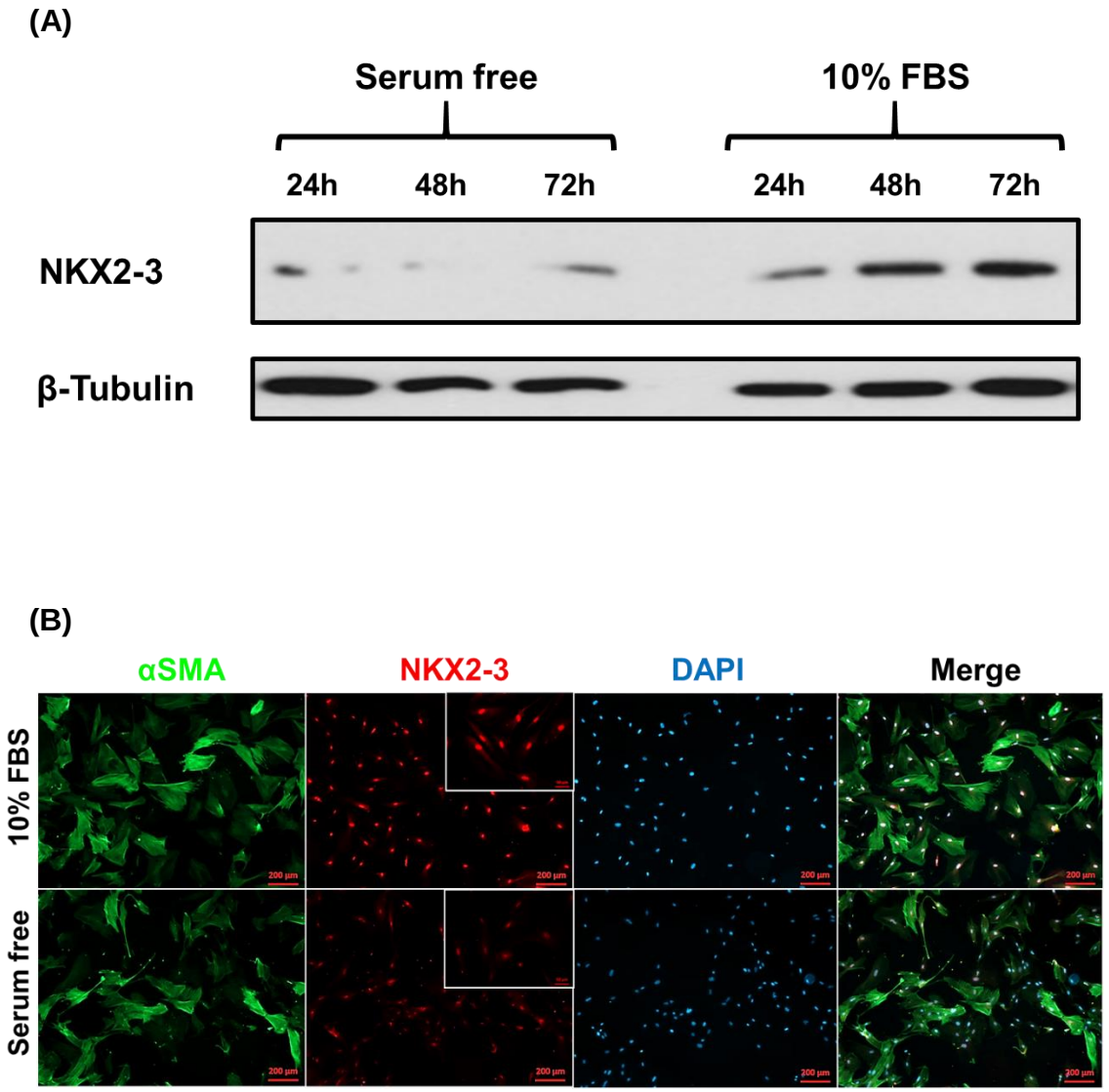

Figure 4.11

The influence of serum on the protein expression of NKX2-3 in myofibroblasts.

(A) Expression of NKX2-3 was upregulated in the presence of 10% FBS as compared to serum starved CCD-18Co. NKX2-3 expression increases overtime more notably under full serum condition. (B) The upregulation of NKX2-3 expression in CCD-18Co maintained in DMEM + 10% FBS for 48 h is visualised with immunofluorescence staining. Weaker NKX2-3 staining intensity was observed in serum free medium-treated group (Magnification: 5x). Enlarged representative images of NKX2-3 from each respective group was included in (B) (Magnification: 20x).

4.2.4 Immunohistochemistry staining of AOC3 and NKX2-3 in parental tumour

Immunohistochemistry (IHC) staining of the FFPE sections from the parental tumours from which myofibroblasts were isolated was performed. Heterogeneous staining intensity of AOC3 was been observed across different samples (**Fig 4.12**). Uniform AOC3 staining in pericryptal cells surrounding the colonic crypt was seen in normal parental tissues in comparison to more irregular staining profile in cancer samples. Strong staining of AOC3 was visualized in Myo 8873 while less fluorescence intensity of AOC3 staining was observed in the other two myofibroblasts (Myo 8835 and Myo 8853). This observation corroborates with previous western blot results (**Fig 4.8**) where Myo 8873 expressed higher protein level in comparison to Myo 8835. As for the parental tumour, the staining of AOC3 evidently shows the accumulation of myofibroblasts surrounding the crypt. It is also noticeable from the staining of the cancerous colon tissues that the tissue organization was highly disrupted due to the formation of the tumour, which is different from normal tissue.

We found discrepancy in the localization of NKX2-3 in IHC staining on FFPE sections thus the result is not shown. Considering previous immunofluorescence result where fixation hugely influenced NKX2-3 staining profile (**Fig 4.6**), NKX2-3 staining using the antibody from LSBio, included in this thesis, should be performed on cryosection of tissue fixed with cold methanol, instead of paraffin-fixed slides.

(A)

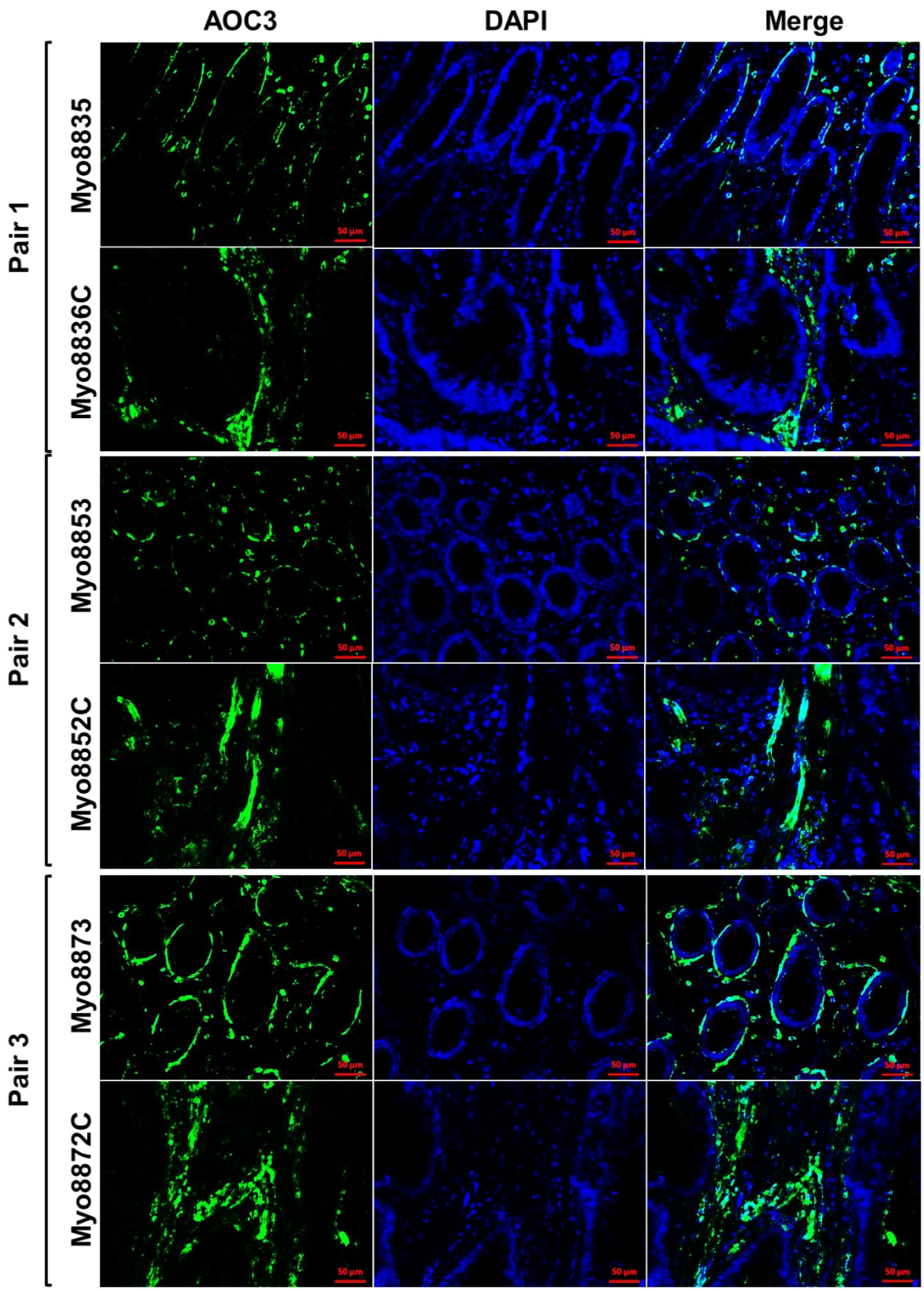

Magnification: 20x

(B)

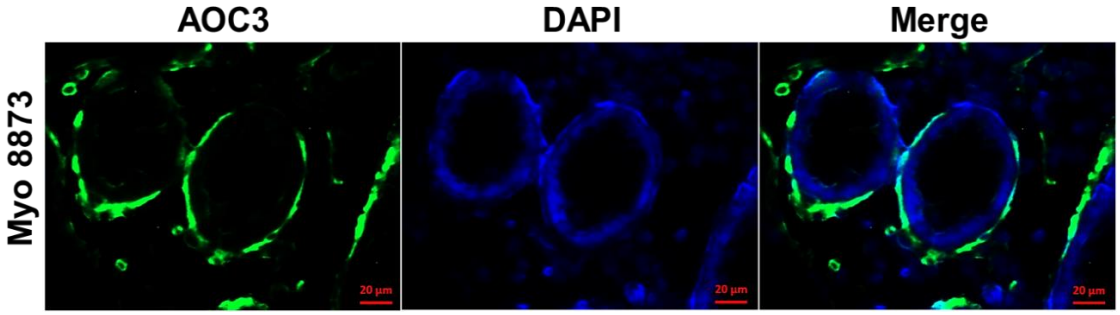

Magnification: 40x

Figure 4.12

IHC staining of AOC3 in matched pairs of parental (A) normal and (B) tumour colon tissues (FFPE sections).

IHC staining patterns of AOC3 (TK8-14, Santa Cruz) on three pairs of normal and tumour parental tissues (Myo 8835 vs 8836C; Myo 8853 vs 8852C and Myo 8873 vs 8872C) are shown in (A) (Magnification: 20x). AOC3 staining localizes at the pericryptal cells. Regular AOC3 staining was found in normal parental tissues while more irregular staining of AOC3 was observed in their matched cancer pairs. Myo 8873 which has highest AOC3 expression shows the strongest staining for AOC3 in myofibroblasts in the normal parental tissue. (B) Enlarged image of AOC3-stained Myo 8873 parental tissue shows staining in the cytoplasmic region of pericryptal myofibroblasts (magnification: 40x). AOC3 (green), DAPI (blue).

4.2.5 Microarray data for other myofibroblast associated genes.

In addition to *AOC3* and *NKX2-3*, several other genes that are apparently associated with the activation of myofibroblasts were studied, namely *ACTA2 MYH11* and *FAP.* Activation of myofibroblasts is often manifested by increase expression of *ACTA2* and *MYH11*, while *FAP* is strongly expressed by stromal fibroblasts of epithelial carcinomas. **Figure 4.13** shows the microarray data for the *ACTA2*, *MYH11* and *FAP* expression in myofibroblasts and skin fibroblasts. Both cell types show positive *ACTA2* expression. Only moderate expression for *MYH11* was found in all myofibroblasts and skin fibroblasts except for Myo 2020 which expressed high mRNA level of the gene. As for CRC cell lines, high expression of *ACTA2* was detected in only 4 of CRC cell lines while only 2 CRC cell lines expressed high level of *MYH11* (**Supplementary data S3**).

Significant expression of *FAP* can be detected in all the myofibroblasts and skin fibroblasts, with Myo 6024 and skin fibro_2, showing markedly higher levels than the others (**Fig 4.13**). The mRNA level of *FAP* in CRC cells is shown in **Figure 4.14**. Nearly all the epithelial cells have very low expression of *FAP.* Only lines OXCO1 and NCIH716 cell lines have markedly high levels of FAP expression but with possibly increased levels in three other lines. Interestingly, both OXCO1 and NCIH716 have been classified by our laboratory as epithelial-mesenchymal transition (EMT)-like CRC cells based on their level of expression of EMT markers.

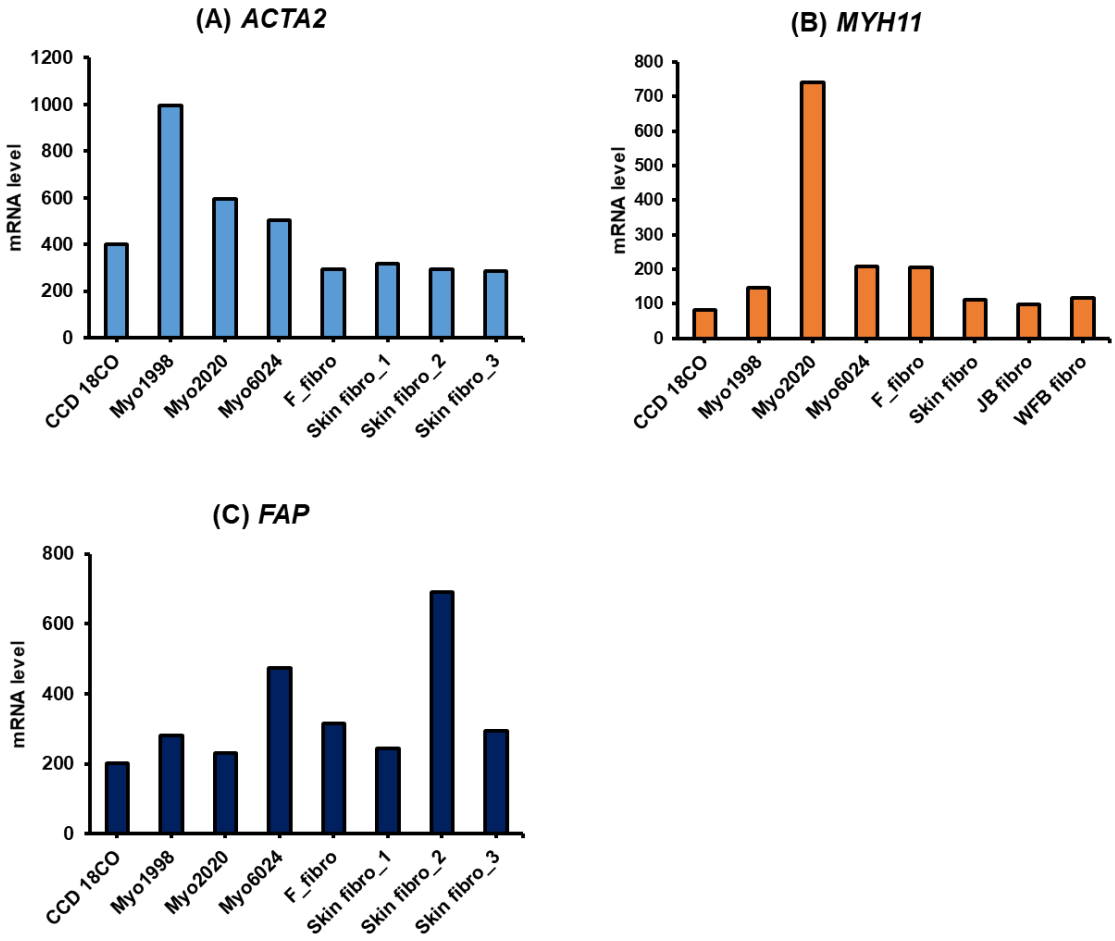

Figure 4.13

Microarray data of *FAP* expression in myofibroblasts and skin fibroblasts. *ACTA2* is highly expressed by different samples of myofibroblasts and skin fibroblasts (A). Moderate expression of *FAP* was found in both cell types (mRNA levels of approximately 200) except for Myo 6024 and skin fibro 2, where higher mRNA values were detected as compared to other samples. *MYH11* expression levels in all samples are lower when compared to the two other genes although a relatively high mRNA level was seen in Myo 2020 (skin fibro: skin fibroblasts).

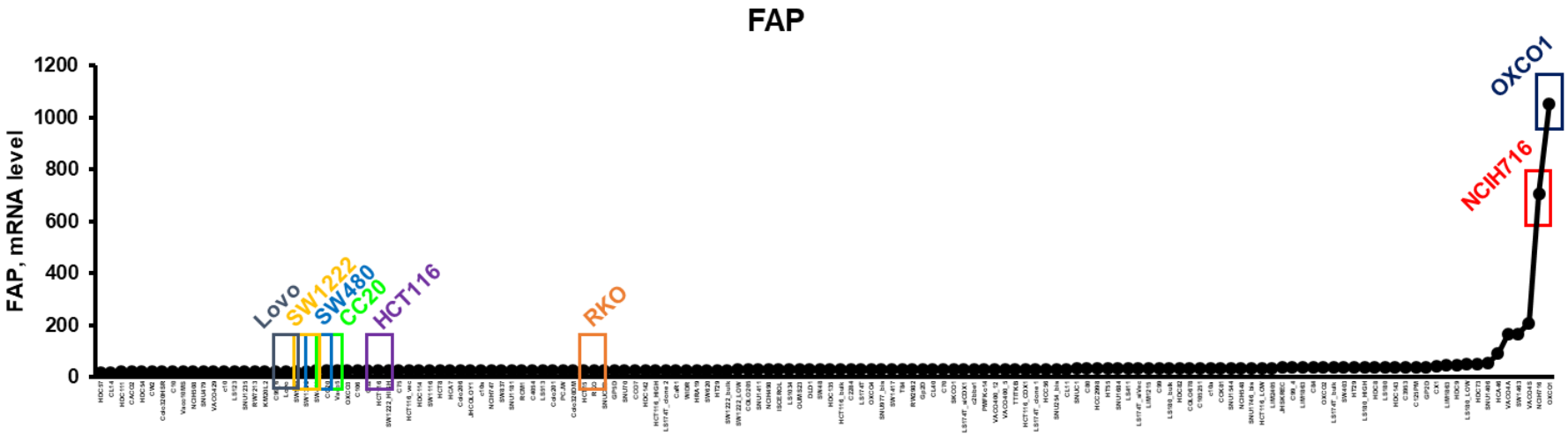

Figure 4.14

The expression of *FAP* in CRC cell lines.

High mRNA level of FAP was only detected in 6 CRC cell lines where OXCO1 and NCIH716 are the two lines with the highest expression of this gene. The FAP expression in OXCO1 and NCIH716 was compared to those lines with low expression of FAP such as Lovo, SW1222, SW480, CC20, HCT116 and RKO, shown in later section of this chapter.

4.2.6 The influence of growth factors on the regulation of AOC3 and NKX2-3 expression in myofibroblasts

Our previous findings clearly indicate the influence of serum on the expression of selected genes in myofibroblasts and this raises fundamental questions concerning the role of the growth factors present in serum in the direct regulation of those genes. The choice of the candidate growth factors tested was based on a thorough literature search on the composition of serum together with previous data from our laboratory. The influence of arrange of growth factors including TGFβ1, EGF, TNFα, FGFβ, HGF, VEGF, PDGF-AA and IGF1 on gene regulation in myofibroblasts was investigated. These growth factors also are potentially secreted by the CRC cells *in vivo* which may lead to certain changes in the properties of the myofibroblasts. The candidate genes to be screened for the effects of growth factors were selected based on the previous microarray analysis performed by our lab of differentially expressed genes between myofibroblasts and fibroblasts, namely *AOC3*, *NKX2-3* and *LRRC17* (high expression in myofibroblasts) and *SHOX2* (low expression in myofibroblasts). *ACTA2* which is expressed at high levels in myofibroblasts, were also included in the screening along with *MYH11*. We were also interested in *FAP* expression as its expression appears to reflect the activation state of myofibroblasts.

The data from qRT-PCR revealed that there was significant downregulation of *AOC3* in CCD-18Co after 72 h treatment with 10% FBS, TGFβ1, EGF and PDGF-AA (**Fig 4.15**). *NKX2.3* is also downregulated in the presence of serum,

which contradicts the previous western blot results (**Fig 4.11**) where the protein expression of NKX2-3 is upregulated after treatment with full serum medium. The discrepancy observed in the regulation of NKX2-3 between gene and protein level is discussed further in Chapter 6. Like *AOC3*, we observed a significant downregulation of *NKX2-3* in the presence of EGF and PDGF-AA.

Strikingly, analysis of the influence of the growth factors on *ACTA2* demonstrates that only TGFβ1 upregulates the *ACTA2* expression in CCD-18Co. Minimal effects on the *ACTA2* expression were observed post-treatment with other growth factors except for EGF and PDGF-AA. Both EGF and PDGF-AA significantly downregulate the *ACTA2* expression. A similar response was seen with *MYH11* where *MYH11* expression was upregulated after incubation with TGFβ1 and downregulated post-treatment with EGF and PDGF-AA. Screening of *LRRC17* in CCD-18Co shows that it is abundantly expressed at basal level. We found that only TGFβ1 treatment upregulated its gene expression. There was no significant effect of growth factors on *SHOX2* and *FAP* expression in CCD-18Co.

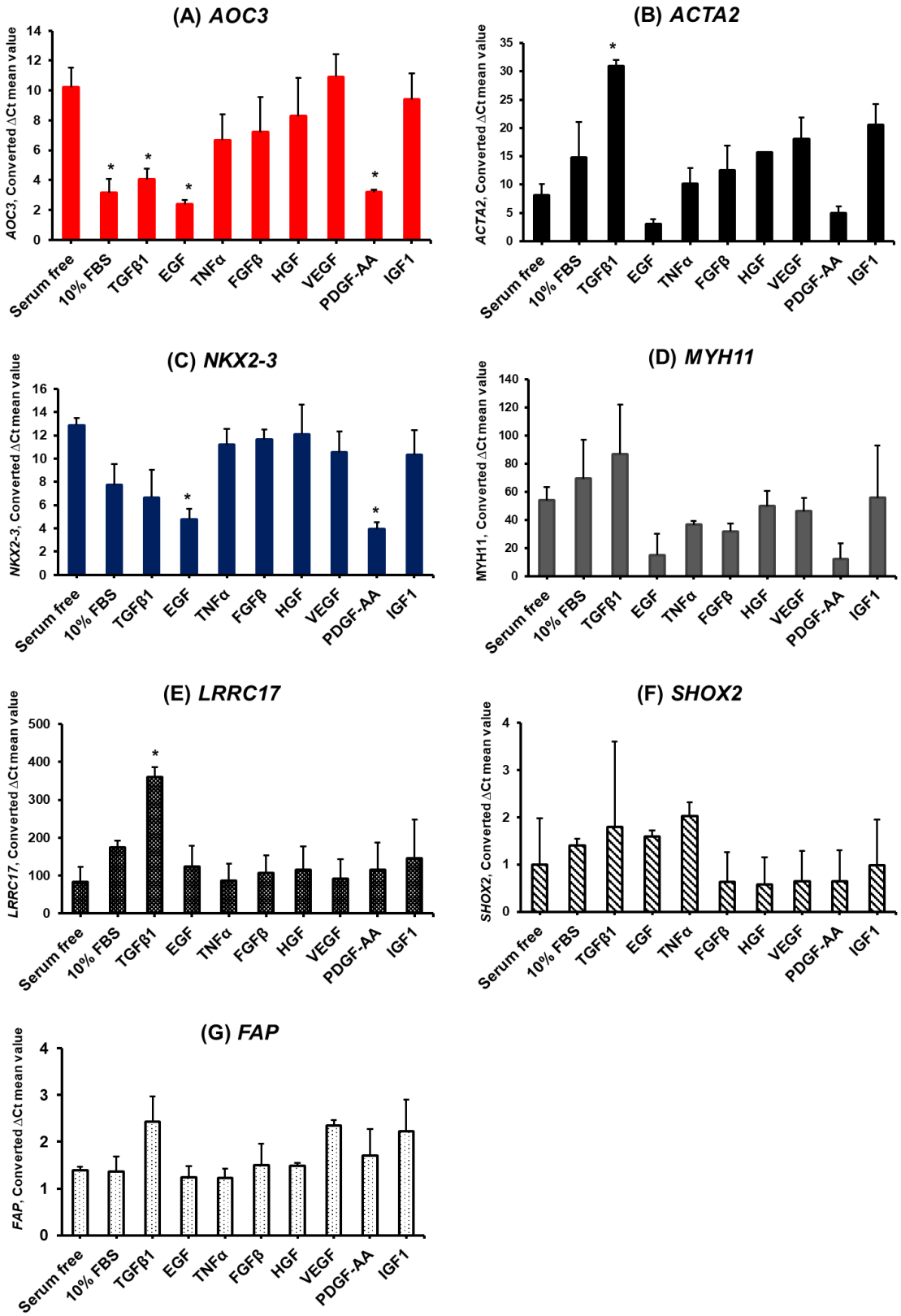

Figure 4.15

The influence of growth factors on (A) *AOC3*; (B) *ACTA2*; C) *NKX2-3*; (D) *MYH11*; (E) *LRRC17*; (F) *SHOX2* and (G) *FAP* expression in CCD-18Co.

The effects of various growth factors on *AOC3* expression were verified at protein level using western blots. There was downregulation of AOC3 protein expression detected in CCD-18Co incubated with TGFβ1, EGF and PDGF-AA, in comparison to serum free conditions (**Fig 4.16**). No significant effects of growth factor treatment were seen on NKX2-3 regulation in CCD-18Co. which, again, is in contradiction with the qPCR data (**Fig 4.15**). Upregulation of αSMA expression was observed upon TGFβ1 treatment although this might not be at a significant level when compared to other growth factor treatments. Treatment with EGF resulted in downregulation of αSMA, which is in agreement with previous qRT-PCR data. The influence of the four growth factors was also confirmed using immunofluorescence staining of CCD-18Co (**Fig 4.17**). Strong AOC3 staining was seen in CCD-18Co treated with serum free condition as opposed to other groups (10% serum, TGFβ1 and EGF) where weak staining of AOC3 was detected which agrees with the western blot data.

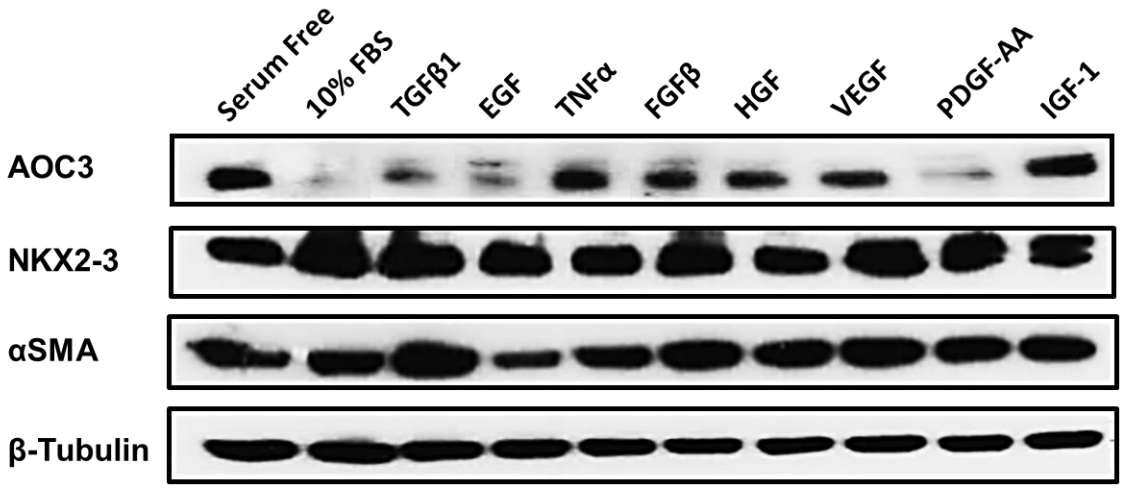

Figure 4.16

The effect of growth factor treatment on the AOC3, NKX2-3 and αSMA protein expression in myofibroblasts

TGFβ1, EGF and PDGF-AA downregulate AOC3 expression. This finding verifies the previous results at gene level (**Fig 4.15**). No significant changes in the NKX2-3 protein expression were observed after incubation with different growth factors. Some downregulation in αSMA expression was found in CCD-18Co treated with EGF.

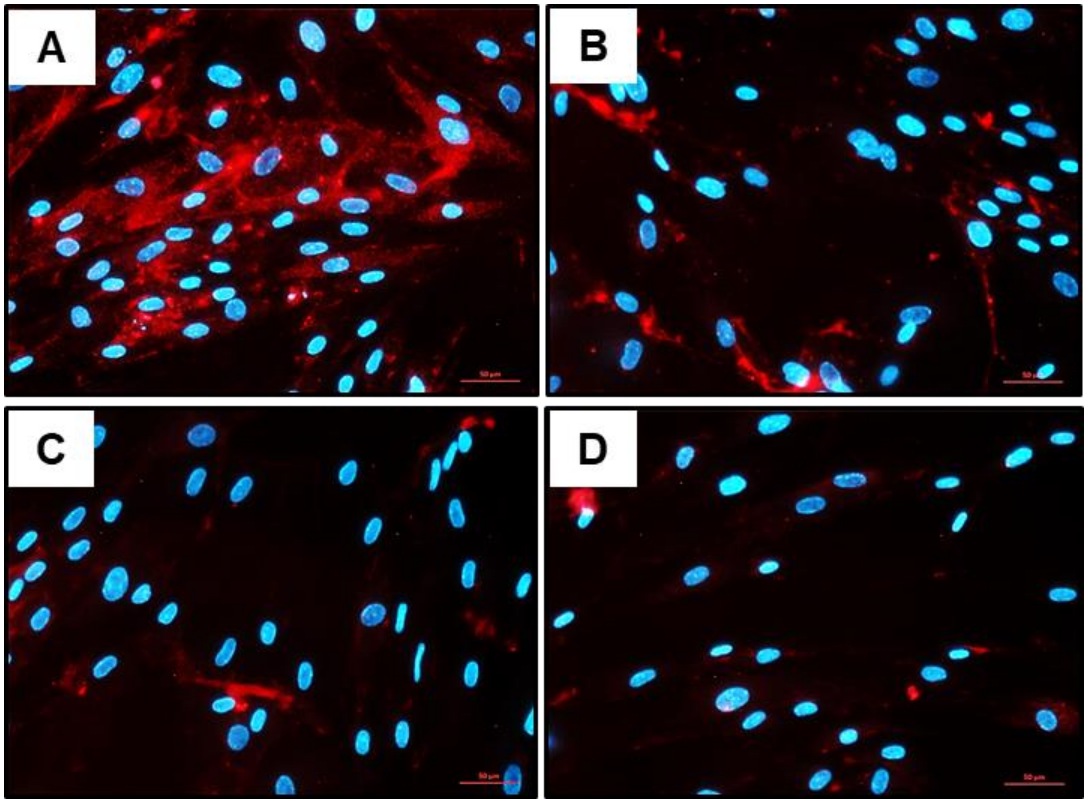

Figure 4.17

The immunofluorescence staining of AOC3 in CCD-18Co incubated with (A) serum free medium; (B) 10% FBS; (C) TGFβ1 and (D) EGF for 72 h.

Strong staining for AOC3 was detected in serum starved CCD-18Co in comparison with other groups indicating upregulation of AOC3 expression after treatment with serum free medium alone.

The effect of various growth factors on protein expression in a primary myofibroblasts from a normal section of colon (Myo 8873) also was performed to confirm the previous finding in CCD-18Co. Western blot results show a similar pattern of AOC3 expression in Myo 8873 and CCD-18Co after incubation with different growth factors except for the IGF1 treatment group (**Fig 4.18**). The presence of serum, TGFβ1, EGF, PDGF-AA and IGF1 downregulated the AOC3 expression in Myo 8873. Minimal affect was observed in NKX2-3 expression after treatment with growth factors.

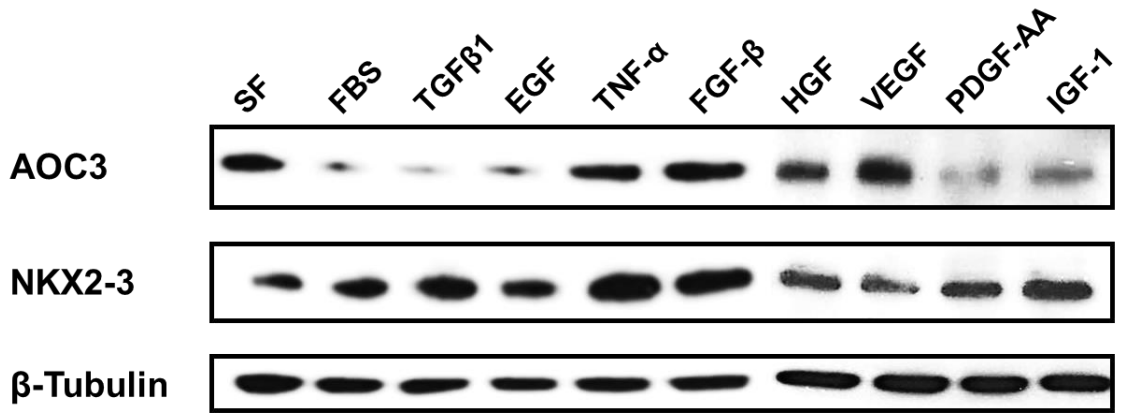

Figure 4.18

The influence of growth factor treatment on the expression AOC3 and NKX2-3 in primary myofibroblasts (Myo 8873).

The presence of 10% serum, TGFβ1, EGF and IGF1 downregulate the AOC3 expression in Myo 8873. Strong expression of NKX2-3 was observed in all the treatment groups.

4.2.7 Microarray data analysis of expression of growth factors and their respective receptors in myofibroblasts and CRC cell lines

Microarray data analysis was performed to identify the CRC cells, which may express the growth factors that influence the regulation of AOC3 in myofibroblasts, namely TGFβ1, EGF, PDGF-A and C (The regulation of AOC3 expression by PDGF-C is explained later in the next section – 4.2.10). Ten of the lowest and highest expressing CRC cells for *TGFβ1*, *EGF*, *PDGF-A* and *C* are listed in **Supplementary data S1**. From the table, only four CRC cells (CC20, OXCO1, CCO7 and c10s) express two or more of the selected growth factors at high levels (top 10 highest). **Figure 4.19** shows the ten CRC cell lines with the highest expression of *TGFβ1*, *EGF*, *PDGF-A* and *C*.

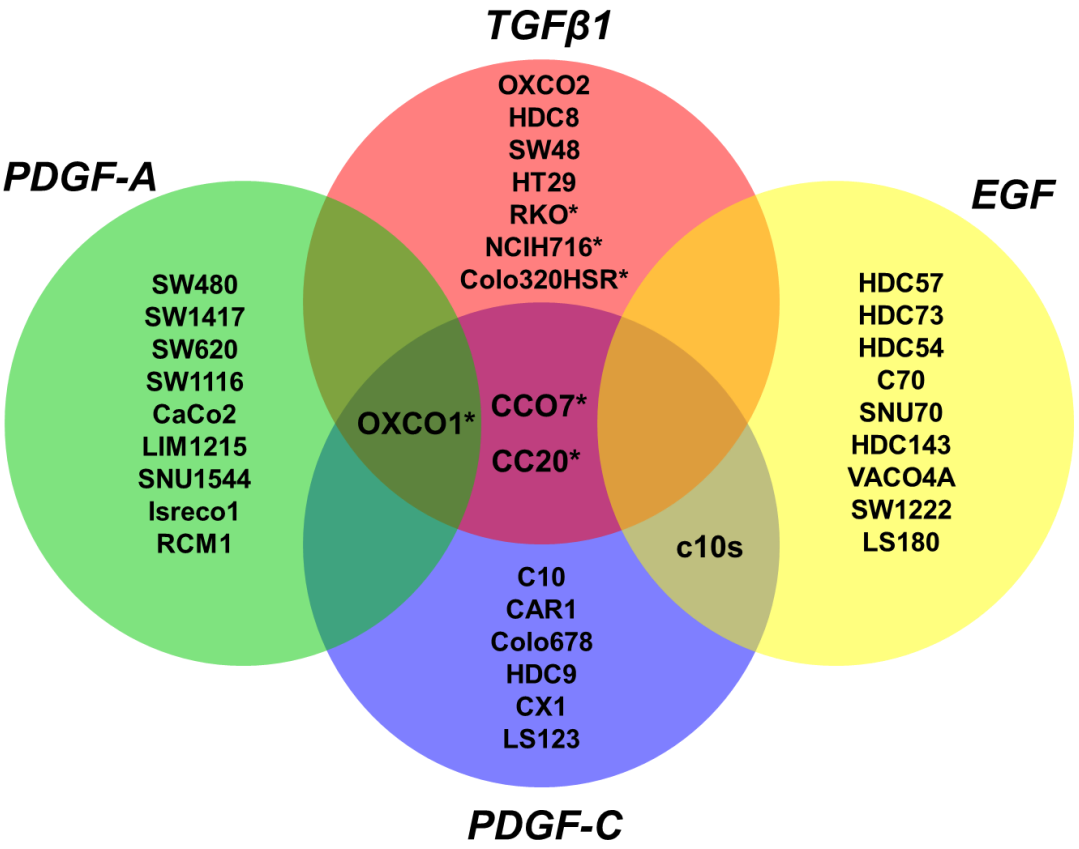

Figure 4.19

Ten of the highest growth factor-expressing CRC cells at mRNA level. OXCO1, CCO7, CC20 and c10s highly express two or more of selected growth factors (*TGFβ1*, *EGF*, *PDGF-A* and *C*) (*denotes the EMT-like cells).

We have used the microarray data available for the CRC cell lines, myofibroblasts and fibroblasts to assess the expression of both the ligands (*TGFβ1*, *EGF*, *PDGF-A* and *C*) and their respective receptors. This analysis was performed to determine the paracrine and/or autocrine signalling pathway between myofibroblasts and CRC cell lines. Paracrine signalling pathway is indicated by the expression of either the ligand or its receptor in cells, while cells that possess high expression of both the ligand and its receptor may indicate the involvement of autocrine signalling. Positive mRNA expression is defined by value more than 100 (High expression: mRNA value of more than 200), while

mRNA value of lower than that signifies low expression of a certain gene. The analysis of the expression of the growth factors (receptors and their ligands) is summarized as below:

a) *TGFBR* – High expression of three different receptors of TGFβ (*TGFBR*), namely *TGFBR1*, *2* and *3*, was found in majority of CRC cells. (**Supplementary data S2**). As shown in **Figure 4.20**, there is strong expression of *TGFBR1*, *2* and *3* in myofibroblasts and skin fibroblasts.

b) TGFBR ligand (*TGFβ1*) – One of the ligands for TGFBR is *TGFβ1*. Positive expression of *TGFβ1* was found in a subset of CRC cell lines (70 cancer cells possesses mRNA level of more than 100). Among the 10 high *TGFβ* expressing CRC cell lines (**Fig 4.19**), a total of six possess EMT-like properties. High expression of *TGFβ1* was observed in all myofibroblasts (**Fig 4.21A**).

c) *EGFR* – Most CRC cell lines expressed EGFR (mRNA level of more than 100). Myofibroblasts and skin fibroblasts have high expression of *EGFR*, with an exception of foreskin fibroblasts (**Fig 4.20**). This is in full agreement with the response of MFs to EGF ligand in respect to the downregulation of *AOC3* and *ACTA2*.

d) EGFR ligand (*EGF*) – Several EGFR ligands has been reported in literatures. The current study mainly focussing on one of ligands, namely EGF. Majority of the CRC cell lines did not express *EGF*. *EGF* expression was found only in 20 CRC cell lines shown in **Figure 4.20**. Low expression of *EGF* was detected in myofibroblasts and skin fibroblasts except for foreskin fibroblasts (**Fig 4.21**).

e) *PDGFR* – Very low mRNA level of both *PDGFRA* and *B* was found in

CRC cell lines (mRNA level below 100). Myofibroblasts have high mRNA level of *PDGFRA* (values of more than 1000) which is a receptor for *PDGF-A* and *C*, except for foreskin fibroblasts (value: 270) (**Fig 4.21**). Moderate expression of *PDGFR-B* was found in myofibroblasts.

f) PDGFR ligands (*PDGF-A* and *C*) – Two isoforms of PDGF which make up PDGF ligands (PDGF-AA and CC) of interest in this study are *PDGF-A* and *C*. Specific binding of these PDGF isoforms to homodimeric and heterodimeric PDGF receptors induces their cellular effects. As shown in **Supplementary data S4**, high expression of both ligands was detected in CRC cell lines. Myofibroblasts and most of skin fibroblasts did not express *PDGF-A*. Foreskin fibroblasts and two of skin fibroblasts have high expression of *PDGF-A* and *C* respectively (**Fig. 4.21**)

Microarray analysis revealed that CRC cells and myofibroblasts only express either the ligand or its receptor with exceptions for *TGFβ1* and *TGFBR*s. High expression of *TGFβ1* was found in 70 CRC cell lines and *TGFBR*s are highly expressed by all cancer cell lines. Myofibroblasts and skin fibroblasts express both high level of *TGFβ1* and *TGFBR*s. The possibility of a paracrine *vs* autocrine signalling pathway between myofibroblasts and CRC cell lines based on our microarray data analysis is discussed further in the discussion section of this chapter.

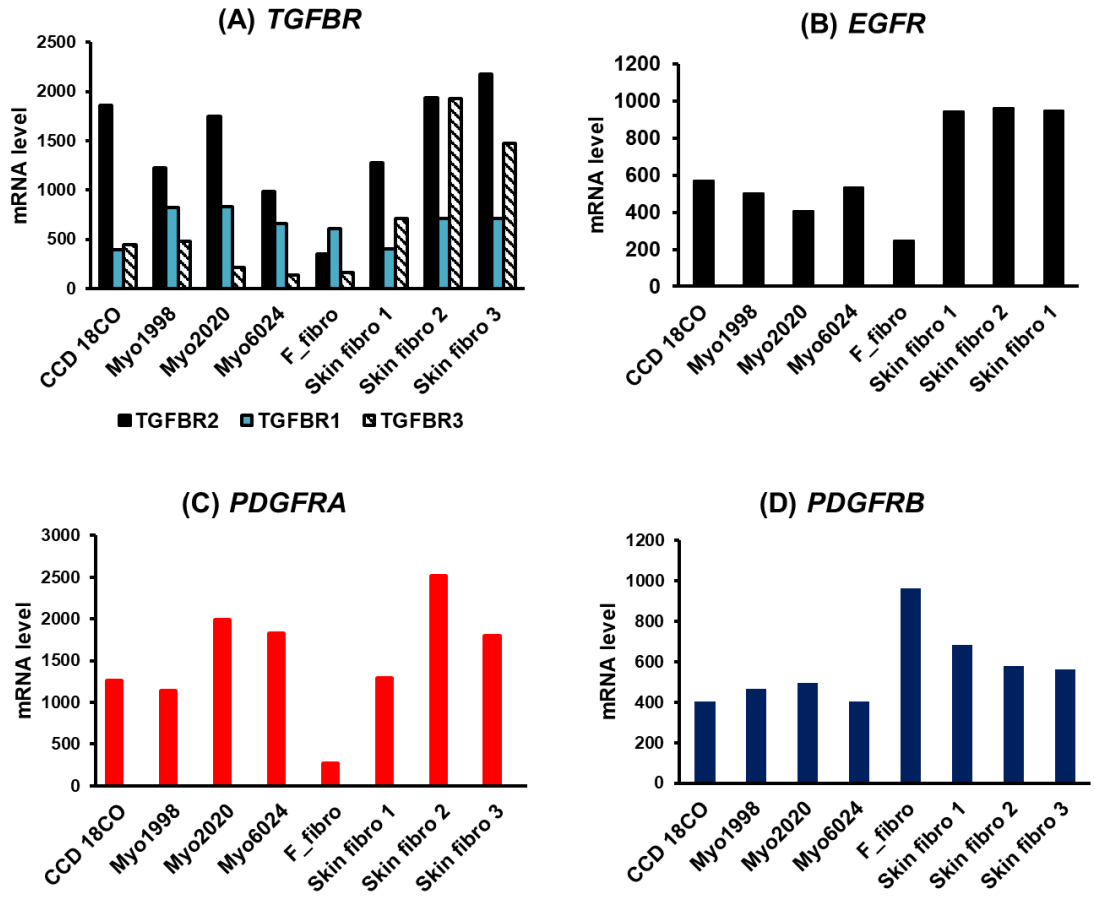

Figure 4.20

Microarray data on expression of *TGFBRs*, *EGFR* and *PDGFRA* in the myofibroblast and skin fibroblast cell lines.

TGFBRs, *EGFR* and *PDGFRA* are highly expressed by all myofibroblasts and skin fibroblasts with an exception of F_fibro where lower mRNA levels of those receptors were found. Differential expression of these genes between F_fibro and other skin fibroblasts and myofibroblasts may be due to its origin of which F_fibro was isolated from a neonate, unlike from other samples which derived from adult tissues (F_fibro: foreskin fibroblasts

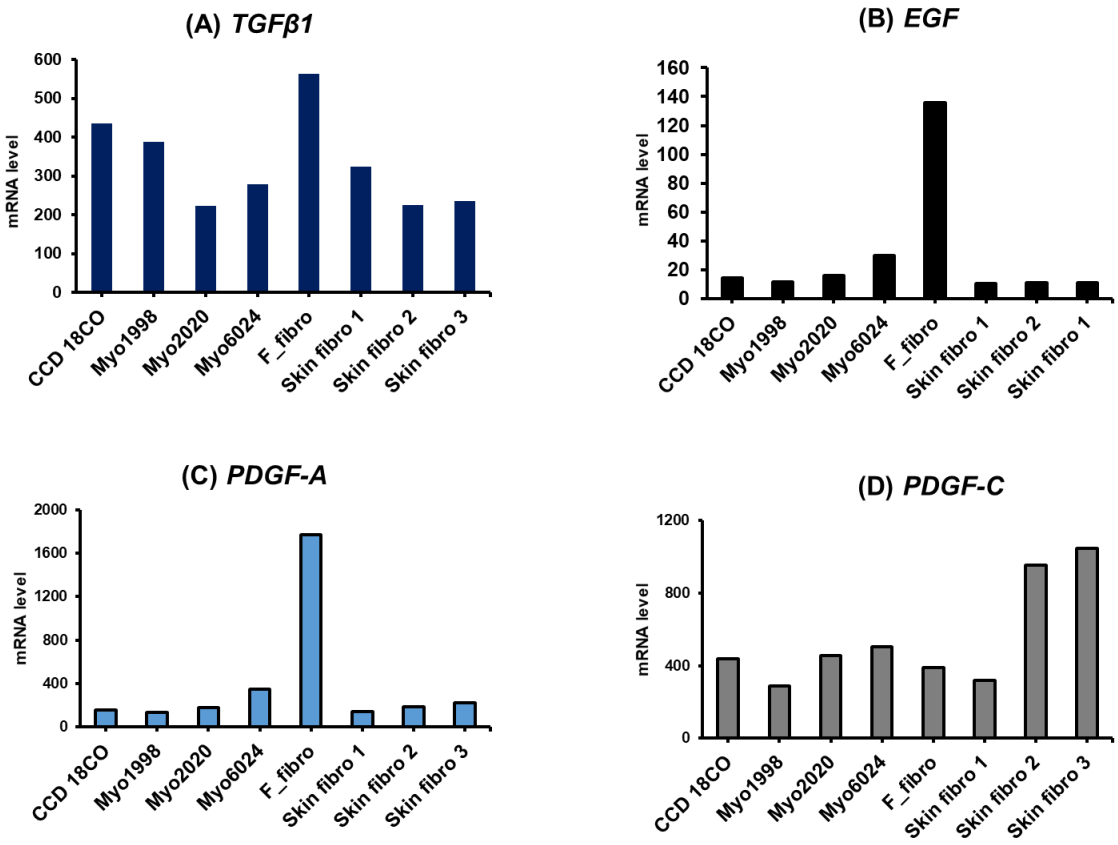

Figure 4.21

Microarray data on the expression of *TGFβ1*, *EGF*, *PDGF-A* and *C* in myofibroblast and skin fibroblast cell lines.

High expression of *TGFβ1* was found in all myofibroblasts and skin fibroblasts, while *EGF* and *PDGF-A* are expressed at low levels in those samples, with an exception for F_fibro. *TGFβ1*, *EGF* and *PDGF-A* are expressed by F_fibro, at much higher levels compared to other myofibroblasts and skin fibroblasts. High mRNA level of *PDGF-C* was found in two of the skin fibroblasts (skin fibro 2 and 3).

4.2.8 Regulation of *AOC3* and *NKX2-3* expression by TGFβ1 in a matched normal and cancer pair of primary myofibroblasts

An important signalling pathway in colorectal cancer is the TGF*β* signalling pathway. The influence of TGFβ1 treatment on the gene expression in primary myofibroblasts (normal and cancerous pair) was studied using qRT-PCR analysis. As demonstrated in CCD-18Co, there was a significant upregulation in *AOC3* expression in Myo 8835 and 8836C maintained in serum free medium for 72 h. Treatment with TGFβ1 downregulated *AOC3* expression in both primary myofibroblasts to comparable level to 10% serum (**Fig 4.22**). It is worth noting that Myo 8836C has a slightly lower *AOC3* mRNA basal level than its normal counterpart. Both myofibroblasts have comparable *NKX2-3* expression and TGFβ1 treatment clearly leads to its downregulation. This finding suggests a stable expression of *NKX2-3* in myofibroblasts, regardless of the origin of the tissue types (normal or cancer). As for TGFβ1's influence on *ACTA2* regulation, its expression in both Myo 8835 and Myo 8836C was elevated post-treatment with TGFβ1. The result also shows that Myo 8836C has higher level basal level (in the presence of 10% FBS) of *ACTA2* when compared to Myo 8835.

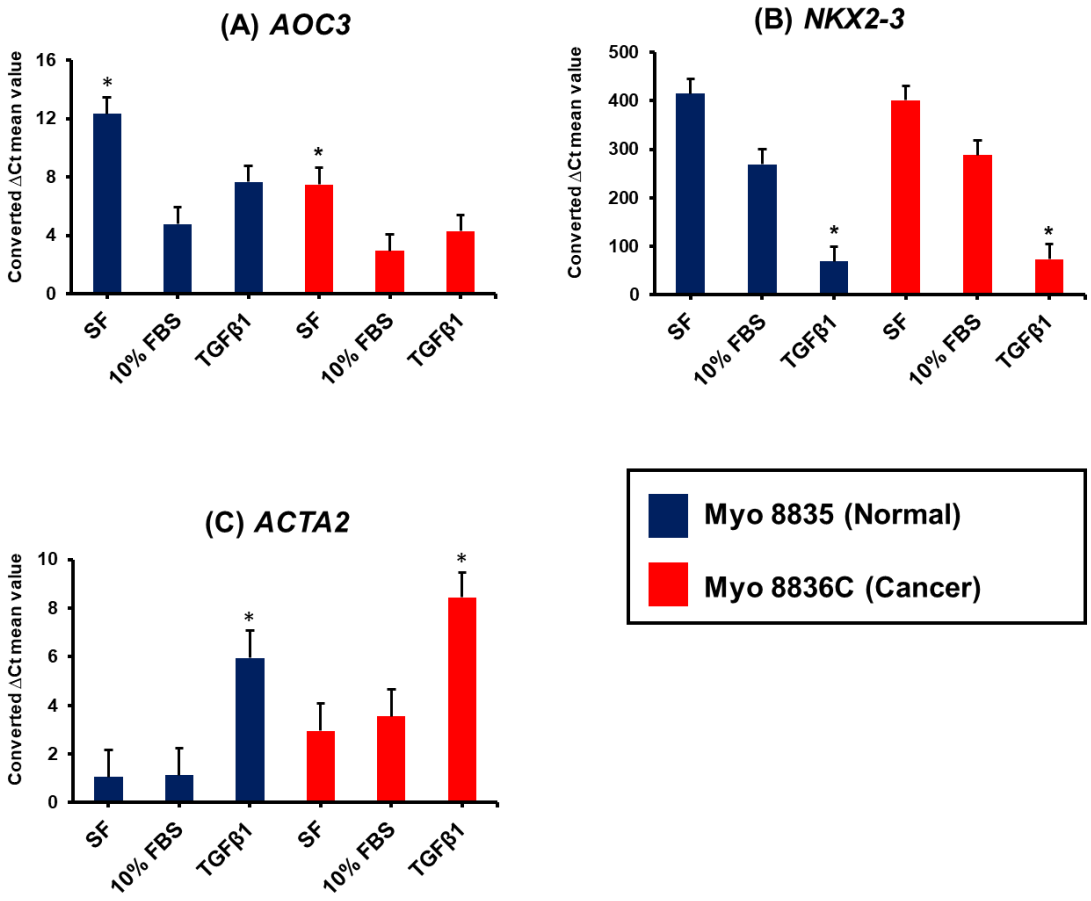

Figure 4.22

Effect of TGFβ1 on *AOC3*, *NKX2-3* and *ACTA2* mRNA expression in myofibroblasts from matched normal (Myo 8835) and cancerous tissue (Myo 8836C).

AOC3 expression in both samples was upregulated in serum free condition. Comparable basal levels of *AOC3* and *NKX2-3* expression (10% FBS) were found in the samples and a higher level of basal *ACTA2* expression was observed in Myo 8836C which is from cancerous colon tissues (*p<0.05 in comparison to 10% FBS from three biological experiments). TGFβ1 downregulated both *AOC3* and *NKX2-3* expression but upregulated *ACTA2* mRNA level in normal and cancer-derived myofibroblasts.

4.2.9 Treatment with EGF and its effect on gene expression in myofibroblasts

EGF is another growth factor of interest that regulates AOC3 expression in myofibroblasts. Over a duration of 72 h, we have compared the mRNA expression of *AOC3* in serum-free conditions with the addition or not of EGF. In the absence of EGF, data shows a gradual increase in the *AOC3* expression over time whereas EGF treatment induced a decrease that remains constant for all time points (**Fig 4.23A**). There is very little explanation of the effect of serum starvation on AOC3 expression. It is likely that unfavourable culture conditions (serum free condition) might lead to accumulation of free radicals and the cells reacted by producing more AOC3 to convert them to hydrogen peroxide and oxygen through enzymatic reaction to maintain optimal state for cell survival. This postulation has yet to be confirmed.

Expression of *NKX2-3* followed the exact same pattern as *AOC3* in both conditions. At protein level, the effect of EGF on the regulation of AOC3 expression in CCD-18Co is more significant at 72 and 96 h of treatment in comparison to serum free condition (**Fig 4.23B**).

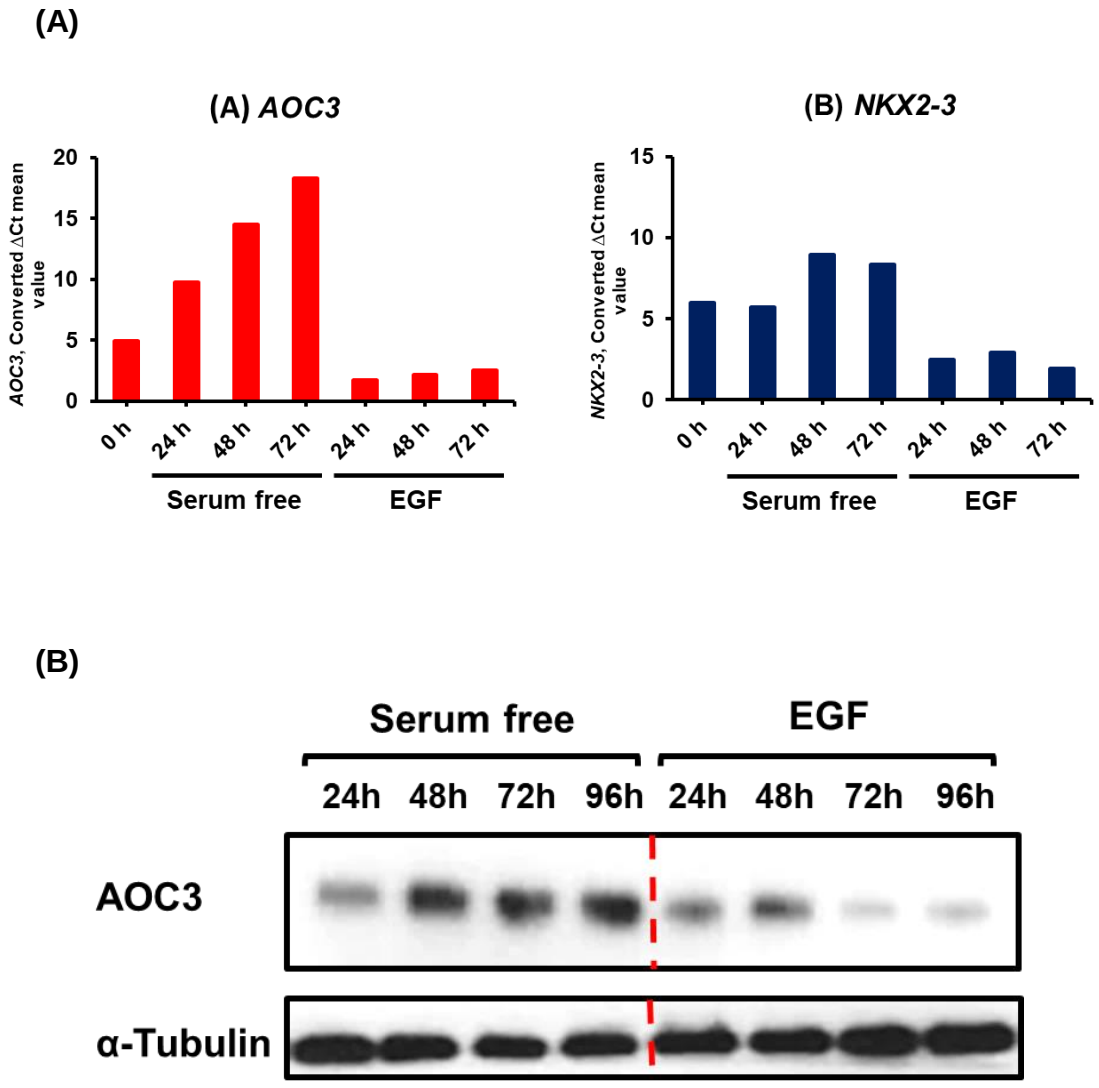

Figure 4.23

Kinetic study of EGF in CCD-18Co.

The qRT-PCR data (A) shows the downregulation of *AOC3* expression in CCD-18Co after treatment with EGF in comparison to serum free conditions (a single experiment). The expression of *AOC3* increases over time in serum starved CCD-18Co. A slight increase in *NKX2-3* expression under same experimental (serum free) condition was observed. (B) The data on the influence of EGF on *AOC3* expression was verified by western blot in which the downregulation of AOC3 expression by EGF was more prominent after 72 h of treatment.

As shown by the microarray data, myofibroblasts do express high levels of *EGFR* and this was validated by flow cytometry data where a significant shift in the expression of EGFR in CCD-18Co was found, when compared to isotype control (**Fig 4.24**). To confirm the specificity of the EGF activity on myofibroblasts, Cetuximab (anti-EGFR monoclonal antibody) was used to block the binding of EGF to its receptor. **Figure 4.25** simplifies the experimental layout that was conducted using this blocking antibody. As expected, *AOC3* mRNA expression was downregulated significantly in EGF-treated CCD-18Co and this was rescued by the pre-treatment with cetuximab. Both addition of cetuximab at 10 µg/mL for either 1 or 3 h prior to EGF treatment lead to significant upregulation of *AOC3* mRNA expression in comparison to treatment with EGF alone due to the blocking activity on EGFR. Cetuximab alone did not affect the regulation of *AOC3*. This finding was confirmed at a protein level using a western blot. The total of 3 h of pre-treatment with cetuximab lead to more efficient blocking of EGF activity on AOC3 regulation. The effect of EGFR blocking on *AOC3* expression also was demonstrated in Myo 7395 where a similar profile of *AOC3* mRNA expression after been pre-treated with cetuximab was produced.

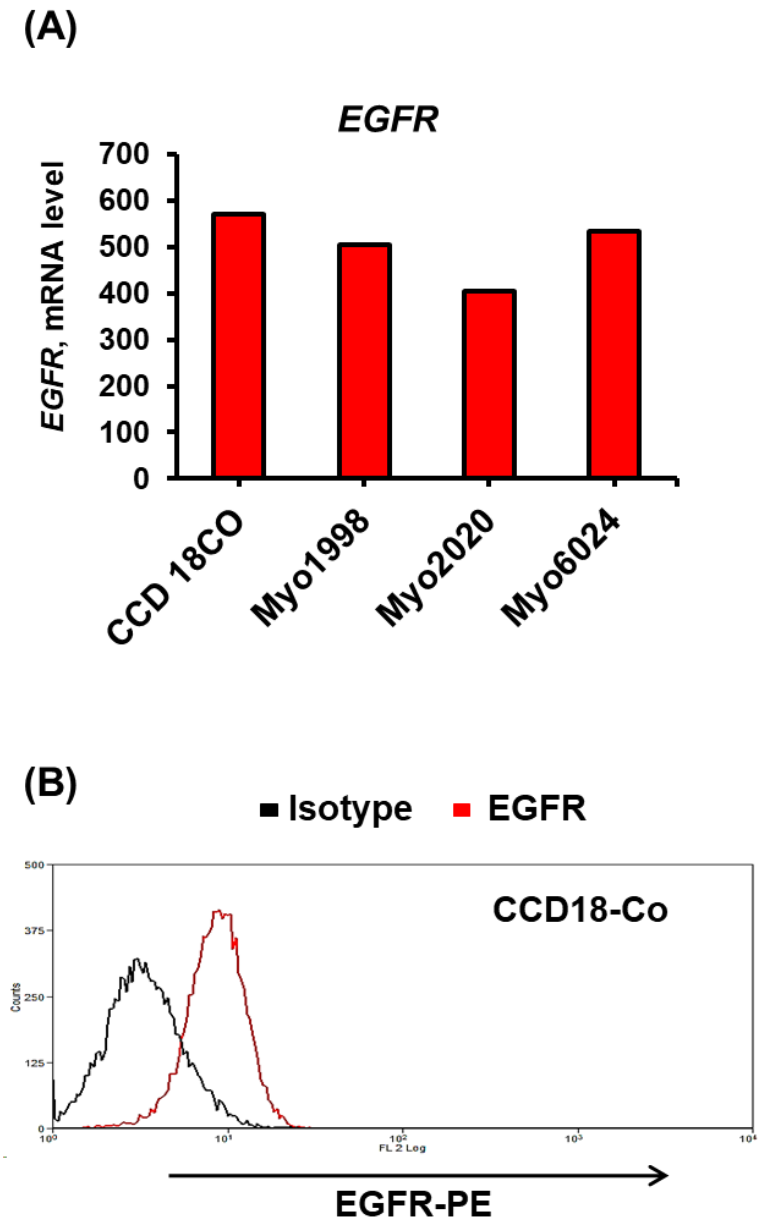

Figure 4.24

The expression of EGFR in myofibroblasts.

Microarray data analysis shows high *EGFR* mRNA level in all candidate myofibroblasts (A). Positive expression of EGFR in CCD-18Co was confirmed using flow cytometry (B) (Data courtesy of Dr Djamila Ouaret, Bodmer lab).

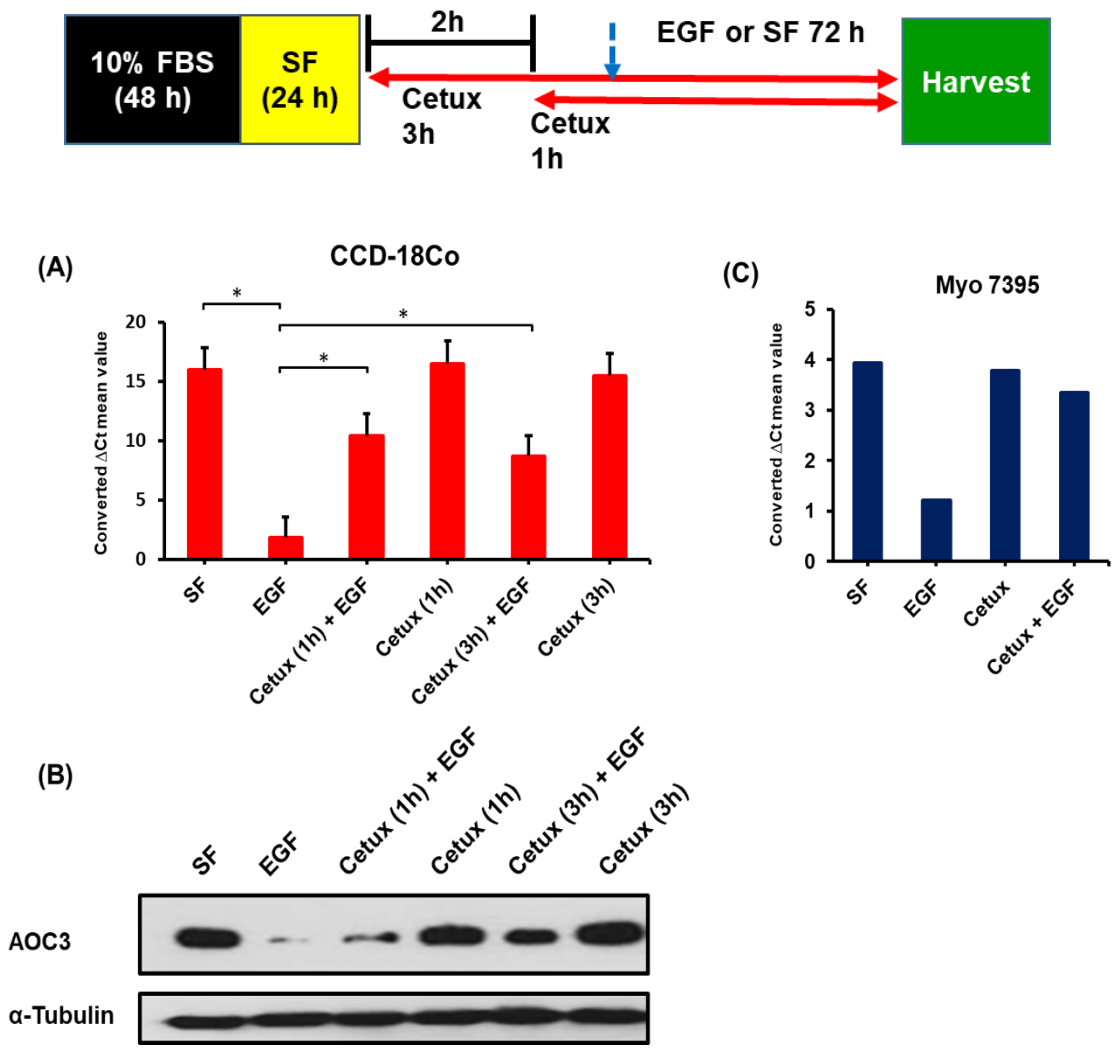

Figure 4.25

Blocking of EGFR activity on AOC3 expression by cetuximab in myofibroblasts.

The activity of EGF on the expression of *AOC3* was blocked by cetuximab shown by (A) qRT-PCR (*p<0.05 as compared to EGF alone) and (B) western blot. Pre-treatment with cetuximab (10 µg/mL) for 3 h was more efficient in inhibiting the EGF activity on AOC3 protein expression in comparison to 1 h of pre-incubation. C) EGFR activity on *AOC3* expression at gene level also was abolished after pre-treatment with cetuximab (3 h) in primary myofibroblasts (Myo 7395) (Cetux; cetuximab; SF: serum free; h: hour).

Two blocking agents against HER2 (human epidermal growth factor receptor 2), namely trastuzumab and pertuzumab were also tested. Both HER2 and EGFR are members of HER/ERBB family of receptor tyrosine kinases (RTKs). As shown in **Figure 4.26**, both anti-HER2 antibodies exhibit lower efficiency in blocking EGF activity of the regulation of AOC3 expression in CCD-18Co, as compared to cetuximab.

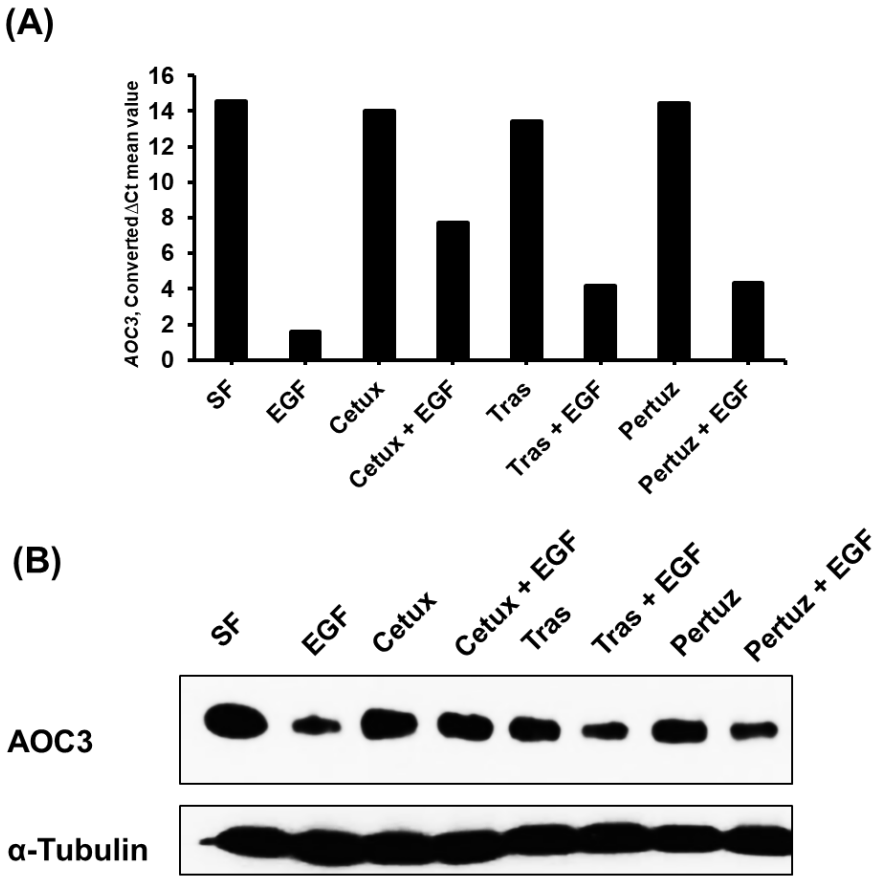

Figure 4.26

Effects of various blocking antibodies (Cetuximab – Cetux; Trastuzumab – Tras and Pertuzumab – Pertuz) of EGFR on AOC3 expression in CCD-18Co.

Blocking activity of cetuximab (EGFR mAb) was proven to be more efficient as analysed by (A) qRT-PCR and (B) western blot, in comparison to Trastuzumab and Pertuzumab (both HER-2 mAb).

4.2.10 PDGF regulation on gene expression in myofibroblasts

One of the tested growth factors that significantly downregulates AOC3 expression is PDGF-AA. Different concentrations of PDGF-AA were tested (20, 50 and 100 ng/mL) and the downregulation of *AOC3* mRNA expression was detected in all treatment groups (**Fig 4.27A**). The screening was repeated using various ranges of PDGF-AA concentrations (1, 5, 10 and 50 ng/mL). Dose-dependent response of *AOC3* expression in CCD-18Co was observed where *AOC3* mRNA level was lower after treatment with high concentrations of PDGF-AA. Similar experimental settings were performed for PDGF-CC, another PDGF ligand. Unlike PDGF-AA, the effect of PDGF-CC on *AOC3* downregulation was less profound Indeed, PDGF-CC at 50 ng/mL did not downregulate *AOC3* expression at a similar extent as in PDGF-AA at the same dosage (**Fig 4.27B**). These results were confirmed at protein level using Western blot analysis (**Fig 4.27C**).

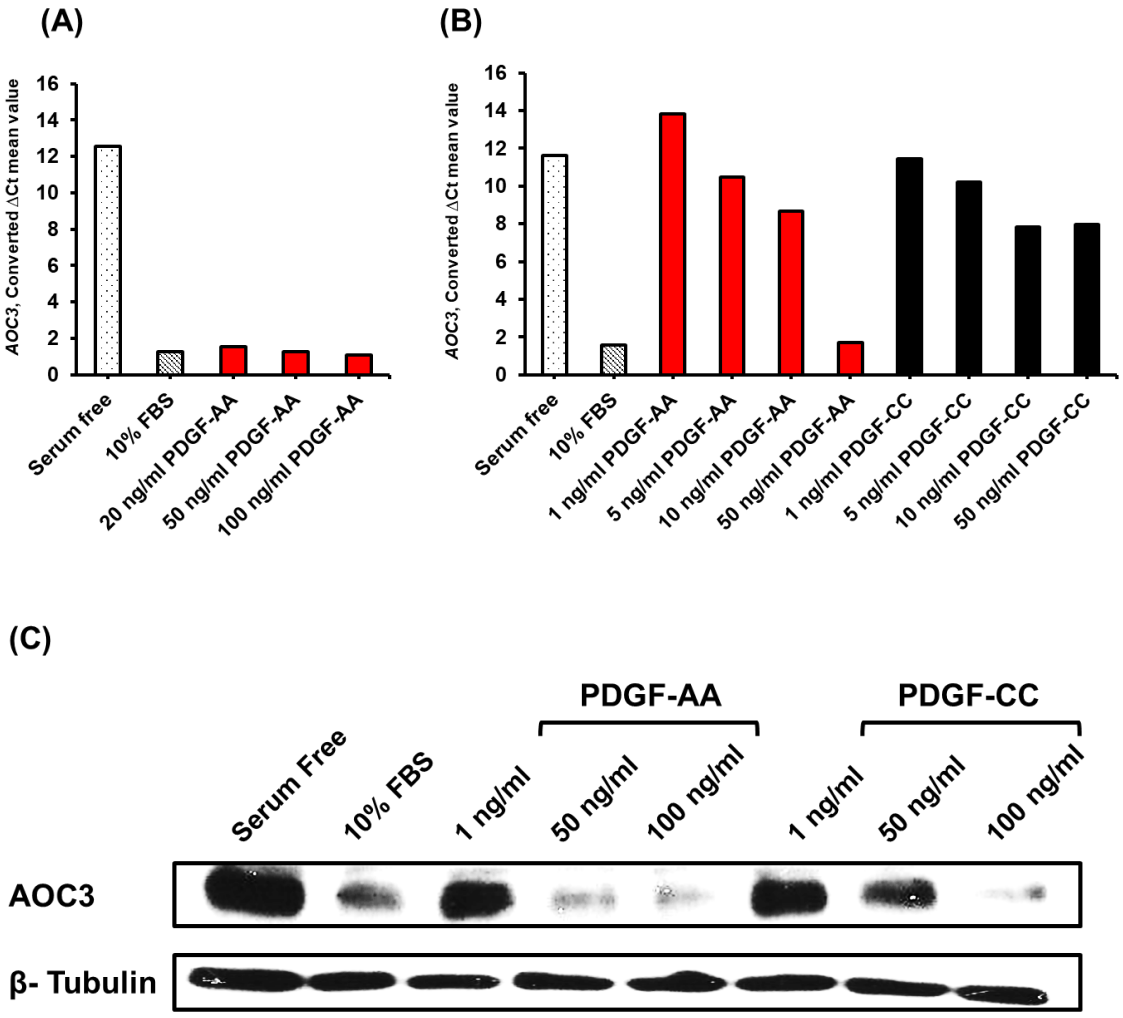

Figure 4.27

The influence of PDGF-AA & CC on the regulation of AOC3 expression in CCD-18Co.

PDGF-AA (different concentrations ranges from 20 to 100 ng/mL) strongly downregulated *AOC3* gene expression as shown in (A). (B) Dose-dependent effects of PDGF-AA and CC on *AOC3* downregulation with the most striking effect observed for 50 ng/mL PDGF-AA. Minimal effect on *AOC3* regulation was observed after similar experimental condition in PDGF-CC-treated CCD18-Co. groups. (C) Western blot analysis demonstrated the greater potency of PDGF-AA to downregulate AOC3 expression in comparison to PDGF-CC.

4.2.11 The effects of conditioned medium from CRC cells on gene expression of myofibroblasts

Experiments using conditioned medium (CM) provide clues on the secreted cytokines and growth factors from CRC cell lines and how they can influence gene expression in myofibroblasts. The selection of CRC cell lines (RKO, HT29, SW480, SW620 and OXCO1) for experiments involving CM was done based on microarray data analysis on the expression of candidate growth factors such as *TGFβ1* and *PDGF-AA*.

The conditioned medium (CM) from CRC cells (RKO, HT29, SW480, SW620 and OXCO1) was collected after 48 h of incubation and incubated with CCD-18Co. The influence of these CM on *AOC3*, *ACTA2*, *FAP* and *LRRC17* expression was summarized in **Figure 4.28**. Two control groups (serum free and 10% FBS) were included in the test. Significant downregulation in *AOC3* expression was observed after treatment with 10% FBS and CM from SW480, SW620 and OXCO1, in comparison to serum free condition. *ACTA2* expression was significantly downregulated after treatment with all CM except for CM from HT29. Interestingly, only CM from OXCO1 upregulated the FAP expression in CCD-18Co. Upregulation of *LRRC17* was observed in CM OXCO1 group whereas this gene was downregulated after treatment with CM from SW620 and RKO, although not at significant level in comparison to serum free (DMEM alone). These data are largely consistent with our microarray data analyses of expression and specific growth factor effects, as discussed further in the discussion part.

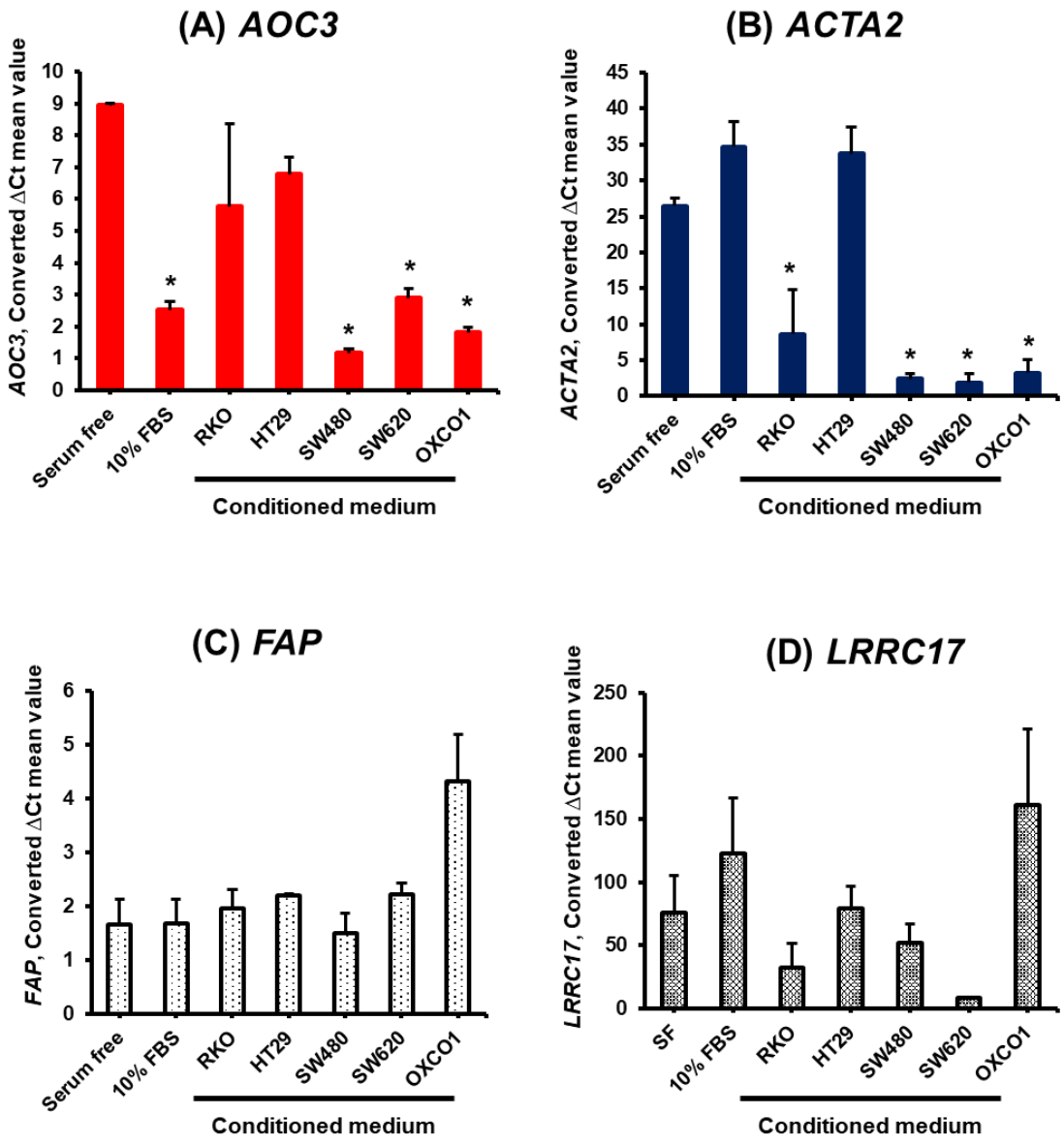

Figure 4.28

The influence of conditioned medium (CM) from CRC cell lines on expression of selected genes in CCD-18Co.

CM of SW480, SW620 and OXCO1 downregulated *AOC3* expression. *ACTA2* expression was suppressed with conditioned medium from RKO, SW480, SW620 and OXCO1. The upregulation of *FAP* and *LRRC17* expression has been observed in the group incubated with CM of OXCO1. CM from SW620 and RKO downregulated *LRRC17* gene expression although at an insignificant level (*$p<0.05$ in comparison to serum free condition, from three biological replicates).

4.2.12 Knockdown of AOC3 and NKX2-3 in myofibroblasts using RNA interference

Kinetic studies of the knockdown of AOC3 and NKX2-3 were performed from 24 to 72 h using RNA interference. Downregulation of *AOC3* mRNA expression in CCD-18Co treated with siAOC3 was observed at 48 h post-transfection and persisted up to 72 h. Similarly, for *NKX2-3*, a significant knockdown was seen at 48 and 72 h after CCD-18Co been transfected with siNKX2-3 (**Fig 4.29A**). Knockdown efficiency at 48 and 72 h was validated by western blots and the results agree with the qPCR data (**Fig 4.29B**).

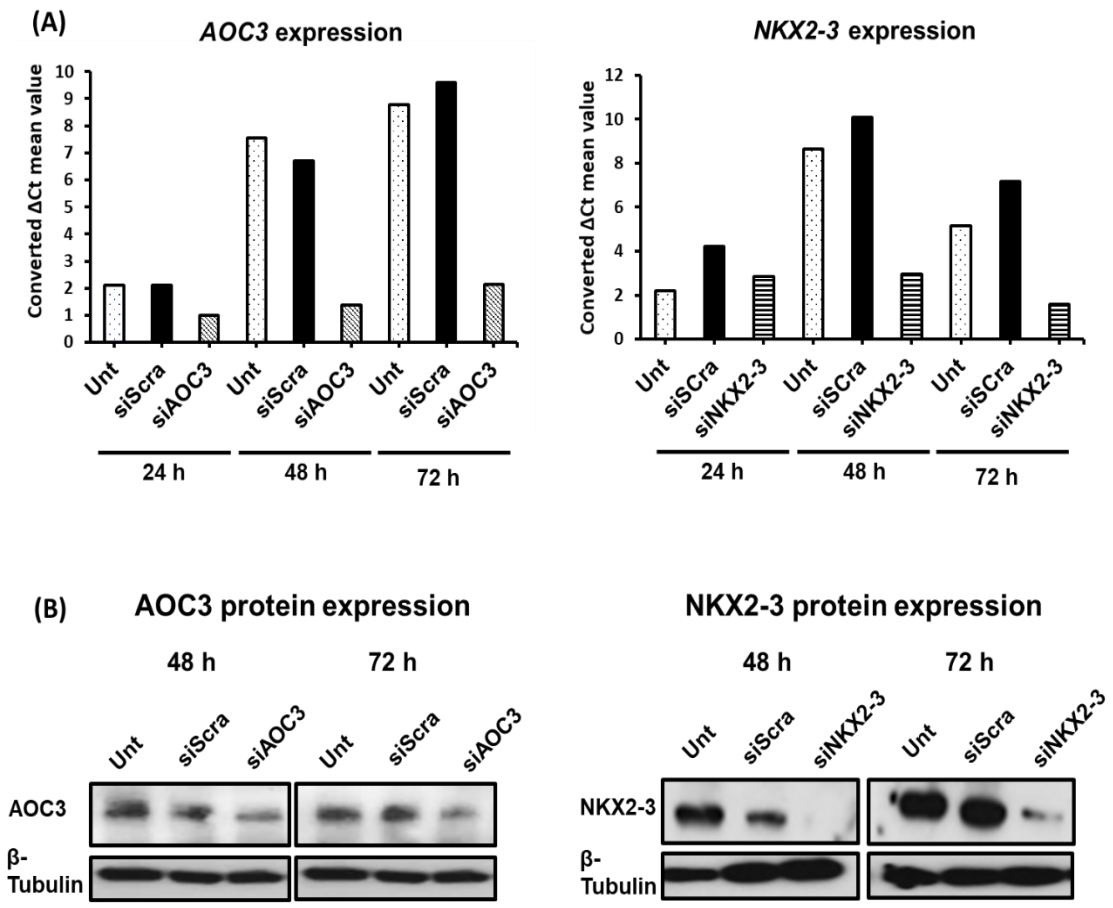

Figure 4.29

Knockdown of AOC3 and NKX2-3 in CCD-18Co.

Quantification using by (A) qRT-PCR shows a significant knockdown of both genes (siAOC3 and siNKX2-3 groups in comparison to siScra) at 48 and 72 h post-transfection. (B) Verification of the knockdown was done by western blot (Unt: untreated; siScra: scrambled siRNA).

The qRT-PCR analysis of the influence of both AOC3 and NKX2-3 knockdown on *AOC3*, *NKX2-3*, *ACTA2* and *FAP* expression is summarized in **Figure 4.30**. Strikingly, NKX2-3 knockdown decreased *AOC3* expression to the same extent as siAOC3. However, AOC3 knockdown did not influence the mRNA expression of *NKX2-3* when compared to siScra-treated CCD-18Co, contradicts from previous observation by Hsia et al. (2016). The discrepancy between our data and Hsia et al (2016) with regards to the effect of siAOC3 on NKX2-3 regulation in CCD-18Co is discussed in Chapter 6. Our results also demonstrated significant downregulation in *ACTA2* expression after transfection with siNKX2-3 whereas this effect was not detected in siAOC3 knock down, as demonstrated before by Hsia et al., (2016). Knockdown of AOC3 or NKX2-3 did not modulate the *FAP* expression.

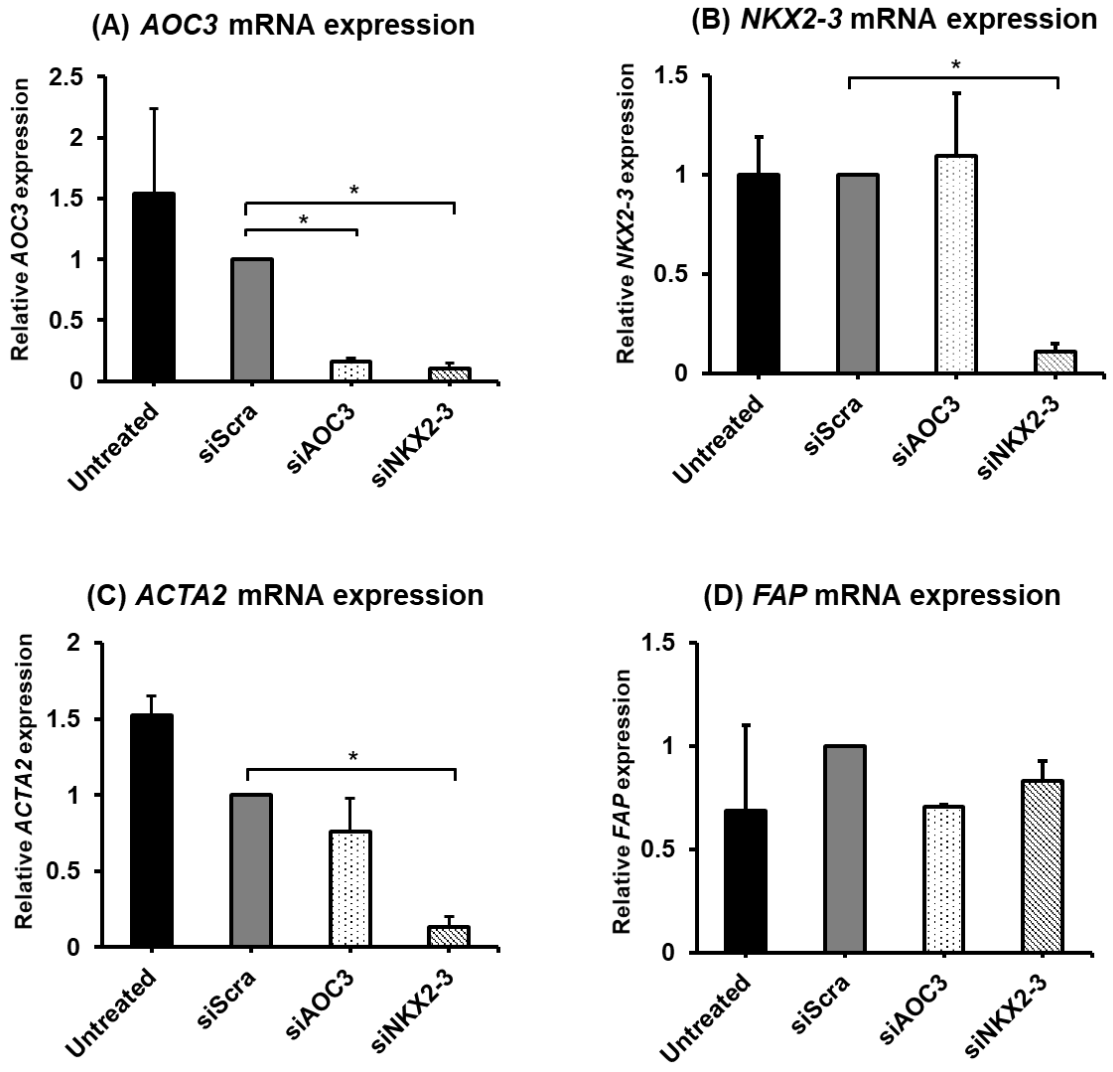

Figure 4.30

The effects of the knockdown of *AOC3* and *NKX2-3* on *AOC3*, *NKX2-3*, *ACTA2* and *FAP* expression in CCD-18Co.

Four independent groups of CCD-18Co consist of untreated, siScra, siAOC3 and siNKX2-3 were included in the siRNA mediated knockdown experiment. Gene expression levels of *AOC3*, *NKX2-3*, *ACTA2* and *FAP* in those respective groups were measured after 48 h of transfection with siRNA. Knockdown of NKX2-3 (siNKX2-3) lead to downregulation of both *NKX2-3* and *AOC3* expression. *NKX2-3* expression remains unaffected in siAOC3 group. *ACTA2* was significantly downregulated after transfection with siNKX2-3. No significant effect of both AOC3 and NKX2-3 knockdown on *FAP* expression was found. The gene expression was calculated relatively to normalized value of siScra to 1

(*p<0.05, significantly different when compared to siScra from three biological replicates) (siScra: scrambled siRNA).

Immunofluorescence staining further clarifies the efficient knockdown of NKX2-3 through transient transfection by siRNA in methanol-fixed CCD-18Co (**Fig 4.31**)**.** As expected from the qPCR data, weaker αSMA staining was observed in siNKX2-3 groups when compared to others. This staining profile also supports the previous finding in **Figure 4.30** where the knockdown of AOC3 did not affect the expression of NKX2-3 in CCD-18Co.

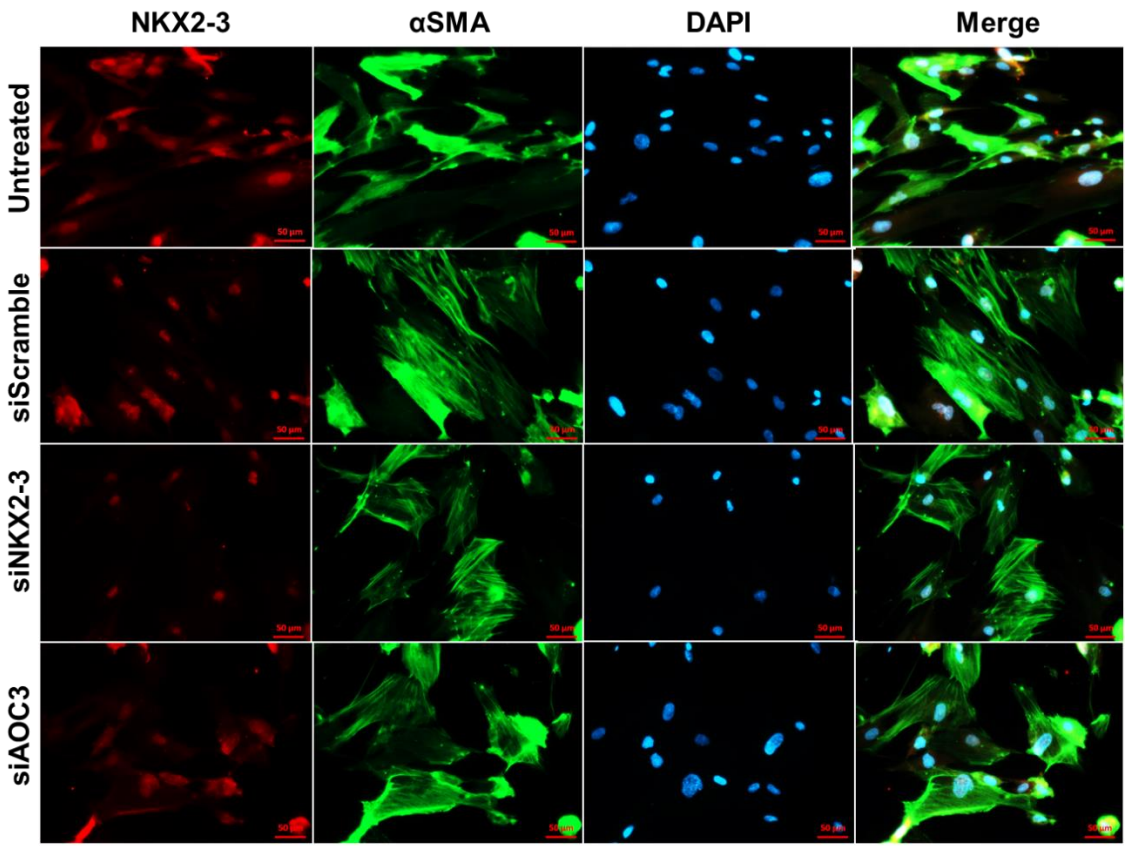

Figure 4.31

Knockdown of NKX2-3 or AOC3 in CCD-18Co.

Representative images of CCD-18Co treated with different siRNA and fixed with cold methanol before stained for NKX2-3 (LSbio) and αSMA (1A4, Sigma) are shown. Efficient knockdown of NKX2-3 protein expression was illustrated in siNKX2-3 treatment group, fixed with cold methanol, after 48 h of transfection. No effects from the knockdown of AOC3 on the expression of NKX2-3 and αSMA was detected. αSMA protein expression was downregulated in siNKX2-3 as indicated by weaker staining intensity of αSMA in comparison to other groups, although the difference in the staining between groups is small (Magnification: 20x).

4.2.13 Functional role AOC3 and NKX2-3 on pro-migratory activity of myofibroblasts

A migration assay using modified Boyden chamber (Transwell assay) was conducted to study one aspect of the functional role of AOC3 and NKX2-3 in myofibroblasts. **Figure 4.32A** shows the representative images of migrated RKO when co-cultured with CCD-18Co transfected with either siAOC3, siNKX2-3 or siScrambled (siScra). An untreated control also was included in the test. Fewer migrated RKO cells (indicated in blue) were found in siAOC3-transfected CCD-18Co co-culture group than in the siScra group. This observation was supported by the quantification of the stained RKO which migrated through the pores of the Transwell **(Fig 4.32B**). A significant reduction in the migration of RKO was found in co-culture condition of CCD-18Co + siAOC3 group when compared to CCD-18Co transfected with scrambled siRNA. Lower numbers of migrated RKO cells were also seen in the siNKX2-3 group although these numbers are not significantly different from siScra group. Contrary to our initial prediction, in which comparable numbers of migrated RKO would be observed in siNKX2-3 and siAOC3 groups, a more significant reduction in the migration of RKO by siAOC3 might indicate the possibility of an upstream gene of *AOC3* that can compensate for the knockdown effect of *NKX2-3*. These data also present the possibility that NKX2.3 has both invasion promoting and invasion suppressing target genes. Nevertheless, as this experiment was conducted with only RKO, further test using more CRC cell lines would be needed to verity this finding.

(A)

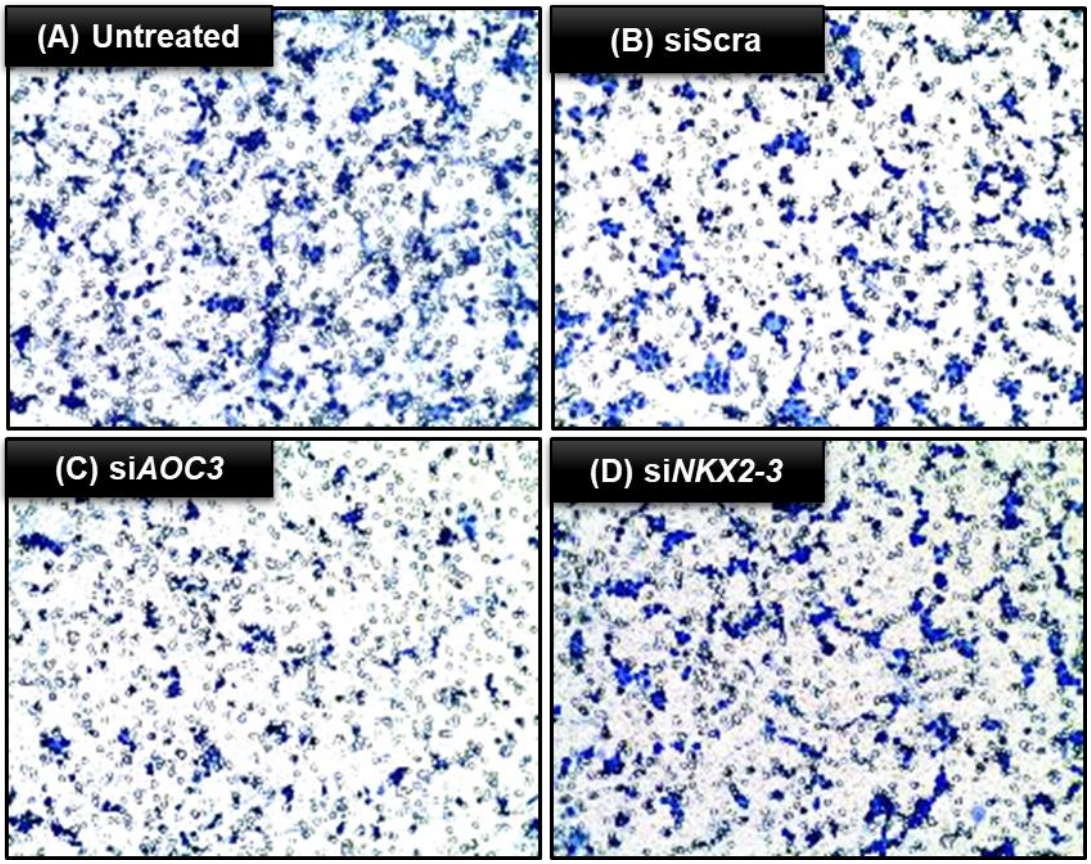
(A) Untreated
(B) siScra
(C) si*AOC3*
(D) si*NKX2-3*

(B)

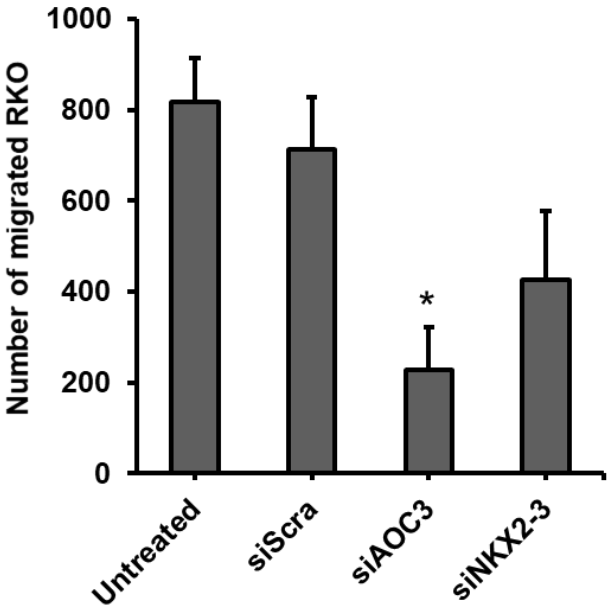
Number of migrated RKO
1000
800
600
400
200
0
*
Untreated
siScra
siAOC3
siNKX2-3

Figure 4.32

Migration of RKO is affected when co-culture with CCD18Co transfected with siAOC3.

Figure (A) shows representative images from Transwell assay, of migrated RKO cells when co-cultured with CCD-18Co treated with either scrambled RNA (siScra), siRNA for AOC3 (siAOC3), NKX2-3 (siNKX2-3) and untreated group for 48 h (Magnification: 20x). B) A significant reduction in the number of migrated RKO cells (stained in black or blue) was found in the co-culture group with myofibroblasts treated with siAOC3 (*$p<0.05$ as compared to control (siScra) from three biological replicates. Fixation, staining and cell counting method used in the experiment are similarly as those described in the Material and Methods section of Transwell assay (**Section 2.7**).

4.2.14 FAP expression in colonic myofibroblasts

Previous microarray data showed a high expression level of *FAP* in myofibroblasts in contrast with almost all CRC cell lines where, the expression is very weak except for OXCO1 and NCIH716 (**Fig 4.14**). This observation was confirmed at a protein level using western blots where a strong band can be detected for CCD-18Co. Very weak bands were observed for all cancer cell lines tested with an exception for OXCO1, although it is at much lower intensity as compared to corresponding FAP band for CCD-18Co (**Fig 4.33**).

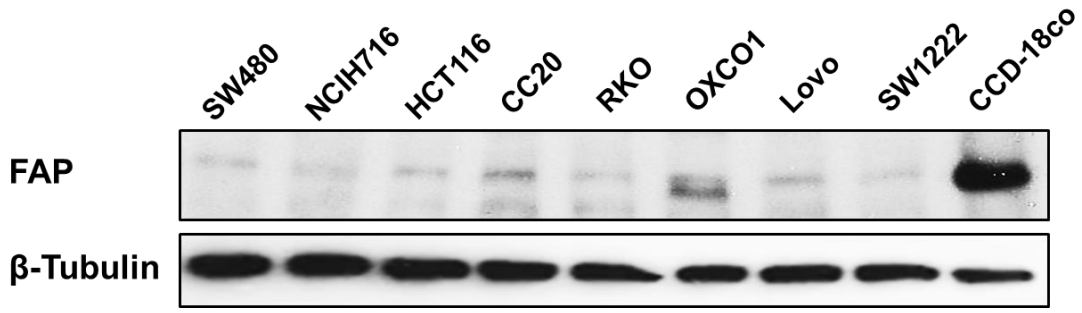

Figure 4.33

FAP protein expression across CRC cells.

Screening of FAP expression in various CRC cell lines (high *vs* low mRNA level of *FAP* from microarray data) shows very weak FAP expression in all but one of the selected cell lines. High expression of FAP was only seen in CCD-18Co signalled by the presence of the strong band of FAP. All cells were incubated in full medium (DMEM + 10% FBS) for 72 h before harvesting.

Immunofluorescence staining of FAP confirms its protein expression in primary myofibroblasts (**Fig 4.34**). Strongest FAP staining intensity was observed in Myo 0164C which is from cancer patient. The staining in its normal matched pair (Myo 0165) looks more heterogeneous showing some strong and weak staining in the same culture. As expected, only faint staining of FAP was detected in skin fibroblasts.

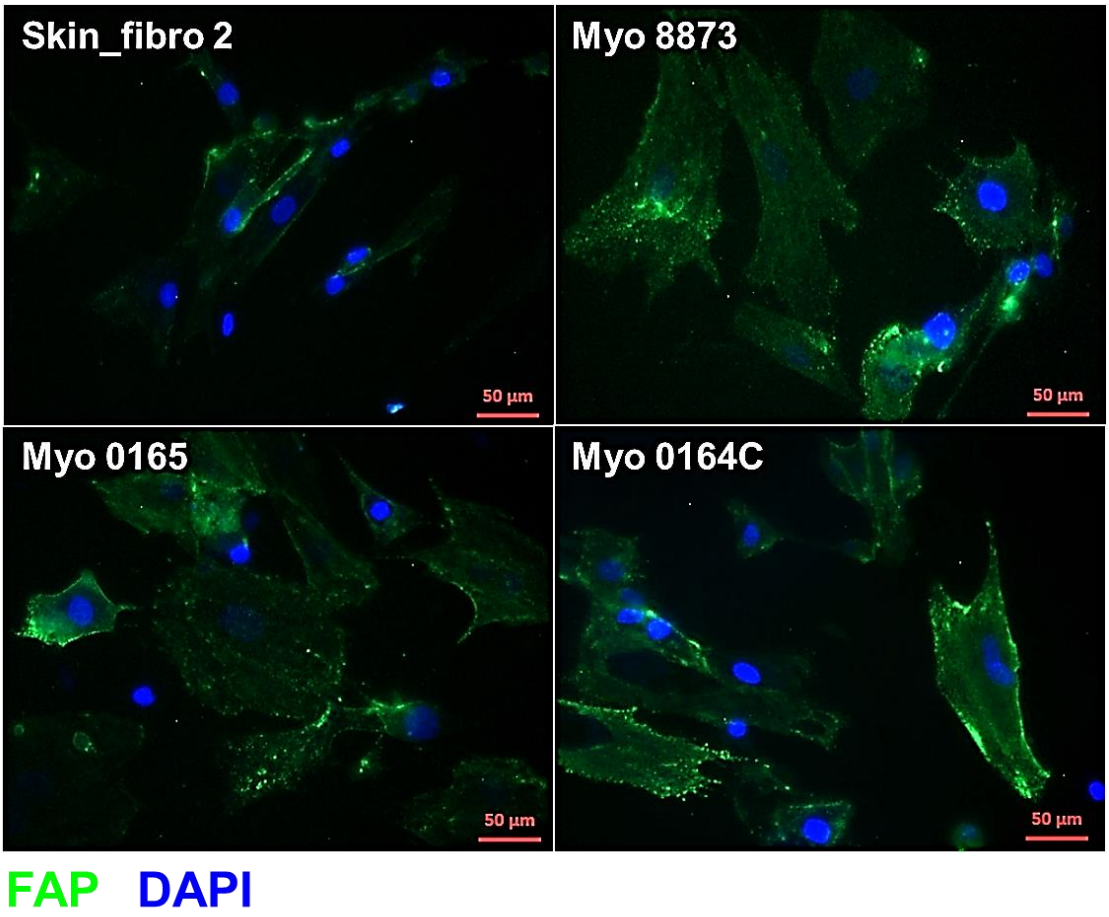

Figure 4.34

Immunofluorescence staining of FAP.

Much greater cytoplasmic FAP (F19) staining intensity was detected in primary myofibroblasts (Myo 0164C, 0165 and 8873) in comparison with skin fibro 2 (skin fibroblasts) A more heterogeneous FAP staining was observed in Myo 0165 (Magnification: 20x). FAP (green), DAPI (blue).

Basal expression of *FAP* in different pairs of myofibroblasts (from cancer and normal colon tissue) was screened along with the expression of *AOC3*, *NKX2-3* and *ACTA2* to look for associations between these gene expression. In general, no obvious correlation was found between these genes' expression at both mRNA and protein level. However, a strikingly high expression of all selected genes (*AOC3*, *NKX2-3* and *ACTA2*) for 8852C was found agreeing with the fact that this myofibroblast line shows high mRNA level in all those genes. All myofibroblast lines express *FAP*, with CCD-18Co having the lowest expression level among those tested (**Fig 4.35**). Except for Myo 8852C and 8853, comparable levels of *FAP* were seen in the other cancer/normal myofibroblasts pairs. A very low expression of *FAP* was observed in skin fibroblasts and no detectable expression of this gene was found in RKO. Positive expression of FAP in myofibroblasts was validated through western blot analysis (**Fig 4.36**).

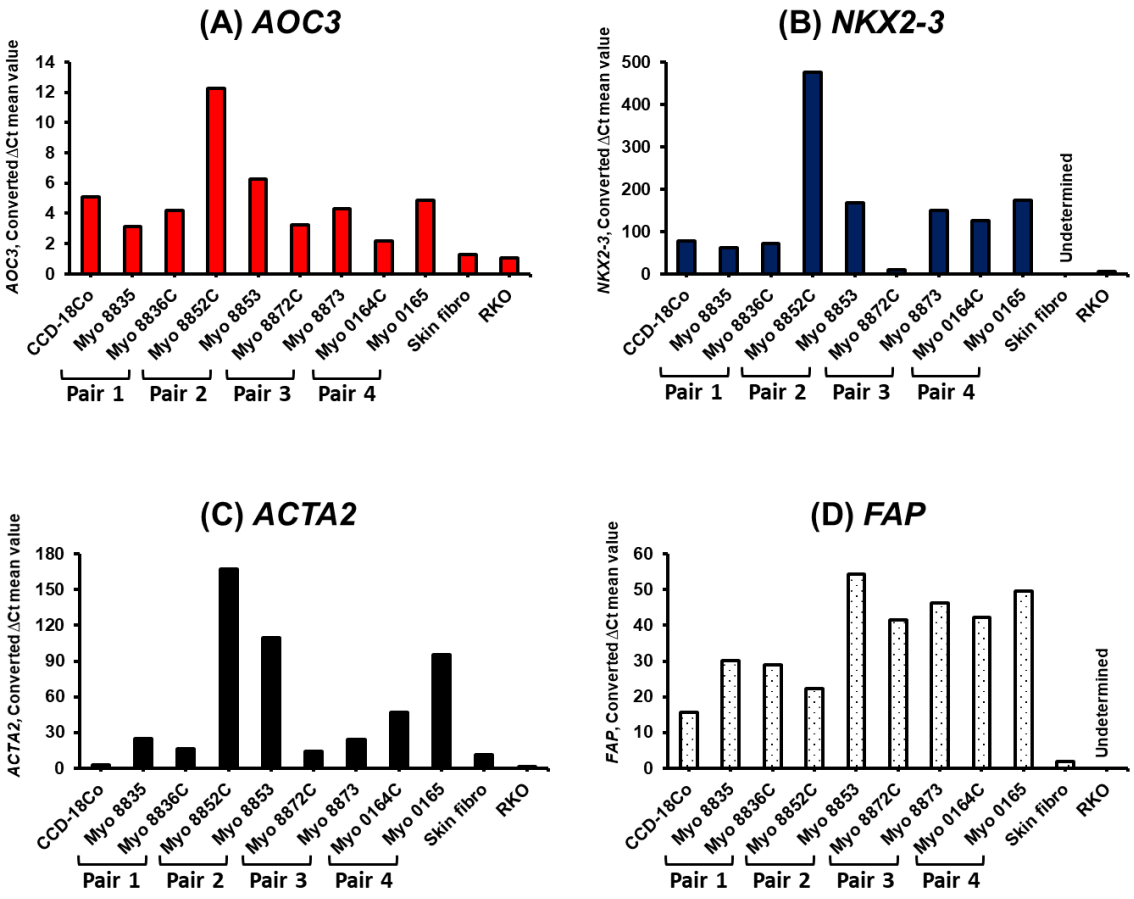

Figure 4.35

Screening of *AOC3*, *NKX2-3*, *ACTA2* and *FAP* expression in different pairs of myofibroblasts using qRT-PCR.

Basal level of the selected genes after 24 h of cell seeding shows no direct correlation between *AOC3*, *NKX2-3* and *ACTA2* and expression of *FAP* in myofibroblasts. However, like *ACTA2*, *FAP* expression level is found to be higher in primary myofibroblasts in comparison to CCD-18Co. Skin fibro_2 and RKO were included as negative controls for *AOC3*, *NKX2-3* and *FAP* while skin fibro_2 serves as a positive control for *ACTA2* (Skin_fibro: skin fibroblasts) (Undetermined: Very low/ undetectable Ct value).

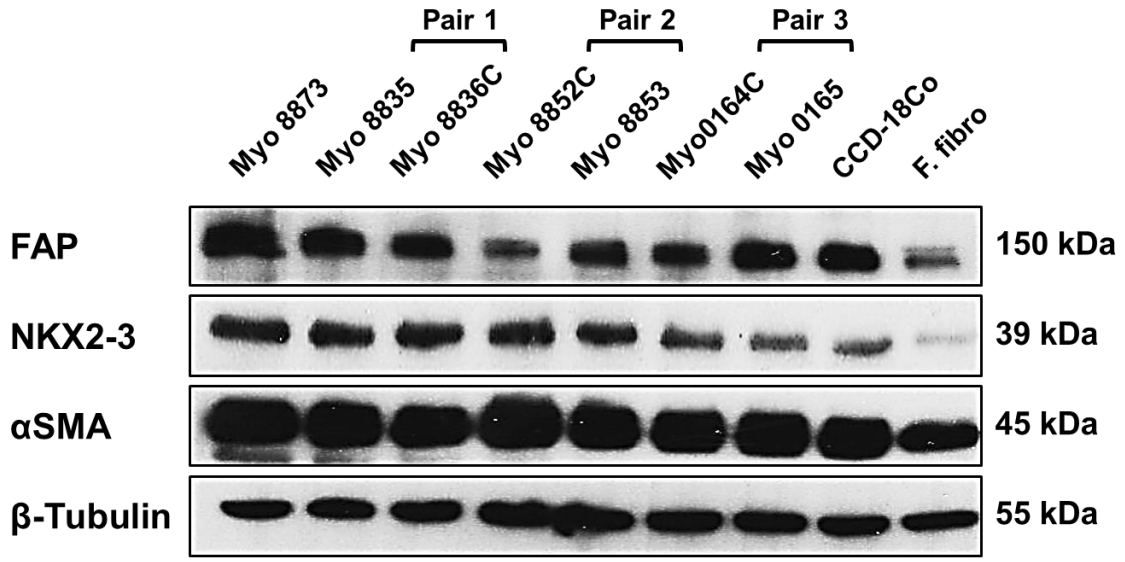

Figure 4.36

Protein expression of FAP, NKX2-3 and αSMA in a range of myofibroblasts, grown in DMEM + 10% FBS.

FAP is expressed at high levels in all primary myofibroblasts but is much lower in F. Fibro (foreskin fibroblasts) (Time exposure of film for FAP detection = 10 sec). Similarly, NKX2-3 is highly expressed in all myofibroblasts but very low in F. Fibro. Myofibroblasts express high levels of αSMA whereas a slightly lower level of expression of αSMA was seen in F. fibro. Screening of these proteins was performed on primary myofibroblasts at cell passage number 4 (P4). The passage numbers for CCD-18Co and foreskin fibroblasts were P17 and P10 respectively.

Screening for the influence of growth factors on *FAP* gene expression in a pair of primary myofibroblasts (Myo 0164C and Myo 0165), revealed that TGFβ1 and PDGF-AA treatment induced significant upregulation of *FAP* expression in Myo1064C, which is derived from a cancer. No significant effect of serum (10% FBS) on *FAP* expression in both primary myofibroblasts was found. Minimal effects of both TGFβ1 and PDGF-AA on *FAP* regulation in Myo 1065 were seen (**Fig 4.37**).

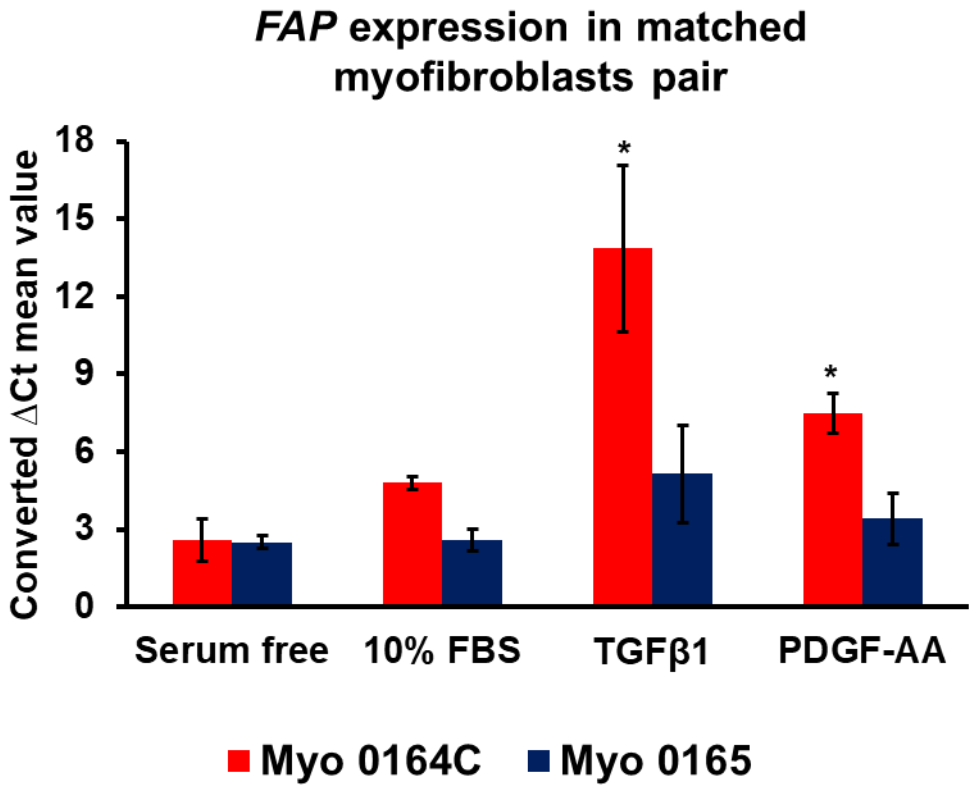

Figure 4.37

The qRT-PCR analysis on the influence of serum (10% FBS), TGFβ1 and PDGF-AA treatment on *FAP* expression in a pair of matched primary myofibroblasts.

Striking upregulation of *FAP* expression was detected in TGFβ1 and PDGF-AA-treated Myo 1064C in comparison to serum free condition (DMEM alone), but not in Myo 1065 under similar experimental conditions (*$p<0.05$ significantly different when compared to serum free condition, from three biological experiments).

To validate these qRT-PCR data, western blot analysis was used to investigate the influence of growth factors (TGFβ1, EGF and PDGF-AA) on FAP protein expression in Myo 0164C and 0165. **Figure 4.38** shows striking differences in the FAP expression profile between myofibroblasts derived from cancer and normal colon. The expression of FAP was upregulated in Myo 0164C after treatment with TGFβ1, EGF and PDGF-AA, but not in Myo 0165 under similar experimental condition. Faint bands of FAP were observed in serum free and 10% FBS treatment groups, for both Myo 1064C and 0165. This result suggests that serum did not affect the FAP protein expression. The expression of αSMA was upregulated in 10% FBS and growth factors-treated Myo 1064C, when compared to the serum free group. Comparable αSMA expression between different treatment groups of Myo 0165 was found.

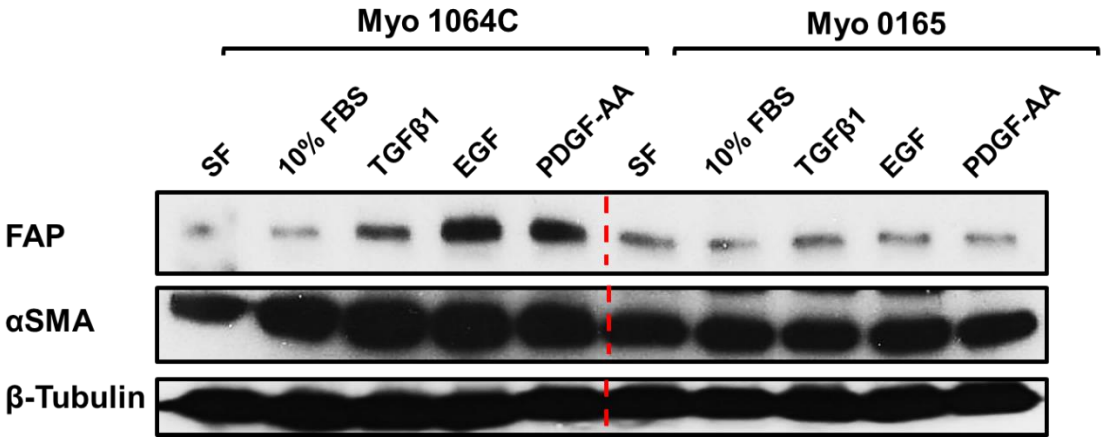

Figure 4.38

The influence of growth factors on FAP expression in primary myofibroblasts from the same patient derived from normal (Myo 0165) and cancerous tissue (Myo 0164C).

Strong upregulation of FAP expression was seen in Myo 0164C treated with TGFβ1, and especially with EGF and PDGF-AA, but not in its normal matched line (Myo 0165) (Time exposure of film for FAP detection = 2 sec). αSMA expression in only Myo 0164C was upregulated in the presence of 10% serum, TGFβ1, EGF and PDGF-AA. Concentrations of TGFβ1, EGF and PDGF-AA used in this experiment were 10, 3 and 100 ng/mL respectively.

As shown in **Figure 4.39**, PDGF-AA upregulated FAP expression in Myo 0164C in a dose-dependent manner. Faint bands of AOC3 were observed in Myo 1064C, regardless of the concentration of PDGF-AA used for the experiment. Treatment with PDGF-AA and 10% FBS upregulated NKX2-3 protein expression in Myo 1064C. Stronger NKX2-3 bands were observed in cells treated with 100 and 150 ng/mL PDGF-AA in comparison to those incubated with lower concentration of the growth factor (25 ng/mL).

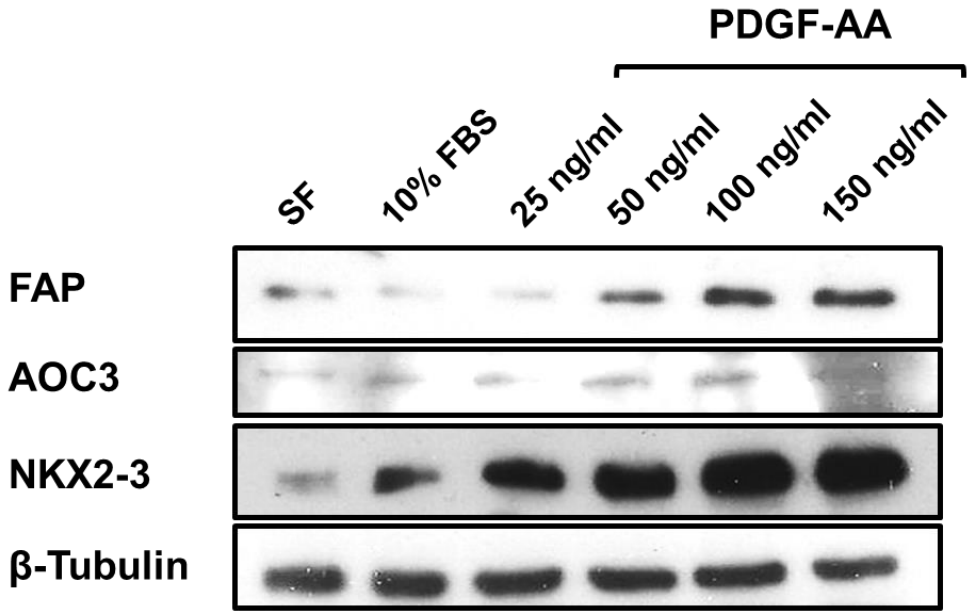

Figure 4.39

Dose-dependent effect of PDGF-AA on FAP expression in Myo 1064C.

Upregulation of FAP expression was observed in Myo 0164C treated with higher concentrations of PDGF-AA (50, 100 and 150 µg/mL). No significant induction of FAP expression after treatment with 25 µg/ml PDGF-AA was found (Time exposure of film for FAP detection = 2 sec). Low levels of AOC3 were found in all treatment groups. There was significant upregulation of NKX2-3 protein expression after incubation with serum, and various concentrations of PDGF-AA.

4.2.13 Cell senescence and its influence on AOC3 and NKX2-3 expression

In contrast to NKX2-3, the expression of AOC3 is more heterogeneous across different myofibroblasts as shown in **Figure 4.8**. A factor that may lead to that is cell senescence, which occurs in fibroblastic cells at later passages.

The different levels of AOC3 depending on the cell passage number might therefore be associated with cell senescence. To relate the beta-galactosidase staining, which is used as a marker of cell senescence, with AOC3 expression, the level of AOC3 protein was studied in different cell passage numbers using CCD-18Co (P11: early, and P19: late passage). Interestingly, there was strong AOC3 expression at P11 and a much fainter band of AOC3 at P19 (**Fig 4.40A**). Stronger NKX2-3 band was seen at late cell passage number (P19) in comparison to P11. Subsequently, beta-galactosidase senescence associated staining was carried out on CCD-18Co from intermediate (P15) and late passage (P21) maintained in 10% serum at FBS. The phenomenon of cell senescence in fibroblasts was defined to be more than 80% cells stained with beta-galactosidase (Itahana et al., 2013). Representative images in **Figure 4.40B** illustrate the presence of a significant number of senescent cells at P21 which are indicated with dark blue green colour. No significant beta-galactosidase staining was detected at P15.

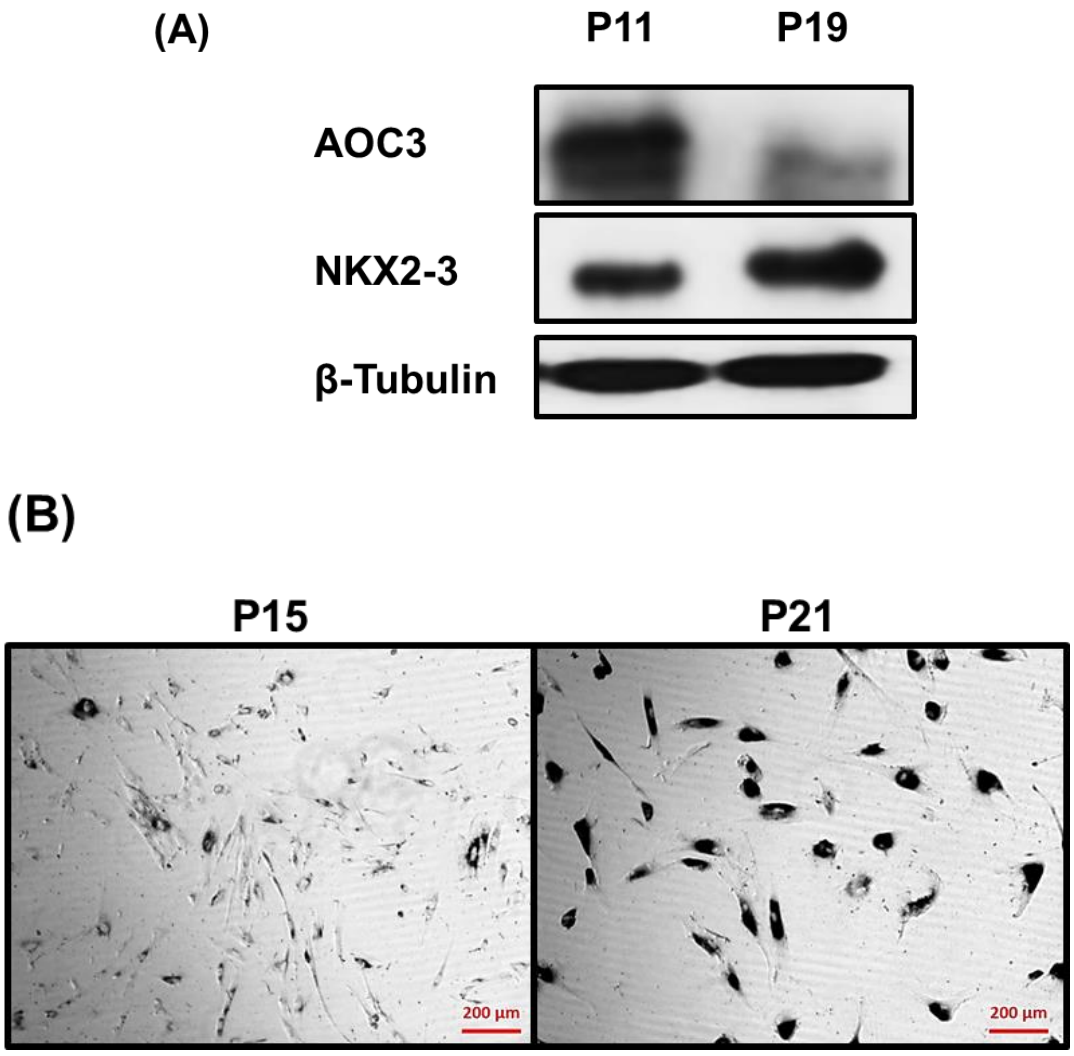

Figure 4.40

Cell senescence at later stages of cell passage (CCD-18Co).

Western blot result (A) shows the downregulation of AOC3 expression at a later passage of CCD-18Co (P19) in comparison to P11 (strong band of AOC3). Moreover, there was upregulation of NKX2-3 expression at P19 when compared to P11. The correlation of AOC3 and cell senescence was studied using beta-galactosidase staining of CCD-18Co at intermediate (P15) and late passages (P21). A phenomenon of replicative senescence was observed in myofibroblasts at late higher number of cell passages (B). Representative images of CCD-18Co at different cell passages indicate the abundance of senescent cells at P21 (dark blue-green staining of beta-galactosidase) as compared to P15 (Magnification: 10x).

Assessment of AOC3 expression level and its association with cell passage number in primary myofibroblasts (Myo 8873) was performed to replicate earlier observations in CCD-18Co. Myo 8873 at three different numbers of cell passages (passage 2, 5 and 8) was harvested and screened for AOC3 protein expression. Passage 2 (P2) is considered as early cell passage, passage 5 (P5) is the intermediate and the later passage is represented by passage 8 (P8). **Figure 4.41A** shows the negative correlation between the cell passage number and the *AOC3* expression. Myo 8873 at P2 has the highest *AOC3* mRNA level compared to P5 and P8 where the expression is decreased by 70% and 75% respectively. *NKX2-3* expression remains constant at P2 and P5 but its level slightly increased at P8. Those results were then confirmed at a protein level by western blot (**Fig 4.41B**). Both results have clearly demonstrated that AOC3 protein expression in Myo 8873 was strongly downregulated at intermediate (P5) and late (P8) cell passages when compared with early cell passage (P2). Similar to CCD18Co, there was an increase in the expression of NKX2-3 at later cell passages of Myo 8873.

It is worth noting that preliminary testing using treatment with TGFβ1 (10 ng/mL for 72 h), which was reported to induce senescence (Senturk et al., 2010) did not lead to any significant increase in the beta-galactosidase staining in myofibroblasts (data not shown). Repetition of the experiment using different concentrations and treatment duration for TGFβ1 or including other agents such as gamma irradiation to induce DNA damage-induced senescence (Noren Hooten and Evans, 2017), may be needed to test the effect of direct induction of senescence on AOC3 and associated genes' expression in myofibroblasts.

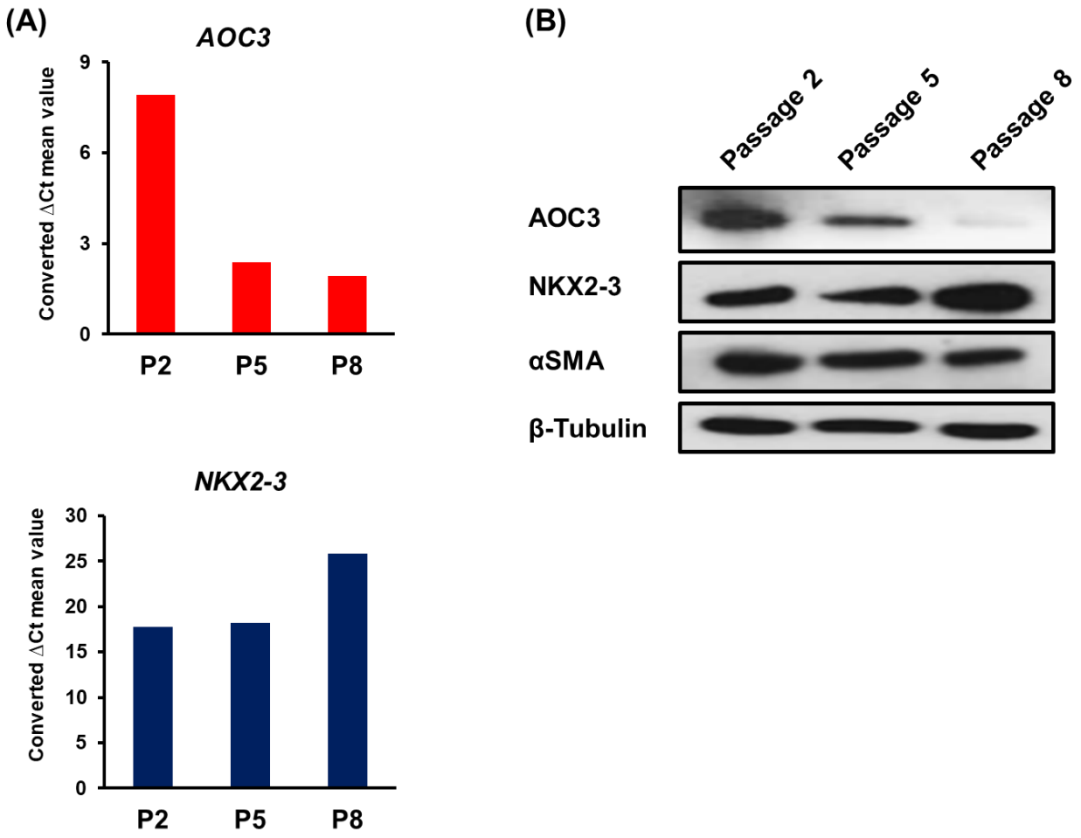

Figure 4.41

The expression of AOC3 and NKX2-3 across different passages of Myo 8873.

The expression of *AOC3* (A) correlates negatively with passage number, the lowest expression being observed at P8. Higher expression of *NKX2-3* was observed at the later passage (one single experiment). Western blot analysis (B) verified the higher AOC3 and NKX2-3 protein expression at P2 when compared to later cell number passages. The protein expression of αSMA was comparable across all cell passages (P = cell passage number).

4.3 Discussion

Myofibroblasts are characterized by the expression of certain genes that differentiate them from normal skin fibroblasts. Our laboratory has identified genes that are differentially expressed between these two types of cells. These include *AOC3*, *NKX2-3* and *LRRC17*, all upregulated in myofibroblasts and downregulated in skin fibroblasts. This chapter discusses the influence of growth factors, primarily on the regulation of AOC3 and NKX2-3 expression in myofibroblasts. Prominent suggested markers of the activated form of myofibroblasts, namely αSMA and FAP, were included in this study to elucidate the effect of the growth factors on the activation of myofibroblasts.

The expression levels of AOC3 and NKX2-3 in myofibroblasts, skin fibroblasts and CRC cell lines were studied at gene and protein levels. Our results (**Fig 4.3 and 4.4**) validate that indeed, AOC3 and NKX2-3 serve as specific markers to distinguish myofibroblasts from skin fibroblasts and CRC cells. Hsia et al. (2016) proved that indeed $AOC3^{+}$ cells isolated from primary tissues using fluorescence cell sorting (FACS) and maintained in culture were myofibroblasts based on their positive expression of AOC3 and NKX2-3. Little is known about the functional role and signalling pathway involving AOC3 and NKX2-3 in the context of the myofibroblasts of the colon.

Immunofluorescence staining of AOC3 and NKX2-3 in CCD-18Co proves the positive expression of these proteins in myofibroblasts. It was found however that NKX2-3 immunostaining profile using commercially available polyclonal

antibody from LSBio, is highly influenced by fixation, as shown in **Figure 4.6A**. This brings up the question of possible cross-reactivity of NKX2-3 antibody used in the present study. We postulated that this observation with NKX2-3 staining pattern may be analogous to that PR2D3, an in-house monoclonal antibody developed by Richman et al. (1987) used to identify pericryptal cells, in which it was found to recognize both AOC3 and MYH11 in colonic muscle lysate (Hsia et al., 2016).

Current data also highlights the heterogeneous AOC3 protein expression as opposed to consistently high NKX2-3 expression in primary myofibroblasts (**Fig 4.8** and **4.10**). This finding was corroborated by IHC staining of AOC3 in parental tissues (**Fig 4.12**) where AOC3 expression in pericryptal cells varied between the samples. As shown by the IHC staining data and western blot screening, it is postulated that NKX2-3 acts as a general marker for myofibroblasts due to its high expressions in primary cells whereas AOC3 expression indicates the activation state of the myofibroblasts. Besides activation, AOC3 expression in myofibroblasts also was regulated by cell senescence (**Fig 4.40** and **4.41**). These results bring the question of the effect of cell senescence on overall gene and protein expression in myofibroblasts.

We screened a panel of growth factors to determine their influence on gene and protein expression of myofibroblasts. The candidate growth factors which were tested in this study include TGFβ1, EGF, TNFα, FGFβ, HGF, VEGF, PDGF-AA, PDGF-CC and IGF1. Our results revealed that certain growth factors regulated gene expression in myofibroblasts (**Table 4.1**). TGFβ1 upregulated *ACTA2* and

MYH11 expression whereas suppression of those genes was detected after incubation with EGF and PDGF-AA. This result is supported by earlier reports that stated EGF and PDGF-AA as two growth factors that downregulate *ACTA2* and *MYH11* (Björkerud, 1991, Liu et al., 2016). The association of the elevated level of *LRRC17*, seen only after treatment with TGFβ1 and myofibroblasts activation, remains to be confirmed. Very small effects, if any, were observed in the regulation of *SHOX2* and *FAP* expression in CCD-18Co after treatment with the selected growth factors.

Growth factor	*AOC3*	*NKX2-3*	*ACTA2*	*MYH11*	*LRRC17*
SF	-	-	-	-	-
10% FBS	↓	↓	↑	↑	-
TGFβ1	↓	↓	↑	↑	↑
EGF	↓	↓	↓	↓	-
TNFα	-	-	-	-	-
FGFβ	-	-	-	-	-
HGF	-	-	-	-	-
VEGF	-	-	-	-	-
PDGF-AA	↓	↓	↓	↓	-
IGF1	-	-	-	-	-

- No changes ↓ Downregulation ↑ Upregulation

Changes in the gene expression, in comparison to serum free (SF) medium alone (-) (highlighted in light grey)

Table 4.1

Influence of growth factors on gene expression (*AOC3*, *NKX2-3*, *ACTA2*, *MYH11* and *LRRC17*) in CCD-18Co, in comparison to serum free (SF) conditions (DMEM alone).

Similar effects on gene regulation in myofibroblasts were found between 10% FBS and TGFβ1 (highlighted in pale red), and EGF and PDGF-AA (highlighted in blue). Three selected growth factors, namely TGFβ1, EGF and PDGF-AA downregulated *AOC3* expression. Downregulation of *NKX2-3* and *ACTA2* expression was found in EGF and PDGF-AA treated CCD-18Co. Similar expression profiles were found between *ACTA2* and *MYH11*.

The opposing effect of EGF and TGFβ1 on *ACTA2*/ αSMA expression of CCD-18Co was verified at mRNA and protein level (**Fig 4.15** and **4.16**). This observation contrasts with the western blot of primary myofibroblasts in **Figure 4.38** where TGFβ1, EGF and PDGF-AA upregulated αSMA expression. These results indicate that growth factors may influence myofibroblast activation differently, depending on their origin and phenotype (activated *vs* nonactivated). Variability in the expression profile between CCD-18Co and other primary myofibroblasts also was indicated through different AOC3 regulation in response to IGF1 observed between CCD-18Co and Myo 8873 (myofibroblast derived from normal colon). IGF1 was found to downregulate AOC3 expression in Myo 8873 (**Fig 4.18**) but not in CCD-18Co (**Fig 4.16**). These results indicate that these myofibroblasts may possess variation in their expression profile such as the expression of IGF1 receptor (IGF1R). The binding of IGF1 to its receptor may affect regulation of AOC3 expression in Myo 8873.

Based on these results on the influence of growth factors on gene expression in myofibroblasts, expression of three growth factors of interest, namely TGFβ1, EGF and PDGFA and their respective receptors in CRC cells, myofibroblasts and skin fibroblasts was analysed using our microarray data. The results are summarized in **Table 4.2**.

Growth factor/ receptor	CRC cell lines	Myofibroblasts	Skin fibroblasts
TGFβ1	**+/-**	**+**	**+**
TGFBRs	**+**	**+**	**+**
EGF	**+/-**	**-**	**- (except for FF)**
EGFR	**+**	**+**	**+ (lowest for FF)**
PDGFA	**++**	**-**	**- (except for FF)**
PDGF-C	**++**	**-**	**- (except for skin fibro 3 and 4)**
PDGFRA	**-**	**+**	**+ (except for FF)**

++ Strong, positive
+ Positive
+/- Moderate
- Negative

Table 4.2

Microarray data on the expression of growth factors and their respective receptors (*TGFβ1* and *TGFBRs*, *EGF* and *EGFR*, *PDGF-A, PDGF-C* and *PDGFRA*) in CRC cell lines, myofibroblasts and skin fibroblasts.

It worth to note that even there was detectable positive expression of *TGFβ1* and *EGF*, it is only at moderate level (mRNA values of less than 700) and only a small subset of CRC cell lines expressed those growth factors. In contrast, approximately 50% of CRC cell lines included in the microarray analysis show strong expression for *PDGF-A*. Another isoform of PDGF, which *PDGF-C* also strongly expressed by CRC cell lines. Positive expression of this gene also was found in two of the skin fibroblasts. The receptor for PDGF-A and C, namely *PDGFRA* is highly expressed by myofibroblasts and skin fibroblasts. EGFR is expressed by almost all CRC cell lines, myofibroblasts and skin fibroblasts. Interestingly, FF (foreskin fibroblasts) possesses striking differences in the expression of *EGFR*, *PDGFA* and *PDGFRA* in comparison to other skin

fibroblasts included in the analysis. With an exception for *TGFβ1*/*TGFRBR*s, CRC cell lines, myofibroblasts and skin fibroblasts only express either the receptor or ligand, not both. This analysis indicates that TGFβ1 signalling between myofibroblasts and CRC cells may occur through paracrine and autocrine mechanisms (due to positive expression of both ligand and its receptor by myofibroblasts and a subset of CRC cell lines) unlike with EGF-EGFR and PDGF-PDGFR which most likely only involve a paracrine signalling pathway as EGF and PDGF-AA/ CC (ligands) are secreted by CRC cells and bind to their receptors on myofibroblasts and these lead to the downstream activation of signalling pathway.

We demonstrated the downregulation of *AOC3* expression in CCD-18Co treated with conditioned medium (CM) from SW480, SW620 and OXCO1 (**Fig 4.28**). This result indicates the presence of secreted components from cancer cells that can influence the property of myofibroblasts. These secretomes may be cell-specific as no significant effect was observed in *AOC3* expression in CCD-18Co after incubation with conditioned medium from RKO and HT29. This finding corroborates with the microarray data where high mRNA level of *PDGF-A* was found in SW480, SW620 and OXCO1, while very low levels of this gene was found in RKO and HT29. As mentioned earlier in this chapter, PDGF-AA is one of the growth factors that downregulates *AOC3* expression in CCD-18Co. The presence of secreted PDGF-AA in the conditioned medium of SW480, SW620 and OXCO1 is postulated by the downregulation of *ACTA2* which mimics the expression profile of PDGF-AA treatment on CCD-18Co. *ACTA2* expression also was downregulated in CCD-18Co when treated with CM from

RKO although RKO is found to be one of the CRC cells with highest expression of TGFβ1. This may be due to the presence of growth factor that been secreted at a higher concentration which masks the effect of TGFβ1 in the medium. OXCO1 also shows higher expression of *TGFβ1* as compared to most of the CRC cells but the values are relatively much lower in comparison to PDGF-A, which may explain the suppression of *ACTA2* expression. No significant changes in *AOC3*, *ACTA2*, *FAP* and *LRRC17* expression was found in CCD-18Co treated with CM from HT29, which do not express TGFβ1, EGF and PDGF-AA. Strikingly, OXCO1 is the only cancer cell line that possesses high mRNA level of three of the growth factors that downregulate the AOC3 expression, namely *TGFβ1*, *PDGF-A* and C. Combination of these three identified growth factors and possibly other unidentified components from OXCO1 lead to the effects seen on the regulation of *AOC3*, *ACTA2*, *FAP* and *LRRC17* expression in CCD-18Co.

The effect of growth factors on the activation of myofibroblasts was studied by comparing FAP expression profiles in a matched myofibroblasts lines from different origins, namely Myo 0165 and 0164C which derived from normal and cancer respectively. Interestingly, large differences in FAP expression were observed between TGFβ1, EGF and PDGF-AA-treated Myo 0164C and 0165 under the same experimental setup, despite them having comparable FAP levels in serum free conditions and in the presence of 10% serum (**Fig 4.38**). That might be explained by Myo 0164C, possessing higher levels of receptors for TGFβ1, EGF and PDGF-AA, which contribute to increased expression of FAP after treatment with the selected growth factors. This hypothesis stems

from reports on the increased expression or activation of TGFBR (Ishimoto et al., 2017), EGFR (Scaltriti and Baselga, 2006) and PDGFR (Pietras et al., 2008) in CAFs through various signalling pathways. The expression of these receptors in the myofibroblast pair (Myo 0165 and 0164C) is discussed further in Chapter 6. The concentration of the growth factor also determines the upregulation of FAP expression in myofibroblasts as higher binding activity of the ligands to the receptor lead to greater induction of FAP expression. Additional screening with more myofibroblast pairs, testing of blocking antibody to specific growth factors (eg. inhibitor for PDGF-AA) and more thorough knockdown experiment will provide more information on the possible pathways and mechanism underlying the activated phenotype of CAFs.

CHAPTER 5

DEVELOPMENT OF SERUM FREE DEFINED MEDIUM FOR MYOFIBROBLASTS

CHAPTER 5: DEVELOPMENT OF SERUM FREE DEFINED MEDIUM FOR MYOFIBROBLASTS

5.1 Introduction

Fetal bovine serum (FBS) is normally included in cell culture media as it contains many essential components that can support cell growth *in vitro*. Despite its routine application in tissue culture, there is a lack of publications on specific constituents of FBS as they may vary between sources and batches of serum. Among the reported growth factors in serum, some such as TGFβ and IGF1 are able to influence the cell properties. To ensure a more controlled experimental setup, a serum free defined medium would be a great advantage for use in such functional tests. In this chapter, the establishment of a serum free defined medium, known as NEW medium is described. The final formulation of NEW medium was optimized from modified PPRF medium, which was designed based on PPRF-msc6 medium formulation, initially described in the literature as a medium that can support mesenchymal cell growth. The development process of the serum free defined medium in this chapter is summarized as below:

The effects of NEW medium on other cell types such as skin fibroblasts and CRC cell lines were also analysed and compared to myofibroblasts under

similar conditions. NEW medium promotes the growth of different myofibroblasts, skin fibroblasts and selected CRC cells. Fetuin and hydrocortisone which are included in NEW medium regulate *AOC3* expression in CCD-18Co. Our analysis shows the potential of NEW medium for use in cell culture work particularly to study myofibroblast and CRC cells in co-culture conditions.

5.2 Results

5.2.1 Early optimization of serum free defined medium formulation - Modified PPRF medium

The serum free defined medium for myofibroblasts was developed and optimized according to the formulation of PPRF-msc6 medium (Jung et al., 2010) that was used to isolate and maintain human mesenchymal stromal cells *in vitro*. PPRF-msc6 medium consists of DMEM/Ham's F12 with 4 mM L-glutamine, 0.1% (v/v) chemically defined lipid concentrate (Invitrogen), 20.5 mM sodium bicarbonate, 4.9 mM HEPES, 4.01 µM bovine insulin, 0.318 mM human transferrin, 55.9 µM putrescine dihydrochloride, 27 nM sodium selenite, 0.018 µM progesterone and 0.7 U/mL heparin (Sigma, St Louis, MO, USA), 4.0 g/L human serum albumin. (HSA; InVitroCare Inc., Frederick, MD, USA), 2 ng/mL FGFβ, 1 ng/mL TGFβ1, 50 µg/mL ascorbic acid, 1 g/L fetuin and 100 nM hydrocortisone. For the current study, we chose to omit several of the elements from the PPRF-msc6 medium such as transferrin and sodium selenite after preliminary test showed that these components inhibited growth of CCD-18Co. This altered PPRF-msc6, which is referred to as modified PPRF medium in the next sections, was used in early optimization of our serum free defined medium. The components of the modified PPRF medium are shown in **Table 5.1**.

Component	Concentration
DMEM/F12 with GlutaMAX	1X
FGFβ	2 ng/mL
TGFβ1	10 ng/mL
L-ascorbic acid-2-phosphate magnesium salt	50 µg/ mL
Hydrocortisone	100 nM
Fetuin	1.0 g/L
Chemically defined lipid concentrate	0.1 % (v/v)

Table 5.1

Components of modified PPRF medium.

Modified PPRF medium was a modification of the PPRF-msc6 medium formulation developed by Jung et al. (2010). This modified PPRF medium comprises of DMEM/F12 (1:1 mixture of DMEM and Ham's F12) with GlutaMAX, chemically defined lipid concentrate, FGFβ, TGβ1, L-ascorbic acid-2- phosphate magnesium salt, fetuin and hydrocortisone.

For the selection of basal medium, two different culture media namely DMEM and DMEM/F12 (1:1 mixture of DMEM and Ham's F12) with GlutaMAX were compared. DMEM/F12 contains more components compared to a more basic DMEM, which is commonly used in cell culture practice. CCD-18Co maintained in DMEM/F12 (both in serum free condition or addition of 10% FBS) demonstrated better growth compared to those cells incubated in DMEM under similar experimental conditions (**Fig 5.1**). Hence, DMEM/F12 was chosen as basal medium for development of serum free defined medium.

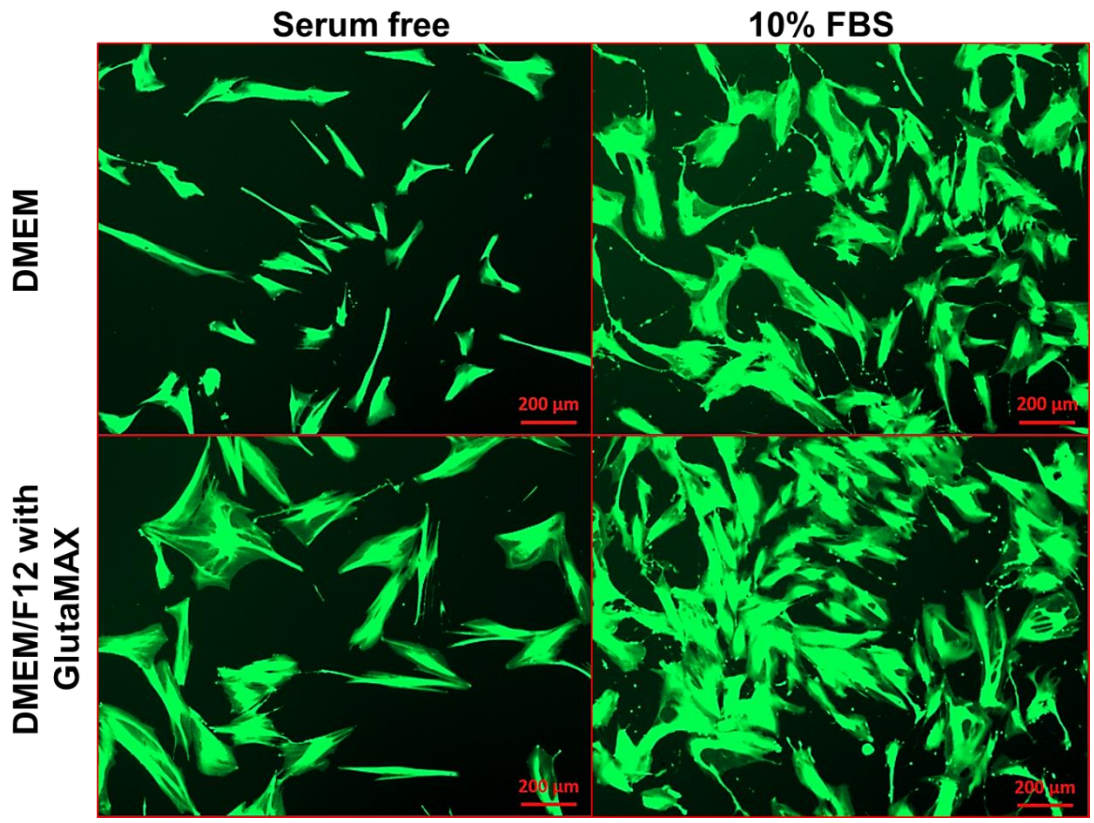

Figure 5.1

CCD-18Co maintained in DMEM or DMEM/F12, either in the presence or absence of serum.

Cells were seeded in DMEM or DMEM/F12 medium + 10% FBS on an uncoated plastic dish and left overnight before medium was changed (either with serum free or medium + 10% FBS). CCD-18Co displayed higher proliferative capacity and better morphology in DMEM/F12 in comparison to DMEM. Viability of cells was assessed using Calcein AM staining (Green) (Magnification: 5x).

Three cell types (myofibroblasts, skin fibroblasts and CRC cells) maintained in the modified PPRF medium displayed different growth rates. After the cells were seeded in 10% FBS and allow to attach overnight, CCD-18Co, skin fibroblasts and HT29 (CRC cells) were incubated with different medium formulations for 6 days. Different percentages of serum (2 and 10%) were included in the experiment to assess the influence of serum concentration on the proliferation of myofibroblasts. Both myofibroblasts and skin fibroblasts displayed better growth after incubation with modified PPRF medium (**Fig 5.2 and 5.3**) in comparison to basal medium alone. This observation was more striking in skin fibroblasts when compared to CCD-18Co. A minimal effect of modified PPRF medium on HT29 proliferation was seen (**Fig 5.4**).

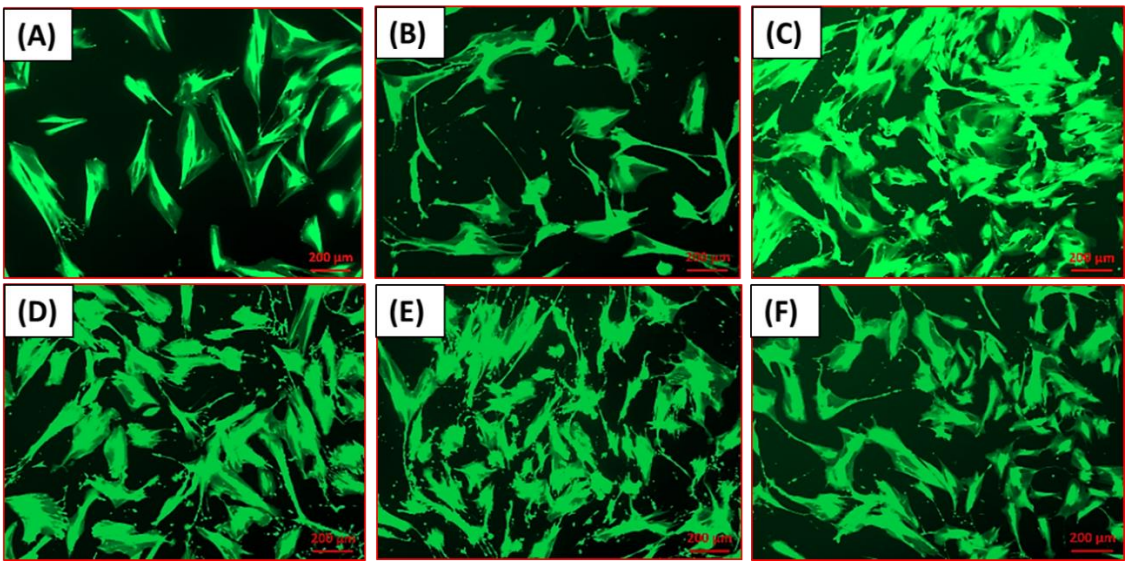

Figure 5.2

Influence of different medium formulations on CCD-18Co.

CCD-18Co maintained in different medium formulations with addition of 0.1% (v/v) chemically defined lipid concentrate; A) DMEM/F12 with GlutaMAX alone; B) DMEM/F12 with GlutaMAX + 2% FBS; C) DMEM/F12 with GlutaMAX + 10% FBS; D) Modified PPRF medium (DMEM/F12 with GlutaMAX alone + H + Fe + A + T + F); E) Modified PPRF medium + 2% FBS and, F) DMEM + 10% FBS for 6 days. Cells were seeded in 10% FBS for 24 h before medium was changed. Viability of cells was assessed by Calcein AM staining (Green) (Magnification: 5x) (Hydrocortisone: H; Fe: Fetuin; A: L-ascorbic acid; T: TGFβ1; F: FGFβ).

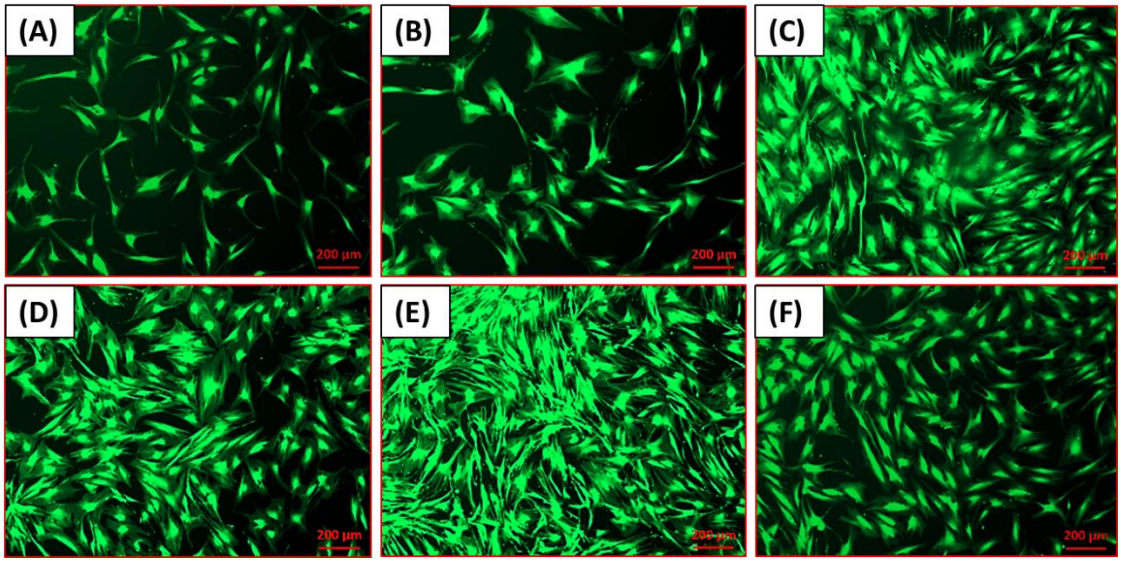

Figure 5.3

Influence of different medium formulations on skin fibroblasts.

Skin fibroblasts (skin fibro_2) maintained in different medium formulations with addition of 0.1% (v/v) chemically defined lipid concentrate; A) DMEM/F12 with GlutaMAX alone; B) DMEM/F12 with GlutaMAX + 2% FBS; C) DMEM/F12 with GlutaMAX + 10% FBS; D) Modified PPRF medium (DMEM/F12 with GlutaMAX alone + H + Fe + A + T + F); E) Modified PPRF medium + 2% FBS and, F) DMEM + 10% FBS for 6 days. Cells were seeded in 10% FBS for 24 h before medium was changed. Viability of cells was assessed by Calcein AM staining (Green) (Magnification: 5x) (Hydrocortisone: H; Fe: Fetuin; A: L-ascorbic acid; T: TGFβ1; F: FGFβ).

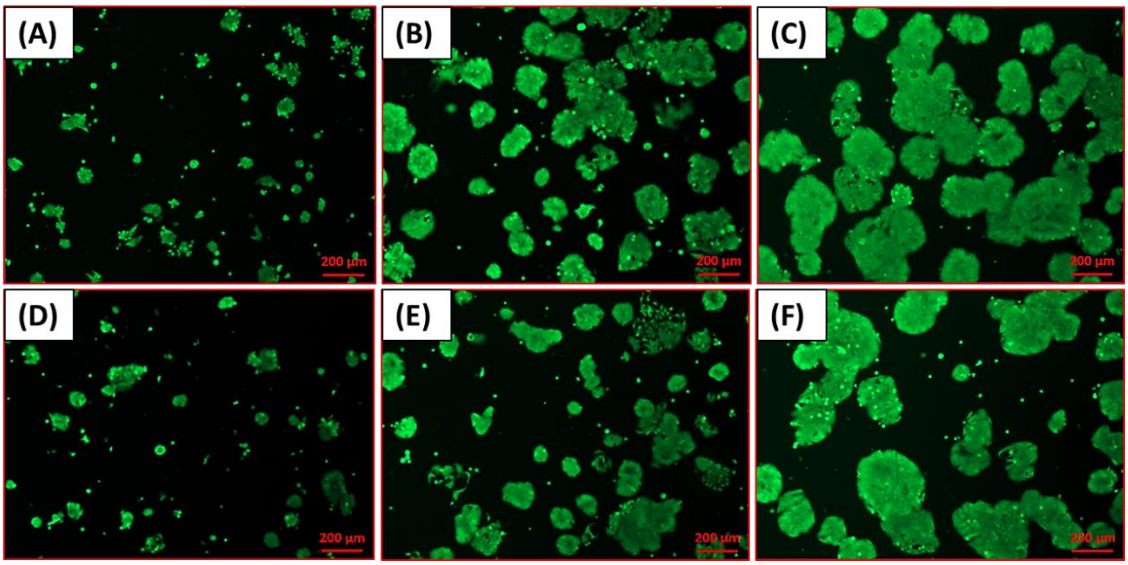

Figure 5.4

Influence of different medium formulations on HT29 (CRC cells).

HT29 maintained in different medium formulations with addition of 0.1% (v/v) chemically defined lipid concentrate; A) DMEM/F12 with GlutaMAX alone; B) DMEM/F12 with GlutaMAX + 2% FBS; C) DMEM/F12 with GlutaMAX + 10% FBS; D) Modified PPRF medium (DMEM/F12 with GlutaMAX alone + H + Fe + A + T + F); E) Modified PPRF medium + 2% FBS and, F) DMEM + 10% FBS for 6 days. Cells were seeded in 10% FBS for 24 h before medium was changed. Viability of cells was assessed by Calcein AM staining (Green) (Magnification: 5x) (Hydrocortisone: H; Fe: Fetuin; A: L-ascorbic acid; T: TGFβ1; F: FGFβ).

Testing using different percentages of FBS for cell culture maintenance revealed that 10% FBS led to optimal proliferation in all selected cells as compared to 2% FBS. Addition of 2% FBS to the modified PPRF medium improved the cell growth although still at lower efficiency than 10% FBS. Greater cell proliferation in the group incubated with DMEM/F12 in comparison to DMEM (both in the presence of 10% FBS) was observed, similarly to previous finding in **Figure 5.1**.

5.2.2 Tissue culture substrate coating material

One of the factors that needs to be considered for an optimal *in vitro* culture environment is cell attachment. Certain cell types do not attach to standard tissue culture plastic or glass unless an appropriate growth factor which mimics the environment of their native counterparts is used to coat its surface (Cooke et al., 2008). We performed a preliminary test to determine whether modified PPRF medium supports the attachment and growth of CCD-18Co by either plating the cells directly into modified PPRF medium or in DMEM/F12 + 10% FBS and replacing the medium with modified PPRF medium after overnight incubation. We found that direct seeding and culture with modified PPRF medium led to adverse effects on their growth. Better cell survival was observed in CCD-18Co seeded in 10% FBS and maintained in modified PPRF medium (data not shown). This observation indicates the need for a substrate which may be essential for cell attachment and FBS most likely contains elements that help cell to attach to the cell culture flasks/plate. Thus, collagen type I rat tail was tested as a possible substrate. In this experiment, CCD-18Co was seeded in a seeding medium, on either collagen type I coated or uncoated plates, and this medium was replaced with fresh culture medium after overnight incubation, which allow cells to adhere to surface. Different medium formulations were tested (serum free – DMEM/F12 alone, DMEM/F12 + 10% FBS and modified PPRF medium).

The results demonstrated that CCD-18Co survived better when seeded and cultured in 10% FBS (**Fig 5.5)**. The absence of collagen coating in CCD-18Co

cultured in modified PPRF medium led to a very minimal cell growth. Interestingly, CCD-18Co thrived when maintained in modified PPRF medium on collagen-coated plates, as shown by the Calcein AM staining. This observation illustrates the importance of collagen for the attachment and growth of myofibroblasts in serum free conditions.

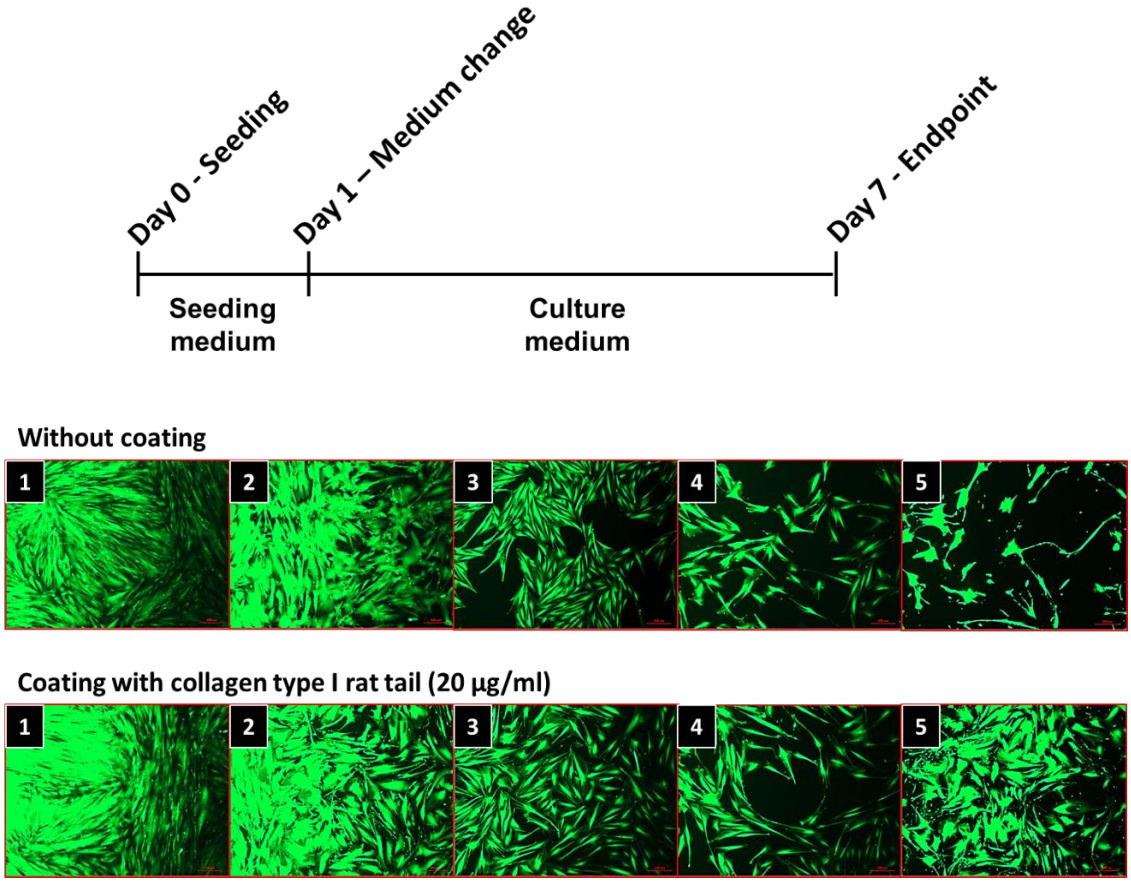

No. of well	1	2	3	4	5
Seeding medium	10% FBS	10% FBS	10% FBS	Serum free	Modified PPRF
Culture medium	10% FBS	Modified PPRF	Serum free	Serum free	Modified PPRF

Figure 5.5

Maintenance of CCD-18Co in various medium formulations, either with and without collagen coating.

CCD-18Co was seeded with seeding medium on coated or uncoated plates and left for overnight at 37˚C. The medium was later changed and CCD-18Co was grown in culture medium for 6 days. Collagen coating supported CCD-18Co attachment. Optimal growth of CCD-18Co was observed in modified PPRF medium + collagen coating although still at lower level compared to 10% FBS

treated group. Viability of cells is shown by Calcein AM staining (Magnification: 5x) (Serum free: DMEM/F12 alone).

5.2.3 NEW medium formulation optimized from modified PPRF medium

The influence of individual components of modified PPRF medium on the growth of CCD-18Co was tested. As shown in **Figure 5.6**, the absence of chemically defined lipid concentrate, FGFβ, fetuin or L-ascorbic acid from modified PPRF medium resulted in slower cell growth and adverse effects on cell viability, indicated by the presence of higher number of DAPI-stained cells in those groups, in comparison to DMEM/F12 alone. CCD-18Co managed to sustain their growth rate when TGFβ1 and hydrocortisone were omitted from the culture medium. A positive control of DMEM/F12 + 10% FBS was included in the experiment.

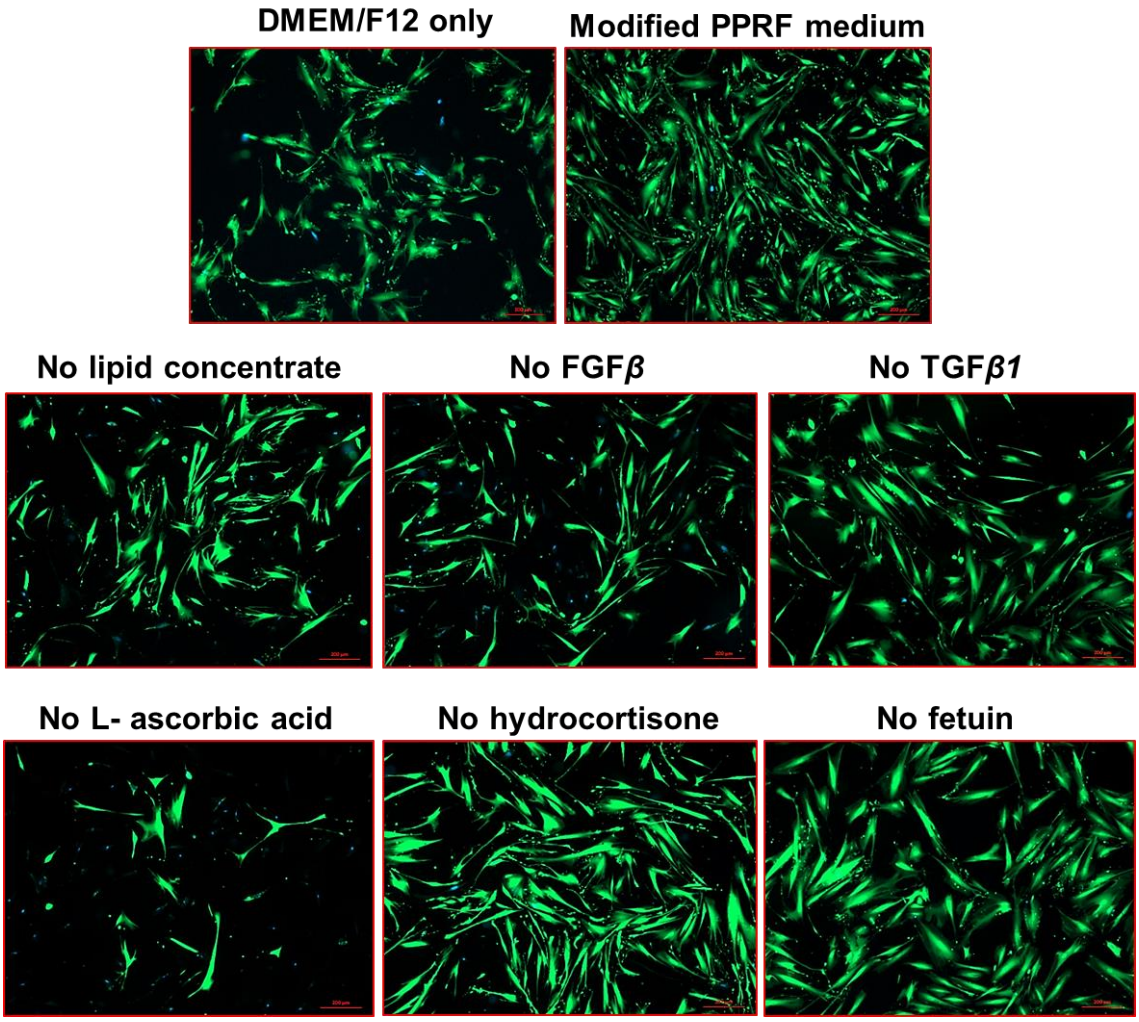

Figure 5.6

Growth and morphology of CCD-18Co maintained in modified PPRF medium depleted with individual components.

Lower cell density was observed in groups treated with the medium in which the following had been omitted one at a time: chemically defined lipid concentrate, FGFβ, TGFβ1, hydrocortisone, fetuin and L-ascorbic acid. All plates were coated with collagen type I. Calcein AM staining indicates the viability of cells. Dead cells are stained with DAPI (Magnification: 5x).

Considering the previous finding in Chapter 4 on the influence of TGFβ1 on the regulation of AOC3 expression, we opted to remove this growth factor from the final formulation of our serum free defined medium. This medium was later renamed as NEW medium which consists of DMEM/F12 with GlutaMAX, chemically defined lipid concentrate, FGFβ, ascorbic acid, fetuin and hydrocortisone. It is worth noting that we found an increase of cell growth when combination of fetuin and hydrocortisone were used, when compared to the addition of fetuin or hydrocortisone alone (data not show). Thus, both components were included in the final formulation of the NEW medium.

Figure 5.7 summarizes the development process of serum free chemically defined medium (NEW medium) which started from alteration of PPRF-msc6 medium formulation, which was renamed as modified PPRF medium. Individual components of the media and their concentrations are listed in the **Figure 5.7** as well. By default, cells maintained in NEW medium were seeded on plates with a thin layer of collagen type I coating and this experimental setup was used throughout the rest of this chapter.

PPRF-msc6 medium → **Modified PPRF medium** → **NEW medium**

Component	Concentration
DMEM/Ham's F12 with glutamine	1X
Chemically defined lipid concentrate	0.1% v/v
Sodium bicarbonate	20.5 mM
HEPES	4.9 mM
Bovine insulin	4.01 µM
Human transferrin	0.318 mM
Putrescine dihydrochloride	55.9 µM
Sodium selenite	27 nM
Progesterone	0.018 µM
Heparin	0.7 U/mL
FGFβ	2 ng/mL
TGFβ1	1 ng/mL
Ascorbic acid	50 µg/mL
Fetuin	1 g/L
Hydrocorstisone	100 nM

Component	Concentration
DMEM/F12 with GlutaMAX	1X
Chemically defined lipid concentrate	0.1% v/v
FGFβ	2 ng/mL
TGFβ1	1 ng/mL
Ascorbic acid	50 µg/mL
Fetuin	1 g/L
Hydrocorstisone	100 nM

Component	Concentration
DMEM/F12 with GlutaMAX	1X
Chemically defined lipid concentrate	0.1% v/v
FGFβ	2 ng/mL
Ascorbic acid	50 µg/mL
Fetuin	1 g/L
Hydrocorstisone	100 nM

Figure 5.7

Development of NEW medium from modified PPRF medium which was optimized from PPRF-msc6.

The initial formulation for serum free chemically defined medium was based on PPRF-msc6 medium (Jung et al., 2010). Modified PPRF medium, which was designed by selecting several essential components from PPRF-msc6 was applied at the initial stages of this study. Final formulation of serum free chemically defined medium, namely NEW medium, was established by excluding TGFβ1 from modified PPRF medium.

5.2.4 NEW medium supports the growth of myofibroblasts

The effect on NEW medium on primary myofibroblast proliferation was tested and compared to CCD-18Co. **Figure 5.8A** illustrates CCD-18Co's distribution and morphology (stained with vimentin and DAPI) when cultured in three different media: serum free medium (DMEM/F12 only), DMEM/F12 + 10% FBS (without collagen coating) and NEW medium. CCD-18Co exhibited a good growth rate when maintained in NEW medium, even without the addition of TGFβ1. Better cell proliferation was observed in the 10% FBS group, while cells treated with serum free medium clearly grew least well. This experiment was repeated with Myo 8873, Myo 0164C and Myo 0165 (**Fig 5.8B**). All primary myofibroblasts displayed better growth when incubated with NEW medium in comparison to serum free condition, although at lower levels compared to 10% FBS.

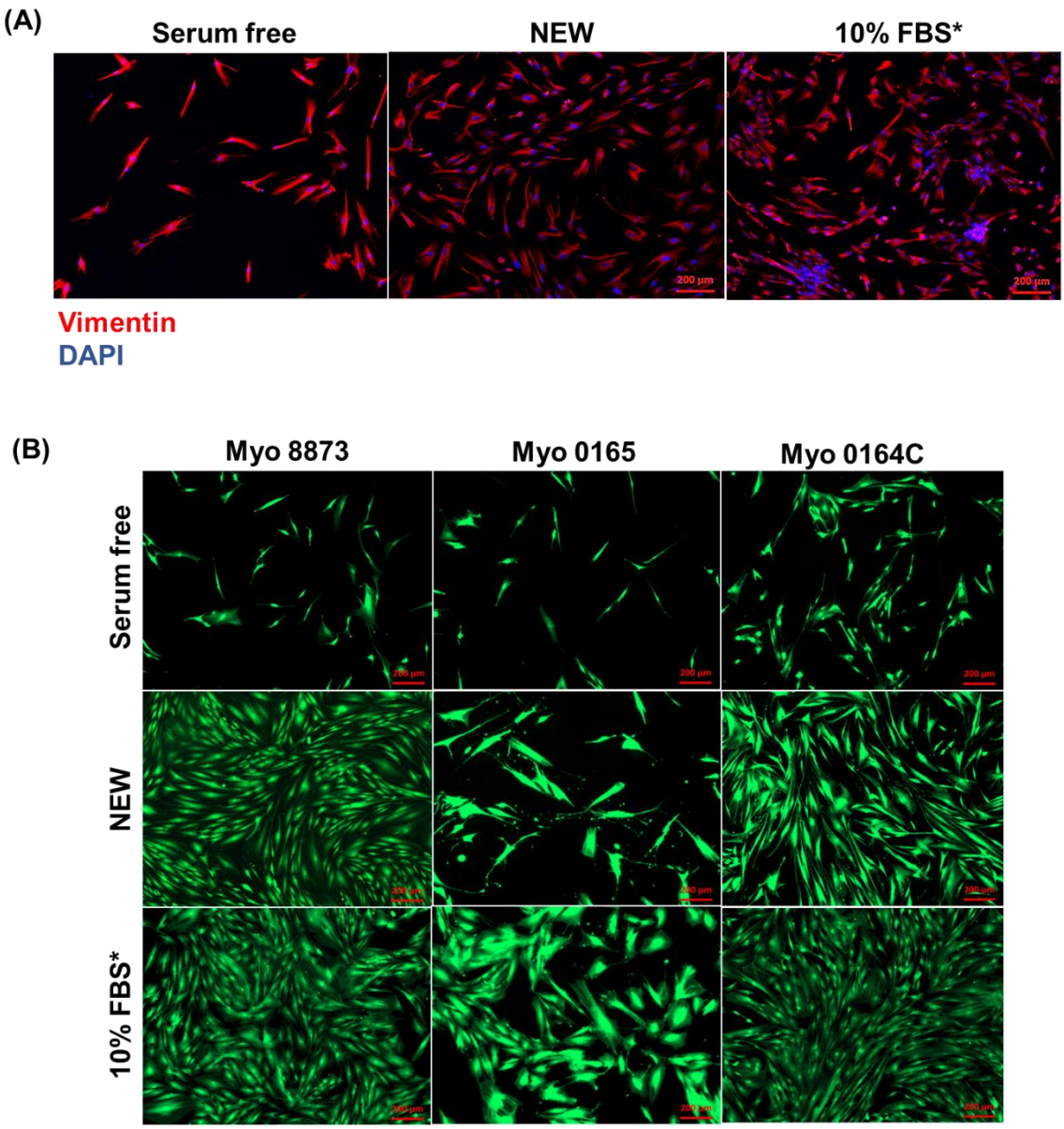

Figure 5.8

The growth of myofibroblasts incubated with NEW medium.

Cells were maintained in either serum free medium (DMEM/F12 alone), NEW medium (DMEM/F12 with GlutaMAX in addition of chemically defined lipid concentrate, FGFβ, L-ascorbic acid, fetuin and hydrocortisone) or DMEM/F12 + 10% FBS for 6 days. NEW medium increased the proliferation of (A) CCD-18Co (stained with vimentin and DAPI) and (B) primary myofibroblasts (Myo 8873, Myo 0165 and Myo 0164C) when compared to DMEM/F12 alone. Viability of primary myofibroblasts was confirmed through Calcein AM staining (*No collagen coating) (Magnification: 5x).

5.2.5 Maintenance of myofibroblasts in NEW medium

A sub-confluence flask of CCD-18Co, maintained in 10% FBS was sub-cultured into different plates where these cells were maintained in either DMEM/F12 alone, DMEM/F12 + 10% FBS and NEW medium for 6 days (Passage 1 – P1). Those cells were then split and grown in their respective medium (DMEM/F12 alone, DMEM/F12 + 10% FBS or NEW medium) for another 6 days. The representative images of CCD-18Co maintained in various medium formulations are shown in **Figure 5.9**. At P1, CCD-18Co grown in NEW medium survived better compared to serum free condition, which agrees with our previous observation, although the cell density is lower compared to DMEM/F12 + 10% FBS group. As expected, at P2, cells incubated with 10% serum managed to survive better as compared to the other groups (serum free and NEW medium treated CCD-18Co). Very little growth was observed in the cells sub-cultured from CCD-18Co maintained in serum free medium at P1. It is worth noting that cells exhibited better proliferative activity in NEW medium in comparison to DMEM/F12 alone even after two cell passages. Optimal growth of CCD-18Co was found in cells sub-cultured from the group previously maintained in 10% FBS at P1. NEW medium seems to support extended *in vitro* culture of CCD-18Co as both cells at P1 and P2 show sufficient growth and better proliferation rate compared to those in serum free conditions.

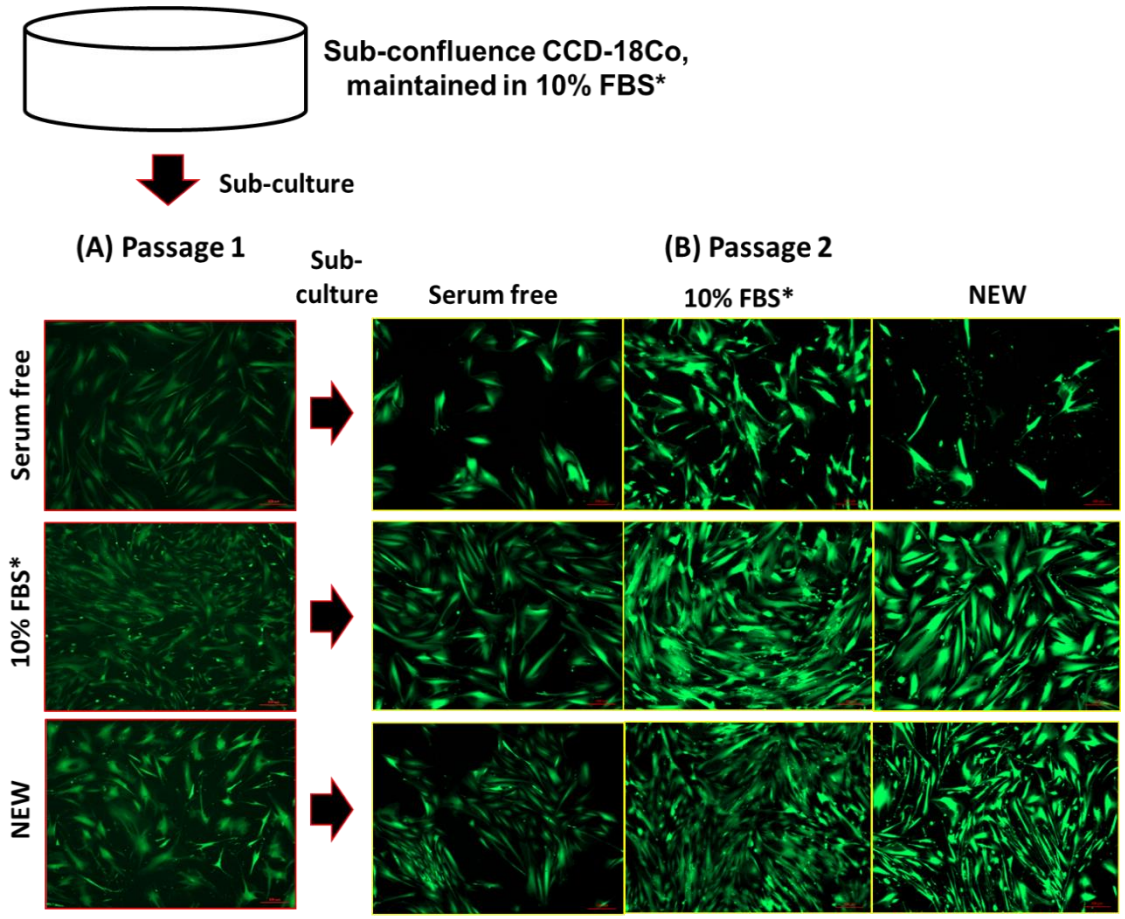

Figure 5.9

Maintenance of myofibroblasts (CCD-18Co) cultured in NEW medium.

The cell distributions after first sub-culture from sub-confluence CCD-18Co, grown in three medium formulations (serum free, 10% FBS and NEW medium) for 6 days are shown in (A). These cells were then split and incubated with different culture media for another 6 consecutive days (P2). CCD-18Co was able to maintain a good number and viability (indicated by Calcein AM) when incubated with NEW medium at P2 (*No collagen coating) (Magnification: 5x). (NEW medium consists of DMEM/F12 with GlutaMAX in addition of chemically defined lipid concentrate, FGFβ, L-ascorbic acid-2-phosphate magnesium salt, fetuin and hydrocortisone).

5.2.6 Influence of NEW medium on *AOC3* expression in CCD-18Co

Although NEW medium supports the growth of myofibroblasts, its influence on specific gene expression in myofibroblasts needs to be tested for. The effect of NEW medium and its individual components on *AOC3* expression in CCD-18Co was analysed using qRT-PCR. **Figure 5.10** shows the experimental layout and results of the experiment. There was a significant downregulation of *AOC3* expression in CCD-18Co after treatment with NEW medium, fetuin alone, hydrocortisone alone, and combination of fetuin and hydrocortisone when compared to DMEM/F12 alone. No significant differences in *AOC3* expression between DMEM/F12 alone and other groups (chemically defined lipid concentrate, ascorbic acid and FGF2 alone) was found. These data demonstrated that gene expression in myofibroblasts is strongly affected by two of the components of NEW medium, namely fetuin and hydrocortisone.

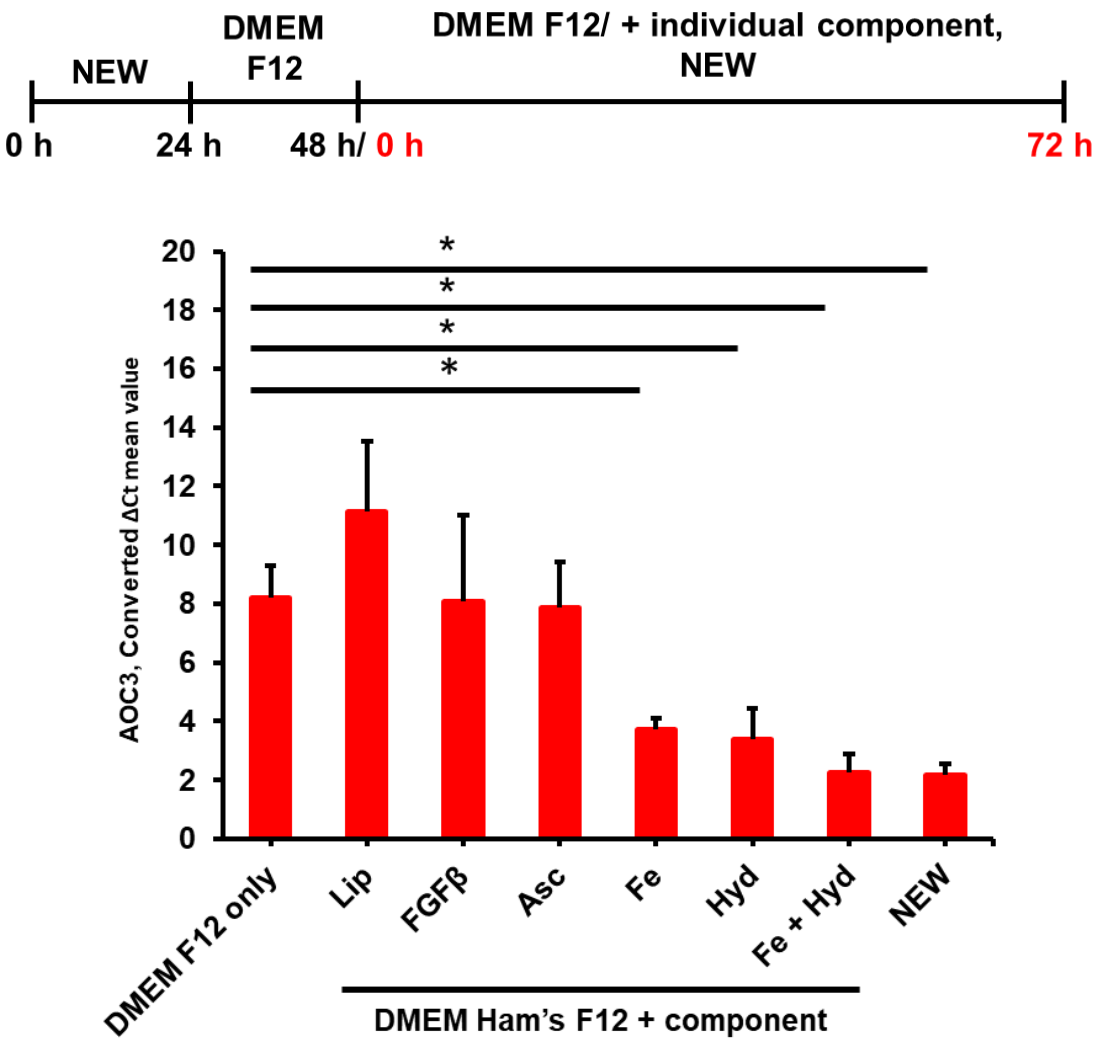

Figure 5.10

The influence of NEW medium and its individual components on *AOC3* expression in CCD-18Co.

Experimental layout and qRT-PCR data of *AOC3* expression in CCD-18Co after incubation with different components of NEW medium are shown as above. Fe, Hyd and combination of Fe + Hyd downregulated *AOC3* expression in CCD-18Co to comparable level as NEW medium. No significant changes in *AOC3* regulation were observed in groups treated with Lip, FGFβ or Asc alone (Lip: chemically defined lipid concentrate; Asc: L-ascorbic acid, Fe: fetuin; Hyd: hydrocortisone) (*$p<0.05$ from triplicates, in comparison to DMEM/F12 (Basal medium) only) (NEW medium consists of DMEM/F12 with GlutaMAX in addition of chemically defined lipid concentrate, FGFβ, L-ascorbic acid-2-phosphate magnesium salt, fetuin and hydrocortisone).

5.2.7 Effect of NEW medium on CRC cell lines

Various CRC cell lines with different characteristics were selected to investigate the proliferative effect of NEW medium on epithelial cells. In this experiment, selected CRC cell lines were seeded directly in NEW medium on collagen type I coated plate (except for 10% FBS treatment groups) and left overnight to attach before medium was changed to either DMEM/F12 alone, NEW medium (DMEM/F12 with GlutaMAX in addition of chemically defined lipid concentrate, FGFβ, L-ascorbic acid-2-phosphate magnesium salt, fetuin and hydrocortisone) or DMEM/F12 + 10% FBS. The cell lines were maintained in those respective medium for 6 days before stained.

Initial screening using RKO, LS180, SW480 and SW620 revealed slight increases in the number of LS180 and SW620 maintained in NEW medium on collagen type I coated plate No positive effects were seen in RKO although it grew better at serum free condition on collagen coated plate (**Fig 5.11A**). No significant changes were observed in SW480 incubated with serum free (DMEM/F12 alone) and NEW medium. Only SW620 grows in NEW medium to any reasonable extent and even that to a much lesser extent than in normal medium containing 10% FBS. A control of CCD-18Co maintained in NEW medium clearly shows better growth rate in comparison to DMEM/F12 (serum free) alone, as shown before.

Further screening using SW1222, SKCO1, HDC9, HCT116 and Colo320DM revealed that these epithelial cell lines exhibited different proliferative activity

under the same treatment (**Fig 5.11B**). Both SKCO1 and HDC9 show minor, insignificant increment in the cell number after incubation with NEW medium. Strikingly, a significant increase in cell proliferation was observed in HCT116 maintained in NEW medium as compared to serum free medium (DMEM/F12 alone). These data collectively demonstrate the difficulty in establishing a completely serum free medium that would satisfy both the requirements of the growth of myofibroblasts and, separately, all the CRC cell lines.

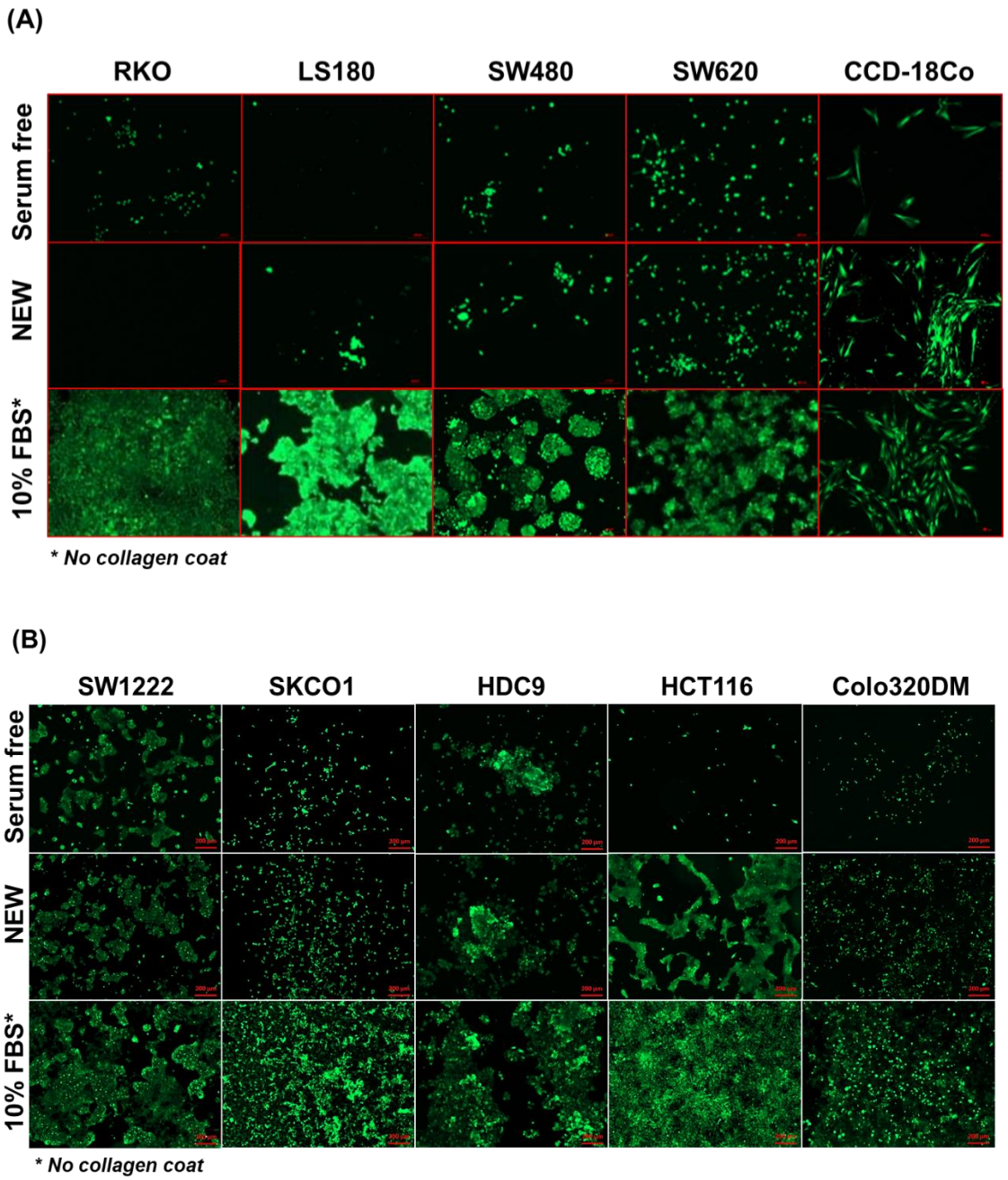

Figure 5.11

Representative images of CRC cell lines and myofibroblasts incubated with serum free (DMEM/F12 alone), NEW medium or DMEM/F12 + 10% FBS.

Various CRC cell lines displayed different survival and growth rate in NEW medium after 6 days. Viability of tested cells was confirmed with Calcein AM staining (Magnification: 5x).

5.2.8 Co-culture of myofibroblasts and CRC cells in NEW medium

Interactions between CRC cells and myofibroblasts can be studied using *in vitro* co-culture assays as described in Chapter 3. Rather than using complete culture medium with addition of 10% FBS, we performed those assays mostly under serum free condition, using DMEM alone without serum, to culture both epithelial cells and myofibroblasts. As most cells require the presence of serum or supplementation to survive well, a more defined medium without serum, which is able to promote cell proliferation would be a better alternative to be used in the *in vitro* assays as it would ensure an optimal cell growth and experimental outcome.

To assess the response of CRC cells and myofibroblasts when co-cultured in NEW medium, two CRC cell lines which show do not grow when grown in NEW medium (**Fig 5.11**), namely HT29 and LS180 were mixed and maintained with CCD-18Co for 7 days in NEW medium on collagen type I coated 24-well plate. After this, CRC cells and CCD-18Co were stained for AUA1 (anti-EpCAM antibody) and vimentin (Vim), respectively to distinguish those two cell types. CRC cells possess positive expression of EpCAM, while CCD-18Co stained for vimentin. Positive control of DMEM/F12 + 10% FBS was included. HT29 formed clusters of “islands” consisting of tightly packed cells in co-culture with CCD-18Co whereas more heterogenous spreading of cells on the culture plate was observed in monoculture. Noticeably, we observed that CCD-18Co grew and surrounded HT29 colonies when incubated in DMEM/F12 + 10% FBS, which was not seen as clearly in serum free conditions (DMEM/F12 alone). most likely

due to fewer myofibroblast cells and less prominent formation of HT29 colonies. Comparison of monoculture between serum free (DMEM/F12 alone) and NEW medium shows that higher numbers of cells were observed in NEW medium although this increment may or may not be significant, as was observed with HCT116 response to NEW medium. HT29 maintained in serum free medium (DMEM/F12 alone) + CCD-18Co was also found to grow at the centre of the well, and at a much lower cell concentration than the 10% FBS co-culture group. HT29 cultured in NEW medium grew evenly across the surface and produced greater cell density as compared to serum free conditions (DMEM/F12 alone). Interestingly, CCD-18Co supports the growth of HT29 as a higher cell number was seen in co-culture (HT29 + CCD-18Co), most notably in those incubated with NEW medium. Representative images of HT29 both in monoculture and co-culture condition are shown in **Figure 5.12A**. A similar experimental setup was applied to study the influence of NEW medium on co-culture of LS180 and CCD-18Co. Higher cell numbers were observed in NEW medium treated groups in comparison to serum free conditions. Additionally, more cells were observed in the LS180 co-culture group compared to monoculture (**Fig 5.12B**). Highest LS180 density was seen in the presence of 10% FBS. It is worth noting that in DMEM/F12 + 10% FBS, LS180 formed colonies or “islands” that were surrounded by CCD-18Co, in a similar manner to HT29 + CCD-18Co. More uniformly growing LS180 was observed in NEW medium.

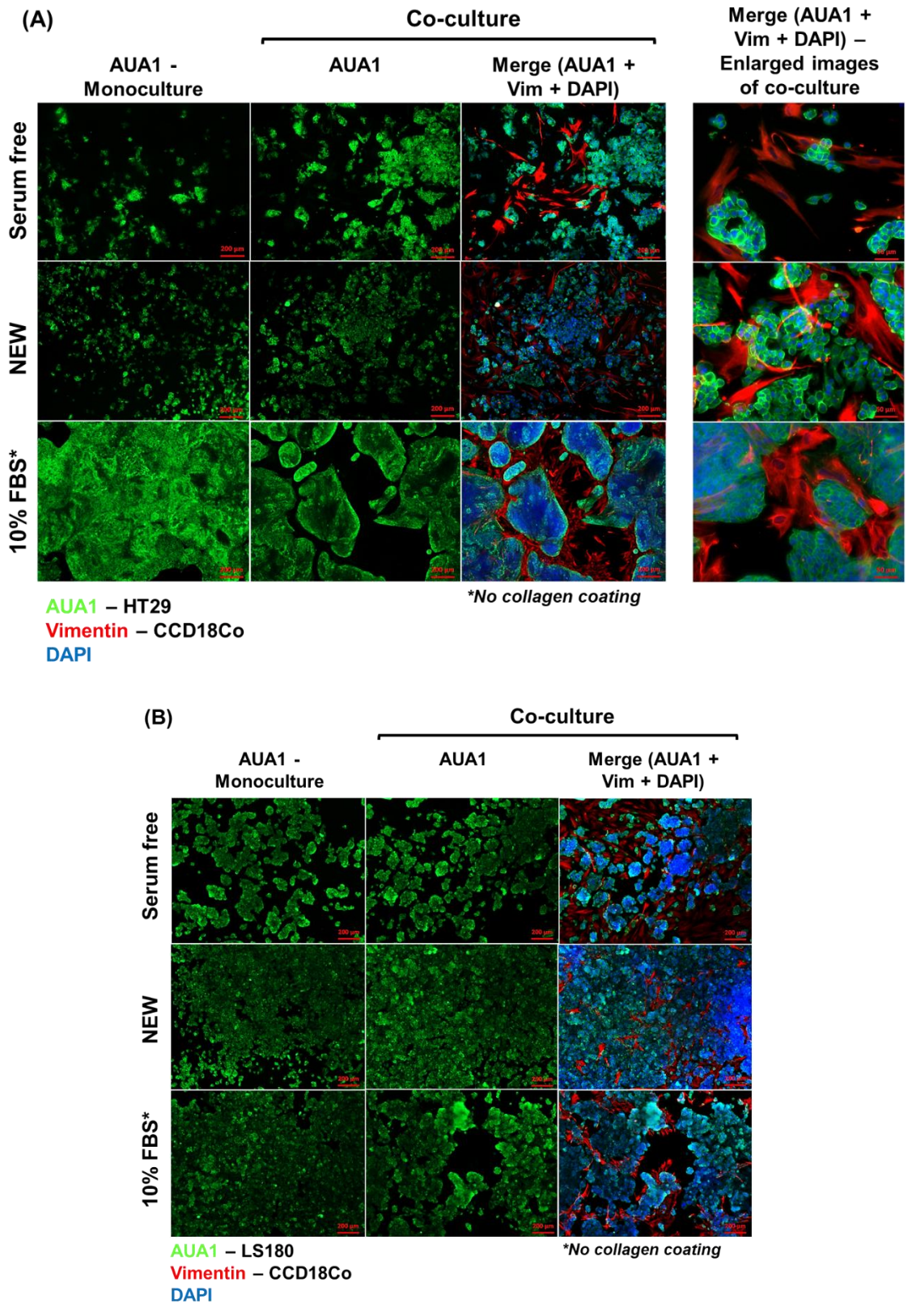

Figure 5.12

Co-culture of (A) HT29 and (B) LS180 and CCD-18Co in NEW medium.

Better growth of CRC cell lines (more prominently with HT29) was found in co-culture using NEW medium as compared to monoculture. This indicates the positive influence of myofibroblasts in supporting the growth of cancer cells. Minimal proliferation of both CCD-18Co and CRC cell lines was observed in serum free (DMEM/F12 alone) condition. Highest cell density was seen in DMEM + 10% FBS groups (Magnification: 5x).

5.3 Discussion

Dulbecco's Modified Eagle's medium (DMEM) with addition of FBS is routinely used to culture human fibroblasts (Rittié and Fisher, 2005). Similar DMEM medium formulation was applied to grow myofibroblasts and skin fibroblasts in this study. Fibroblasts have a reasonably high proliferation rate when maintained in culture medium supplemented with serum. However, the exact composition of serum is poorly defined, and different lots of serum may lead to variability in the experimental outcome.

Jung et al. (2010) described a serum free defined medium for isolation and expansion of human mesenchymal stromal cells, known as PPRF-msc6. Alteration of the PPRF-msc6 formulation without 2% serum was performed and this modified PPRF medium was tested at earlier stages of the current study. TGFβ1 was later excluded from the final formulation of the modified PPRF medium, which was later renamed as NEW medium. The components of NEW medium were listed earlier in this chapter and in the materials and methods section.

DMEM/F12 with GlutaMAX was chosen as the basal medium for the NEW medium as better cell growth was observed when myofibroblasts were maintained in this medium as compared to DMEM. This may be due to the additional components in DMEM/F12 that provide better supplementation for myofibroblasts. The comparison of the composition between DMEM/F12 and DMEM is listed in **Supplementary data S5**.

Our result revealed that several of the components of NEW medium (FGFβ, chemically defined lipid concentrate, L-ascorbic acid and fetuin) are crucial for growth of myofibroblasts as compared to others. The properties of those individual components are discussed below:

a) FGFβ

FGFβ was suggested as a supplement in cell culture medium (Haley and Kim, 2014). This growth factor promotes survival and protects the cells through resistance to radiation-induced-programmed cell death (Fuks et la., 1994) via modulation of apoptosis pathway (Zhang et al., 2010).

b) Chemically defined lipid concentrate

Studies have shown that the chemically defined lipid concentrate supported growth of different types of cells (Rajala et al., 2007; Chijimatsu et al., 2017; Lin et al., 2017). **Supplementary data S6** lists the components of this mixture which include a combination of unsaturated and saturated free fatty acids (FFA). The importance of lipids in cell growth has been documented by Hang et al. (2012).

c) L-ascorbic acid-2-phosphate magnesium salt (APM)

L-ascorbic acid-2-phosphate magnesium salt (APM) is a more stable form of ascorbic acid. L-Ascorbic acid also known as vitamin C is sometimes used as an additive in culture medium and it possesses different biochemical functions including promotion of collagen synthesis in skin fibroblasts (Chan et al., 1990, Pinnell, 1985), phagocytosis of

polymorphonuclear leukocytes (Thomas and Holt, 1978) and differentiation of various mesenchymal cell types (Duarte and Lunec, 2005). L-ascorbic acid-2-phosphate also was reported to stimulate proliferation of skin fibroblasts (Hata and Senoo, 1989). Moreover, APM promotes the synthesis of type 1 collagen synthesis and reduces cell damage by suppressing H_2O_2-induced intracellular reactive oxygen species (ROS) (Tsutsumi et al., 2011). Ascorbic acid also has been reported to elevate the expression of TGF*β*1-induced genes, including *DDR1* and *CCN2 (*Piersma et al., 2017).

d) Fetuin

Fetuin family protein members include fetuin A and B which can form dimers that are thought to contribute to their functional effects. They are carrier proteins rather like albumin and found in the serum (Olivier et al., 2000). Fetuin-A homologues have been identified as a major protein in bovine, sheep, pig, goat, human and rodent sera (Dziegielewska et al., 1992). Fetuin-A (also called α2-Heremans or Schmid glycoprotein (α2-HS glycoprotein/Ahsg)) has been used in tissue culture for its promotion of cellular attachment and its functions probably depend on its carrier properties (Nie, 1992; Rodan and Rodan, 1997; Sakwe et al., 2010).

e) Hydrocortisone

Hydrocortisone is a glucocorticoid. It has been reported to be able to induce changes in gene regulation and promote cell differentiation (Lu et al., 2011; Shiomi and Watanabe, 2014).

f) Collagen I as substrate

Our finding strongly suggests that myofibroblasts requires a substrate such as collagen for their attachment. Collagen type I has been proposed to be the basis of a 3D matrix which is a better representative of physiological conditions of tissue rather than using plastic dishes for fibroblast and myofibroblast culture (Kanta, 2015). Collagen type I supports the attachment and growth of fibroblasts without the transient use of FBS. It is clear from the present study that FBS provides components that help cells to attach and proliferate as the omission of serum (in uncoated plate) leads to minimal cell survival.

Two of the NEW medium components, namely fetuin and hydrocortisone downregulated *AOC3* expression in CCD-18Co. This observation mimics the effect of TGFβ1 on expression of *AOC3*, prompted us to investigate association between fetuin and hydrocortisone with TGFβ1 activity. The fetuin A protein structure composed of a) two cystatin-like domains (Kellermann et al., 1989); b) a calcium phosphate-binding site near the N-terminus (Schinke et al., 1996) and c) a TGFβ cytokine-binding motif (Demetriou et al., 1996). The later shares homology in sequence with extracellular domain of TGFβ receptor type II (TGβRII). These peptides bind to TGFβ and BMP cytokines. The TGFβ/BMP antagonistic property of fetuin A (Szweras et al., 2002) may suggest that fetuin acts in a similar mechanism as TGFβ1 which leads to the downregulation of *AOC3* expression observed in fetuin-treated CCD-18Co). As for hydrocortisone,

it was reported to supress the production of TGFβ mRNA in human fetal lung fibroblasts (Wen et al., 2003).

Hydrocortisone treatment also affects gene regulation (eg. downregulating genes involve in the innate immune/inflammatory responses such as IL-1, IL-6, Toll-like receptor (TLR) and TNF-α signalling) (Lu et al., 2011; Rautava et al., 2016). Thus, we speculated that hydrocortisone induces upregulation of gene(s) that may influence the *AOC3* expression in CCD-18Co, in a similar manner to TGFβ1. Our data shows that fetuin and hydrocortisone were able to downregulate *AOC3* expression without the presence of TGFβ. This may indicate the independence of fetuin and hydrocortisone activity from TGFβ. The nature and mechanisms by which fetuin and hydrocortisone influence *AOC3* will require further investigation.

CRC cells and myofibroblasts were tested to analyse the influence of NEW medium on the growth of different cell types. Various epithelial cells responded differently when incubated with NEW medium. Some CRC cell lines seem to need minimal requirements to proliferate, whereas the others are more stringent and selective with respect to their growth requirements (Boyd et al., 1988; Huschtscha et al., 1991). Myofibroblasts (CCD-18Co and myofibroblast lines established from surgical samples) and selected CRC cells such as HT29 and LS180, survived well under co-culture condition using NEW medium which suggests the potential for this medium to be used for future work involving *in vitro* co-culture of those two cell types.

CHAPTER 6

GENERAL DISCUSSION

CHAPTER 6: GENERAL DISCUSSION

6.1 NKX2-3 is a key regulator of myofibroblast phenotype and AOC3 is an activation marker for myofibroblasts

Our microarray data has identified differentially expressed genes (DEGs) between myofibroblasts and skin fibroblasts. The genes that are upregulated in myofibroblasts and downregulated in fibroblasts include *AOC3* and *NKX2-3*. The specificity of AOC3 and NKX2-3 expression in myofibroblasts has been demonstrated both at gene and protein levels in the present study. As myofibroblasts express high levels of *AOC3* and *NKX2-3*, these genes can be used as markers for myofibroblasts (Hsia et al., 2016; Hulikova et al., 2016), to distinguish them from skin fibroblasts and CRC cell lines.

Our IHC staining result (**Fig 4.12**) on FFPE sections verified the presence of AOC3 stained-pericryptal cells (myofibroblasts) which uniformly surround the epithelial cells in the normal colonic crypt. More irregular AOC3 staining in tumour samples was seen due to disorganized colon structure. This finding corroborates with previous publications which reported different architectures between normal and tumour tissues (Kalluri and Zeisberg, 2006; Medema and Vermeulen, 2011). IHC staining results for NKX2-3 on FFPE section remains inconclusive as unreliable staining profiles were found. Future IHC staining on sections of methanol-fixed tissue would be required to verify the NKX2-3 expression in parental tissue.

Screening of both NKX2-3 and AOC3 expression in various myofibroblasts revealed heterogeneous expression of AOC3 across myofibroblasts samples while NKX2-3 is highly expressed in all of them. This result serves as an indicator of two different populations of myofibroblasts, identified generally as NKX2-3^{+} (positive expression of NKX2-3), and are characterized by either high or low AOC3 expression (AOC3^{+} or AOC3^{-}). Western blot results in **Figure 4.10** show that AOC3^{-}, NKX2-3^{+} myofibroblasts correspond to more activated myofibroblasts which are derived from cancer tissues, while AOC3^{+}, NKX2-3^{+} expression profile was found in myofibroblast lines isolated from the normal matched pair.

Although low AOC3 and high NKX2-3 expression indicates a more activated state of myofibroblasts, this expression profile also is found in senescent myofibroblasts (**Fig 4.40** and **4.41**). It has been shown that senescent cells exhibit the upregulation of secreted proteins and microenvironment modulators that include the senescent-associated secretory phenotype (SASP) or senescence messaging secretome. Increased expression and release of these secretome products, such as PDGF-AA, TGFβ and matrix metalloproteinase-2 (MMP2), may contribute to the suggested cancer promoting property of senescent cells (Kuilman and Peeper, 2009; Coppé et al., 2010; Hassona et al., 2013; Demaria et al., 2014).

AOC3 can be used to define a sub-type of myofibroblasts based on their functional properties (activation state). Variability in AOC3 expression among myofibroblasts further highlights the heterogeneity of myofibroblasts present in

the colon. Hence, data from this thesis suggest that NKX2-3 should be used as a general marker to define the myofibroblast phenotype while AOC3 is an activation marker of myofibroblasts.

The expression of AOC3 in cancer has been reported, before where analysis of the RNA expression patterns for the human copper (Cu) proteome in cancer versus normal tissues from The Cancer Genome Atlas (TCGA) database showed that *AOC3* expression is downregulated in many cancers (≥6 out of 18) such as bladder, stomach, bile duct, prostate, colorectal (CRC) and lung (Blockhuys et al., 2017. Considering that epithelial cells do not express AOC3, at least in CRCs, it is suspected that contamination with myofibroblasts may contribute to the AOC3 expression shown in the database. Downregulation of AOC3 in cancer-derived myofibroblasts in comparison to its normal counterpart may explain the differential expression of AOC3 between those tissues, as found in the TCGA database.

6.2 Activation of myofibroblasts is represented by increased FAP expression

FAP has been described in many publications as a marker for activated myofibroblasts or CAFs. FAP has also been identified as one of several proteins that are upregulated in activated myofibroblasts besides αSMA, fibroblast specific protein-1 (FSP1), PDGFRA, PDGFRB, Forkhead box F1 (FOXF1), SPARC, Podoplanin (PDPN), and COL11A1 (Gascard and Tlsty, 2016). Higher basal levels of FAP were found in myofibroblasts in comparison to skin fibroblasts and CRC cell lines, which do not express any FAP. This proves

FAP's specificity in distinguishing cancer stromal cells from other cell types (**Fig 4.33** and **4.36**).

Activation of myofibroblasts is characterized by positive expression of FAP and upregulation of classical markers of activation such as *ACTA2* (Gene name: αSMA) and *MYH11*, as seen in the current study. More activated stromal cells or CAFs may play a crucial role in promoting cancer progression. **Figure 4.37** and **4.38** indicate that myofibroblasts from different origins responded differently to growth factor treatment. For example, upregulation of FAP expression was found in more activated myofibroblasts, namely Myo 0164C, which are derived from a cancer but not in Myo 0165, which was isolated from normal colon. These results are summarized in **Table 6.1**.

Myofibroblasts	10% FBS	TGFβ1	EGF	PDGF-AA
Myo 0165	-	-	-	-
Myo 0164C	-	+	+	+

- : No changes, + : Upregulation

Table 6.1

Influence of growth factors on FAP expression in Myo 1065 and Myo 0164C, in comparison to serum free condition (DMEM alone).

No changes in the FAP expression were found in serum (10% FBS)-treated groups in comparison to serum free (DMEM alone) conditions in both Myo 0165 and 0164C. However, the concentration of TGFβ1 in FBS, which has been identified as a component in FBS (Areström et al., 2012), may be insufficient to upregulate FAP expression to a comparable level to TGFβ1-treated Myo 0164C.

Despite similar experimental conditions of growth factor treatment with any of TGFβ1, EGF or PDGF-AA, no significant changes in FAP expression profile of non-activated myofibroblasts (Myo 0165) were found. This finding shows that the activated features of myofibroblasts are not a direct, rapid result of stimuli through secreted growth factors or chemokines from surrounding cells such as cancer cells, but rather a process which occurs early in the development of myofibroblasts. This hypothesis arises from the earlier publication from Rettig et al. (1993) where they proposed possible mechanisms for the conversion of resting (low expression of FAP - FAP^-) fibrocytes to activated and proliferating fibroblasts, characterized by positive FAP expression (FAP^+). This process involves discrete steps, each of which may be triggered by specific signals. The first signal induces FAP^- fibrocytes to enter a program of activation that includes *de novo* synthesis of FAP without increasing their growth rate. While these FAP^+ fibroblasts may be incapable of dividing, a second signal, from known mitogenic peptides or by other external, undefined factors will induce their proliferation. They also postulated the possibility that FAP itself may serve as the stimulant for the putative second signal.

The role of FAP as therapeutic agent for cancer has been studied previously. It has been reported that silencing FAP lead to reduce growth and metastasis of oral squamous cell carcinoma (OSCC), through inactivation of PTEN/PI3K/AKT and Ras-ERK and its downstream signalling pathway which regulate proliferation, migration and invasion of cancer cells (Wang et al., 2014).

6.3 Origin and heterogeneity of activated myofibroblasts and CAFs in the colon and rectum

As mentioned earlier, short-term treatment with various growth factors, namely TGFβ1, EGF and PDGF-AA, was not able to switch on the activation response in Myo 0165 so that it became more like its cancer matched pair (Myo 0164C). This observation brings up the question of the origin and processes that contribute to the variation of myofibroblast features (eg. activation state). It is widely reported that heterogeneous populations of myofibroblasts may be a result of their possibly different origins (Worthley et al., 2010) and there are indeed phenotypic differences between myofibroblasts associated with normal colonic epithelium and CAFs (Olumi et al., 1999; Kuperwasser et al., 2004). Still, the nature of activation of myofibroblasts is poorly understood (Herrera et al., 2013).

The mechanisms involved in the formation and differentiation of myofibroblast populations which are derived from the same patient remain debatable. Some have proposed that stable changes in the gene expression of CAFs may be a result of epigenetic changes such as DNA methylation (Hu et al., 2005; Du and Che, 2017; Robertson, 2005). This seems intrinsically unlikely as it would require selection for this changed relatively stable state in what are essentially terminally differentiated cells. An even less plausible proposal for the process that may contribute to development of CAFs is somatic mutation (Weber et al., 2007). The somatic evolutionary process in cancer which involves a series of mutational steps has been discussed in great length by, for example Bodmer

(1996). As more mutational steps occur, there is a higher probability that the subsequent change will lead to exponential growth and so cancer progression. We propose that cancer changes the balance of the outgrowth of the different types of differentiated myofibroblasts from yet not clearly defined progenitor or myofibroblast adult stem cell, leading to a preferential outgrowth of the differentiated form of myofibroblasts that are now recognised as CAFs.

6.4 Differential expression between myofibroblasts from different origins (normal colon *vs* cancer)

The gene expression profile of CAFs and its association with cancer progression has been reported before (Peng et al., 2013). Comparative analysis of the DEGs between CAFs and matched myofibroblasts from normal colonic mucosa shows the upregulation of genes in CAFs which are associated with expression of growth factors (eg. HGF, CDNF, and CSH1), members of the Wnt signalling pathway and other signalling cascades, among others (Mrazek et al., 2014). Candidate genes such as TNFSF4, ST6GALNAC5, TGFB2, TFAP2C and LEF1 are found to be the most overexpressed whereas NOVA1, PDE3B, SLIT3, AKR1C1, AKR1C2 are among the most under-expressed in CAFs derived from CRC (Berdiel-Acer et al., 2014). The lack of myofibroblast pairs included in the microarray analysis in the present study limits the information that can be gathered with respect to DEGs between normal colon and cancer-derived myofibroblasts, although our results clearly show FAP as a reliable marker for CAFs.

Upregulation of FAP expression observed in Myo 0164C treated with TGFβ1, EGF and PDGF-AA (**Fig 4.38**) may be attributed to overexpression of their receptors, namely TGFβ1, EGFR and PDGFRA to which the ligands bind. This hypothesis is based on publications which reported on the elevated levels of those respective receptors in CAFs (The Cancer Genome Atlas Network, 2012, Gascard and Tlsty, 2016). Preliminary screening of EGFR expression in Myo 1064C and 1065 using flow cytometry, shows higher levels of EGFR protein in myofibroblasts derived from cancer when compared to normal colon (**Fig 6.1**). Upregulation in the mRNA level of receptors for TGFβ1 (*TGFBR1*) also was found in Myo 0164C when compared to Myo 0165. However, in contrast to our above suggestion, we found slightly lower levels of *PDGFRA* in Myo 0164C in comparison to Myo 0165 (**Fig 6.2**).

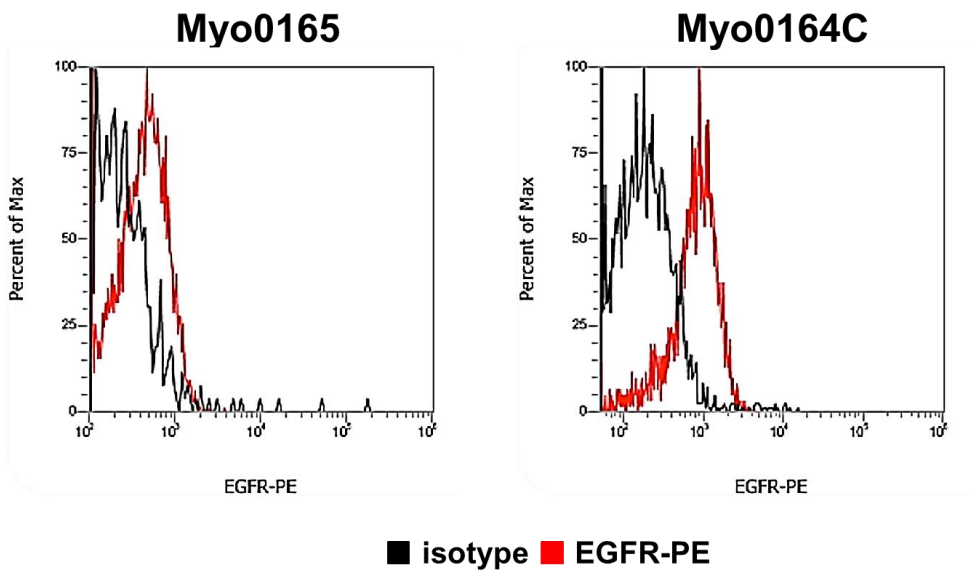

Figure 6.1

Flow cytometry analysis of EGFR expression in Myo 0165 and 0164C.

Myo 1064C expresses a higher level of EGFR protein than Myo 1065 although the difference detected between the lines is not major. It is worth noting that both myofibroblasts expressed significant levels of EGFR. Data courtesy of Dr

Djamila Ouaret, Bodmer's lab (EGFR-PE: EGFR antibody conjugated to phycoerythrin).

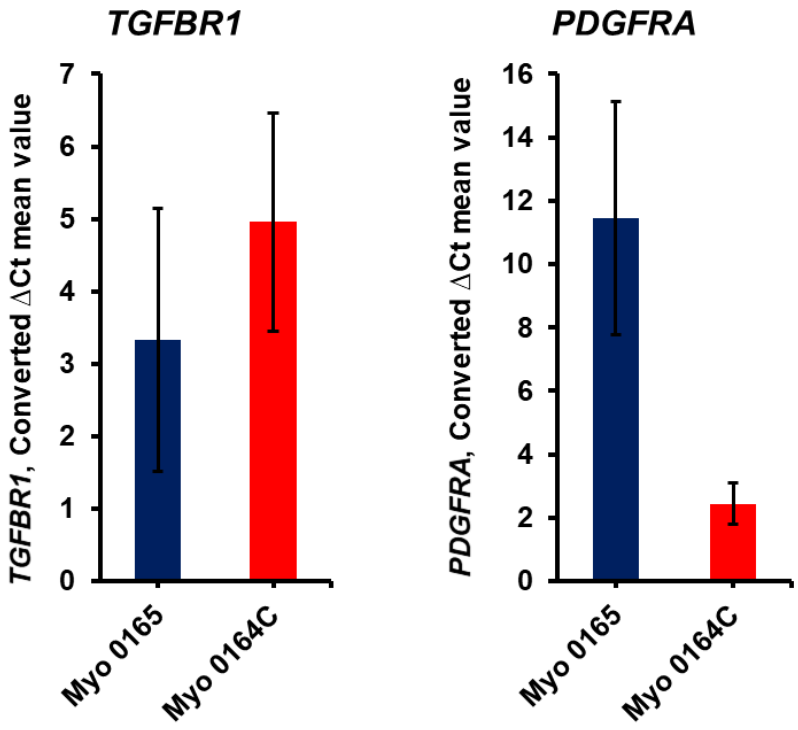

Figure 6.2

The expression of *TGFβR1* and *PDGFRA* in Myo 0165 and 0164C.

The qRT-PCR result shows higher *TGFβR1* expression in Myo 1064C than Myo 0165. A lower *PDGFRA* expression level was detected in cancer-derived Myo 0164C in comparison to its matched normal pair. No significant difference ($p>0.05$) in *TGFβR1* and *PDGFRA* mRNA levels between both samples was found from two biological replicates.

Further screening of TGFBR and PDGFRA expression at protein level in those myofibroblast lines need to be performed to verify our finding. These results show that the activation of myofibroblasts may not be solely characterized by high expression of certain receptors. Other involved mechanisms may influence how the cells respond to growth factors or cytokines for them to acquire the more activated state.

6.5 Activated state of myofibroblasts is represented by suppression of AOC3, positive NKX2-3 expression and stimulation of FAP, αSMA and LRRC17 expression

Collectively, our data suggest the involvement of several crucial genes/ proteins, namely AOC3, NKX2-3, αSMA, FAP and LRRC17, in the activation of myofibroblasts. The activated state of myofibroblasts is characterized by lower levels of AOC3, and increased expression of αSMA, FAP and LRRC17. NKX2-3 is a key regulator for the basic myofibroblast phenotype along with negative expression of SHOX2. Myofibroblast populations (activated *vs* nonactivated) which are classified according to the expression of genes of interest, analysed in the current study are shown in **Figure 6.3**.

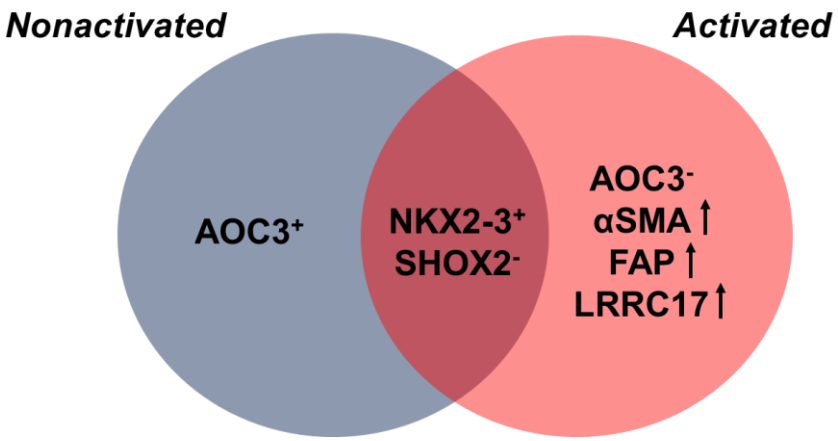

Figure 6.3

Activated and nonactivated myofibroblasts from colon are respectively distinguished by high and low AOC3 expression.

Myofibroblasts in the colon are divided into two major groups (Activated and nonactivated). Both groups express NKX2-3, and no expression of SHOX2 (marker for skin fibroblasts). Increased expression of αSMA, FAP and LRRC17 was found in activated myofibroblasts, but not in nonactivated cells.

6.6 Regulation of AOC3, NKX2-3, αSMA and FAP expression in myofibroblasts

siRNA knockdown experiment suggests that *NKX2-3* is the key regulator of *AOC3* and *ACTA2* expression in CCD-18Co, which is in agreement with Hsia et al (2016). The knockdown of NKX2-3, which is presumably the upstream controlling gene of *AOC3* and *ACTA2*, leads to the downregulation of both *AOC3* and *ACTA2*. We however found a discrepancy in our current result with the previous publication by Hsia et al. As shown in **Figure 4.30** and **4.31**, *NKX2-3* expression in siAOC3-treated CCD-18Co remains unaffected after the transfection, which contradicts the results reported by Hsia et al. They have reported a negative effect on *NKX2-3* expression by siRNA knockdown of AOC3 which suggested the ability of AOC3 to mediate NKX2-3 transcriptional regulation in myofibroblasts. Several factors may contribute to these contradictory results. It is worth noting that Hsia et al. performed the expression analysis after 24 h of transfection with siAOC3 while we analysed the gene expression 48 h post-transfection with siRNA. Moreover, the previous knockdown experiment by Hsia was conducted using siRNA produced by a different company (OriGene), instead of the siRNA from Dharmacon which was used in the current study, although similar concentrations of siRNAs and transfection protocols were included in both experiments.

The discrepancy between these results also might indicate the possibility of off-target activity of siRNA. Although highly sequence specific siRNA mediates the cleavage of target mRNA, the unintended off-target silencing of endogenous

genes can be observed in cells (Fedorov et al., 2006). For example, siRNA-induced sequence-dependent regulation of unintended transcripts, through partial sequence complementarity to their 3′ UTRs, can lead to false-positive phenotypes (Jackson and Linsley, 2010). Moreover, these off-target effects have also been reported to induce apoptosis in various cell lines transfected with siRNAs (Fedorov et al., 2006). Several protocols can be followed to help reduce the off-target effects of siRNAs such as siRNA redundancy, siRNA pooling or chemical modification (eg. 2′-*O*-methyl modification) (Jackson and Linsley, 2010). Experiments involving testing different siRNAs or reducing the concentrations of the siRNAs could be performed to verify our data.

Our initial hypothesis, in which *NKX2-3* is the upstream controlling gene of *AOC3*, is in agreement with our present data that the knockdown of AOC3 would not affect NKX2-3 expression. The NKX2-3 role as the mediator for AOC3 expression was indicated by the qRT-PCR result (**Fig 4.15**) where comparable expression profiles of *NKX2-3* and *AOC3* after treatment with growth factors were found. *AOC3* expression is on this hypothesis influenced by the transcriptional output of *NKX2-3* and thus follows the pattern of *NKX2-3* gene expression. A striking difference on NKX2-3 regulation between gene and protein levels was found where, in the presence of serum, *NKX2-3* mRNA level was supressed (**Fig 4.15**) while its protein expression was upregulated (**Fig 4.11**), in comparison to serum free conditions. We postulate that this result may be an indication of a negative feedback loop in NXK2-3 regulation where the accumulation of NKX2-3 protein may subsequently inhibit production of *NKX2-3*

transcripts. Little is known regarding the protein turnover rate of NKX2-3 which may also explain its high protein expression in serum-treated myofibroblasts.

AOC3 and NKX2-3 regulation also influences other myofibroblast-associated genes or proteins such as *ACTA2*/ αSMA and FAP. The knockdown experiment suggests that NKX2-3 is the regulator for *ACTA2*/ αSMA expression (**Fig 4.30**). As for FAP, its expression is independent of AOC3 and NKX2-3 regulation although in activated myofibroblasts, similarly to AOC3 and NKX2-3, FAP expression is also affected by different growth factors and cytokines. The regulation of AOC3, NKX2-3, *ACTA2*/ αSMA and FAP in myofibroblasts is summarized in **Figure 6.4.**

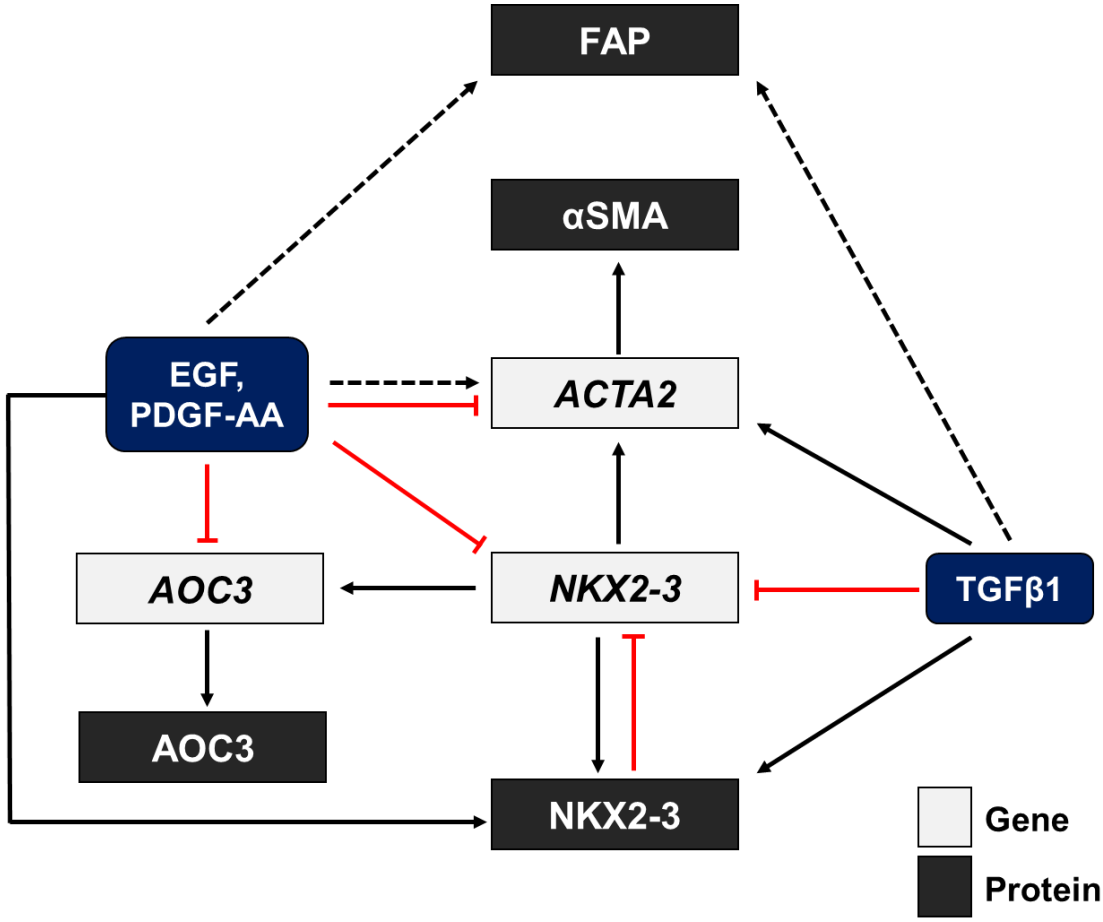

Figure 6.4

Regulation of genes and proteins of interest in myofibroblasts.

NKX2-3 is the regulator of AOC3 and *ACTA2*/ αSMA expression. High NKX2-3 protein level will in turn inhibit its transcript production through a negative feedback loop mechanism. TGFβ1 elevates *ACTA2* and NKX2-3 protein levels but downregulates AOC3 expression which suggests a more activated state of myofibroblasts. Similarly, to TGFβ1, two other growth factors, namely EGF and PDGF-AA downregulate *AOC3* and *NKX2-3* gene expression. EGF and PDGF-AA supress *ACTA2* expression in myofibroblasts derived from normal colon, which contrasts with the observation in cancer-derived myofibroblasts where both growth factors upregulate *ACTA2*/ αSMA expression. TGFβ1, EGF and PDGF-AA induce FAP expression in myofibroblasts isolated from cancer, but not normal colon. Black and dotted lines denote the activation mechanism in myofibroblasts derived from normal colon and cancer respectively. Inhibition of the signalling pathway is represented by the red line.

6.7 Interactions between myofibroblasts and CRC cell lines are facilitated by the growth factors and cytokines

Results obtained from the *in vitro* assays (Chapter 3) provide valuable insights on the interactions between epithelial cells and stromal cells that may promote CRC progression. We found an increase in the migration of myofibroblasts when co-cultured with different CRC cells. Moreover, these assays also demonstrated increased migratory activity and cell differentiation of CRC cell lines when incubated together with myofibroblasts. Our data also show positive effects of co-culture (myofibroblasts and CRC cell lines) on proliferation of both cell types, even in the absence of serum. These results indicate the secretion of growth factors and cytokines from myofibroblasts which influence the property of CRC cells and *vice versa*.

Among the studied growth factors in this thesis, we highlighted mainly the effects of three of them, namely TGFβ1, EGF and PDGF-AA based on their influence on AOC3 and NKX2-3 expression in myofibroblasts. All three growth factors downregulate *AOC3* expression in CCD-18Co (**Fig 4.15**) and upregulate FAP expression in cancer-derived myofibroblasts (**Fig 4.38**). Interestingly, only TGFβ1 treatment leads to the upregulation of *LRRC17*, which is a key gene that defines the myofibroblast characteristics. The upregulation of *LRRC17* in TGFβ1-treated CCD-18Co suggests that *LRRC17* could be an indicator for activation and differentiation of myofibroblasts. SMAD4, which is a mediator of the TGF signalling pathway, has been found to bind at the 5’ transcription start

site (TSS) of *LRRC17* which may lead to an elevated level of the expression of this gene upon treatment with TGFβ1 (Kennedy et al., 2011).

Our data also show different effects of TGFβ1, EGF and PDGF-AA on *ACTA2* regulation in CCD-18Co (**Fig 4.15**) where in contrast to TGFβ1, EGF and PDGF-AA downregulate *ACTA2* expression, which differs from observations in myofibroblasts derived from a patient's sample **(Fig 4.38).** PDGF-BB, another dimer of PDGF, was reported to be a potent negative regulator of smooth muscle-selective gene expression (Blank and Owens, 1990; Li et al., 1997; Owens et al. (2004) which may explain repressive effects on *ACTA2* in CCD-18Co by PDGF-A. Phenotypic differences between CCD-18Co and cancer-derived myofibroblasts may contribute their opposing response to PDGF-AA with respect to *ACTA2*/ αSMA expression.

Collectively, considering our findings from conditioned medium experiments and microarray data analysis on CRC cells and myofibroblasts, PDGF-AA may potentially play a much more important role in the interactions between myofibroblasts and CRC cells, than either TGFβ1 or EGF. High expression of *PDGF-AA* was found in over 50% CRC cell lines (mRNA level of more than 200). Only moderate expression of *TGFβ1* and *EGF* was found in a small number of our CRC cell lines which suggest at most a minimal role for the TGFβ1 and EGFR ligand-dependent signalling pathway *in vivo*. Higher mRNA levels of other EGFR ligands, namely *TGFα*, amphiregulin and epiregulin (**Supplementary data S7**), were detected in most of the CRC cells which could indicate their more significant involvement in CRC progression through the

EGFR signalling pathway, in comparison to EGF. This is supported by Khelwatty et al. (2017) who found abundant expression of TGFα, amphiregulin and epiregulin in CRC tissues, in comparison to EGF. Again, it is still unclear what might be the role of these EGFR ligands in myofibroblast-epithelial cell interactions.

6.8 PDGF-AA and CC as key players in communications between myofibroblasts and CRC cell lines

As mentioned before, PDGF-AA may act as an important factor that is involved in the communications between myofibroblasts and epithelial cells. Interestingly, another family member of PDGF, namely PDGF-CC also produced similar effects, although not as potent as PDGF-AA, on the regulation of AOC3 expression in myofibroblasts (**Fig 4.27**). High expression of *PDGF-C* was observed in almost 40% of cell lines in CRC panel. This expression data agrees with a previous publication which reported the secretion of PDGF-AA and CC by epithelial cells and binding of these ligands to the PDGFR receptor which is expressed on myofibroblasts, as reported by Yasuhiko et al. (2006). The expression of both genes was compared using microarray data, shown in **Figure 6.5**. Clearly, the data shows that CRC cell lines predominantly expressed either one but not both ligands, except for OXCO1 where high mRNA levels for both *PDGF-A* and *C* were found. Our findings on the influence of PDGF-AA and CC on AOC3 expression and microarray expression data on these ligands, and their receptor (*PDGFRA*) strongly suggest an essential role

for the PDGF-AA and CC/PDGFR signalling pathway in controlling the interactions between myofibroblasts and CRC cells.

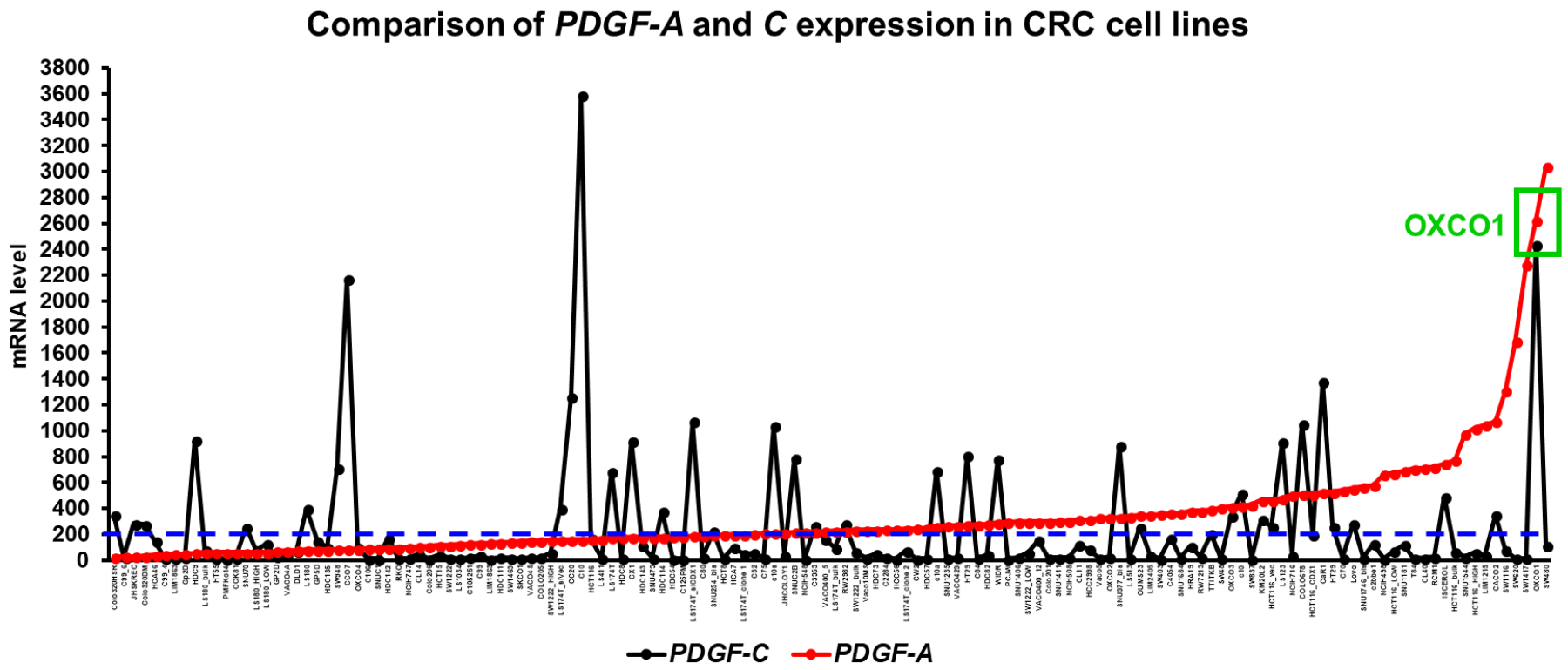

Figure 6.5

Comparison of the expression of PDGF-A and C in CRC cell lines panel.

Mutually exclusive expression of PDGF-A and C was found in CRC cell lines. Only OXCO1 expressed high levels of both ligands. However, ISCEROL and Caco2 may also be double expressers, and to a lesser extent also Lovo and OUMS23. The blue dotted line indicates the cut off mRNA value at 200, in which any value lower than this is to be considered as low or absent expression.

Overactivity of PDGF signalling contributes to the development of certain malignant diseases including cancer, characterized by excessive cell proliferation. The binding of PDGF ligand to its receptor induces dimerization and autophosphorylation of receptors. This leads to activation recruitment and binding and activation of the cytoplasmic SH2-domain containing signal transduction molecules to specific phosphor-tyrosine residues. This initiates different signalling pathways, which stimulate primary tumour growth and survival, as well as reorganization of actin, differentiation, migration and metastasis (Heldin et al., 1998; Östman, 2017). PDGFRs overexpression is associated with poor prognosis for patients (Kitadai et al., 2006). The potential role of PDGF-AA and CC/PDGFRA in myofibroblasts-CRC cell lines interactions is illustrated in **Figure 6.6**.

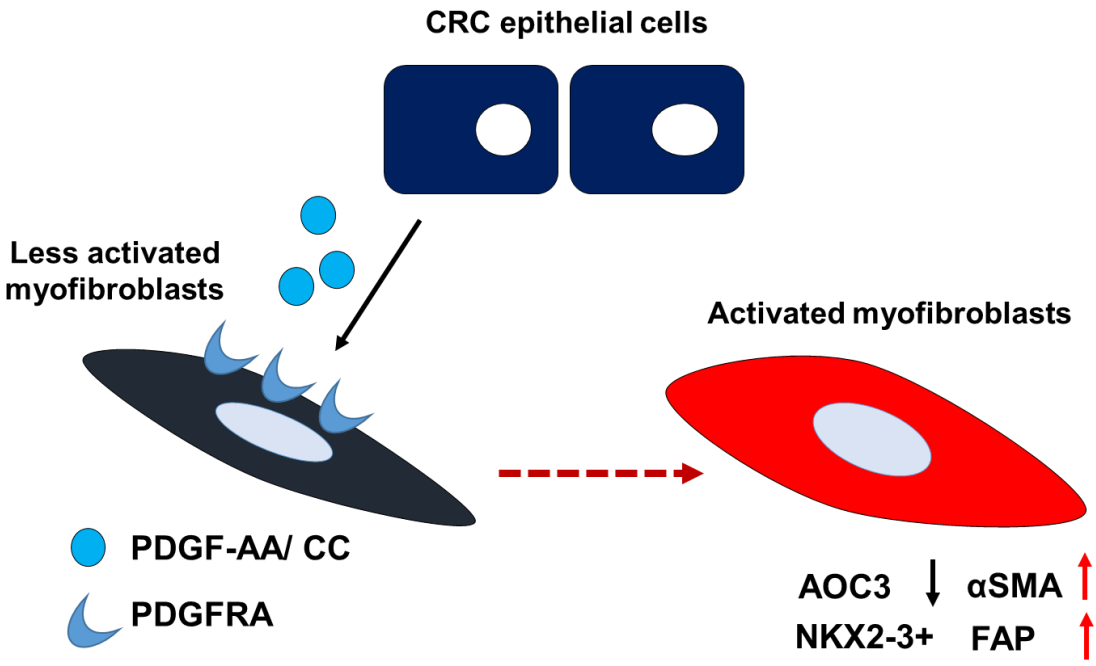

Figure 6.6

Interactions between myofibroblasts and CRC cells through PDGF signalling pathway.

PDGF-AA or CC secreted by the cancer cells bind to PDGFRA on myofibroblasts. Upon stimulation by PDGF-AA/CC binding to the receptor followed by activation of a cascading signalling pathway, myofibroblasts (NKX2-3^{+}) acquire a more activated state represented by decreased AOC3 expression and increased of αSMA and FAP expression.

Previous work from our laboratory (Kalugin's thesis, unpublished, 2017) highlighted the association of PDGF-A and C (isoforms that make up PDGF-AA and CC ligands, respectively) expressed by CRC cells in influencing the migration of myofibroblasts under co-culture conditions. Using a Matrigel-blob assay, he discovered significant recruitment or migration of myofibroblasts when co-cultured with high expressing CRC cells in either *PDGF-A* or *C*. Mutually exclusive expression of *PDGF-A* and *C* in the myofibroblast-recruiting cell lines suggests that these ligands may substitute for one another, which is in agreement with data shown in **Figure 6.6**. As shown by our microarray data, different from most of the CRC cell lines, OXCO1 is the only line that expressed both *PDGF-A* and *C* at high levels. As shown in **Figure 4.28**, conditioned medium from OXCO1 which potentially contains PDGF-A and C, downregulated *AOC3* expression which mimics the previous finding of the influence of PDGF-AA and CC on AOC3 expression in CCD-18Co (**Fig 4.15** and **4.27**).

The role of PDGFs and PDGFRs in CRC has been reported before although these publications emphasized other PDGF family members such as PDGF-AB and BB (Yu et al., 2003; Nakamura et al., 2008). We do not find any significant expression of *PDGF-B* in our CRC cell lines, which is not in agreement with the previous report by Ito et al., 1990. Furthermore, only moderate expression of *PDGFRB* (receptor for PDGF-B) was detected in myofibroblasts (**Fig 4.20**), which suggests a less prominent role, if any, for the PDGF-BB/PDGFRB signalling pathway in bidirectional communications between CRC cell lines and myofibroblasts.

The involvement of the PDGF-AA and CC/PDGFRA axis in the interplay between myofibroblasts and CRC cells was reported before in liver metastasis cases where colorectal cancer cell invasion of the liver lead to upregulation of PDGFRA of hepatic stellate cells (HSCs), which are a source of liver myofibroblasts (Lemoinne et al., 2013). Moreover, PDGFRA also promotes TGFβ signalling of cultured HSCs, which leads to more activated state of HSCs (Liu et al., 2014). The influence of PDGFRA on stromal cell activation and carcinogenesis agrees with reports by Shinagawa et al. (2013) where blocking of PDGFRA in CAFs by imatinib in an orthotopic nude mice model of colon cancer supressed growth and metastasis of human colon cancer. The PDGF/PDGFR signalling pathway was reported to be more significant in cancer than in normal colonic tissue (Raica and Cimpean, 2010).

6.9 Other relevant signalling pathways that influence cross-talk between myofibroblasts and CRC cells

Other signalling pathways that have been associated with CRC include CXCR4–CXCL12 and PD-L1-PD-1, as discussed in the next section. Increased expression of CXCR4 in cancer cells, which is a receptor for CXCL12 that is secreted by stromal myofibroblasts, has been linked to poor prognosis of CRC (Kim et al., 2005). The positive expression of CXCR4 and CXCL12 in epithelial cells and myofibroblasts respectively, agrees with our microarray data (data not shown). Downregulation of the CXCR4/CXCL12 axis led to a reduction in colon cancer cell line growth and metastasis via blocking of Wnt/β-catenin pathway in cancer cells (Song et al., 2015).

Another widely studied pathway in cancer is the PD-L1-PD-1 pathway which is implicated in the regulation of T-cell function (Latchman et al., 2001). CAFs express the programmed death ligands 1 (PD-L1 or CD274) and PD-L2 which can bind to programmed death 1 receptor (PD-1) on T cells and inhibit their activity (Nazareth et al., 2007). This anti-tumour response of T cells by CAFs may in certain situations promote cancer progression presumably by suppressing T cell attack on the cancer (Kakarla et al., 2012). PD-L1 expression is regulated by interferon gamma (Mimura et al., 2018). A previous study has reported positive PD-L1 expression in human colonic myofibroblasts (Pinchuk et al., 2008) which is in agreement with our microarray data on CCD-18Co. PD-L1 expression was found to be varied across myofibroblasts and skin fibroblasts samples (**Fig 6.7**). Our data found no direct correlations between AOC3, NKX2-3 and PD-L1 expression in myofibroblasts, although more thorough analysis needs to be conducted to confirm this.

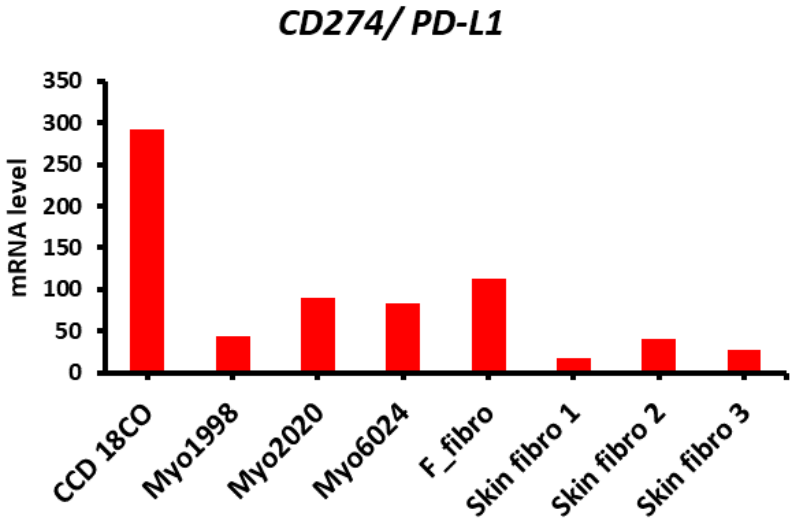

Figure 6.7

***PD-L1* mRNA level in our panel of myofibroblasts and skin fibroblasts (F. fibro: foreskin fibroblasts; skin fibro: skin fibroblasts).**

With regard to other growth factors of interest, HGF, which is secreted by stromal cells such as myofibroblasts, would bind to its receptor (c-MET) on epithelial cells. This interaction has been suggested to possesses pro-carcinogenic properties as it has been found to promote cancer formation by protecting CRC cells against glucose starvation-induced apoptosis (Mira et al., 2017). Positive expression of *HGF* was found in our panel of myofibroblasts (**Fig 6.8**). Unpublished work from our laboratory (Kalugin, 2017) shows that HGF inhibited the differentiation of one of the CRC cell lines (HT29).

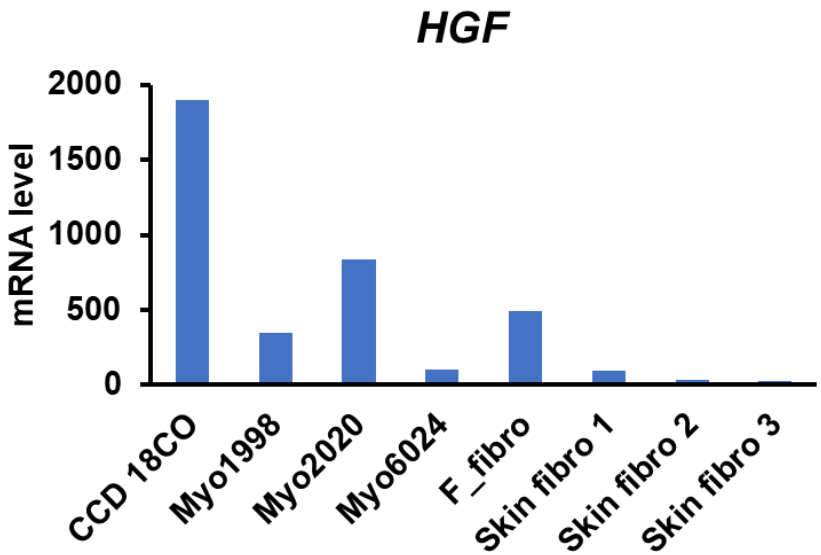

Figure 6.8

***HGF* mRNA level in our panel of myofibroblasts and skin fibroblasts.**

F. fibro: foreskin fibroblasts; skin fibro: skin fibroblasts.

6.10 Establishment of serum free defined medium for co-culture experiments to study interactions between CRC cells and myofibroblasts

The addition of serum in cell culture medium to recapitulate the *in vivo* condition is highly debatable. Various studies employ different concentrations of serum for the experimental purposes, ranging from low or minimal serum (0-2% FBS) to full serum (10-20% FBS). Many researchers have opted to use serum free defined medium for a more controlled experimental setting. NEW medium was developed to enable good growth of myofibroblasts in contrast to DMEM, alone which only supported a much lower rate of cell proliferation.

The compatibility of the NEW medium for co-culture of myofibroblasts and CRC cells was proven, as shown in **Figure 5.12**. Higher cell growth of HT29 was observed when co-cultured with CCD-18Co in NEW medium. This observation indicates the release of growth factors and chemokine from CCD-18Co which promote the proliferation of HT29. Sufficient growth of CCD-18Co was seen when maintained in NEW medium, better than in DMEM/F12 alone (basal medium only). This cell culture setup will enable future studies on the influence of specific growth factors and cytokines and their inhibitors on both cancer cells and myofibroblasts, when they are incubated together.

6.11 Summary

In this thesis, we have provided solid evidence on the nature of the *in vitro* bidirectional communication between myofibroblasts and CRC cell lines, facilitated by secretion of growth factors and cytokines. We also further characterize NKX2-3 as a regulator which defines the overall myofibroblast phenotype and AOC3 absence as an activation marker for myofibroblasts. Analysis of FAP expression and other classical markers for activation including αSMA in myofibroblasts from different origins (normal *vs* cancer) revealed heterogeneity in the populations of myofibroblasts. Our current work also demonstrated the influence of growth factors and cytokines particularly PDGF-AA, secreted by epithelial cells on AOC3 and NKX2-3 regulation in myofibroblasts. Further work on identifying different, heterogeneous subpopulations of myofibroblasts with respect to their activation state (activated or nonactivated) will help tremendously in understanding the nature of myofibroblasts in the colon and how interactions between myofibroblasts and cancer cells occur *in vivo*.

REFERENCES

REFERENCES

ABELLA, A., GARCIA-VICENTE, S., VIGUERIE, N., ROS-BARO, A., CAMPS, M., PALACIN, M., ZORZANO, A. & MARTI, L. (2004) Adipocytes release a soluble form of VAP-1/SSAO by a metalloprotease-dependent process and in a regulated manner. *Diabetologia,* 47**,** 429-438.

ADEGBOYEGA, P. A., MIFFLIN, R. C., DIMARI, J. F., SAADA, J. I. & POWELL, D. W. (2002) Immunohistochemical study of myofibroblasts in normal colonic mucosa, hyperplastic polyps, and adenomatous colorectal polyps. *Archives of Pathology & Laboratory Medicine,* 126**,** 829-836.

AERTGEERTS, K., LEVIN, I., SHI, L., SNELL, G., JENNINGS, A., SRIDHAR PRASAD, G., ZHANG, Y., L KRAUS, M., SALAKIAN, S., SRIDHAR, V., WIJNANDS, R. & TENNANT, M. (2005) Structural and kinetic analysis of the substrate specificity of human fibroblast activation protein Alpha. *The Journal of biological chemistry,* 280**,** 19441-4.

AIRENNE, T. T., NYMALM, Y., KIDRON, H., SMITH, D. J., PIHLAVISTO, M., SALMI, M., JALKANEN, S., JOHNSON, M. S. & SALMINEN, T. A. (2005) Crystal structure of the human vascular adhesion protein-1: Unique structural features with functional implications. *Protein Science,* 14**,** 1964-1974.

ARAI, T., KAKUTA, Y., KINOUCHI, Y., KIMURA, T., NEGORO, K., AIHARA, H., ENDO, K., SHIGA, H., KANAZAWA, Y., KUROHA, M., MOROI, R., NAGASAWA, H., SHIMODAIRA, Y., TAKAHASHI, S. & SHIMOSEGAWA, T. (2011) Increased expression of NKX2.3 mRNA transcribed from the risk haplotype for ulcerative colitis in the involved colonic mucosa. *Human Immunology,* 72**,** 587-591.

ARESTRÖM, I., ZUBER, B., BENGTSSON, T. & AHLBORG, N. (2012) Measurement of human latent transforming growth factor-β1 using a latency associated protein-reactive ELISA. *Journal of Immunological Methods,* 379**,** 23-29.

ARVILOMMI, A.-M., SALMI, M. & JALKANEN, S. (1997) Organ-selective regulation of vascular adhesion protein-1 expression in man. *European Journal of Immunology,* 27**,** 1794-1800.

ASHLEY, N., YEUNG, T. M. & BODMER, W. F. (2013) Stem cell differentiation and lumen formation in colorectal cancer cell lines and primary tumors. *Cancer Research,* 73**,** 5798-5809.

AUGSTEN, M. (2014) Cancer-associated fibroblasts as another polarized cell type of the tumor microenvironment. *Frontiers in Oncology,* 4**,** 62.

BELLA, J., HINDLE, K. L., MCEWAN, P. A. & LOVELL, S. C. (2008) The leucine-rich repeat structure. *Cellular and Molecular Life Sciences,* 65**,** 2307-2333.

BERDIEL-ACER, M., SANZ-PAMPLONA, R., CALON, A., CUADRAS, D., BERENGUER, A., SANJUAN, X., PAULES, M. J., SALAZAR, R., MORENO, V., BATLLE, E., VILLANUEVA, A. & MOLLEVÍA, D. G. (2014) Differences between CAFs and their paired NCF from adjacent colonic mucosa reveal functional heterogeneity of CAFs, providing prognostic information. *Molecular Oncology,* 8**,** 1290-1305.

BIBEN, C., WANG, C. C. & HARVEY, R. P. (2002) NK-2 class homeobox genes and pharyngeal/oral patterning: Nkx2-3 is required for salivary gland and tooth morphogenesis. *The International Journal of Developmental*

Biology, 46**,** 415-422.
BJÖRKERUD, S. (1991) Effects of transforming growth factor-beta 1 on human arterial smooth muscle cells in vitro. *Arteriosclerosis, Thrombosis, and Vascular Biology,* 11**,** 892-902.
BLANK, R. S. & OWENS, G. K. (1990) Platelet-derived growth factor regulates actin isoform expression and growth factor regulates actin isoform expression and growth state in cultured rat aortic smooth muscle cells. *Journal of Cellular Physiology,* 142**,** 635-642.
BLOCKHUYS, S., CELAURO, E., HILDESJO, C., FEIZI, A., STAL, O., FIERRO-GONZALEZ, J. C. & WITTUNG-STAFSHEDE, P. (2017) Defining the human copper proteome and analysis of its expression variation in cancers. *Metallomics,* 9**,** 112-123.
BOCHATON-PIALLAT, M. L., GABBIANI, G. & HINZ, B. (2016) The myofibroblast in wound healing and fibrosis: answered and unanswered questions. *F1000Research,* 5**,** F1000 Faculty Rev-752.
BODMER, W. F. (1996) The somatic evolution of cancer. *The Harveian Oration*.
BOYD, D. D., LEVINE, A. E., BRATTAIN, D. E., MCKNIGHT, M. K. & BRATTAIN, M. G. (1988) Comparison of growth requirements of two human intratumoral colon carcinoma cell lines in monolayer and soft agarose. *Cancer Research,* 48**,** 2469-2474.
BRENNEN, W. N., ISAACS, J. T. & DENMEADE, S. R. (2004) Rationale behind targeting fibroblast activation protein-expressing carcinoma-associated fibroblasts as a novel chemotherapeutic strategy. *Molecular Cancer Therapeutics,* 11**,** 257-266.
BROKOPP, C. E., SCHOENAUER, R., RICHARDS, P., BAUER, S., LOHMANN, C., EMMERT, M. Y., WEBER, B., WINNIK, S., AIKAWA, E., GRAVES, K., GENONI, M., VOGT, P., LÜSCHER, T. F., RENNER, C., HOERSTRUP, S. P. & MATTER, C. M. (2011) Fibroblast activation protein is induced by inflammation and degrades type I collagen in thin-cap fibroatheromata. *European Heart Journal,* 32**,** 2713-2722.
CALON, A., LONARDO, E., BERENGUER-LLERGO, A., ESPINET, E., HERNANDO-MOMBLONA, X., IGLESIAS, M., SEVILLANO, M., PALOMO-PONCE, S., TAURIELLO, D. V. F., BYROM, D., CORTINA, C., MORRAL, C., BARCELÓ, C., TOSI, S., RIERA, A., ATTOLINI, C. S.-O., ROSSELL, D., SANCHO, E. & BATLLE, E. (2015) Stromal gene expression defines poor-prognosis subtypes in colorectal cancer. *Nature Genetics,* 47**,** 320-329.
CHAN, D., LAMANDE, S. R., COLE, W. G. & BATEMAN, J. F. (1990) Regulation of procollagen synthesis and processing during ascorbate-induced extracellular matrix accumulation in vitro. *Biochemical Journal,* 269**,** 175-181.
CHANRION, M. A., NEGRE, V., FONTAINE, H. L. N., SALVETAT, N., BIBEAU, F. D. R., GROGAN, G. T. M., MAURIAC, L., KATSAROS, D., MOLINA, F., THEILLET, C. & DARBON, J.-M. (2008) A gene expression signature that can predict the recurrence of tamoxifen-treated primary breast cancer. *Clinical Cancer Research,* 14**,** 1744-1752.
CHASE, L. G., LAKSHMIPATHY, U., SOLCHAGA, L. A., RAO, M. S. & VEMURI, M. C. (2009) A novel serum-free medium for the expansion of human mesenchymal stem cells. *Stem Cell Research & Therapy,* 1**,** 8-8.
CHENG, J. D., VALIANOU, M., CANUTESCU, A. A., JAFFE, E. K., LEE, H.-O.,

WANG, H., LAI, J. H., BACHOVCHIN, W. W. & WEINER, L. M. (2005) Abrogation of fibroblast activation protein enzymatic activity attenuates tumor growth. *Molecular Cancer Therapeutics,* 4**,** 351-360.

CHIEREGATO, K., CASTEGNARO, S., MADEO, D., ASTORI, G., PEGORARO, M. & RODEGHIERO, F. (2011) Epidermal growth factor, basic fibroblast growth factor and platelet-derived growth factor-bb can substitute for fetal bovine serum and compete with human platelet-rich plasma in the ex vivo expansion of mesenchymal stromal cells derived from adipose tissue. *Cytotherapy,* 13**,** 933-943.

CHIJIMATSU, R., IKEYA, M., YASUI, Y., IKEDA, Y., EBINA, K., MORIGUCHI, Y., SHIMOMURA, K., HART, D. A., YOSHIKAWA, H. & NAKAMURA, N. (2017) Characterization of mesenchymal stem cell-like cells derived from human iPSCs via neural crest development and their application for osteochondral repair. *Stem Cells International,* 2017**,** 18.

CHRISTIANSEN, V., JACKSON, K., N LEE, K. & MCKEE, P. (2007) Effect of fibroblast activation protein and α2-Antiplasmin cleaving enzyme on collagen types I, III and IV. *Archives of Biochemistry and Biophysics,* 457**,** 177-86.

COOKE, M. J., PHILLIPS, S. R., SHAH, D. S., ATHEY, D., LAKEY, J. H. & PRZYBORSKI, S. A. (2008) Enhanced cell attachment using a novel cell culture surface presenting functional domains from extracellular matrix proteins. *Cytotechnology,* 56**,** 71-79.

COPPÉ, J.-P., DESPREZ, P.-Y., KRTOLICA, A. & CAMPISI, J. (2010) The senescence-associated secretory phenotype: The dark side of tumor suppression. *Annual review of pathology,* 5**,** 99-118.

COSTA, A., KIEFFER, Y., SCHOLER-DAHIREL, A., PELON, F., BOURACHOT, B., CARDON, M., SIRVEN, P., MAGAGNA, I., FUHRMANN, L., BERNARD, C., BONNEAU, C., KONDRATOVA, M., KUPERSTEIN, I., ZINOVYEV, A., GIVEL, A.-M., PARRINI, M.-C., SOUMELIS, V., VINCENT-SALOMON, A. & MECHTA-GRIGORIOU, F. (2018) Fibroblast heterogeneity and immunosuppressive environment in human breast cancer. *Cancer Cell,* 33**,** 463-479.e10.

DE WEVER, O., DEMETTER, P., MAREEL, M. & BRACKE, M. (2008) Stromal myofibroblasts are drivers of invasive cancer growth. *International Journal of Cancer,* 123**,** 2229-2238.

DEMARIA, M., OHTANI, N., YOUSSEF, S. A., RODIER, F., TOUSSAINT, W., MITCHELL, J. R., LABERGE, R.-M., VIJG, J., VAN STEEG, H., DOLLÉ, M. E. T., HOEIJMAKERS, J. H. J., DE BRUIN, A., HARA, E. & CAMPISI, J. (2014) An essential role for senescent cells in optimal wound healing through secretion of PDGF-AA. *Developmental cell,* 31**,** 722-733.

DEMETRIOU, M., BINKERT, C., SUKHU, B., TENENBAUM, H. C. & DENNIS, J. W. (1996) Fetuin/α2-HS glycoprotein is a transforming growth factor-β type II receptor mimic and cytokine antagonist. *Journal of Biological Chemistry,* 271**,** 12755-12761.

DU, H. & CHE, G. (2017) Genetic alterations and epigenetic alterations of cancer-associated fibroblasts. *Oncology Letters,* 13**,** 3-12.

DUARTE, T. L. & LUNEC, J. (2005) Review: When is an antioxidant not an antioxidant? A review of novel actions and reactions of vitamin C. *Free Radical Research,* 39**,** 671-686.

DZIEGIELEWSKA, K. M., BROWN, W. M., GOULD, C. C., MATTHEWS, N.,

SEDGWICK, J. E. C. & SAUNDERS, N. R. (1992) Fetuin: an acute phase protein in cattle. *Journal of Comparative Physiology B,* 162**,** 168-171.

EBERLEIN, C., ROONEY, C., ROSS, S. J., FARREN, M., WEIR, H. M. & BARRY, S. T. (2015) E-Cadherin and EpCAM expression by NSCLC tumour cells associate with normal fibroblast activation through a pathway initiated by integrin [alpha]v[beta]6 and maintained through TGF[beta] signalling. *Oncogene,* 34**,** 704-716.

EKBOM, A., HELMICK, C., ZACK, M. & ADAMI, H.-O. (1990) Ulcerative colitis and colorectal cancer. *New England Journal of Medicine,* 323**,** 1228-1233.

ENRIQUE-TARANCÓN , G., CASTAN, I., MORIN, N., MARTI, L., ABELLA, A., CAMPS, M., CASAMITJANA, R., PALACÍN, M., TESTAR, X., DEGERMAN, E., CARPÉNÉ, C. & ZORZANO, A. (2000) Substrates of semicarbazide-sensitive amine oxidase co-operate with vanadate to stimulate tyrosine phosphorylation of insulin-receptor-substrate proteins, phosphoinositide 3-kinase activity and GLUT4 translocation in adipose cells. *Biochemical Journal,* 350**,** 171-180.

ERDOGAN, B. & WEBB, D. J. (2017) Cancer-associated fibroblasts modulate growth factor signaling and extracellular matrix remodeling to regulate tumor metastasis. *Biochemical Society Transactions,* 45**,** 229-236.

FARMER, P., BONNEFOI, H., ANDERLE, P., CAMERON, D., WIRAPATI, P., BECETTE, V., ANDRE, S., PICCART, M., CAMPONE, M., BRAIN, E., MACGROGAN, G., PETIT, T., JASSEM, J., BIBEAU, F., BLOT, E., BOGAERTS, J., AGUET, M., BERGH, J., IGGO, R. & DELORENZI, M. (2009) A stroma-related gene signature predicts resistance to neoadjuvant chemotherapy in breast cancer. *Nature Medicine,* 15**,** 68-74.

FEDOROV, Y., ANDERSON, E., BIRMINGHAM, A., REYNOLDS, A., KARPILOW, J., ROBINSON, K., LEAKE, D., S MARSHALL, W. & KHVOROVA, A. (2006) Off-target effects by siRNA can induce toxic phenotype. *RNA (New York, N.Y.),* 12**,** 1188-1196.

FEIG, C., O JONES, J., KRAMAN, M., WELLS, R., DEONARINE, A., S CHAN, D., M CONNELL, C., W ROBERTS, E., ZHAO, Q., L CABALLERO, O., A TEICHMANN, S., JANOWITZ, T., I JODRELL, D., A TUVESON, D. & T FEARON, D. (2013) Targeting CXCL12 from FAP-expressing carcinoma-associated fibroblasts synergizes with anti-PD-L1 immunotherapy in pancreatic cancer. *Proceedings of the National Academy of Sciences of the United States of America,* 110**,** 20212-20217.

FISCHER, R. S., MYERS, K. A., GARDEL, M. L. & WATERMAN, C. M. (2012) Stiffness-controlled three-dimensional extracellular matrices for high-resolution imaging of cell behavior. *Nature Protocols,* 7**,** 10.1038/nprot.2012.127.

FISHER, S. A., TREMELLING, M., ANDERSON, C. A., GWILLIAM, R., BUMPSTEAD, S., PRESCOTT, N. J., NIMMO, E. R., MASSEY, D., BERZUINI, C., JOHNSON, C., BARRETT, J. C., CUMMINGS, F. R., DRUMMOND, H., LEES, C. W., ONNIE, C. M., HANSON, C. E., BLASZCZYK, K., INOUYE, M., EWELS, P., RAVINDRARAJAH, R., KENIRY, A., HUNT, S., CARTER, M., WATKINS, N., OUWEHAND, W., LEWIS, C. M., CARDON, L., THE WELLCOME TRUST CASE CONTROL, C., LOBO, A., FORBES, A., SANDERSON, J., JEWELL, D. P., MANSFIELD, J. C., DELOUKAS, P., MATHEW, C. G., PARKES, M. &

SATSANGI, J. (2008) Genetic determinants of ulcerative colitis include the ECM1 locus and five loci implicated in Crohn's disease. *Nature Genetics,* 40**,** 710-712.
FLETCHER, C. D. M. (1998) Myofibroblastic tumors: an update. *Verhandlungen der Deutschen Gesellschaft für Pathologie* 82**,** 75-82.
FLIER, L. G. V. D. & CLEVERS, H. (2009) Stem cells, self-renewal, and differentiation in the intestinal epithelium. *Annual Review of Physiology,* 71**,** 241-260.
FRANTZ, C., STEWART, K. M. & WEAVER, V. M. (2010) The extracellular matrix at a glance. *Journal of Cell Science,* 123**,** 4195-4200.
FRESHNEY, R. I. (1987) *Culture of Animal Cells: A Manual of Basic Technique*, Alan R. Liss.
FUKS, Z., PERSAUD, R. S., ALFIERI, A., MCLOUGHLIN, M., EHLEITER, D., SCHWARTZ, J. L., SEDDON, A. P., CORDON-CARDO, C. & HAIMOVITZ-FRIEDMAN, A. (1994) Basic fibroblast growth factor protects endothelial cells against radiation-induced programmed cell death in vitro and in vivo. *Cancer Research,* 54**,** 2582-2590.
GAO, M. Q., KIM, B. G., KANG, S., CHOI, Y. P., PARK, H., KANG, K. S. & CHO, N. H. (2010) Stromal fibroblasts from the interface zone of human breast carcinomas induce an epithelial-mesenchymal transition-like state in breast cancer cells in vitro. *Journal of Cell Science,* 123**,** 3507-3514.
GARCIA-FERNÀNDEZ, J. (2005) The genesis and evolution of homeobox gene clusters. *Nature Reviews Genetics,* 6**,** 881-892.
GARIN-CHESA, P., OLD, L. J. & RETTIG, W. J. (1990) Cell surface glycoprotein of reactive stromal fibroblasts as a potential antibody target in human epithelial cancers. *Proceedings of the National Academy of Sciences of the United States of America,* 87**,** 7235-7239.
GASCARD, P. & TLSTY, T. D. (2016) Carcinoma-associated fibroblasts: orchestrating the composition of malignancy. *Genes & Development,* 30**,** 1002-1019.
GREICIUS, G., KABIRI, Z., SIGMUNDSSON, K., LIANG, C., BUNTE, R., SINGH, M. K. & VIRSHUP, D. M. (2018) PDGFRα+ pericryptal stromal cells are the critical source of Wnts and RSPO3 for murine intestinal stem cells in vivo. *Proceedings of the National Academy of Sciences,* 115**,** E3173-E3181.
GSTRAUNTHALER, G. (2003) Alternatives to the use of fetal bovine serum: serum-free cell culture. *ALTEX,* 20**,** 275-281.
HALEY, E. M. & KIM, Y. (2014) The role of basic fibroblast growth factor in glioblastoma multiforme and glioblastoma stem cells and in their in vitro culture. *Cancer Letters,* 346**,** 1-5.
HALL, P. A., COATES, P. J., ANSARI, B. & HOPWOOD, D. (1994) Regulation of cell number in the mammalian gastrointestinal tract: the importance of apoptosis. *Journal of Cell Science,* 107**,** 3569-3577.
HANG, T. C., LAUFFENBURGER, D. A., GRIFFITH, L. G. & STOLZ, D. B. (2012) Lipids promote survival, proliferation, and maintenance of differentiation of rat liver sinusoidal endothelial cells in vitro. *American Journal of Physiology - Gastrointestinal and Liver Physiology,* 302**,** G375-G388.
HARAMIS, A. P. G., BEGTHEL, H., VAN DEN BORN, M., VAN ES, J., JONKHEER, S., OFFERHAUS, G. J. A. & CLEVERS, H. (2004) De novo

crypt formation and juvenile polyposis on BMP inhibition in mouse intestine. *Science,* 303**,** 1684-1686.

HASSONA, Y., CIRILLO, N., HEESOM, K., PARKINSON, E. K. & PRIME, S. S. (2013) Senescent cancer-associated fibroblasts secrete active MMP-2 that promotes keratinocyte dis-cohesion and invasion. *British Journal of Cancer,* 111**,** 1230-1237.

HATA, R. I. & SENOO, H. (1989) L-ascorbic acid 2-phosphate stimulates collagen accumulation, cell proliferation, and formation of a three-dimensional tissuelike substance by skin fibroblasts. *Journal of Cellular Physiology,* 138**,** 8-16.

HELDIN, C.-H., ÖSTMAN, A. & RÖNNSTRAND, L. (1998) Signal transduction via platelet-derived growth factor receptors. *Biochimica et Biophysica Acta (BBA) - Reviews on Cancer,* 1378**,** F79-F113.

HERRERA, M., ISLAM, A. B. M. M. K., HERRERA, A., MARTÍN, P., GARCÍA, V., SILVA, J., GARCIA, J. M., SALAS, C., CASAL, I., DE HERREROS, A. G., BONILLA, F. & PEÑA, C. (2013) Functional heterogeneity of cancer-associated fibroblasts from human colon tumors shows specific prognostic gene expression signature. *Clinical Cancer Research,* 19**,** 5914-5926.

HINZ, B., PHAN, S. H., THANNICKAL, V. J., PRUNOTTO, M., DESMOULIÈRE, A., VARGA, J., DE WEVER, O., MAREEL, M. & GABBIANI, G. (2012) Recent developments in myofibroblast biology. *The American Journal of Pathology,* 180**,** 1340-1355.

HOMMINGA, I., PIETERS, R., LANGERAK, ANTON W., DE ROOI, JOHAN J., STUBBS, A., VERSTEGEN, M., VUERHARD, M., BUIJS-GLADDINES, J., KOOI, C., KLOUS, P., VAN VLIERBERGHE, P., FERRANDO, ADOLFO A., CAYUELA, JEANÂ M., VERHAAF, B., BEVERLOO, H. Â B., HORSTMANN, M., DE HAAS, V., WIEKMEIJER, A.-S., PIKE-OVERZET, K., STAAL, FRANK J. T., DE LAAT, W., SOULIER, J., SIGAUX, F. & MEIJERINK, JULES P. P. (2011) Integrated transcript and genome analyses reveal NKX2-1 and MEF2C as potential oncogenes in T Cell acute lymphoblastic leukemia. *Cancer Cell,* 19**,** 484-497.

HOMMINGA, I., PIETERS, R. & MEIJERINK, J. P. P. (2011) NKL homeobox genes in leukemia. *Leukemia,* 26**,** 572-581.

HSIA, L. T., ASHLEY, N., OUARET, D., WANG, L. M., WILDING, J. & BODMER, W. F. (2016) Myofibroblasts are distinguished from activated skin fibroblasts by the expression of AOC3 and other associated markers. *Proceedings of the National Academy of Sciences of the United States of America,* 113**,** E2162-E2171.

HU, Y., YAN, C., MU, L., HUANG, K., LI, X., TAO, D., WU, Y. & QIN, J. (2015) Fibroblast-derived exosomes contribute to chemoresistance through priming cancer stem cells in colorectal cancer. *PLoS ONE,* 10**,** e0125625.

HULIKOVA, A., BLACK, N., HSIA, L.-T., WILDING, J., BODMER, W. F. & SWIETACH, P. (2016) Stromal uptake and transmission of acid is a pathway for venting cancer cell-generated acid. *Proceedings of the National Academy of Sciences,* 113**,** E5344-E5353.

HUSCHTSCHA, L., ROZENGURT, E. & BODMER, W. F. (1991) Growth factor requirements of human colorectal tumour cells: Relations to cellular differentiation. *European Journal of Cancer and Clinical Oncology,* 27**,** 1680-1684.

IRJALA, H., SALMI, M., ALANEN, K., GRÉNMAN, R. & JALKANEN, S. (2001) Vascular adhesion protein 1 mediates binding of immunotherapeutic effector cells to tumor endothelium. *The Journal of Immunology,* 166**,** 6937-6943.

ISHIMOTO, T., MIYAKE, K., NANDI, T., YASHIRO, M., ONISHI, N., HUANG, K. K., LIN, S. J., KALPANA, R., TAY, S. T., SUZUKI, Y., CHO, B. C., KURODA, D., ARIMA, K., IZUMI, D., IWATSUKI, M., BABA, Y., OKI, E., WATANABE, M., SAYA, H., HIRAKAWA, K., BABA, H. & TAN, P. (2017) Activation of transforming growth factor beta 1 signaling in gastric cancer-associated fibroblasts increases their motility, via expression of rhomboid 5 homolog 2, and ability to induce invasiveness of gastric cancer cells. *Gastroenterology,* 153**,** 191-204.

ITAHANA, K., ITAHANA, Y. & DIMRI, G. P. (2013) Colorimetric detection of senescence-associated β Galactosidase. *Methods in Molecular Biology (Clifton, N.J.),* 965**,** 143-156.

ITO, M., YOSHIDA, K., KYO, E., AYHAN, A., NAKAYAMA, H., YASUI, W., ITO, H. & TAHARA, E. (1990) Expression of several growth factors and their receptor genes in human colon carcinomas. *Virchows Archiv B,* 59**,** 173-178.

IWASA, S., OKADA, K., CHEN, W.-T., JIN, X., YAMANE, T., OOI, A. & MITSUMATA, M. (2005) Increased expression of seprase, a membrane-type serine protease, is associated with lymph node metastasis in human colorectal cancer. *Cancer Letters,* 227**,** 229-236.

JACKSON, A. L. & LINSLEY, P. S. (2010) Recognizing and avoiding siRNA off-target effects for target identification and therapeutic application. *Nature Reviews Drug Discovery,* 9**,** 57-67.

JALKANEN, S., KARIKOSKI, M., MERCIER, N., KOSKINEN, K., HENTTINEN, T., ELIMA, K., SALMIVIRTA, K. & SALMI, M. (2007) The oxidase activity of vascular adhesion protein-1 (VAP-1) induces endothelial E- and P-selectins and leukocyte binding. *Blood,* 110**,** 1864-1870.

JALKANEN, S. & SALMI, M. (2008) VAP-1 and CD73, endothelial cell surface enzymes in leukocyte extravasation. *Arteriosclerosis, Thrombosis, and Vascular Biology,* 28**,** 18-26.

JOSH, F., TOBITA, M., TANAKA, R., ORBAY, H., OGATA, K., SUZUKI, K., HYAKUSOKU, H. & MIZUNO, H. (2013) Concentration of PDGF-AB, BB and TGF-beta1 as valuable human serum parameters in adipose-derived stem cell proliferation. *Journal of Nippon Medical School,* 80**,** 140-147.

JUNG, S., SEN, A., ROSENBERG, L. & A BEHIE, L. (2010) Identification of growth and attachment factors for the serum-free isolation and expansion of human mesenchymal stromal cells. *Cytotherapy,* 12**,** 637-57.

KAKARLA, S., SONG, X. T. & GOTTSCHALK, S. (2012) Cancer-associated fibroblasts as targets for immunotherapy. *Immunotherapy,* 4**,** 1129-1138.

KALER, P., OWUSU, B. Y., AUGENLICHT, L. & KLAMPFER, L. (2014) The Role of STAT1 for crosstalk between fibroblasts and colon cancer cells. *Frontiers in Oncology,* 4**,** 88.

KALLURI, R. & ZEISBERG, M. (2006) Fibroblasts in cancer. *Nat Rev Cancer,* 6**,** 392-401.

KALUGIN, P. (2017) Myofibroblast migration and signaling in in vitro colorectal cancer models. *Department of Oncology.* University of Oxford.

KANTA, J. (2015) Collagen matrix as a tool in studying fibroblastic cell behavior.

Cell Adhesion & Migration, 9**,** 308-316.
KEANE, F. M., CHOWDHURY, S., YAO, T. W., NADVI, N. A., GALL, M. G., CHEN, Y., OSBORNE, B., RIBEIRO, A. J. V., CHURCH, W. B., MCCAUGHAN, G. W., GORRELL, M. D. & YU, D. M. T. (2012) Chapter 5 Targeting Dipeptidyl Peptidase-4 (DPP-4) and Fibroblast Activation Protein (FAP) for Diabetes and Cancer Therapy. *Proteinases as Drug Targets***,** 118-144.
KELLERMANN, J., HAUPT, H., AUERSWALD, E. A. & MÜLLER-ESTER, W. (1989) The arrangement of disulfide loops in human alpha 2-HS glycoprotein. Similarity to the disulfide bridge structures of cystatins and kininogens. *Journal of Biological Chemistry,* 264**,** 14121-14128.
KELLY, T. (2005) Fibroblast activation protein-α and dipeptidyl peptidase IV (CD26): Cell-surface proteases that activate cell signaling and are potential targets for cancer therapy. *Drug Resistance Updates,* 8**,** 51-58.
KEMIK, O., SÜMER, A., KEMIK, A. S., İTIK, V., DULGER, A. C., PURISA, S. & TUZUN, S. (2010) Human vascular adhesion protein-1 (VAP-1): Serum levels for hepatocellular carcinoma in non-alcoholic and alcoholic fatty liver disease. *World Journal of Surgical Oncology,* 8**,** 83.
KENNEDY, B. A., DEATHERAGE, D. E., GU, F., TANG, B., CHAN, M. W. Y., NEPHEW, K. P., HUANG, T. H. M. & JIN, V. X. (2011) ChIP-seq defined genome-wide map of TGFβ/SMAD4 targets: Implications with clinical outcome of ovarian cancer. *PLoS ONE,* 6**,** e22606.
KHELWATTY, S., ESSAPEN, S., BAGWAN, I., GREEN, M., SEDDON, A. & MODJTAHEDI, H. (2017) The impact of co-expression of wild-type EGFR and its ligands determined by immunohistochemistry for response to treatment with cetuximab in patients with metastatic colorectal cancer. *Oncotarget,* 8**,** 7666-7677.
KIM, J., TAKEUCHI, H., LAM, S. T., TURNER, R. R., WANG, H.-J., KUO, C., FOSHAG, L., BILCHIK, A. J. & HOON, D. S. B. (2005) Chemokine receptor CXCR4 expression in colorectal cancer patients increases the risk for recurrence and for poor survival. *Journal of Clinical Oncology,* 23**,** 2744-2753.
KIM, T., KIM, K., LEE, S. H., SO, H.-S., LEE, J., KIM, N. & CHOI, Y. (2009) Identification of LRRc17 as a negative regulator of receptor activator of NF-κB Ligand (RANKL)-induced osteoclast differentiation. *The Journal of Biological Chemistry,* 284**,** 15308-15316.
KITADAI, Y., SASAKI, T., KUWAI, T., NAKAMURA, T., BUCANA, C. D., HAMILTON, S. R. & FIDLER, I. J. (2006) Expression of activated platelet-derived growth factor receptor in stromal cells of human colon carcinomas is associated with metastatic potential. *International Journal of Cancer,* 119**,** 2567-2574.
KOBE, B. & DEISENHOFER, J. (1994) The leucine-rich repeat: a versatile binding motif. *Trends in Biochemical Sciences,* 19**,** 415-421.
KOBE, B. & KAJAVA, A. V. (2001) The leucine-rich repeat as a protein recognition motif. *Current Opinion in Structural Biology,* 11**,** 725-732.
KOJIMA, M. & OCHIAI, A. (2016) Special cancer microenvironment in human colonic cancer: Concept of cancer microenvironment formed by peritoneal invasion (CMPI) and implication of subperitoneal fibroblast in cancer progression. *Pathology International,* 66**,** 123-131.
KOSTORO, J., CHANG, S.-J., CLARK LAI, Y.-C., WU, C.-C., CHAI, C.-Y. &

KWAN, A.-L. (2016) Overexpression of vascular adhesion protein-1 is associated with poor prognosis of astrocytomas. *APMIS,* 124**,** 462-468.
KUILMAN, T. & PEEPER, D. S. (2009) Senescence-messaging secretome: SMS-ing cellular stress. *Nature Reviews Cancer,* 9**,** 81-94.
KUPERWASSER, C., CHAVARRIA, T., WU, M., MAGRANE, G., GRAY, J. W., CAREY, L., RICHARDSON, A. & WEINBERG, R. A. (2004) Reconstruction of functionally normal and malignant human breast tissues in mice. *Proceedings of the National Academy of Sciences of the United States of America,* 101**,** 4966-4971.
LALOR, P. F., SUN, P. J., WESTON, C. J., MARTIN-SANTOS, A., WAKELAM, M. J. O. & ADAMS, D. H. (2007) Activation of vascular adhesion protein-1 on liver endothelium results in an NF-κB–dependent increase in lymphocyte adhesion. *Hepatology,* 45**,** 465-474.
LASORSA, V. A., FORMICOLA, D., PIGNATARO, P., CIMMINO, F., CALABRESE, F. M., MORA, J., ESPOSITO, M. R., PANTILE, M., ZANON, C., DE MARIANO, M., LONGO, L., HOGARTY, M. D., DE TORRES, C., TONINI, G. P., IOLASCON, A. & CAPASSO, M. (2016) Exome and deep sequencing of clinically aggressive neuroblastoma reveal somatic mutations that affect key pathways involved in cancer progression. *Oncotarget,* 7**,** 21840-21852.
LATCHMAN, Y., WOOD, C. R., CHERNOVA, T., CHAUDHARY, D., BORDE, M., CHERNOVA, I., IWAI, Y., LONG, A. J., BROWN, J. A., NUNES, R., GREENFIELD, E. A., BOURQUE, K., BOUSSIOTIS, V. A., CARTER, L. L., CARRENO, B. M., MALENKOVICH, N., NISHIMURA, H., OKAZAKI, T., HONJO, T., SHARPE, A. H. & FREEMAN, G. J. (2001) PD-L2 is a second ligand for PD-1 and inhibits T cell activation. *Nature Immunology,* 2**,** 261-8.
LEE, K. N., JACKSON, K., CHRISTIANSEN, V., DOLENCE, K. & MCKEE, P. (2011) Enhancement of fibrinolysis by inhibiting enzymatic cleavage of precursor α2-antiplasmin. *Journal of thrombosis and haemostasis: JTH,* 9**,** 987-996.
LEE, K. N., JACKSON, K. W., CHRISTIANSEN, V. J., CHUNG, K. H. & MCKEE, P. A. (2004) A novel plasma proteinase potentiates α_2--antiplasmin inhibition of fibrin digestion. *Blood,* 103**,** 3783-3788.
LEE, K. N., JACKSON, K. W., CHRISTIANSEN, V. J., LEE, C. S., CHUN, J.-G. & MCKEE, P. A. (2006) Antiplasmin-cleaving enzyme is a soluble form of fibroblast activation protein. *Blood,* 107**,** 1397-1404.
LEIBOVITZ, A., STINSON, J. C., MCCOMBS, W. B., MCCOY, C. E., MAZUR, K. C. & MABRY, N. D. (1976) Classification of human colorectal adenocarcinoma cell lines. *Cancer Research,* 36**,** 4562-4569.
LEMOINNE, S., CADORET, A., EL MOURABIT, H., THABUT, D. & HOUSSET, C. (2013) Origins and functions of liver myofibroblasts. *Biochimica et Biophysica Acta (BBA) - Molecular Basis of Disease,* 1832**,** 948-954.
LEVY, M. T., MCCAUGHAN, G. W., ABBOTT, C. A., PARK, J. E., CUNNINGHAM, A. M., MÜLLER, E., RETTIG, W. J. & GORRELL, M. D. (1999) Fibroblast activation protein: A cell surface dipeptidyl peptidase and gelatinase expressed by stellate cells at the tissue remodelling interface in human cirrhosis. *Hepatology,* 29**,** 1768-1778.
LI, X., VAN PUTTEN, V., ZARINETCHI, F., NICKS, M. E., THALER, S., HEASLEY, L. E. & NEMENOFF, R. A. (1997) Suppression of smooth-

muscle alpha-actin expression by platelet-derived growth factor in vascular smooth-muscle cells involves Ras and cytosolic phospholipase A2. *Biochemical Journal,* 327**,** 709-716.

LICKERT, H., DOMON, C., HULS, G., WEHRLE, C., DULUC, I., CLEVERS, H., MEYER, B. I., FREUND, J. N. & KEMLER, R. (2000) Wnt/(beta)-catenin signaling regulates the expression of the homeobox gene Cdx1 in embryonic intestine. *Development,* 127**,** 3805-3813.

LIN, C., SONG, L., GONG, H., LIU, A., LIN, X., WU, J., LI, M. & LI, J. (2013) Nkx2-8 downregulation promotes angiogenesis and activates NF-κB in esophageal cancer. *Cancer Research,* 73**,** 3638-3648.

LIN, Y., LINASK, K. L., MALLON, B., JOHNSON, K., KLEIN, M., BEERS, J., XIE, W., DU, Y., LIU, C., LAI, Y., ZOU, J., HAIGNEY, M., YANG, H., RAO, M. & CHEN, G. (2017) Heparin promotes cardiac differentiation of human pluripotent stem cells in chemically defined albumin-free medium, enabling consistent manufacture of cardiomyocytes. *STEM CELLS Translational Medicine,* 6**,** 527-538.

LIOTTA, L. A. & KOHN, E. C. (2001) The microenvironment of the tumour-host interface. *Nature,* 411**,** 375.

LIPKIN, M. (1983) Proliferation and differentiation of normal and diseased gastrointestinal cells. IN JOHNSON, L. R. (Ed.) *Physiology of the Gastrointestinal Tract.* New York, Raven Press.

LIU, C., LI, J., XIANG, X., GUO, L., TU, K., LIU, Q., SHAH, V. H. & KANG, N. (2014) PDGF receptor-α promotes TGF-β signaling in hepatic stellate cells via transcriptional and posttranscriptional regulation of TGF-β receptors. *American Journal of Physiology - Gastrointestinal and Liver Physiology,* 307**,** G749-G759.

LIU, R., BAUER, A. J. & MARTIN, K. A. (2016) A new editor of smooth muscle phenotype. *Circulation Research,* 119**,** 401-403.

LOCHTER, A., STERNLICHT, M. D., WERB, Z. & BISSELL, M. J. (1998) The significance of matrix metalloproteinases during early stages of tumor progression. *Annals of the New York Academy of Sciences,* 857**,** 180-193.

LU, L., LI, T., WILLIAMS, G., PETIT, E., BOROWSKY, M. & WALKER, W. A. (2011) Hydrocortisone induces changes in gene expression and differentiation in immature human enterocytes. *American Journal of Physiology - Gastrointestinal and Liver Physiology,* 300**,** G425-G432.

LU, X., TANG, L., LI, K., ZHENG, J., ZHAO, P., TAO, Y. & LI, L. X. (2014) Contribution of NKX2-3 polymorphisms to inflammatory bowel diseases: A meta-analysis of 35358 subjects. *Scientific Reports,* 4**,** 3924.

MAESHIMA, A. M., TOCHIGI, N., YOSHIDA, A., ASAMURA, H., TSUTA, K. & TSUDA, H. (2002) Histological scoring for small lung adenocarcinomas 2 cm or less in diameter: A reliable prognostic indicator. *Journal of Thoracic Oncology,* 5**,** 333-339.

MARKOWSKA, M., STĘPNIAK, P., WOJDAN, K. & ŚWIRSKI, K. (2014) Smooth muscle contamination analysis in clinical oncology gene expression research. *Acta Biochimica Polinica,* 61**,** 333-340.

MARTI, L., MORIN, N., ENRIQUE-TARANCON, G., PREVOT, D., LAFONTAN, M., TESTAR, X., ZORZANO, A. & CARPÉNÉ, C. (1998) Tyramine and vanadate synergistically stimulate glucose transport in rat adipocytes by amine oxidase-dependent generation of hydrogen peroxide. *The Journal*

of Pharmacology and Experimental Therapeutics, 285**,** 342-349.
MARTIN, C. L., PICCINI, A., CHEVALOT, I., OLMOS, E., GUEDON, E. & MARC, A. (2015) Serum-free media for mesenchymal stem cells expansion on microcarriers. *BMC Proceedings,* 9**,** P70-P70.
MARTTILA-ICHIHARA, F., CASTERMANS, K., AUVINEN, K., OUDE EGBRINK, M., JALKANEN, S., W GRIFFIOEN, A. & SALMI, M. (2010) Small-molecule inhibitors of vascular adhesion protein-1 reduce the accumulation of myeloid cells into tumors and attenuate tumor growth in mice. *The Journal of Immunology,* 184**,** 3164-3173.
MATHE, A., WONG-BROWN, M., LOCKE, W. J., STIRZAKER, C., BRAYE, S. G., FORBES, J. F., CLARK, S. J., AVERY-KIEJDA, K. A. & SCOTT, R. J. (2016) DNA methylation profile of triple negative breast cancer-specific genes comparing lymph node positive patients to lymph node negative patients. *Scientific Reports,* 6**,** 33435.
MATSUSHIMA, N., ENKHBAYAR, P., KAMIYA, M., OSAKI, M. & H. KRETSINGER, R. (2005) Leucine-Rich Repeats (LRRs): Structure, function, evolution and interaction with ligands. *Drug Design Reviews - Online,* 2**,** 305-322.
MATSUSHIMA, N., MIKAMI, T., TANAKA, T., MIYASHITA, H., YAMADA, K. & KUROKI, Y. (2009) Analyses of non-leucine-rich repeat (non-LRR) regions intervening between LRRs in proteins. *Biochimica et Biophysica Acta (BBA) - General Subjects,* 1790**,** 1217-1237.
MATSUSHIMA, N., TACHI, N., KUROKI, Y., ENKHBAYAR, P., OSAKI, M., KAMIYA, M. & KRETSINGER, R. H. (2005) Structural analysis of leucine-rich-repeat variants in proteins associated with human diseases. *Cellular and Molecular Life Sciences CMLS,* 62**,** 2771-2791.
MCGINNIS, W. & KRUMLAUF, R. (1992) Homeobox genes and axial patterning. *Cell,* 68**,** 283-302.
MEDEMA, J. P. & VERMEULEN, L. (2011) Microenvironmental regulation of stem cells in intestinal homeostasis and cancer. *Nature,* 474**,** 318-26.
MEGGYESI, N., KISS, L. S., KOSZARSKA, M., BORTLIK, M., DURICOVA, D., LAKATOS, L., MOLNAR, T., LENICEK, M., VÍTEK, L., ALTORJAY, I., PAPP, M., TULASSAY, Z., MIHELLER, P., PAPP, J., TORDAI, A., ANDRIKOVICS, H., LUKAS, M. & LAKATOS, P. L. (2010) NKX2-3 and IRGM variants are associated with disease susceptibility to IBD in Eastern European patients. *World Journal of Gastroenterology: WJG,* 16**,** 5233-5240.
MENDELSOHN, J. & BASELGA, J. (2003) Status of epidermal growth factor receptor antagonists in the biology and treatment of cancer. *Journal of Clinical Oncology,* 21**,** 2787-2799.
MIMURA, K., TEH, J. L., OKAYAMA, H., SHIRAISHI, K., KUA, L. F., KOH, V., SMOOT, D. T., ASHKTORAB, H., OIKE, T., SUZUKI, Y., FAZREEN, Z., ASUNCION, B. R., SHABBIR, A., YONG, W. P., SO, J., SOONG, R. & KONO, K. (2018) PD-L1 expression is mainly regulated by interferon gamma associated with JAK-STAT pathway in gastric cancer. *Cancer Science,* 109**,** 43-53.
MIRA, A., MORELLO, V., CÉSPEDES, M. V., PERERA, T., COMOGLIO, P. M., MANGUES, R. & MICHIELI, P. (2017) Stroma-derived HGF drives metabolic adaptation of colorectal cancer to angiogenesis inhibitors. *Oncotarget,* 8**,** 38193-38213.

MRAZEK, A. A., CARMICAL, J. R., WOOD, T. G., HELLMICH, M. R., ELTORKY, M., BOHANON, F. J. & CHAO, C. (2014) Colorectal cancer-associated fibroblasts are genotypically distinct. *Current Cancer Therapy Reviews,* 10**,** 97-218.

NAGEL, S., SCHERR, M., KEL, A., HORNISCHER, K., CRAWFORD, G. E., KAUFMANN, M., MEYER, C., DREXLER, H. G. & MACLEOD, R. A. F. (2007) Activation of *TLX3* and *NKX2-5* in t(5;14) (q35;q32) T-cell acute lymphoblastic leukemia by remote 3′-*BCL11B* enhancers and coregulation by PU.1 and HMGA1. *Cancer Research,* 67**,** 1461-1471.

NAKAMURA, Y., TANAKA, F., YOSHIKAWA, Y., MIMORI, K., INOUE, H., YANAGA, K. & MORI, M. (2008) PDGF-BB is a novel prognostic factor in colorectal cancer. *Annals of Surgical Oncology,* 15**,** 2129-2136.

NAZARETH, M. R., BRODERICK, L., SIMPSON-ABELSON, M. R., KELLEHER, R. J., YOKOTA, S. J. & BANKERT, R. B. (2007) Characterization of human lung tumor-associated fibroblasts and their ability to modulate the activation of tumor-associated T cells. *The Journal of Immunology,* 178**,** 5552-5562.

NOREN HOOTEN, N. & EVANS, M. K. (2017) Techniques to induce and quantify cellular senescence. *Journal of visualized experiments: JoVE*.

ÖHLUND, D., HANDLY-SANTANA, A., BIFFI, G., ELYADA, E., ALMEIDA, A. S., PONZ-SARVISE, M., CORBO, V., ONI, T. E., HEARN, S. A., LEE, E. J., CHIO, I. I. C., HWANG, C.-I., TIRIAC, H., BAKER, L. A., ENGLE, D. D., FEIG, C., KULTTI, A., EGEBLAD, M., FEARON, D. T., CRAWFORD, J. M., CLEVERS, H., PARK, Y. & TUVESON, D. A. (2017) Distinct populations of inflammatory fibroblasts and myofibroblasts in pancreatic cancer. *The Journal of Experimental Medicine,* 214**,** 579-596.

OLIVIER, E., SOURY, E., RISLER, J.-L., SMIH, F., SCHNEIDER, K., LOCHNER, K., JOUZEAU, J.-Y., FEY, G. H. & SALIER, J.-P. (1999) A novel set of hepatic mRNAs preferentially expressed during an acute inflammation in rat represents mostly intracellular proteins. *Genomics,* 57**,** 352-364.

OLIVIER, E., SOURY, E., RUMINY, P., HUSSON, A., PARMENTIER, F., DAVEAU, M. & SALIER, J. P. (2000) Fetuin-B, a second member of the fetuin family in mammals. *Biochemical Journal,* 350**,** 589-597.

OLUMI, A. F., GROSSFELD, G. D., HAYWARD, S. W., CARROLL, P. R., TLSTY, T. D. & CUNHA, G. R. (1999) Carcinoma-associated fibroblasts direct tumor progression of initiated human prostatic epithelium. *Cancer Research,* 59**,** 5002-5011.

OOTANI, A., LI, X., SANGIORGI, E., HO, Q. T., UENO, H., TODA, S., SUGIHARA, H., FUJIMOTO, K., WEISSMAN, I. L., CAPECCHI, M. R. & KUO, C. J. (2009) Sustained in vitro intestinal epithelial culture within a Wnt-dependent stem cell niche. *Nature Medicine,* 15**,** 701-706.

ORIMO, A. & WEINBERG, R. (2007) Heterogeneity of stromal fibroblasts in tumors. *Cancer Biology & Therapy,* 6**,** 618-619.

ÖSTMAN, A. (2017) PDGF receptors in tumor stroma: Biological effects and associations with prognosis and response to treatment. *Advanced Drug Delivery Reviews,* 121**,** 117-123.

OWENS, G. K., KUMAR, M. S. & WAMHOFF, B. R. (2004) Molecular regulation of vascular smooth muscle cell differentiation in development and disease. *Physiological Reviews,* 84**,** 767-801.

ÖZDEMIR, B. C., PENTCHEVA-HOANG, T., CARSTENS, J. L., ZHENG, X., WU, C.-C., SIMPSON, T. R., LAKLAI, H., SUGIMOTO, H., KAHLERT, C., NOVITSKIY, S. V., DE JESUS-ACOSTA, A., SHARMA, P., HEIDARI, P., MAHMOOD, U., CHIN, L., MOSES, H. L., WEAVER, V. M., MAITRA, A., ALLISON, J. P., LEBLEU, V. S. & KALLURI, R. (2014) Depletion of carcinoma-associated fibroblasts and fibrosis induces immunosuppression and accelerates pancreas cancer with reduced survival. *Cancer Cell,* 28**,** 831-833.

PABST, O., ZWEIGERDT, R. & ARNOLD, H. H. (1999) Targeted disruption of the homeobox transcription factor Nkx2-3 in mice results in postnatal lethality and abnormal development of small intestine and spleen. *Development,* 126**,** 2215-2225.

PARK, J. E., LENTER, M. C., ZIMMERMANN, R. N., GARIN-CHESA, P., OLD, L. J. & RETTIG, W. J. (1999) Fibroblast activation protein, a dual specificity serine protease expressed in reactive human tumor stromal fibroblasts. *The Journal of biological chemistry,* 274**,** 36505-12.

PARKES, M., BARRETT, J. C., PRESCOTT, N., TREMELLING, M., ANDERSON, C. A., FISHER, S. A., ROBERTS, R. G., NIMMO, E. R., CUMMINGS, F. R., SOARS, D., DRUMMOND, H., LEES, C. W., KHAWAJA, S. A., BAGNALL, R., BURKE, D. A., TODHUNTER, C. E., AHMAD, T., ONNIE, C. M., MCARDLE, W., STRACHAN, D., BETHEL, G., BRYAN, C., DELOUKAS, P., FORBES, A., SANDERSON, J., JEWELL, D. P., SATSANGI, J., MANSFIELD, J. C., THE WELLCOME TRUST CASE CONTROL, C., CARDON, L. & MATHEW, C. G. (2007) Sequence variants in the autophagy gene IRGM and multiple other replicating loci contribute to Crohn disease susceptibility. *Nature genetics,* 39**,** 830-832.

PATTABIRAMAN, D. R. & WEINBERG, R. A. (2014) Tackling the cancer stem cells - what challenges do they pose? *Nature reviews. Drug discovery,* 13**,** 497-512.

PENG, Q., ZHAO, L., HOU, Y., SUN, Y., WANG, L., LUO, H., PENG, H. & LIU, M. (2013) Biological characteristics and genetic heterogeneity between carcinoma-associated fibroblasts and their paired normal fibroblasts in human breast cancer. *PLoS ONE,* 8**,** e60321.

PIERSMA, B., WOUTERS, O. Y., DE ROND, S., BOERSEMA, M., GJALTEMA, R. A. F. & BANK, R. A. (2017) Ascorbic acid promotes a TGFβ1-induced myofibroblast phenotype switch. *Physiological Reports,* 5**,** e13324.

PIETRAS, K., PAHLER, J., BERGERS, G. & HANAHAN, D. (2008) Functions of paracrine PDGF signaling in the proangiogenic tumor stroma revealed by pharmacological targeting. *PLoS Medicine,* 5**,** e19.

PINCHUK, I. V., SAADA, J. I., BESWICK, E. J., BOYA, G., QIU, S. M., MIFFLIN, R. C., RAJU, G. S., REYES, V. E. & POWELL, D. W. (2008) PD-1 ligand expression by human colonic myofibroblasts/fibroblasts regulates CD4(+) T cell activity. *Gastroenterology,* 135**,** 1228-1237.e2.

PINNELL, S. R. (1985) Regulation of collagen biosynthesis by ascorbic acid: a review. *The Yale Journal of Biology and Medicine,* 58**,** 553-559.

POWELL, D. W., PINCHUK, I. V., SAADA, J. I., CHEN, X. & MIFFLIN, R. C. (2011) Mesenchymal cells of the intestinal lamina propria. *Annual Review of Physiology,* 73**,** 213-237.

RAICA, M. & CIMPEAN, A. M. (2010) Platelet-Derived growth factor

(PDGF)/PDGF receptors (PDGFR) axis as target for antitumor and antiangiogenic Therapy. *Pharmaceuticals,* 3**,** 572-599.

RAJALA, K., HAKALA, H., PANULA, S., AIVIO, S., PIHLAJAMÄKI, H., SUURONEN, R., HOVATTA, O. & SKOTTMAN, H. (2007) Testing of nine different xeno-free culture media for human embryonic stem cell cultures. *Human Reproduction,* 22**,** 1231-1238.

RAUTAVA, S., WALKER, W. A. & LU, L. (2016) Hydrocortisone-induced anti-inflammatory effects in immature human enterocytes depend on the timing of exposure. *American Journal of Physiology - Gastrointestinal and Liver Physiology,* 310**,** G920-G929.

RETTIG, W. J., GARIN-CHESA, P., HEALEY, J. H., SU, S. L., OZER, H. L., SCHWAB, M., ALBINO, A. P. & OLD, L. J. (1993) Regulation and heteromeric structure of the fibroblast activation protein in normal and transformed cells of mesenchymal and neuroectodermal origin. *Cancer Research,* 53**,** 3327-3335.

RETTIG, W. J., SU, S. L., FORTUNATO, S. R., SCANLAN, M. J., MOHAN RAJ, B. K., GARIN-CHESA, P., HEALEY, J. H. & OLD, L. J. (1994) Fibroblast activation protein: Purification, epitope mapping and induction by growth factors. *International Journal of Cancer,* 58**,** 385-392.

RICHMAN, P. I., TILLY, R., JASS, J. R. & BODMER, W. F. (1987) Colonic pericrypt sheath cells: characterisation of cell type with new monoclonal antibody. *Journal of Clinical Pathology,* 40**,** 593-600.

RITTIÉ, L. & FISHER, G. J. (2005) Isolation and culture of skin fibroblasts. IN VARGA, J., BRENNER, D. A. & PHAN, S. H. (Eds.) *Fibrosis Research: Methods and Protocols.* Totowa, NJ, Humana Press.

ROBERTSON, K. D. (2005) DNA methylation and human disease. *Nature Reviews Genetics,* 6**,** 597-610.

ROBLES, E. F., MENA-VARAS, M., BARRIO, L., MERINO-CORTES, S. V., BALOGH, P. T., DU, M.-Q., AKASAKA, T., PARKER, A., ROA, S., PANIZO, C., MARTIN-GUERRERO, I., SIEBERT, R., SEGURA, V., AGIRRE, X., MACRI-PELLIZERI, L., ALDAZ, B., VILAS-ZORNOZA, A., ZHANG, S., MOODY, S., CALASANZ, M. J., TOUSSEYN, T., BROCCARDO, C., BROUSSET, P., CAMPOS-SANCHEZ, E., COBALEDA, C., SANCHEZ-GARCIA, I., FERNANDEZ-LUNA, J. L., GARCIA-MUNOZ, RICARDO, PENA, E., BELLOSILLO, B., SALAR, A., BAPTISTA, M. J., HERNANDEZ-RIVAS, J. M., GONZALEZ, M., TEROL, M. J., CLIMENT, J., FERRANDEZ, A., SAGAERT, X., MELNICK, A. M., PROSPER, F., OSCIER, D. G., CARRASCO, Y. R., DYER, M. J. S. & MARTINEZ-CLIMENT, J. A. (2016) Homeobox NKX2-3 promotes marginal-zone lymphomagenesis by activating B-cell receptor signalling and shaping lymphocyte dynamics. *Nature Communications,* 7**,** 11889.

RODAN, S. B. & RODAN, G. A. (1997) Integrin function in osteoclasts. *Journal of Endocrinology,* 154**,** S47-S56.

SAKWE, A. M., KOUMANGOYE, R., GOODWIN, S. J. & OCHIENG, J. (2010) Fetuin-A (α2HS-Glycoprotein) is a major serum adhesive protein that mediates growth signaling in breast tumor cells. *The Journal of Biological Chemistry,* 285**,** 41827-41835.

SALMI, M. & JALKANEN, S. (2001) VAP-1: an adhesin and an enzyme. *Trends in Immunology,* 22**,** 211-216.

SALMI, M. & JALKANEN, S. (2005) Cell-surface enzymes in control of leukocyte

trafficking. *Nature Reviews Immunology,* 5**,** 760-771.
SAPPINO, A.-P., DIETRICH, P.-Y., SKALLI, O., WIDGREN, S. & GABBIANI, G. (1989) Colonic pericryptal fibroblasts. Differentiation pattern in embryogenesis and phenotypic modulation in epithelial proliferative lesions. *Virchows Archiv. A, Pathological anatomy and histopathology,* 415**,** 551-557.
SCALTRITI, M. & BASELGA, J. (2006) The epidermal growth factor receptor pathway: A model for targeted therapy. *Clinical Cancer Research,* 12**,** 5268-5272.
SCHINKE, T., AMENDT, C., TRINDL, A., PÖSCHKE, O., MÜLLER-ESTERL, W. & JAHNEN-DECHENT, W. (1996) The serum protein α2-HS glycoprotein/fetuin inhibits apatite formation in vitro and in mineralizing calvaria cells: A possible role in mineralization and calcium homeostasis. *Journal of Biological Chemistry,* 271**,** 20789-20796.
SEMBA, S., KODAMA, Y., OHNUMA, K., MIZUUCHI, E., MASUDA, R., YASHIRO, M., HIRAKAWA, K. & YOKOZAKI, H. (2009) Direct cancer-stromal interaction increases fibroblast proliferation and enhances invasive properties of scirrhous-type gastric carcinoma cells. *British Journal of Cancer,* 101**,** 1365-1373.
SENTURK, S., MUMCUOGLU, M., GURSOY-YUZUGULLU, O., CINGOZ, B., AKCALI, K. C. & OZTURK, M. (2010) Transforming growth factor-beta induces senescence in hepatocellular carcinoma cells and inhibits tumor growth. *Hepatology,* 52**,** 966-974.
SHINAGAWA, K., YASUHIKO, K., MIWAKO, T., TOMONORI, S., MIEKO, O., MAYU, O., EIJI, O., YUKIHITO, H., SHINJI, T., WATARU, Y. & KAZUAKI, C. (2013) Stroma-directed imatinib therapy impairs the tumor-promoting effect of bone marrow-derived mesenchymal stem cells in an orthotopic transplantation model of colon cancer. *International Journal of Cancer,* 132**,** 813-823.
SHIOMI, N. & WATANABE, K. (2014) Effects of hydrocortisone, glycerophosphate and retinol on the differentiation of mesenchymal stem cells and vascular endothelial cells to osteoblasts. *Journal of Biomedical Science and Engineering,* 7**,** 1056-1066.
SIMON-ASSMANN, P., KEDINGER, M., DE ARCANGELIS, A., ROUSSEAU, V. & SIMO, P. (1995) Extracellular matrix components in intestinal development. *Experientia,* 51**,** 883-900.
SMITH, D. J., SALMI, M., BONO, P., HELLMAN, J., LEU, T. & JALKANEN, S. (1998) Cloning of vascular adhesion protein 1 reveals a novel multifunctional adhesion molecule. *The Journal of Experimental Medicine,* 188**,** 17-27.
SMITH, R., OWEN, L. A., TREM, D. J., WONG, J. S., WHANGBO, J. S., GOLUB, T. R. & LESSNICK, S. L. (2006) Expression profiling of EWS/FLI identifies NKX2.2 as a critical target gene in Ewing's sarcoma. *Cancer Cell,* 9**,** 405-416.
SONG, Z. Y., GAO, Z. H., CHU, J. H., HAN, X. Z. & QU, X. J. (2015) Downregulation of the CXCR4/CXCL12 axis blocks the activation of the Wnt/β-catenin pathway in human colon cancer cells. *Biomedicine & Pharmacotherapy,* 71**,** 46-52.
STAPPENBECK, T. S., WONG, M. H., SAAM, J. R., MYSOREKAR, I. U. & GORDON, J. I. (1998) Notes from some crypt watchers: regulation of

renewal in the mouse intestinal epithelium. *Current Opinion in Cell Biology,* 10**,** 702-709.
STERNLICHT, M. D., LOCHTER, A., SYMPSON, C. J., HUEY, B., ROUGIER, J.-P., GRAY, J. W., PINKEL, D., BISSELL, M. J. & WERB, Z. (1999) The stromal proteinase MMP3/Stromelysin-1 promotes mammary carcinogenesis. *Cell,* 98**,** 137-146.
STOLEN, C., YEGUTKIN, G., KURKIJARVII, R., BONO, P., ALITALO, K. & JALKANEN, S. (2004) Origins of serum semicarbazide-sensitive amine oxidase. *Circulation Research,* 95**,** 50-57.
SU, S., CHEN, J., YAO, H., LIU, J., YU, S., LAO, L., WANG, M., LUO, M., XING, Y., CHEN, F., HUANG, D., ZHAO, J., YANG, L., LIAO, D., SU, F., LI, M., LIU, Q. & SONG, E. (2018) CD10+GPR77+ cancer-associated fibroblasts promote cancer formation and chemoresistance by sustaining cancer stemness. *Cell,* 172**,** 841-856.e16.
SUN, L., XIA, W., ZHAO, S., LIU, N., LIU, S., XIU, P., LI, L., CAO, X. & GAO, J. (2016) An asymmetrically dimethylarginated nuclear 90 kDa protein (p90aDMA) induced by interleukin (IL)-2, IL-4 or IL-6 in the tumor microenvironment is selectively degraded by autophagy. *International Journal of Oncology,* 48**,** 2461-2471.
SZWERAS, M., LIU, D., PARTRIDGE, E. A., PAWLING, J., SUKHU, B., CLOKIE, C., JAHNEN-DECHENT, W., TENENBAUM, H. C., SWALLOW, C. J., GRYNPAS, M. D. & DENNIS, J. W. (2002) α2-HS glycoprotein/fetuin, a transforming growth factor-β/bone morphogenetic protein antagonist, regulates postnatal bone growth and remodeling. *Journal of Biological Chemistry,* 277**,** 19991-19997.
TENOPOULOU, M., KURZ, T., DOULIAS, P.-T., GALARIS, D. & BRUNK, ULFÂ T. (2007) Does the calcein-AM method assay the total cellular 'labile iron pool' or only a fraction of it? *Biochemical Journal,* 403**,** 261-266.
THE CANCER GENOME ATLAS, N. (2012) Comprehensive molecular characterization of human colon and rectal cancer. *Nature,* 487**,** 330-337.
THE WELLCOME TRUST CASE CONTROL, C. (2007) Genome-wide association study of 14,000 cases of seven common diseases and 3,000 shared controls. *Nature,* 447**,** 661-678.
THOMAS, W. R. & HOLT, P. G. (1978) Vitamin C and immunity: an assessment of the evidence. *Clinical and Experimental Immunology,* 32**,** 370-379.
TOIYAMA, Y., MIKI, C., INOUE, Y., KAWAMOTO, A. & KUSUNOKI, M. (2009) Circulating form of human vascular adhesion protein-1 (VAP-1): Decreased serum levels in progression of colorectal cancer and predictive marker of lymphatic and hepatic metastasis. *Journal of Surgical Oncology,* 99**,** 368-372.
TOMASEK, J. J., GABBIANI, G., HINZ, B., CHAPONNIER, C. & BROWN, R. A. (2002) Myofibroblasts and mechano-regulation of connective tissue remodelling. *Nature Reviews Molecular Cell Biology,* 3**,** 349.
TOROK, N. J. (2015) VAP-1 in NASH: A novel biomarker? *Hepatology (Baltimore, Md.),* 62**,** 1313-1315.
TORRE, L. A., BRAY, F., SIEGEL, R. L., FERLAY, J., LORTET TIEULENT, T. & JEMAL, A. (2015) Global cancer statistics, 2012. *CA: A Cancer Journal for Clinicians,* 65**,** 87-108.
TOTHILL, R. W., TINKER, A. V., GEORGE, J., BROWN, R., FOX, S. B., LADE,

S., JOHNSON, D. S., TRIVETT, M. K., ETEMADMOGHADAM, D., LOCANDRO, B., TRAFICANTE, N., FEREDAY, S., HUNG, J. A., CHIEW, Y.-E., HAVIV, I., GERTIG, D., DEFAZIO, A. & BOWTELL, D. D. L. (2008) Novel molecular subtypes of serous and endometrioid ovarian cancer linked to clinical outcome. *Clinical Cancer Research,* 14**,** 5198-5208.

TRABER, P. G. (1994) Differentiation of intestinal epithelial cells: lessons from the study of intestine-specific gene expression. *The Journal of Laboratory and Clinical Medicine,* 123**,** 467-477.

TSUJINO, T., SESHIMO, I., YAMAMOTO, H., NGAN, C. Y., EZUMI, K., TAKEMASA, I., IKEDA, M., SEKIMOTO, M., MATSUURA, N. & MONDEN, M. (2007) Stromal myofibroblasts predict disease recurrence for colorectal cancer. *Clinical Cancer Research,* 13**,** 2082-2090.

TSUTSUMI, K., FUJIKAWA, H., KAJIKAWA, T., TAKEDACHI, M., YAMAMOTO, T. & MURAKAMI, S. (2011) Effects of L-ascorbic acid 2-phosphate magnesium salt on the properties of human gingival fibroblasts. *Journal of Periodontal Research,* 47**,** 263-271.

WANG, C. C., BIBEN, C., ROBB, L., NASSIR, F., BARNETT, L., DAVIDSON, N. O., KOENTGEN, F., TARLINTON, D. & HARVEY, R. P. (2000) Homeodomain factor Nkx2-3 controls regional expression of leukocyte homing coreceptor MAdCAM-1 in specialized endothelial cells of the viscera. *Developmental Biology,* 224**,** 152-167.

WANG, H., WU, Q., LIU, Z., LUO, X., FAN, Y., LIU, Y., ZHANG, Y., HUA, S., FU, Q., ZHAO, M., CHEN, Y., FANG, W. & LV, X. (2014) Downregulation of FAP suppresses cell proliferation and metastasis through PTEN/PI3K/AKT and Ras-ERK signaling in oral squamous cell carcinoma. *Cell Death and Disease,* 5**,** e1155.

WANG, L. C., NASSIR, F., LIU, Z. Y., LING, L., KUO, F., CROWELL, T., OLSON, D., DAVIDSON, N. O. & BURKLY, L. C. (2002) Disruption of hedgehog signaling reveals a novel role in intestinal morphogenesis and intestinal-specific lipid metabolism in mice. *Gastroenterology,* 122**,** 469-482.

WANG, X., ZBOU, C., QIU, G., FAN, J., TANG, H. & PENG, Z. (2008) Screening of new tumor suppressor genes in sporadic colorectal cancer patients. *Hepatogastroenterology,* 55**,** 2039-2044.

WARD, S., WESTON, C., SHEPHERD, E., HEJMADI, R., ISMAIL, T. & ADAMS, D. (2016) Evaluation of serum and tissue levels of VAP-1 in colorectal cancer. *BMC Cancer,* 16.

WEBER, F., XU, Y., ZHANG, L., PATOCS, A., SHEN, L., PLATZER, P. & ENG, C. (2007) Microenvironmental genomic alterations and clinicopathological behavior in head and neck squamous cell carcinoma. *JAMA,* 297**,** 187-195.

WEIR, B. A., WOO, M. S., GETZ, G., PERNER, S., DING, L., BEROUKHIM, R., LIN, W. M., PROVINCE, M. A., KRAJA, A., JOHNSON, L. A., SHAH, K., SATO, M., THOMAS, R. K., BARLETTA, J. A., BORECKI, I. B., BRODERICK, S., CHANG, A. C., CHIANG, D. Y., CHIRIEAC, L. R., CHO, J., FUJII, Y., GAZDAR, A. F., GIORDANO, T., GREULICH, H., HANNA, M., JOHNSON, B. E., KRIS, M. G., LASH, A., LIN, L., LINDEMAN, N., MARDIS, E. R., MCPHERSON, J. D., MINNA, J. D., MORGAN, M. B., NADEL, M., ORRINGER, M. B., OSBORNE, J. R., OZENBERGER, B., RAMOS, A. H., ROBINSON, J., ROTH, J. A.,

RUSCH, V., SASAKI, H., SHEPHERD, F., SOUGNEZ, C., SPITZ, M. R., TSAO, M.-S., TWOMEY, D., VERHAAK, R. G. W., WEINSTOCK, G. M., WHEELER, D. A., WINCKLER, W., YOSHIZAWA, A., YU, S., ZAKOWSKI, M. F., ZHANG, Q., BEER, D. G., WISTUBA, I. I., WATSON, M. A., GARRAWAY, L. A., LADANYI, M., TRAVIS, W. D., PAO, W., RUBIN, M. A., GABRIEL, S. B., GIBBS, R. A., VARMUS, H. E., WILSON, R. K., LANDER, E. S. & MEYERSON, M. (2007) Characterizing the cancer genome in lung adenocarcinoma. *Nature,* 450**,** 893-898.

WEN, F.-Q., KOHYAMA, T., SKÖLD, C. M., ZHU, Y. K., LIU, X., ROMBERGER, D. J., STONER, J. & RENNARD, S. I. (2003) Glucocorticoids modulate TGF-β production by human fetal lung fibroblasts. *Inflammation,* 27**,** 9-19.

WITSCH, E., SELA, M. & YARDEN, Y. (2010) Roles for growth factors in cancer progression. *Physiology (Bethesda, Md.),* 25**,** 85-101.

WORTHLEY, D. L., GIRAUD, A. S. & WANG, T. C. (2010) Stromal fibroblasts in digestive cancer. *Cancer Microenvironment,* 3**,** 117-125.

WU, J. B., SHAO, C., LI, X., LI, Q., HU, P., SHI, C., LI, Y., CHEN, Y.-T., YIN, F., LIAO, C.-P., STILES, B. L., ZHAU, H. E., SHIH, J. C. & CHUNG, L. W. K. (2014) Monoamine oxidase A mediates prostate tumorigenesis and cancer metastasis. *The Journal of Clinical Investigation,* 124**,** 2891-2908.

XIE, T., WANG, Y., DENG, N., HUANG, G., TAGHAVIFAR, F., GENG, Y., LIU, N., KULUR, V., YAO, C., CHEN, P., LIU, Z., STRIPP, B., TANG, J., LIANG, J., NOBLE, P. W. & JIANG, D. (2018) Single-cell deconvolution of fibroblast heterogeneity in mouse pulmonary fibrosis. *Cell Reports,* 22**,** 3625-3640.

YAMAGUCHI, T., HOSONO, Y., YANAGISAWA, K. & TAKAHASHI, T. (2013) NKX2-1/TTF-1: An enigmatic oncogene that functions as a double-edged sword for cancer cell survival and progression. *Cancer Cell,* 23**,** 718-723.

YAO, T. & ASAYAMA, Y. (2017) Animal-cell culture media: History, characteristics, and current issues. *Reproductive Medicine and Biology,* 16**,** 99-117.

YASUDA, H., TOIYAMA, Y., OHI, M., MOHRI, Y., MIKI, C. & KUSUNOKI, M. (2011) Serum soluble vascular adhesion protein-1 is a valuable prognostic marker in gastric cancer. *Journal of Surgical Oncology,* 103**,** 695-699.

YASUHIKO, K., TAKAMITSU, S., TOSHIO, K., TORU, N., D., B. C., R., H. S. & J., F. I. (2006) Expression of activated platelet-derived growth factor receptor in stromal cells of human colon carcinomas is associated with metastatic potential. *International Journal of Cancer,* 119**,** 2567-2574.

YAZHOU, C., WENLV, S., WEIDONG, Z. & LICUN, W. (2004) Clinicopathological significance of stromal myofibroblasts in invasive ductal carcinoma of the breast. *Tumor Biology,* 25**,** 290-295.

YEUNG, T. M., BUSKENS, C., WANG, L. M., MORTENSEN, N. J. & BODMER, W. F. (2013) Myofibroblast activation in colorectal cancer lymph node metastases. *British Journal of Cancer,* 108**,** 2106-2115.

YU, J., USTACH, C. & CHOI KIM, H.-R. (2003) Platelet-derived growth factor signaling and human cancer. *Journal of biochemistry and molecular biology,* 36**,** 49-59.

YU, P., MA, D. & XU, M. (2005) Nested genes in the human genome. *Genomics,* 86**,** 414-422.

YU, W., LIN, Z., PASTOR, D. M., HEGARTY, J. P., CHEN, X., KELLY, A. A.,

WANG, Y., PORITZ, L. S. & KOLTUN, W. A. (2010) Genes regulated by Nkx2-3 in sporadic and inflammatory bowel disease-associated colorectal cancer cell lines. *Digestive Diseases and Sciences,* 55**,** 3171-3180.

ZAKA, M. U., PENG, Y. & SUTTON, C. W. (2014) Microarray big data integrated analysis to identify robust diagnostic signature for triple negative breast cancer. *2014 IEEE Symposium on Computational Intelligence in Big Data (CIBD).*

ZHANG, L., SUN, W., WANG, J., ZHANG, M., YANG, S., TIAN, Y., VIDYASAGAR, S., PEÑA, L. A., ZHANG, K., CAO, Y., YIN, L., WANG, W., ZHANG, L., SCHAEFER, K. L., SAUBERMANN, L. J., SWARTS, S. G., FENTON, B. M., KENG, P. C. & OKUNIEFF, P. (2010) Mitigation effect of an FGF-2 peptide on acute gastrointestinal syndrome after high-dose ionizing radiation. *International Journal of Radiation Oncology, Biology, Physics,* 77**,** 261-268.

ZHENG, X., BAKER, H., HANCOCK, W. S., FAWAZ, F., MCCAMAN, M. & PUNGOR, E. (2006) Proteomic analysis for the assessment of different lots of fetal bovine serum as a raw material for cell culture. Part IV. application of proteomics to the manufacture of biological drugs. *Biotechnology Progress,* 22**,** 1294-1300.

APPENDIX

SUPPLEMENTARY DATA

Growth factor (Probe set)	Low	mRNA level	High	mRNA level
TGFβ1 (203085_s_at)	C99 (lowest)	12	OXCO2 (Highest)	660
	LIM1863	12	HDC8	638
	PCJW	15	OXCO1*	604
	HCC56	16	SW48	539
	SW403	17	HT29	534
	HT55	17	RKO*	497
	HRA19	17	NCIH716*	484
	C80	17	CCO7*	446
	HDC57	17	CC20*	437
	C125PM	18	Colo320HSR*	426
EGF (206254_at)	HDC8 (lowest)	11	HDC57 (highest)	308
	LIM1863	12	HDC73	283
	COLO678	13	HDC54	276
	ISCEROL	13	C70	268
	C105251	13	SNU70	239
	OXCO3	14	HDC143	198
	HDC9	14	c10s	189
	SW1116	14	VACO4A	179
	HCT116	14	SW1222	177
	RW7213	15	LS180	168
PDGF-A (229830_at)	Colo320HSR	26	SW480 (highest)	3039
	(lowest)	31	OXCO1	2628
	JHSKREC	35	SW1417	2281
	Colo320DM	41	SW620	1690
	HCA46	50	SW1116	1309
	LIM863	52	CaCo2	1074
	Gp2D	57	LIM1215	1045
	HDC9	60	SNU1544	1020
	HT55	61	ISCEROL	976
	PMFKo14	63	RCM1	774
	CCK81			
PDGF-C (218718_at)	NCIH548 (lowest)	10	C10 (highest)	3591
	Colo206	12	OXCO1	2437
	SW837	12	CCO7*	2170
	SW403	12	CAR1	1381
	PMFKo14	12	CC20*	1263
	SNUC1	12	Colo678	1074
	CW2	13	c10s	1054
	C125PM	13	HDC9	1039
	HDC54	13	CX1	929
	NCIH498	13	LS123	923

Supplementary data S1
Ten of the highest and lowest growth factor-expressing CRC cells (*denotes the EMT cells
OXCO1, CCO7, CC20 and c10s highly express two or more of selected growth factors (*TGFβ1*, *EGF* and *PDGF-A)*

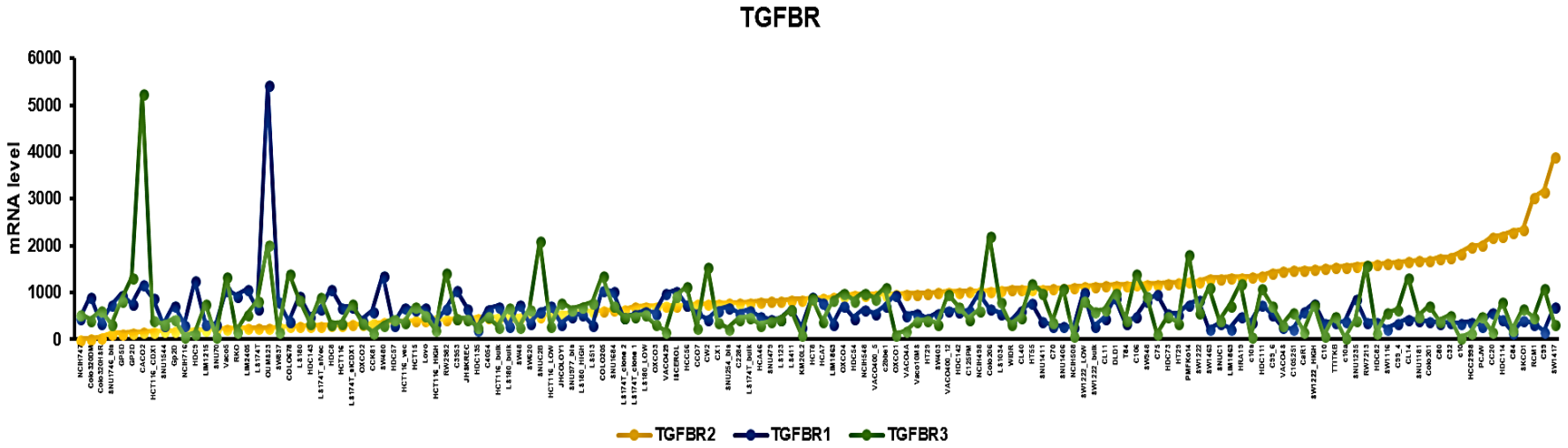

Supplementary data S2
Microarray data analysis on the expression of *TGFBR1*,*2* and *3* of CRC cell lines.

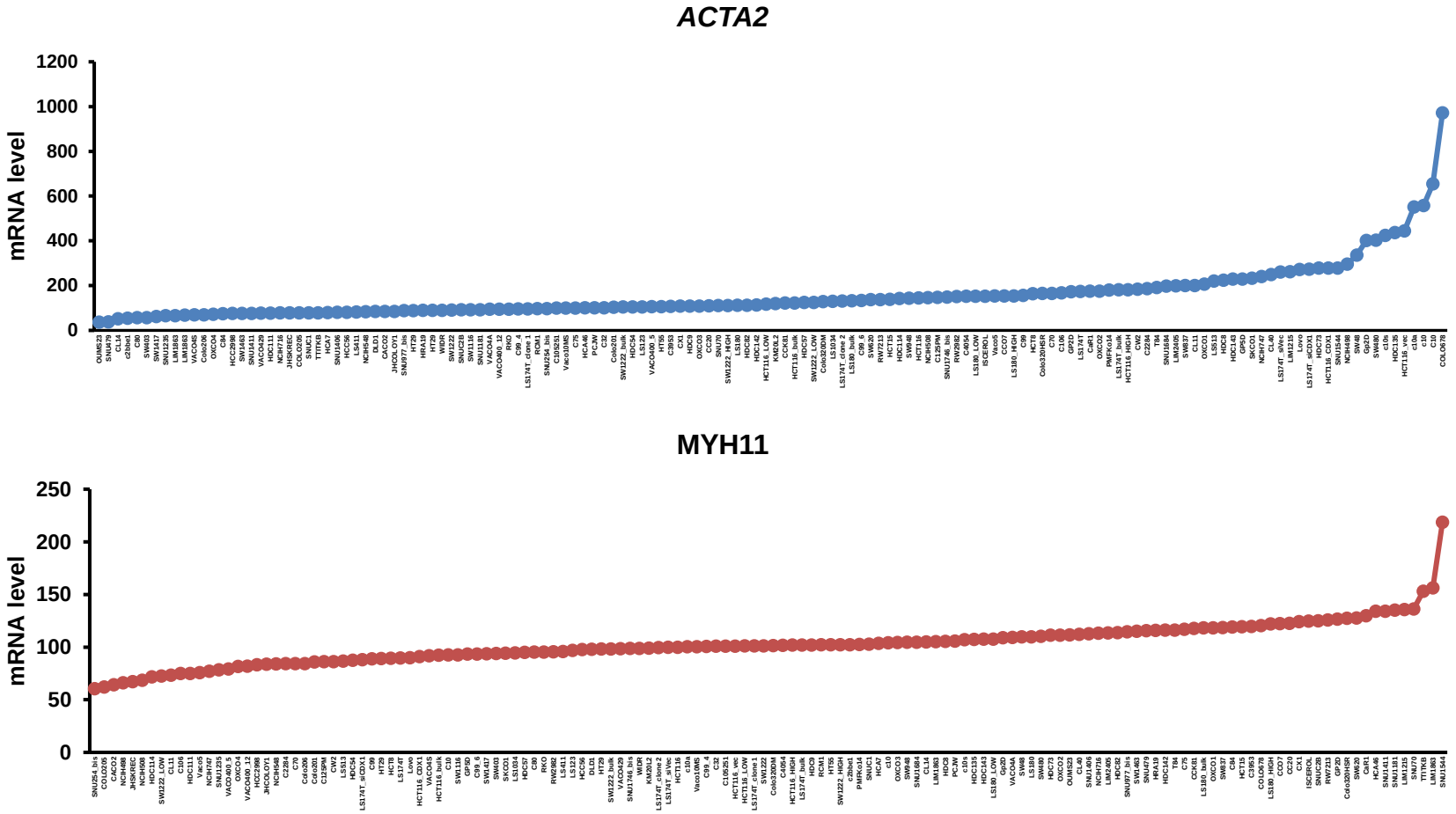

Supplementary data S3
Microarray data analysis of *ACTA2* and *MYH11* expression in CRC cell lines.
Only a small subsets of CRC cell lines express detectable levels of ACTA2 (6 cell lines) and MYH11 (2 cell lines)

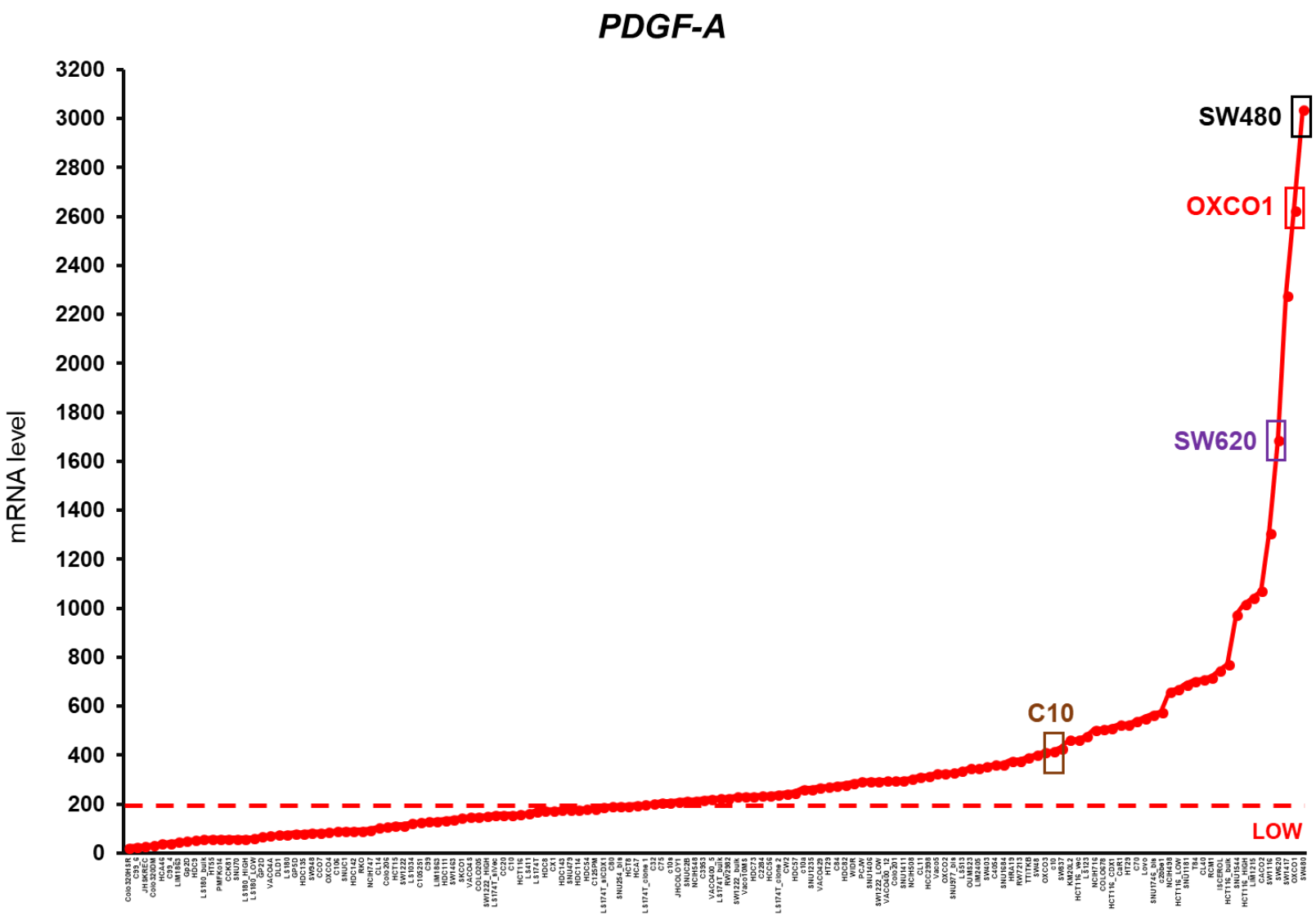
PDGF-A
mRNA level
3200
3000
2800
2600
2400
2200
2000
1800
1600
1400
1200
1000
800
600
400
200
0
SW480
OXCO1
SW620
C10
LOW

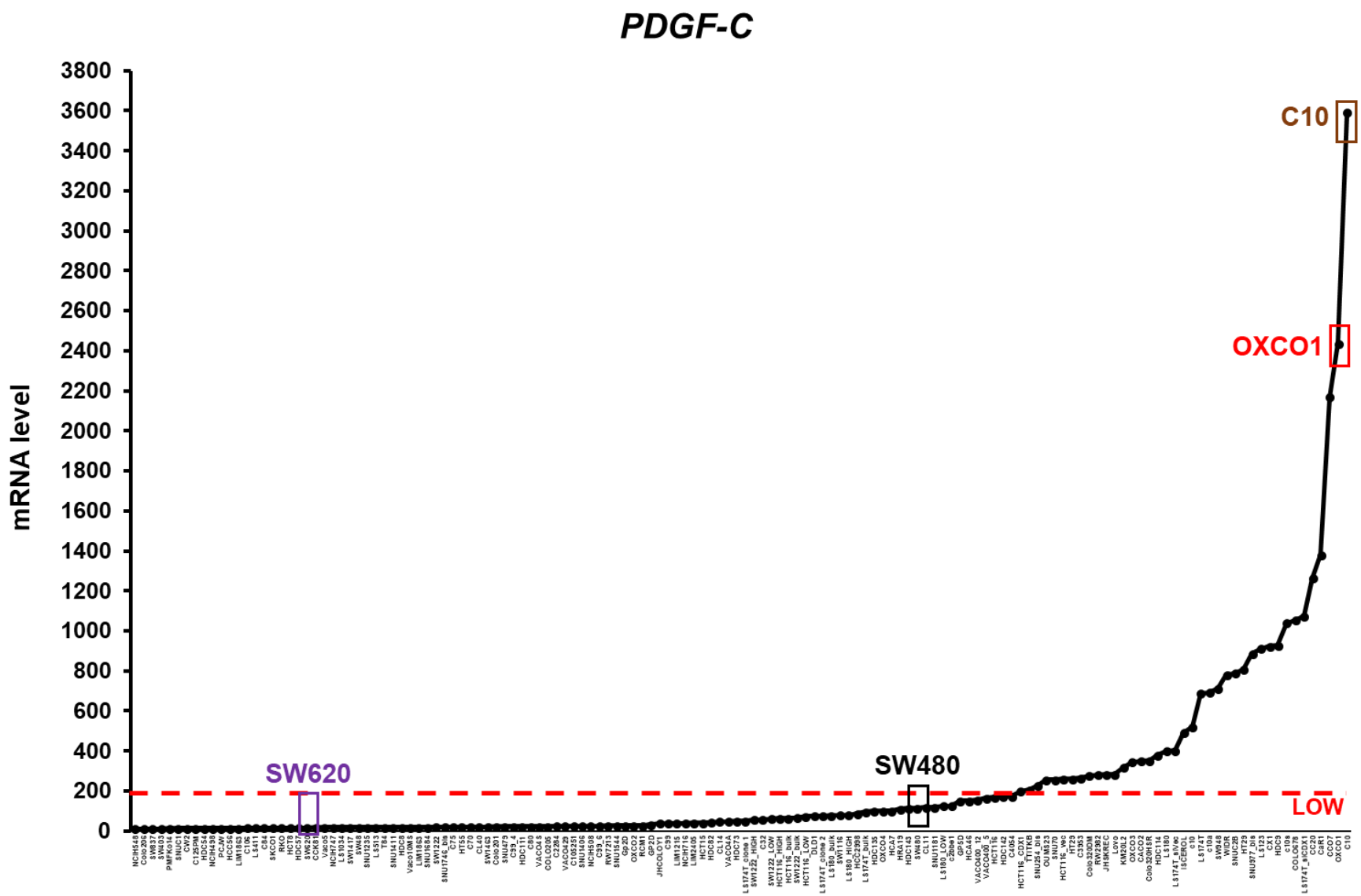
PDGF-C
mRNA level
3800
3600
3400
3200
3000
2800
2600
2400
2200
2000
1800
1600
1400
1200
1000
800
600
400
200
0
C10
OXCO1
SW620
SW480
LOW

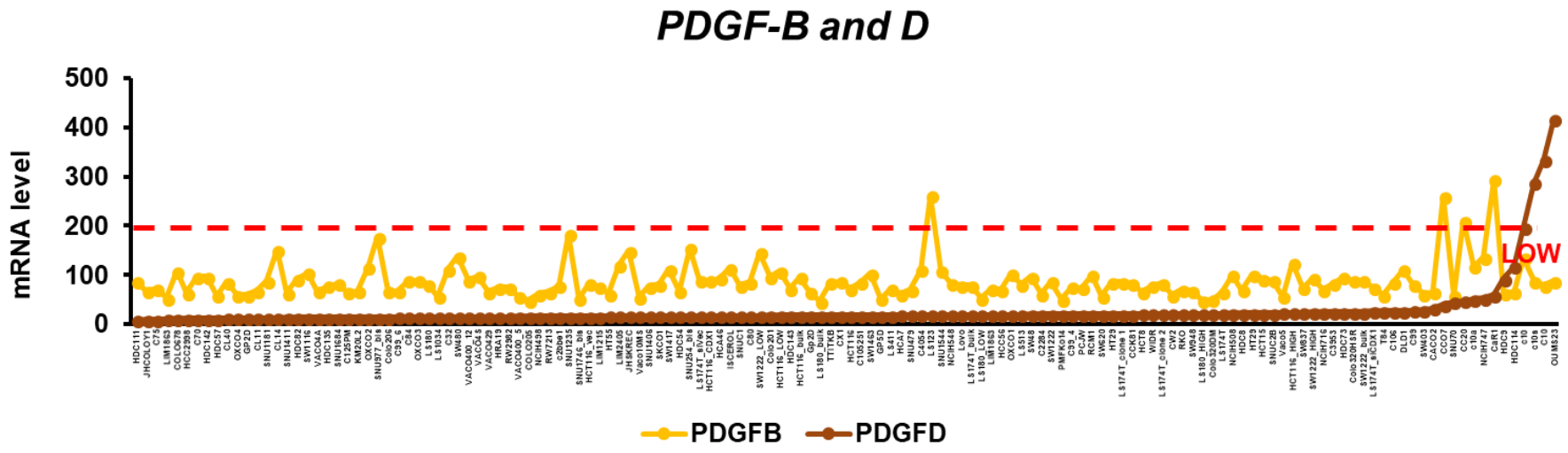

Supplementary data S4

Microarray data on the expression levels of *PDGF-A*, *C*, *B* and *D* in CRC cell lines

CRC cell lines with high expression of either one, or both of *PDGF-A* and *C* (OXCO1, SW480, SW620 and C10) are denoted by boxes. High expression of either *PDGF-A* or *C* was found in most of CRC cell lines (approximately 50% and 40% of CRC cell lines for *PDGF-A* and *C*, respectively). No CRC cell lines expressed significant level of *PDGF-B* and *D* (Strong positive expression: mRNA level more than 200)

A) Amino acid

DMEM, high glucose, pyruvate (41966, Life Technologies)	Concentration (mg/L)	DMEM/F12 with GlutaMAX (10565, Life Technologies)	Concentration (mg/L)
Glycine	30.0	Glycine	18.75
L-Arginine hydrochloride **	84.0	L-Alanine *	4.45
L-Cystine 2HCl	63.0	L-Alanyl-L-Glutamine *	542.0
L-Glutamine **	580.0	L-Arginine hydrochloride	147.5
L-Histidine hydrochloride-H_2O	42.0	L-Asparagine-H_2O *	7.5
L-Isoleucine	105.0	L-Aspartic acid *	6.65
L-Leucine	105.0	L-Cysteine hydrochloride-H_2O *	17.56
L-Lysine hydrochloride	146.0	L-Cystine 2HCl	31.29
L-Methionine	30.0	L-Glutamic acid *	7.35
L-Phenylalanine	66.0	L-Histidine hydrochloride-H_2O	31.48
L-Serine	42.0	L-Isoleucine	54.47
L-Threonine	95.0	L-Leucine	59.05
L-Tryptophan	16.0	L-Lysine hydrochloride	91.25
L-Tyrosine	72.0	L-Methionine	17.24
L-Valine	94.0	L-Phenylalanine	35.48
		L-Proline *	17.25
		L-Serine	26.25
		L-Threonine	53.45
		L-Tryptophan	9.02
		L-Tyrosine disodium salt dihydrate *	55.79
		L-Valine	52.85

B) **Vitamins**

DMEM, high glucose, pyruvate (41966, Life Technologies)	Concentration (mg/L)	DMEM /F12 with GlutaMAX (10565, Life Technologies)	Concentration (mg/L)
Choline chloride	4.0	Biotin *	0.0035
D-Calcium pantothenate	4.0	Choline chloride	8.98
Folic acid	4.0	D-Calcium pantothenate	2.24
Niacinamide	4.0	Folic acid	2.65
Pyridoxine hydrochloride	4.0	Niacinamide	2.02
Riboflavin	0.4	Pyridoxine hydrochloride	2.031
Thiamine hydrochloride	4.0	Riboflavin	0.219
i-Inositol	7.2	Thiamine hydrochloride	2.17
		Vitamin B12 *	0.68
		i-Inositol	12.6

C) Inorganic salt

DMEM, high glucose, pyruvate (41966, Life Technologies)	Concentration (mg/L)	DMEM/F12 with GlutaMAX (10565, Life Technologies)	Concentration (mg/L)
Calcium chloride	264.0	Calcium chloride	116.6
Ferric nitrate	0.1	Cupric sulfate *	0.0013
Magnesium sulfate	200.0	Ferric nitrate	0.05
Potassium chloride	400.0	Ferric sulfate *	0.417
Sodium bicarbonate	3700.0	Magnesium chloride *	28.64
Sodium chloride	6400.0	Magnesium sulfate	48.84
Sodium phosphate monobasic	141.0	Potassium chloride	311.8
		Sodium bicarbonate	2438.0
		Sodium chloride	6999.5
		Sodium phosphate dibasic *	71.02
		Sodium phosphate monobasic	62.5
		Zinc sulfate *	0.432

D) Other components

DMEM, high glucose, pyruvate (41966, Life Technologies)	Concentration (mg/L)	DMEM/F12 with GlutaMAX (10565, Life Technologies)	Concentration (mg/L)
D-Glucose (Dextrose)	4500.0	D-Glucose (Dextrose)	3151.0
Phenol red	15.0	Hypoxanthine Na *	2.39
Sodium pyruvate	110.0	Linoleic acid *	0.042
		Lipoic acid *	0.105
		Phenol red	8.1
		Putrescine 2HCl *	0.081
		Sodium pyruvate	55.0
		Tyhmidine *	0.365

Supplementary data S5
Composition of commercially available culture media; DMEM *vs* DMEM/F12 with GlutaMAX (Components in DMEM which are not included in DMEM/F12) (*Components in DMEM/F12 which are not included in DMEM) (Information taken from Life Technologies website).**

Component	Concentration (mg/L)
Arachidonic acid	2.0
Cholesterol	220.0
DL-alpha-Tocopherol acetate	70.0
Ethyl alcohol 100%	Confidential
Linoleic acid	10.0
Linolenic acid	10.0
Myristic acid	10.0
Oleic acid	10.0
Palmitic acid	10.0
Palmitoleic acid	10.0
Pluronic F-68	90000.0
Stearic acid	10.0
Tween 80®	2200.0

Supplementary data S6
Components of chemically defined lipid concentrate (11905, Life Technologies) (Information taken from Life Technologies website).

EGFR ligand (Probe set)	CRC cells	mRNA level
EGF (206254_at)	HDC57 (highest)	308
	HDC73	283
	HDC54	276
	C70	268
	SNU70	239
	HDC143	198
	c10s	189
	VACO4A	179
	SW1222	177
	LS180	168
TGF alpha (205016_at)	CaR1 (highest)	2472
	SNU1235	1882
	c10a	1638
	LS123	1448
	c10	1418
	SW1417	1308
	c10s	1294
	HDC8	1223
	DLD1	1214
	C10	1118
Epiregulin (205767_at)	DLD1 (highest)	5094
	Colo201	4022
	SNU70	3995
	HCT116	3728
	SNU1684	3700
	CL14	3524
	NCIH548	3388
	OXCO3	3372
	LS1034	3191
	Lovo	3104
Amphiregulin (205239_at)	HCA7 (highest)	9192
	Colo201	7460
	NCIH548	5730
	LS1034	4909
	HCT116	4804
	KM20L2	4526
	CL14	4475
	OXCO3	4442
	CaR1	4128
	C70	3929

Supplementary data S7
Microarray data of ten of the highest EGFR ligands-expressing CRC cells.
The mRNA levels of three selected EGFR ligands, namely *TGF alpha*, epiregulin and amphiregulin are shown. Higher expression of *TGF alpha*, epiregulin and amphiregulin in CRC cell lines was found in comparison to EGF.

Number	Myofibroblasts	Location	Type of tissue
1.	Myo 1998	Normal colon	Normal
2.	Myo 2156	CRC	Cancer
3.	Myo 6024	Rectum	Normal
4.	Myo 6536	Sigmoid colon	Normal
5.	Myo 6544	Descending colon	Normal
6.	Myo 6526	Sigmoid colon	Normal
7.	Myo 6550[1]	Sigmoid colon	Normal
8.	Myo 6551C[1]	Sigmoid colon	Cancer
9.	Myo 6769[2]	Ascending colon	Normal
10.	Myo 6769C[2]	Ascending colon	Cancer
11.	Myo 7395	Sigmoid colon	Normal
12.	Myo 7659	Sigmoid colon	Normal
13.	Myo 8835[3]	Sigmoid colon	Normal
14.	Myo 8836C[3]	Sigmoid colon	Cancer
15.	Myo 8849	Ascending colon	Normal
16.	Myo 8852C[4]	Rectum	Cancer
17.	Myo 8853[4]	Sigmoid colon	Normal
18.	Myo 8872C[5]	Ascending colon	Cancer
19.	Myo 8873[5]	Ascending colon	Normal
20.	Myo 0164C[6]	Caecum	Cancer
21.	Myo 0165[6]	Ascending colon	Normal
22.	Myo 8958C (W)	CRC	Cancer

Supplementary data S8
The primary myofibroblasts isolated from surgical samples.
Myofibroblasts from the same patient are given identical numbers following the cell line name.